

Electrogreffage et photogreffage de couches organiques sur des substrats conducteurs et semi-conducteurs

Avni Berisha

▶ **To cite this version:**

Avni Berisha. Electrogreffage et photogreffage de couches organiques sur des substrats conducteurs et semi-conducteurs. Chimie-Physique [physics.chem-ph]. Université Pierre et Marie Curie - Paris VI, 2011. Français. NNT : . pastel-00649488

HAL Id: pastel-00649488
https://pastel.hal.science/pastel-00649488

Submitted on 8 Dec 2011

HAL is a multi-disciplinary open access archive for the deposit and dissemination of scientific research documents, whether they are published or not. The documents may come from teaching and research institutions in France or abroad, or from public or private research centers.

L'archive ouverte pluridisciplinaire **HAL**, est destinée au dépôt et à la diffusion de documents scientifiques de niveau recherche, publiés ou non, émanant des établissements d'enseignement et de recherche français ou étrangers, des laboratoires publics ou privés.

THESE DE DOCTORAT DE

L'UNIVERSITE PIERRE ET MARIE CURIE

Spécialité
Electrochimie
(Chimie Physique et Chimie Analytique de Paris Centre, ED 388)

Présentée par

Avni BERISHA

Pour obtenir le grade de

DOCTEUR de l'UNIVERSITÉ PIERRE ET MARIE CURIE

Sujet de la thèse :

Electrografting and photografting of organic layers onto conducting and semi-conducting surfaces

Electrogreffage et photogreffage de couches organiques sur des substrats conducteurs et semi-conducteurs

Soutenue en 13 Septembre 2011

devant le jury composé de:

Mme. Catherine COMBELLAS	Directeur de recherche CNRS	Directrice de thèse
M. Fetah PODVORICA	Professeur, Université de Prishtina	Codirecteur de thèse
Mme. Zineb MEKHALIF	Professeur, Université de Namur	Rapporteur
Mme. Christine VAUTRIN-UL	Professeur, Université d'Orléans	Rapporteur
M. Emmanuel MAISONHAUTE	Professeur, Université Pierre et Marie Curie	Examinateur
M. Ramë VATAJ	Professeur associé, Université Prishtina	Examinateur

THESE DE DOCTORAT DE

L'UNIVERSITE PIERRE ET MARIE CURIE

Spécialité
Electrochimie
(Chimie Physique et Chimie Analytique de Paris Centre, ED 388)

Présentée par

Avni BERISHA

Pour obtenir le grade de

DOCTEUR de l'UNIVERSITÉ PIERRE ET MARIE CURIE

Sujet de la thèse :

Electrografting and photografting of organic layers onto conducting and semi-conducting surfaces

Electrogreffage et photogreffage de couches organiques sur des substrats conducteurs et semi-conducteurs

Soutenue en 13 Septembre 2011

devant le jury composé de:

Mme. Catherine COMBELLAS	Directeur de recherche CNRS	Directrice de thèse
M. Fetah PODVORICA	Professeur, Université de Prishtina	Codirecteur de thèse
Mme. Zineb MEKHALIF	Professeur, Université de Namur	Rapporteur
Mme. Christine VAUTRIN-UL	Professeur, Université d'Orléans	Rapporteur
M. Emmanuel MAISONHAUTE	Professeur, Université Pierre et Marie Curie	Examinateur
M. Ramë VATAJ	Professeur associé, Université Prishtina	Examinateur

R e m e r c i e m e n t s

J’ai réalisé cette thèse au sein du Laboratoire des sciences analytiques, bioanalytiques et miniaturisation (LSABM) de l’ESPCI.

J’aimerais à présent adresser mes plus vifs remerciements à mes directeurs de thèses Catherine Combellas et Fetah Podvorica. Catherine Combellas m’a accepté au sein de son équipe, encadré et fourni des conseils au cours de discussions très intéressantes ; elle a aussi relu très précisément mon manuscrit. C’est grâce a Fetah Podvorica que je obtenu la bourse qui m’a permis d’effectuer cette thèse a Paris. Il m’a faite profiter de ca très grande expérience du greffage de surfaces. Je suis extrêmement reconnaissant au professeur émérite Jean Pinson : ‘’ Jean cette thèse n'aurait pas vu le jour sans ton aide précieuse, tes conseils, ta patience et le temps que tu as consacré à donner plus de rigueur à ma plume qui à tendance quelquefois à déraper ‘’. Merci pour tout.

Merci à toutes les trois d’être parvenus à maintenir au sein du laboratoire une ambiance à la fois pleine de travail et de bonne humeur ce qui est très appréciable. Je n’oublierai pas se sitôt ce laboratoire exceptionnel !

Durant ces trois années plusieurs personnes ont contribué au quotidien à l’environnement scientifique et amical. Aux thèsards Nadia Ktari (maintenant jeune docteur) et Sorin Munteanu (doctorant en troisième année), merci pour toutes ces années passées ensemble. Un grand merci a Sandra Nunige et Géraldine Hallais pour leur aide au cours des mesures MEB et Tof-SIMS.

Je remercie également Fréderic Kanoufi que j’ai eu le privilège de connaître et côtoyer ainsi que Hassan Hazimeh, et rendre hommage à leurs immenses qualités scientifiques et humaines qui font que de simples discussions deviennent de passionnants échanges.

Je suis très honore que Mme Zineb Mekhalif professeur à Namur (Belgique) et Mme Christine Vautrin-Ul professeur à l’Université d’Orléans, aient acceptées de juger mon travail de thèse en tant que rapporteurs. Je remercie aussi les autres membres de jury d’avoir bien voulu juger mon travail.

Je voudrais remercier l’ambassade de France au République du Kosovo pour l’aide financière durant 18 mois et la fondation Langlois pour 3 mois de financement.

Un grand remerciement également a la famille Tershnjaku (Fadil, Perparime et leurs enfants) pour m’avoir m’accueilli dans leur famille pendant plusieurs mois durant mes séjours à Paris.

Je voudrais enfin remercier mes parents (Riza et Lirije), mes cinq sœurs et mes deux frères pour leur soutien. Vous m’avez laissé libre de choisir la voie que je voulais suivre sans même savoir où tout cela allait me mener ! Merci pour cette confiance sans faille.

Je dédie tout ce travail à mes parents et à Valbona qui a su m’écouter, m’encourager et supporter mes moments de stress durant ces trois années, particulièrement lors de la rédaction de ce manuscrit. J’essaierai d’être toujours à la hauteur.

Table of contents

General introduction 1

Chapter 1 : Surface Coatings, a Review 3

I. Formation of organic films on different substrates 3

I. SAMs 3

I.1. Fatty Acids 4

I.2. Silanes 4

I.3. Phosphonic acids 7

I.4. Thiols 7

I.5. Alkyl Monolayers on Silicon 9

II. Formation of organic nano/micro layers through electrochemistry 10

II.1. Oxidation of amines 10

II.2. Oxidation of carboxylates 11

II.3. Oxidation of alcohols 12

II.4. Oxidation of Grignard reagents 13

II.6. Grafting of diazonium salts 14

II.6.1. Electrochemistry of diazonium salts 15

II.6.2. Stability of the layers 16

II.6.3. Different diazonium salts 16

II.6.4. Different grafting methods 17

II.6.5. Post grafting modification 19

II.6.6. Monolayer vs. multilayer 21

II.6.7. Patterning using the reduction of diazoniums 23

II.6.8. Techniques for the characterization of the grafted layers 24

II.6.9. Applications of diazonium salts grafting reactions. 33

II.7. Reduction of alkyl halides 38

II.8. Reduction of vinylics 39

III. UV photochemical modification of surfaces 43

III.1. Modification using unsaturated compounds 43

III.2. Modification using arylazides 45

References 49

Chapter 2 : Indirect Grafting of Acetonitrile-Derived Films on Metallic Substrates 67

2.1. Introduction 67

2.2. Paper 69
2.3. Supporting informations 77
2.4. Analysis 80
Chapter 3 : Photochemical grafting and Patterning of Metallic Surfaces by Organic Layers Derived from Acetonitrile 81
3.1. Introduction 81
3.2. Paper 83
3.3. Supporting informations 110
3.4. Analysis 123
Chapter 4 : Physisorption vs grafting of aryldiazonium salts onto iron: A corrosion study 125
4.1. Introduction 125
4.2. Paper 127
4.3. Analysis 132
General conclusions 133
Annexes 135
Annex 1: Water contact angles 135
Annex 2: Ellipsometry 136
Annex 3: Profilometry 137
Annex 4: IRRAS spectroscopy 138
Annex 5: Tof-SIMS 139
Annex 6: SEM, EDX 140
Annex 7: AFM 141
Annexes references 142

List of figures

Figure. 1. Fatty acid SAM structure. _____ 4

Figure. 2. Silane SAM obtention and the structure of the formed layer. _____ 4

Figure. 3. Silane structure dependency on the amount of water in solution. _____ 6

Figure. 4. SAM monolayers formation: a. monodentate or b. bidentate linkage with substrate. _____ 7

Figure. 5. Different reactions for the construction of monolayers on silicon. _____ 9

Figure. 6. Grafting of amine by oxidation. _____ 10

Figure. 7. Grafting of carboxylates onto carbon materials. _____ 12

Figure. 8. Mechanism of alcohol oxidation on carbon material. _____ 12

Figure. 9. Mechanism for grafting Grignard reagents onto hydrogenated silicium surface through oxidation (h= electron hole, SH=solvent). _____ 13

Figure. 10. 1) The mechanism of diazonium grafting to different substrates (C-carbon materials, M-metals, SC-semiconductors and P-polymers) and 2) formation of aryl anion from the reduction of the aryl radical. _____ 15

Figure. 11. Different means to initiate the diazonium grafting. _____ 18

Figure. 12. The mechanism for the electrochemical reduction in acidic aqua media of the grafted layer containing $-NO_2$ group into $-NH_2$ group. _____ 19

Figure. 13. Attachment of anthraquinone to a carbon surface through a protection-deprotection method _ 20

Figure. 14. The mechanism for the formation of multilayer during the grafting of diazoniums _____ 21

Figure. 15. Grafting a monolayer using the ''formation/degradation'' approach : A) using the formation of a multilayer of diaryl disulfides and its reductive cleavage to a monolayer of nucleophilic thiophenolate [360] and B) using a grafted long chain alkyl hydrazone and its cleavage in acidic media to a monolayer of benzaldehyde[359]. _____ 22

Figure. 16. Influence of the steric effects on the voltammetric behavior during the grafting of 4 mM ubstituted diazoniums salts in ACN + 0.1M NBu_4BF_4, Reference Ag/AgCl, 1,2) 2 mm glassy carbon electrode, scan rate 0.1 V s^{-1}. 3) 1 mm copper electrode, scan rate 50 mV s^{-1}. 1) (A) 2,6-dimethylbenzene diazonium, (a) first, (b) second, and (c) tenth scan, and (B) 2-ethylbenzenediazonium, (a) first, (b) second, and (c) fourth scan. 2) (A) 2,4- and (B) 3,5- dimethylbenzene diazonium, (a) first, (b) second, (c) third, and (d) fourth scan.[394] 3) 3,5-bis-*tert*-butylbenzenediazonium (a) first scan; (b) second scan; (0) blank. [392] _____ 25

Figure. 17. Influence of immersion time on FT-IRRAS reflection spectra of nitrophenyl modified Zn surfaces. Modification of zinc surfaces consists in dipping the substrate in 10 mM 4-nitrobenzenediazonium tetrafluoroborate solution in ACN for 5, 30 and 120 min[302]. _____ 27

Figure. 18. Tapping mode images for a biphenyl-modified PPF surface following a contact mode scratch. Single derivatization scans from +0.4 to 0, -0.2, -0.4, and -0.6 V vs Ag/Ag+ were used to modify the PPF surface, as indicated[258]. _____ 30

Figure. 19. **AFM images of: bare zinc, bare nickel, and Zn and Ni surfaces modified with diethylaminobenzenediazonium by immersion of the sample for 5 min and 15 h in 10 mM 4-nitrobenzenediazonium tetrafluoroborate solution in ACN [302]. _____ 30**

Figure. 20. **SEM image of the modified graphite flake a) with 4-aminophenyl groups and b) subsequent transformation of $-NH_2$ group into diazo group followed by the covalent attachment of Si particles [245]. _____ 31**

Figure. 21. **TEM image of the modified oxide powder $Li_{1.1}V_3O_8$ with 4-nitrobenzene layer b) t=10min and c) t=60min [410]. _____ 31**

Figure. 22. **Constant-current STM image (650 x 650 nm^2) of a HOPG substrate collected in air following 2 deposition cycles in 0.5 mM 4-diazo-*N*, *N*-diethylaniline fluoroborate. Bias voltage) 100 mV; tunneling current) 100 pA[248]._____ 32**

Figure. 23. **STM 5nm x 5nm image of: a) SiH (111) surface and b) the same surface modified by bromphenyl groups[333]. _____ 32**

Figure. 24. **Grafting mechanism of the reduction of alkyl halides on Si-H _____ 38**

Figure. 25. **Cyclic voltametry on a GC electrode (*d* =3 mm) in ACN+ 0.1 M NBu_4BF_4 of $I(CH_2)_2C_8F_{17}$ (*c* =10 mM), (a) first; (b) second and (c) third scans. Reference Ag/AgCl, v= 0.1 V s^{-1} [441]. _____ 39**

Figure. 26. **Mechanism for the formation of an organic layer by electrografting of $^{\bullet}CH_2CN$. [442] _____ 39**

Figure. 27. **Mechanism for the cathodic electrografting of the vinylics (i.e methacrylonitrile) _____ 40**

Figure. 28. Left: **Schematic view of the different electrochemical and chemical reactions occurring on the substrate, at the tip, and in the tip/substrate gap. *Right:* Reproduction of the "Madeleine" painted by Henri Matisse (inset) printed on the gold substrate by coupling SECM with Elecdraw software. (Conditions: [Acrylic Acid] = 2.0 mol L^{-1}, [DNB] = $2 \cdot 10^{-3}$ mol L^{-1}, $[H_2SO_4]$ = 0.25 mol L^{-1}.) [452] _____ 42**

Figure. 29. **Mechanism of photochemical grafting in Si-H: A) by excitaction and surface radical formation;B) by photoemission and nucleophilic attack of the alkene. _____ 44**

Figure. 30. **Modification of polymers surface through photochemical process using azides._____ 46**

General introduction

Coating of surfaces includes important industrial processes such as Physical Vapor Deposition (PVD), Chemical Vapor Deposition (CVD), Electroplating, Electrophoresis and many others, the objects obtained with these methods are part of our daily life such as microelectronic equipments or car bodies…. Other methods for the modification of surfaces include the reaction of oxidized surfaces with silanes and phosphonates as well as Self Assembled Monolayers. More recently electrografting has appeared as method for the strong (covalent) attachment of organic layers to a variety of substrates from diamond to polymers. A number of chemical groups (amines, carboxylates, alcohols, Grignard reagents, diazonium salts, vinylics, alkyl halides) have been found as suitable for electrografting. Besides electrografting a number of other procedures have been developed (spontaneous grafting, grafting by scribing, by ultrasonication, etc). These methods appear of some interest as, for example, grafting of diazonium salts has now reached the industrial stage (either by electrochemistry or as a spontaneous reaction). Besides, a number of sensors have been described in academic publications.

Nevertheless, adding new chemicals or new procedures to the list above is a valuable research goal, as one can expect faster, more efficient, or more easily scaled up reactions. The search of new reactions is the topic of this thesis, particularly the search for easily available molecules that can be grafted to surfaces. We report the rather unexpected indirect and photochemical grafting of a common, easily accessible solvent: acetonitrile.

General introduction

In most cases, deposition of an organic layer onto a metal does not lead to the formation of a bond between the substrate and the layer. There are a number of methods available for the deposition of an organic layer on a metal, painting is the simplest one, but also roll coating (where the polymer sheet is pressed between two rolls on a metal sheet), spraying polymer onto metals, etc.

This thesis describes something very different. It deals with chemical reactions that permit the formation of a chemical bond between the substrate (carbon, metal, semiconductor) and the organic layer. Some reactions of this type have already been described and the following introduction gives a brief account of these methods.

In the first chapter, we present the bibliographic studies of different methods that permit surface modification. These methods are divided in two groups: a) the class of molecules that form self assembled monolayers without electrochemical induction and b) the molecules that form organic layers on the substrate involving electrochemistry as a means to initiate and perform modification (both oxidation and reduction). We start by describing the formation of self assembled monolayers using different classes of compounds like fatty acids, silanes, thiols, phosphonic acids and alkyl monolayers on silicon. For each class, we represent shortly the substrates that can be used, basic modes to prepare these substrates, bonding mechanism, stability and some applications. Photochemical modification is described separately, together with two important classes of molecules used (alkanes and arylazides).

The second chapter deals with the electrografting of metals (gold, copper) and semiconductors (SiH) with a newly developed strategy using the sterically hindered 2,6-dimethylbenzenediazonium salt to generate and graft radicals derived from the solvent (acetonitrile), this leads finally to an amino layer. It is interesting to note that the layer can be formed spontaneously in the case of copper. We analyse these layers by different techniques and present a mechanism accounting for the formation of the layers.

The third chapter involves the photochemical grafting of acetonitrile under UV irradiation. This simple method only necessitates a small UV lamp and a very common solvent, acetonitrile. The amino layer that is obtained is identical to that of the second chapter, but

through a different mechanism. It is characterized by IRRAS, Tof-SIMS, SEM, EDX. Whatever the induction mode (electrochemical or photochemical), the amino groups of the surface could be used as a platform for attachment of different biomolecules.

The fourth chapter investigates an important point in the grafting of diazonium salts. An adsorption step takes place before the grafting (bonding) step when diazonium salts are attached to graphene or carbon nanotubes (CNTs). We investigate the possibility of an adsorption of the diazonium salts prior to grafting on metals. A corrosion study points to the absence of such an adsorption step on metals.

Chapter 1

Surface Coatings, a Review

Chapter 1 : Surface Coatings, a Review

I. Formation of organic films on different substrates

This thesis describes the covalent modification of various surfaces (carbon, metals) with organic layers, including surface patterning.

There are now quite a number of methods that permits bonding of an organic layer to a surface, even if the presence of a bond its not clearly demonstrated. This introduction gives a brief account of these methods. There are also many ways to deposit, without formation of a specific bond, an organic layer on a metal by spraying, roll coating …etc.

In the first part of the chapter, we describe the methods that permit to create these layers without any induction – these reactions can be regarded as purely chemical and involve surface groups of the substrates (activated or not) and the head group of the molecule intended to bind to those surfaces. Although these methods are simple, in most cases, they are limited to one surface type (i.e thiols on gold, phosphonic acids and silanes on hydroxylated surfaces) or suffer from weak interaction/bonding with the surface (i.e thiol, fatty acids). One of the important aspects of their chemistry is the formation of i) organized monolayers (thiols), ii) more or less organized layers (silanes, phosphonic acids, alkyl groups on silicon), and iii) possible further functionalization and patterning, etc. Hereafter, we will briefly and simply describe their chemistry, utility and stability.

The second part of this chapter describes the powerful, electrochemically based methods for attaching covalently different compound types, their characterization and their applications.

I. SAMs

A **self assembled monolayer** (**SAM**) is an organized layer of amphiphilic[1] molecules in which one end of the molecule, the “head group” shows a special affinity for a substrate and the ‘’tail’’, which contains a functional group at the terminal end. Different class of molecules can form SAMs[1]:

[1] **Amphiphile** (from the Greek αμφις, amphis: both and φιλία, philia: love, friendship) - term describing a chemical compound possessing both hydrophilic (*water-loving*) and lipophilic (*fat-loving*) properties.

I.1. Fatty Acids

These monolayers are formed from spontaneous adsorption of long-chain *n*-alkanoic acids ($C_nH_{2n+1}COOH$) on Al_2O_3[2-6], TiO_2[7], Ag(AgO)[8-10], stainless steel[11], CeO_2[12] nanoparticles, ZnO[13] nanowires , ITO[14].

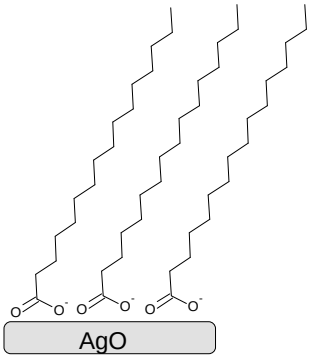


Figure. 1. Fatty acid SAM structure.

The reaction leading to the formation of the monolayer is an acid-base reaction between the carboxylate anion and a surface metal cation (Figure 1). This ionic bonding between the substrate and the SAM is reflected in their poor stability towards hydrolysis[6].

I.2. Silanes

For the formation of these monolayers, the substrate to be modified needs to be hydroxylated. The self-assembling molecules consist generally of three parts: the head group, the alkyl chain and the terminal end group[15].

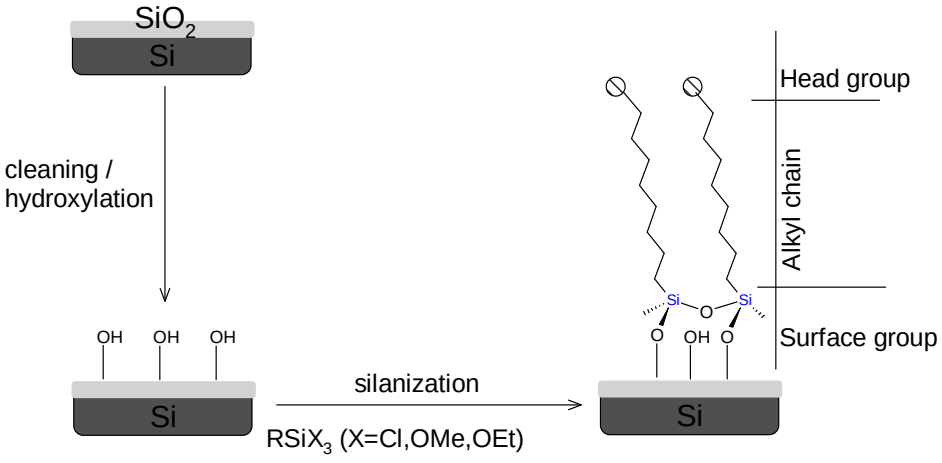


Figure. 2. Silane SAM obtention and the structure of the formed layer.

The head group, i.e., trichloro-, trimethoxy- or triethoxysilane, is responsible for the anchoring of the molecules onto the substrate. The alkyl chain provides the stability of the

monolayer, due to van der Waals interactions, and has a significant influence on the ordering of the SAM; the terminal end group introduces a chemical functionality into the monolayer system and can be further chemically modified to tailor surface properties in a controllable fashion[16-18]. The SAM in Figure 2 is a polysiloxane layer that is connected to the surface silanol groups via –Si-O-Si bonds.

A clean and hydroxylated thin oxide layer on a silicon surface is mandatory before the formation of the layer. Two methods are mainly used for this purpose:

- The Si wafer is cleaned by dipping it many times in a mixture of concentrated sulfuric acid and hydrogen peroxide, and then in an alkaline mixture of de-ionized water, ammonium hydroxide and hydrogen peroxide (to remove organic and inorganic contaminants as well as unwanted particules from the wafer). Afterwards, the SiO_2 layer is removed using dilute hydrofluoric acid and finally, pure native oxide is formed by treating the wafer in a bath of hydrochloric acid and hydrogen peroxide. This last step affords an hydroxylated surface. In the last step, the wafer is rinsed with de-ionized water and dried under nitrogen.
- The silicon wafer is submitted to the following successive steps: i) Sonication in chloroform to degrease and remove organic contamination; (ii) Photochemical precleaning by UV radiation in an oxygen atmosphere for 15 min to transform organic compounds (hydrocarbons and oils) into gases or watersoluble species such as fatty acids; (iii) Piranha cleaning for ~10 min, (immersion of the wafer into a freshly prepared mixture of sulfuric acid and hydrogen peroxide), (iv) thorough rinsing with DI water and (v) finally, further dry photochemical oxidation for~45 min to remove the last traces of contaminants.

To prepare the SAM, the clean hydroxylated Si wafer is dipped into a reaction bath containing the silane molecule $R(CH_2)_nSiX_3$ n(X = Cl, OCH_3 or OC_2H_5) dissolved in an alkane/carbon tetrachloride mixture.

On silicon-oxide surfaces, SAMs as above can be be formed directly using silane based precursor molecules[19] as above or by activating the substrate with $SiCl_4$ and $HNEt_2$, and further addition of hydroxyl functionalized molecules[20][21].

Silane SAMS can be formed on a variety of substrates such as silicon oxide [19][22-28], mica[34], glass[29-32], quartz[27][33], Al_2O_3[35-40], ZnSe[41][35], GeO_2[41], TiO_2[42-47], ZnO[48], ITO[22], ZrO_2[47],

GaN[49], poly-SiGe[50], BN[51] (cubic boron nitride) and nanoparticules: ZnO[52], Fe_3O_4[53][54], $EuLu_2O_3$[55], nanodiamond[56], SiO_2[57], (-OH)CNT[58-60], TiO_2[61], ZrO_2[62] (nanocrystal).

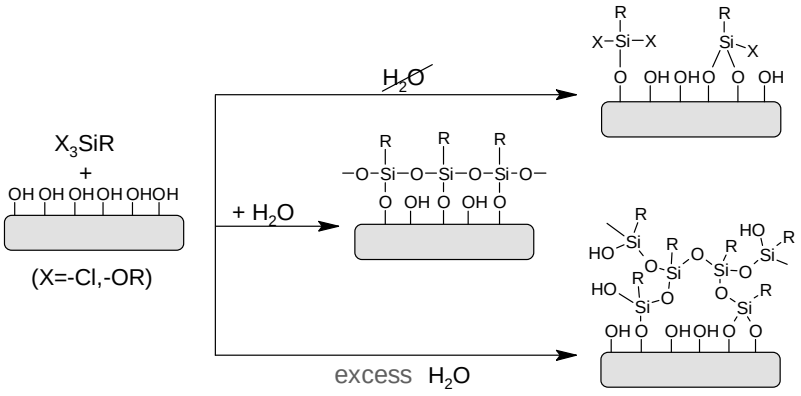


Figure. 3. Silane structure dependency on the amount of water in solution.

To obtain a good quality silane monolayer, one of the most important parameters is the water content of the reaction medium (Figure 3) – in the absence of water, the formed layer is incomplete[63]; with an exces of water, the silane polymerizes, leading to the formation of polysiloxanes, which in turn form islands of multilayer films[28]. The optimal water content is estimated to be 0.15 mg H_2O per 100 mL of solvent[29]. If the bonded silane has a terminal hydroxyl group (or a precursor of it through a chemical reaction), it can be further modified to form multilayers.

The silanes are used in different applications such as: forming patterned assembly of single-walled carbon nanomaterials onto oxide surfaces[22]; depositing controlled assembly of silane-based copolymers, which are resistant to piranha solution for several hours [64]; creating superhydrophobic layers on Al (using perfluorinatedchlorosilanes), lowering adhesion[38]; improving the corrosion protection of metals - and possible use as replacement for chromate in general in corrosion control and paint adhesion[65][66]-; micropaterning functionalized surfaces by photoreaction of the formed silane layer[67]; biosensing applications[16]; grafting surfaces with PEG (PolyEthyleneGlycol) through modification by aminopropylsilane to increase chemical stability[68]; linking biotin to ZnO nanoparticules[52]; preventing agglomeration of nanodiamond particules[56]; patterning proteins onto poly-SiGe via lithography[50]; functionalizing silica coated porous alumina membrane for advanced molecular separation[69]; for cell adhesion [42] and attachment [43] to Ti surface ,etc.

Monolayers are thermally very stable[70-73], depending on the molecule type, they withstand temperatures up to 350°C[74], they resist some mechanical wear[75][76], and chemical attack[77]. The chemical stability of these silane films has been tested by monitoring contact angles, ellipsometry or infrared spectroscopy upon repeated washing at room temperature, showing very little change of contact angle, film thickness and a slight shift of the metylene stretch to higher frequencies. But when such films were placed in boiling water the change in contact angle, thickness was significant due to the film hydrolysis[26].

I.3. Phosphonic acids

SAMs from phosphonic acids (Figure 4) can be formed on different substrates: Al[78-81], Ti[82-85], Fe[86], Si[87][88], ITO[89][90], Zn[91], Cr[92], Cu[92], GaN[93], HfO_2[94]. Diphosphonic acids can also form SAMs on: Zn[95][96], Si[97] , Ti[97], Fe[97].

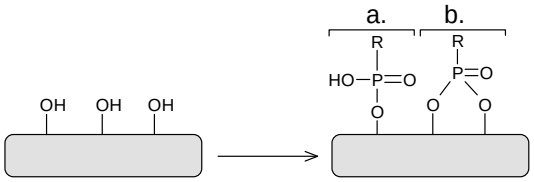


Figure. 4. SAM monolayers formation: a. monodentate or b. bidentate linkage with substrate.

These layers are used in corrosion protection[95], as biosensors[90], etc. They have good stability under acidic and neutral conditions, but a decreased stability under basic conditions[93][97], they are thermally stable up to 400°C[98].

I.4. Thiols

The most common protocol for thiol-SAMs preparation is the immersion of the clean substrate into a dilute (1-10 mM) ethanolic solution of thiols for 12-18h[99]. Dense surface coverage of thiol is obtained some minutes after immersion of the substrate into the solution, but the organization process requires time to achieve a maximal density and minimal defects. The quality and the formation rate of the resulting SAM is affected by different factors[99]:

- *Solvent* - ethanol is used most often due to its low toxicity, and good solubility. Other solvents can also be used: tetrahydrofuran, dimethylformamide, acetonitrile, which can give a SAM of the same quality[100][101] as that formed in ethanol. The rate of formation in other solvens such as heptane or hexane can be faster than in ethanol[102].

- *Temperature* – increasing the temperature of the solution improves the kinetics of formation and reduces the defects of the formed layer[103], the benefit of this increase can also be the desorption of adventitious materials possibly present on the surface.
- *Concentration and immersion time* – when the concentration of the thiol is low, the time of immersion is long. Typically, the formation time is 12-18h, but sometimes more time is required to obtain a better quality SAM.
- *Thiols purity* – the impurities presented in thiols, are in most cases, their oxidation products (disulfides), which up to a concentration <5% do not change the structure of the formed SAM[101].
- *Adsorbate or surface purity* – is one of the important factors, because any adventitious material present on the substrate decreases the quality of the formed SAM, or increases the formation time.
- *Oxygen concentration in solution* – degassing the solvent with an inert gas prior to the preparation of the thiol solution and maintaining an inert atmosphere in the course of the modification improves the reproducibility of SAM[101]. Oxygen content is significant when the substrate to be modified is different from gold, because it leads to surface oxidation of the substrate (ex. Pd, Ag, Cu, etc). Other benefit is that the reduced oxygen content is reflected in the stability of the dissolved thiol (in the presence of oxygen, some extent of the thiols is oxidized into a disulfide).

SAMS can be formed with a vast range of substrates: Au[104], Cu[104], Ge[105], Hg[106][107], Ni[108], Pt[109][110], Pd[101], Zn[111][112], GaAs[113], InP[114][115], ZnSe[116]; nanostructures (particules, clusters, rods) : Au [117-119], Pt[120], Ir[121], Pd[121], Cu[122], Ru[123], clusters of AuAg, AuCu and Au_xPd_{1-x} [122], CdTe[124][125], CdSe[126], CdS[127][128], FePt[129-131], HgTe[125], GaAs[113][132], PbS[133], PdAg[122], ZnS[134].

The terminal group of the SAM can be further modified and tailored [135][136], which broadens the scope of thiol chemistry, especially when accounting for the possibility of surface patterning to nm scale [137-139]. Thiol-SAMs are used in vast fields of academic applications[99][140]: protein immobilization and biosensing , corrosion inhibition, molecular junctions , sensors, etc.

The mechanism for the SAM formation from thiols is not well understood[1][99]; on gold, the mechanism is an oxidative addition of the S-H bond to the surface, followed by reductive elimination of hydrogen.

$$R\text{-}S\text{-}H + Au_n^0 \rightarrow R\text{-}S^-Au^+ {}^*Au_{n-1}^0 + \tfrac{1}{2}H_2$$

The SAM layer withstands temperatures to 200-220°C[141][142], and is electrochemically stable till -1 V ±0.25 V, depending on the SAM quality and type of thiol[143-145]. Under ambient conditions, the layer is not stable and degrades, due to reactions[146][147]:

$$2\ RS\text{–}Au \rightarrow RSSR + 2\ Au$$

This limited stability under ambient conditions has restricted their use to the academic field.

I.5. Alkyl Monolayers on Silicon

The formation of alkyl monolayers bonded to a Si-H surface was first achieved via an hydrosilylation reaction, providing a versatile pathway for formation a stable Si-C bond[148][149]. For the reaction to occur, the Si-H bond needs to be activated, this can be achieved thermally (heating to 120-200°C)[150], by UV[149] or by white light irradiation[151][152], by electrochemistry[153], by using Lewis acid-mediated initiators[153], Grignard reagents (Si-Cl surface)[153] (Figure 5).

The layer can be formed from 1-alkynes without external activation; under the same conditions 1-alkenes[154] show little or are hardly any reactivity - which emphasizes the superior reactivity of 1-alkynes. The density of adsorbed molecules from long alkyl chains to form a monolayer is about 1:2, with the remaining Si atoms being H-bound to silicium. An important feature of this method is the possibility to pattern[155][156] and to further chemically modify the layer[157]. These SAMS can be used in different applications[157][158]: chemical and biochemical sensing, electronics, etc.

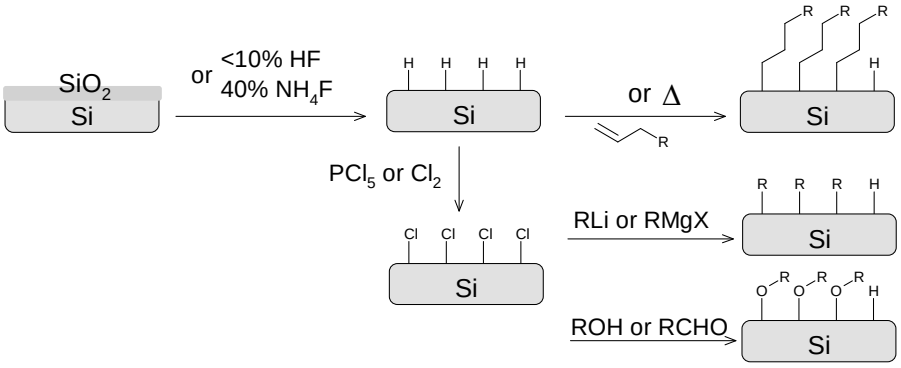


Figure. 5. Different reactions for the construction of monolayers on silicon.

The layer improves the lifetime of the surface in ambient atmosphere by several orders of magnitude, compared to a hydrogenated surface[159]. Monolayers formed from 1-alkynes

(containing Si-C- bonds) are more stable in aqueous HF and Na_2CO_3 solution compared to those formed from alcohols and aldehydes (both forming Si-O-C-)[160]. The alkyl monolayers formed from the reaction of 1-alkenes with SiH are thermally stable up to 340°C [161].

II. Formation of organic nano/micro layers through electrochemistry.

The formation of thin organic layers by electrochemistry can be achieved via reduction or oxidation. For the oxidation process, the substrate needs to withstand relatively high potentials and this puts a limit on the type of substrate that can be modified. For this reason, the reductive methods are more general.

II.1. Oxidation of amines

This electrografting process can be only done on a limited type of substrates, due to the high potential that is needed for grafting (often higher than +1.2 V vs. SCE), which imposes the use of noble substrates that withstand oxidation such as: carbon fibers[162][163], glassy carbon (GC)[164][165], carbon felt[166], pyrolized photoresist film[167], Au[165], Pt[165], ITO[168], carbon nanotubes, p-Si[169].

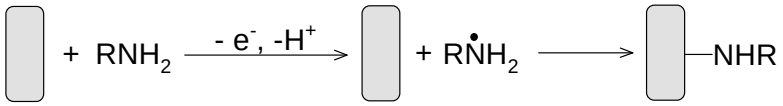


Figure. 6. Grafting of amine by oxidation.

The grafting mechanism proceeds via the one-electron oxidation of the amine group to the corresponding radical cation, which deprotonates to give a carbon radical and an aminyl radical. This radical reacts with the carbon surface, leading to the covalent attachment of the compound via an N-C linkage[165] (Figure 6). It is estimated that grafted diamines are bridged with both amino groups to the surface and only 25% of them are bonded with one amino group[162]; in order to overcome this issue, one can use N-protected amines i.e protected N-Boc-ethylenediamine (Boc : *tert*-butyloxycarbonyl)[170][171].

The efficiency of the modification depends on the type of amine intended to be grafted - while primary amines are efficient for this purpose, secondary amines are less reactive and tertiary ones do not react due to steric hindrance with surfaces[164]. Surface modification of some metals (Au, Pt, Cu, Fe) and GC with alkyl amines can be performed without electrochemical induction[172]; a mechanism has been proposed for this reaction. Different classes of amino

groups containg compounds can also be used in addition to aliphatic amines[162][164][165]: aromatic amines[173-175], amino acids[176-178]. In addition to organic anhydrous solvents (such as ethanol[164], DMF[179] or ACN[179]), the modification can also be done in aqueous solutions[164][166][173-175], ionic liquid media[168] or in pure amine (ethylendiamine[169][180][181]). The attachment of amine to surfaces through oxidation is usually achived at fairly elevated potentials. In the case of conjugated molecules combining both an amino and an organometallic moiety,[182] the amine moiety can be indirectly oxidized through an intra-molecular electron transfer from the ferrocenyl group to the amino moiety at +0.40 V.

The thickness of the formed layers range from monolayer (using protected N-Boc-ethylenediamine[170][171]), to nanometric[183] or micrometric thick layers[169]. The surface can be patterned using SECM (Scanning Electrochemical Microscopy)[184], the strategy involves the formation of an amine generated at the SECM tip by reduction of a nitro-containing compound and the derivatization of the substrate by oxidation of the electrogenerated amine after diffusion in the interelectrode space.

Electrochemical oxidation of amines permits the immobilization of dopamine[164], amine-terminated polyamidoamine dendrimers[185], gold nanoparticules[177], different redox systems[179], laccase[171], iridium and ruthenium complexes[186], Au@Fe_3O_4 nanoparticles[178], gold nanoparticules[187], nitrogen macrocycles[167], azacrown ethers[183]. The formation of linear polyethyleneimine coatings[188] is possible, it can be used for pH sensing by grafting pure ethylenediamine, charged with lithium trifluoromethanesulfonate[181][169], the grafted layer also permits anion exchange[163]. The suppression of protein adsorption [189], can be used to attach derivatives of 1,3-dihydroxybenzene[190]. Other applications involve: increasing the performance of a fuel cell in methanol oxidation[191], improving the toughness of carbon-epoxy composites[162], simultaneous determination of hydroquinone and catechol[192], simultaneous determination of uric acid and ascorbic acid[177][187], selective detection of neurotransmitter serotonin[176], determination of nitrite[178], sensor for phenol quantification[193], lead detection through a system based on cyclam-modified graphite felt electrode[194].

II.2. Oxidation of carboxylates

Since the oxidation of carboxylates is achieved -as the oxidation of amines -at relatively high potentials (E = 1.0 ± 0.15V[195][196]), this method is also limited to non oxidizable substrates such as GC[195][196], HOPG[195], carbon felts[197-199], PPF[200].

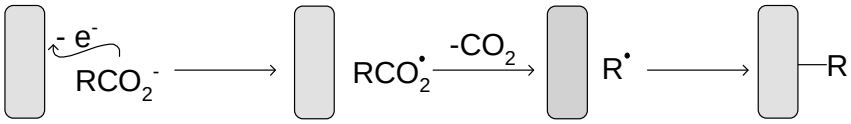


Figure. 7. Grafting of carboxylates onto carbon materials.

The grafting mechanism involves the formation of the radical through electrooxidation of the carboxylate ion, leading to the attachment of the radical to the surface (Figure 7).

Grafted molecules include substituated aryl[195-198] and alkyl acetates (using ferrocene derivatives as electron transfer mediators)[201][202]. The grafting medium usually consists of an organic solvent (ACN[195-197], DMF[203]) containing an inert electrolyte or an aqueous medium[198].

The stability of the layers has been examined. Based on redox probes, the grafted layers can be oxidatively removed in an acetonitrile + inert electrolyte solution by scanning the potential at a slightly more positive value than the grafting potential[195], although there is evidence that the measured film thickness does not change after positive cycling of film to potentials as high as +2V. The grafted film has a multilayer[200][202] structure.

Further reactions can be performed: a modified felt substrate can be used as a possible support for combinatorial chemistry[199], it shows electrocatalytic oxygen reduction properties[203], it can be used for anchoring bipyridine ligand complexes[204].

II.3. Oxidation of alcohols

Even more than the methods above, this reaction suffers from the fact that the substrate needs to withstand high potentials as the oxidation of alcohols is achieved at elevated potentials. Thus it can only be used to modifiy carbonaceous materials GC[205-211], graphite felt[212]. The modification is usually carried out in an aqueous solution using H_2SO_4[205][206] or $LiClO_4$[208][209] as supporting electrolyte, the latter one giving better results[209]. The reaction mechanism has not been clearly established (Figure 8).

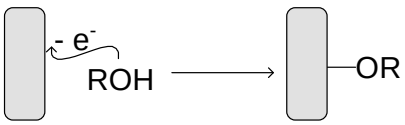


Figure. 8. Mechanism of alcohol oxidation on carbon material.

Applications involve: suppression of GC electrode fouling from non-specific adsorption of serum proteins[205]; attachment of phenanthroline alcohol ligand on which a catalyst (a ruthenium complex) is immobilized, which shows a good selectivity for the oxidation of primary alcohols to aldehydes[212]; anchoring of dendrimer-Pt(II) complexes ($G4OHPt_{EC}$) on GC, which shows electrocatalytic activity for oxygen reduction[213]; electrochemical detection of dopamine[206]; immobilization of TEMPO on the grafted layer at GC electrode[211]; immobilization of laccase [214].

II.4. Oxidation of Grignard reagents

Modification of different[215][216] silicon surfaces and other substrates like Ga-Cl with Grignard reagents is achieved either electrochemically by oxidation[2] on Si-H[217][218][219] or spontaneously (Si-H[220][221][222], Si-Cl[223][153][224], Ga-Cl[225], porous silicon[226][227]). The spontaneous[223] reactions are also possible using alkyl or aryl lithium reagents. The grafted molecules involve different Grignard derivatives (like alkyl[226], vinyl (and other unsaturated hydrocarbons moieties)[220], ethynyl [228][219], aryl[226][227]) or alkyl lithium[223] / aryl lithium[227] derivatives.

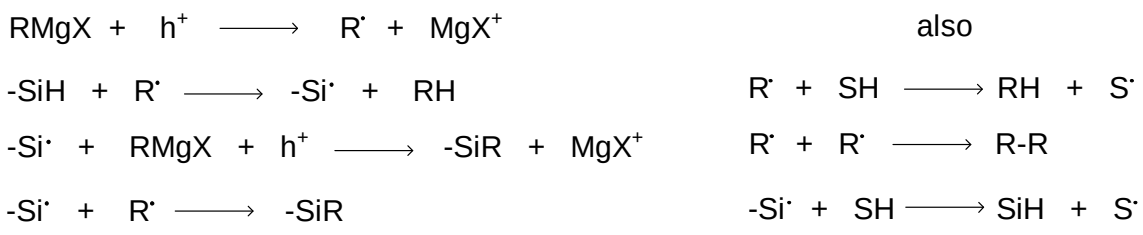


Figure. 9. Mechanism for grafting Grignard reagents onto hydrogenated silicium surface through oxidation (h= electron hole, SH=solvent).

The grafting mechanism is presented in Figure 9. The oxidation of the Grignard reagent provides a $R^{\bullet}$ radical, this radical abstracts an hydrogen from the surface to give a silyl radical. This formed silyl radical can react with an $R^{\bullet}$ radical to give Si-R the modified surface.

Concerning the spontaneous grafting mechanism of the aryl lithium reagent on porous silicon the reactions proceeds by addition to a Si-Si surface bond, resulting in a Si-aryl bond[227]. The anodic oxidation of CH_3MgI leads to a fully methylated[229] silicium surface (100%

[2] Note that Si is an easly oxidized material – the electrografting is performed in a glove box in the absence of water and oxygen.

substitution of hydrogen atoms by methyl groups in Si-H). The Si-Cl has been reacted with Na-C≡CH, giving a Si-C≡CH surface[230]. The thickness of the films can range from monolayer[231] to nanometer (few layers)[219][232] or micrometer films[233]. The electrochemical grafting of Grignard reagents is a more efficient for surface passivisation than the thermal one and provides more uniform films [234].

Si surfaces derivatized with longer alkyl chains are resistant to oxidation (formation of the oxide layer on these surfaces is slower than that on the unmodified surface) and the formed alkyl layer resists immersion for 15 min in boiling solvents (aerated chloroform and water)[223]; in air these modified surfaces resist oxidation for a period of ~50 h, much longer than SiH surfaces. The pulsed photoluminescence of Si surface, modified electrochemically with ethynyl groups, shows a higher intensity and a lower surface photovoltage than the unmodified ones. This is an indication of a low amount of defects at the interface (better passivation)[228]. The formed monolayer[235] can be further modified and functionalized, thus broadening the usage utility of these surfaces.

This is an interesting method, but it suffers from the need to operate in highly flammable solvents and in a dry box.

II.6. Grafting of diazonium salts

Surface modification using the reduction of diazonium salts is a very efficient and versatile means of grafting organic moieties to many substrates[236-238]. The electrochemical reduction of these salts at a glassy carbon electrode allows the attachment of organic moieties through the formation of the corresponding aryl radical[239][240]. This electrografting method involves a reduction and is applicable to many substrates: other carbon materials (nanotubes, particules, etc), coinage and precious metals, metal oxides, semiconductors and even polymers.

Substrates

- ***Carbon materials*** - glassy carbon[239-242], graphite[243-245], highly ordered pyrolytic graphite (HOPG)[246-250], graphene[251-257], pyrolized photo resists (PPF)[258-262], carbon felts[263][199], carbon blacks[241][264-267], carbon fibers[239][268][269], carbon nanotubes[270-275] or nanohorns[276][277], ordered mesoporous carbon[278-281], ultrananocrystalline diamond[282-285], boron-doped diamond (BDD)[286-290], diamond particles (nanoparticules) [291-294] and nanowires[295].

- ***Metals, oxides and semiconductors*** - Fe[296-305], Zn[298][302], Ni[303][306], Cu[298][302][307][308], Co[303][306], Cr[309], TaN/Ta[301], Zn, Ni[310], Au[298][311-316], gold nanoparticules: [317][318] Pd[319], Pt[320-325], indium tin oxide (ITO)[326-328], SnO_2[302], SiO_2[329]; Fe_3O_4 nanocrystals[330], different Si substrates[331-339], GaAs[319], Ge nanowires[340].
- ***Polymers*** - Teflon®[341], polyaniline (PANI)[342][343].

II.6.1. Electrochemistry of diazonium salts

The electrochemical grafting involves a one electron reduction of the diazonium cation to the aryl radical (this is accompanied with the loss of a nitrogen molecule) and the binding of this radical to the substrate (1), this formed radical can be also reduced into the anion (2).

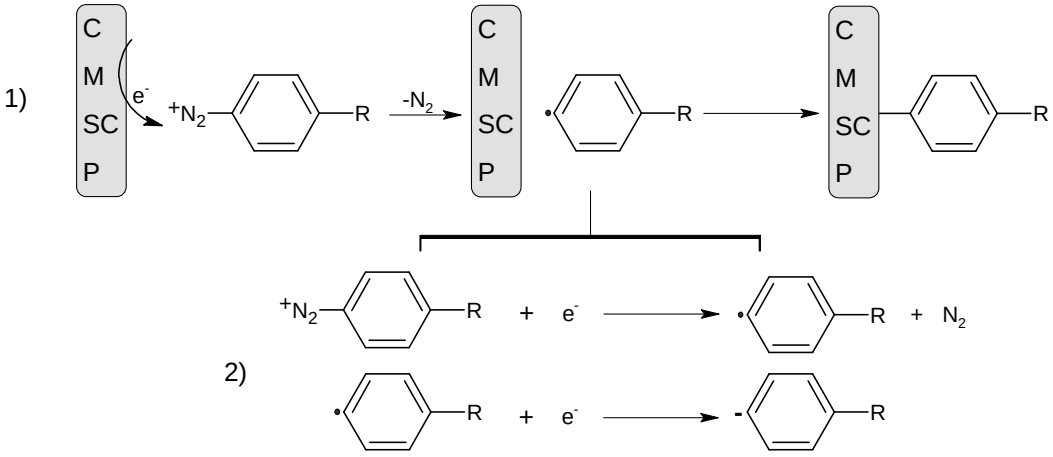


Figure. 10. 1) The mechanism of diazonium grafting to different substrates (C-carbon materials, M-metals, SC-semiconductors and P-polymers) and 2) formation of aryl anion from the reduction of the aryl radical.

The mechanism (Figure 10. 1) is shown to involve an electron transfer concerted with the cleavage of the C-N bond and the loss of dinitrogen molecule[344]. The reduction of the aryl radical to the corresponding anion takes place at more negative potentials (Figure 10. 2), this is sometime observed by a secondary small wave at $E_p = -0.64\,V/SCE$ during the cyclic voltammetry scan and corresponds to the reduction of residual aryl radicals that did not dimerize or undergo further reaction. The redox potential could be obtained from the simulation of the voltammogram $E^0_{Ar^{\cdot}/Ar^-} = +0.05V/SCE$. The reduction potential was also obtained by measuring the number of electrons consumed at different potential values during the reduction of other aryl radical sources finding a potential of $E^0_{Ar^{\cdot}/Ar^-} = -0.95V$. These values of the redox potential for $Ar^{\cdot}/Ar^-$ are quite different, this is certainly related with

experimental difficulties. The diazenyl radical •N=N-Ar can be observed (for example, by pulse radiolysis in strong acidic media), but it should not be an intermediate under normal grafting conditions at low potentials.

During the reductive electrografting around 0 V, when the potential is scanned toward negative values, an irreversible wave is obtained, which on the second or third scan, completely disappears; this decrease of the current is related to the formation of an organic layer, which blocks any further reduction reaction at the electrode surface. If the grafting is performed by chronoamperometry, the current drops very rapidly, it does not decrease along a Cotrell law -f($t^{-1/2}$)- as it should expected for a reduction reaction without coupled chemical reactions; this behavior is related to the blocking of the electrode surface during the grafting.

II.6.2. Stability of the layers

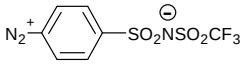
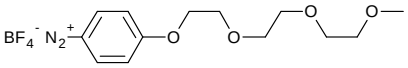
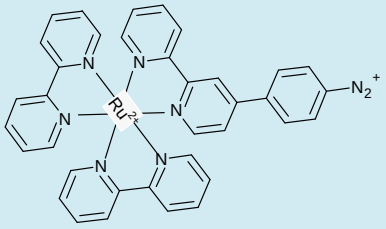
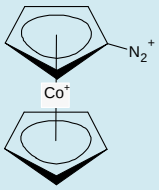
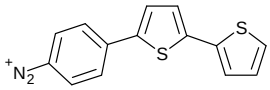
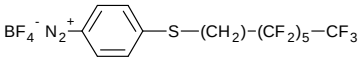
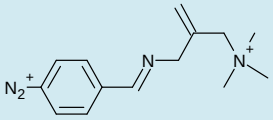
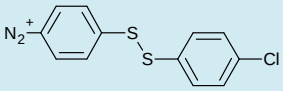
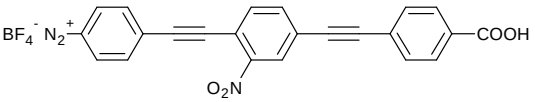
The layers formed during the grafting of diazonium salts are very stable, they resist prolonged ultrasonic cleaning (ACN, dimethylformamide, dimethyl sulfoxide, benzene, benzonitrile, acetone, methanol, ethanol, dichloromethane and chloroform for 15 min each), boiling in different solvents and a long time of exposure to ambient conditions[236]. The resistance of these layers in the case 4-bromophenyl groups grafted on Si is 2 min when treated with aggressive 40% solution of hydrofluoric acid and one min when treated with a 10 mol/L solution of ammonium fluoride[236]. In the case of SiH grafted with bromophenyl groups, the layers are stable in air 6 months and no loss of the Br signal is observed during this time[331]. The existence of the bond between the substrate and the organic layer has been calculated by the Density Functional Theory (DFT), this bonding energy is highest on silicon with the value of -292.6 kJ/mol, -171.4 kJ/mol on iron and -100.3 kJ/mol on gold[345].

II.6.3. Different diazonium salts

The grafted diazonium cations include a variety of substituents (methyl, *t*-butyl, ethyl, naphtyl, carbonyl, anthraquinonyl, carboxyl, cyano, fluoro, perfluoro chains, chloro, bromo, iodo, etc) but also large or complex molecules, some of which are presented in Table 1.

Usually the grafting reaction is performed using diazonium tetrafluoroborates in ACN + electrolyte[236] or it can be performed in acidic[296][346], neutral[347] or basic[348] aqueous media (in these last two cases, diazoates are the reactive species). Grafting can also be performed directly without isolation of diazonium salts through the '*in situ*' procedure starting from an aromatic amine and adding sodium nitrite at low pH in acidic medium[349][264] or by dissolving the amine in ACN and adding *t*-butylnitrite[350].

Table 1. Some interesting grafted diazonium salt structures and their uses.

 (during the reduction of the zwitterions, an electrolyte layer is formed [351])	 (creation, on GC, of an interface, which resists non specific adsorption of proteins[352])
 (covalent attachment of the ruthenium complexes to carbon nanotubes [353], the reduced form of the grafted complexes shows strong affinity toward CO_2 [354])	 (construction of organometallic electrodes, which have approximately a monolayer surface coverage [355] of redox species)
 (reversible tunable electrochemical switches having a diode-like behavior [356][357])	 (grafted layers show outstanding wear resistance with low contact resistance [358])
 (provides a monolayer of benzaldehyde after chemical acid cleavage step[359])	 (provides a monolayer of thiophenolate after electrochemical reductive cleavage step[360])
diazotized - P R O T E I N (reaction of amino groups from rabbit IgG proteins with 4-aminophenylacetic acid, ‘’*in situ*’’ diazotation of these amino groups and covalent attachment of the protein to the surface[243])	 (wiring enzymes to electrodes to achieve direct electron transfer to native glucose oxydase [361])

II.6.4. Different grafting methods

The reduction of diazonium salts can also be spontaneous on reducing metals[346][347][362], on glassy carbon[363], carbon nanotubes[273], graphene[251] , diamond[284], and carbon black, but also on silicon[364]. The spontaneous reduction of a particular diazonium salt on metals depends on the reducing power of the metal (it follows the order of open circuit potential) and the reduction potential of the salt; reduction is more efficient with more reducing metals and with more easily reducible diazonium salts[302]. Spontaneous grafting on copper is less efficient in acidic water than in acetonitrile[308]. During the spontaneous modification of gold

by 4-nitrobenzenediazonium (NBD) in 0.1 M H_2SO_4 at open-circuit potential, it has been proposed, rather surprisingly, that the grafting reaction involves electron transfer from gold to the NBD cation[346].

Spontaneous or electrochemical grafting in neutral and basic aqueous media involves a different grafting mechanism; in these media, the diazonium salts react with hydroxyl ions forming transient diazohydroxides, which are deprotonated to diazoates which in turn react with the surface[348]. In the case of GC, in organic media, spontaneous grafting only occurs with 4-nitrobenzenediazonium which is easily reducible and the grafting does not take place with diazoniums that are less reducible (diethyl, aminodiphenyl and triphenylaniline). The electrochemical grafting of diazoniums is possible in many ionic liquids; in such media, the grafting efficiency decreases with ionic liquid viscosity [365].

The grafting can be initiated by irradiating charge transfer complexes (including an electron donor such as dimethoxybenzene and a diazonium salt); with this method various polymers such as polypropylene, polyethylteraphtalate and also inorganic substrates such as SiO_2, TiN could be derivatized [366].

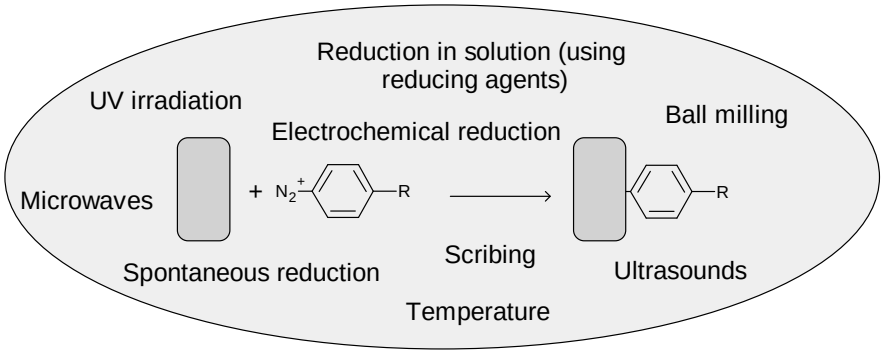


Figure. 11. Different means to initiate the diazonium grafting.

The formation of an organic layer, on different substrates, by reduction of diazonium cations can be achieved with hydrophosphorous acid as reducing agent; in this manner, graphite, carbon nanotubes and carbon powder have been derivatized[367]. Modification of CNT with diazonium salts can be assisted by microwave[368] (the modification of nanohorns can be achieved in solvent free process by using microwave irradiation[277]) or by thermal reaction[369]. Ultrasounds can be also used as a mean to perform grafting (diamond[370], ITO[328]). On SiO_2, the formation of an organic layer can be achieved by simply scribing it with a diamond in the presence of 4-nitrobenzenediazonium[371]. The GC spheres are modified

by an organic film through a ball milling reaction with diazonium salts (nitrophenyl, anthraquinonylbenzene diazonium).

II.6.5. Post grafting modification

Due to the impossible isolation of diazonium salts that contain an amino group attached directly to the phenyl ring (the amino group is a good nucleophile and thus reacts with the diazo group), the general methodology to obtain a grafted layer containing amino groups involves grafting the nitrobenzenediazonium salt and then reducing the grafted layer to amino groups (Figure 12); however the - NO_2 groups are not totally converted to $–NH_2$. It is interesting to note that this electrochemical transformation of $–NO_2$ to $-NH_2$ is substrate dependent - the rate of electron transfer for the conversion is lower on gold than on glassy carbon and the conversion by chronoamperometry (under the same conditions) is only complete on gold but not on glassy carbon[372].

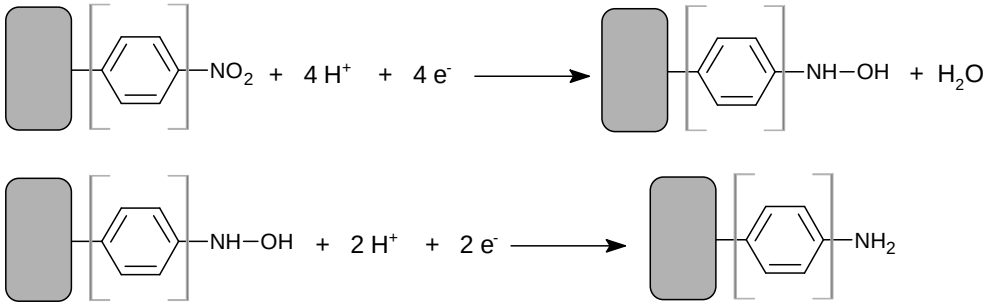


Figure. 12. The mechanism for the electrochemical reduction in acidic aqua media of the grafted layer containing - NO_2 group into $–NH_2$ group.

Another possibility to attach the aminophenyl group is the protection/deprotection approach - first the protected diazonium NHBoc-CH_2-C_6H_4-N_2^+ (Boc = *tert*-Butyloxycarbonyl) is grafted and then deprotected to give the $–NH_2$ group[373]. The elegant and simpler solution that avoids the deprotection step involves the use of diamines that are monodiazotized; this is usually done in an acidic solution by adding 1 equivalent of sodium nitrite to the amine[374][375], but this transformation is also possible in organic solvents using amine + 1 equivalent of isoamyl nitrite.

It is possible to graft simultaneously two different diazonium salts on GC by using mixtures of two diazoniums: 1) 4-nitrophenyldiazonium and 4-bromophenyl diazonium cations and 2) 4-bromophenyl diazonium and N,N-diethylaniline diazonium cations. The higher grafting efficiency is obtained with the substituted phenyl group for which the corresponding diazonium cation is the most easily reduced. Its surface proportion is higher than its

proportion in the deposition solution[376]. Grafting layers on top of each other is obtained by attaching a rather thick conductive polyphenylene layer to the substrate and then grafting 4-nitrobenzenediazonium or 4-bromophenyl diazonium on top of the first polymer layer. The deposition of copper is also possible on the polyphenylene layer[301].

The surface functionality of the grafted layer can be changed through electrochemical or chemical post transformation. The grafted layer of nitrophenyl groups can be transformed through electrochemical reduction into phenylhydroxylamine groups (-1.7 V/Ag wire in ACN). The transformation of a phenylcarboxylic layer chemically (1 M BH_3/THF) or electrochemically into a benzylalcohol layer is also possible[377]. The grafted layer of benzylchloride (*GC*-$C_6H_4CH_2$-Cl) on GC can be chemically modified with 4,4'-bipyridine at room temperature in an aqueous solution with a 5 day reaction time to give *GC*-$C_6H_4CH_2$-($^+$Py)-(Py), Cl^-. This surface can, in turn, be reacted with benzyl iodide to give: *GC*-$C_6H_4CH_2$-($^+$Py)-(Py$^+$)-CH_2-(Py), Cl^-, I^-.[378] The amino group of the GC grafted with 4-(2-aminoethyl)phenyl groups layer can be transformed into an urea function by reaction with p-substituted phenylisocyanates (ONC-PhX; X = NO_2, COPh, Cl, H, and NMe_2); this is done by immersing the grafted layer containing the amino group in a 20 mM solution of isocyante in toluene for several hours[379]. Nucleophilic reactions using thiolates as nucleophiles can be performed on grafted carbon felt functionalized with a benzyl chloride layer using an extended reaction time (t = 108 h) and elevated temperatures in order to increase the reaction yields[199]. Grafting covalently protected amino group BocNHCH$_2$C$_6$H$_4$, removing the Boc group (a, Figure 13) and reacting with anthraquinonecarboxylic acid (as redox model) (b, Figure 13), gives a layer with bonded anthraquinone groups[380].

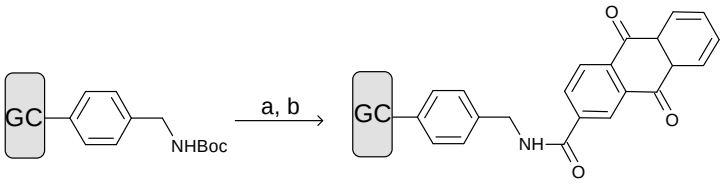


Figure. 13. Attachment of anthraquinone to a carbon surface through a protection-deprotection method.

The reduction of a grafted nitrophenyl layer to an aminophenyl layer and the attachment of EDTA molecule to the –NH_2 groups in the presence of a coupling agent is also possible to obtain a complexing layer[381].

The grafted surface can be used for anchoring nanobjects like fullerenes[382], nanotubes[383-387] and nanoparticules[388-391].

II.6.6. Monolayer vs. multilayer

During the grafting, depending on the experimental conditions and on the molecule to be grafted, layers can vary from nanometer to micrometer thickness[301][305] – i.e. ranging from monolayers[333][359][392][393] to multilayers-[248].

The mechanism for the electrochemical attachment of aryl groups to carbon or metallic surfaces has been assigned to the reaction of an aryl radical, produced concertedly with the electron transfer to the diazonium salt, and further reaction of this radical with the carbon surface (***R1*** + ***R2*** in Figure 14). The transfer of a second electron to another diazonium salt leads to the formation of dinitrogen and a new radical, which would attack the first grafted nitrophenyl group to give a cyclohexadienyl radical along reaction ***R3***. In order for the layer to grow, this radical must be reoxidized - this can be achieved by electron exchange with another nitrophenyl diazonium cation along reaction ***R4***. Due to high reactivity of the diazonium salts, multilayered films are formed even during spontaneous modification of gold in acidic media[346].

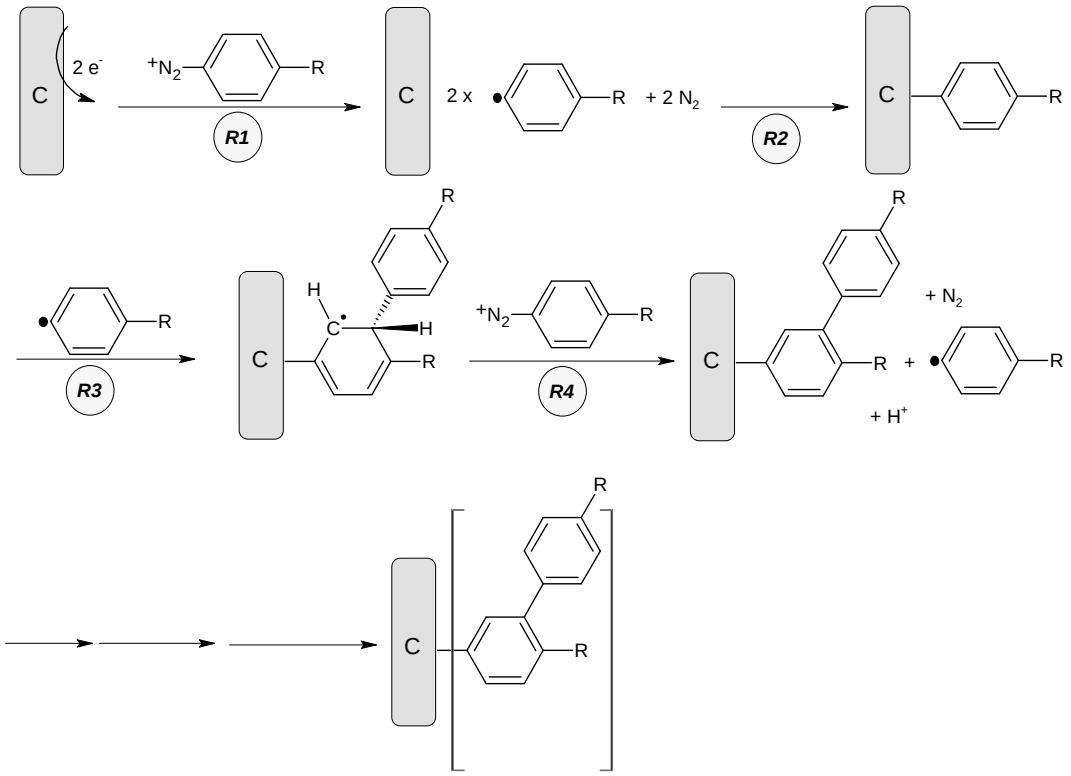


Figure. 14. The mechanism for the formation of multilayer during the grafting of diazoniums.

The formation of monolayer films can be achieved by precisely controlling the cycling conditions in cyclic voltammetry; on PPF, this is done by a single scan from -0.4 to -0.6V/ vs.

Ag^+/Ag (scan rate = 200 mV/s) in a 1 mM concentration of biphenyl and 4-nitrobiphenyldiazonium salt in acetonitrile; conversely upon repetitive scans, the formation of poly 4-nitrophenylene multilayers is achieved[258]. By monitoring the charge Q and by proper choice of the potential during the grafting of Si-H with bromophenyl and bromobenzyl diazonium, it is possible to obtain dense and ordered monolayers[333].

By using the diazonium salt of diaryl disulfides during the grafting, a multilayer of diaryl disulfide is obtained, which is reductively cleaved to a monolayer of thiophenolate (the thickness of the layers, measured by AFM, is 3±1 and 1.5±0.5 nm respectively before or after the cleaving step) (Figure 15 A)[360] . This same ‘’formation/degradation‘‘ approach has been applied to hydrazones in which the first step is the grafting of a long-chain of bulky alkyl hydrazone to minimize multilayer formation and the second step is the deprotection of this group by acidic hydrolysis to give a monolayer of phenylcarboxaldehyde groups ($\Gamma=4x10^{-10}$ mol/cm^2) (Figure 15 B)[359] .

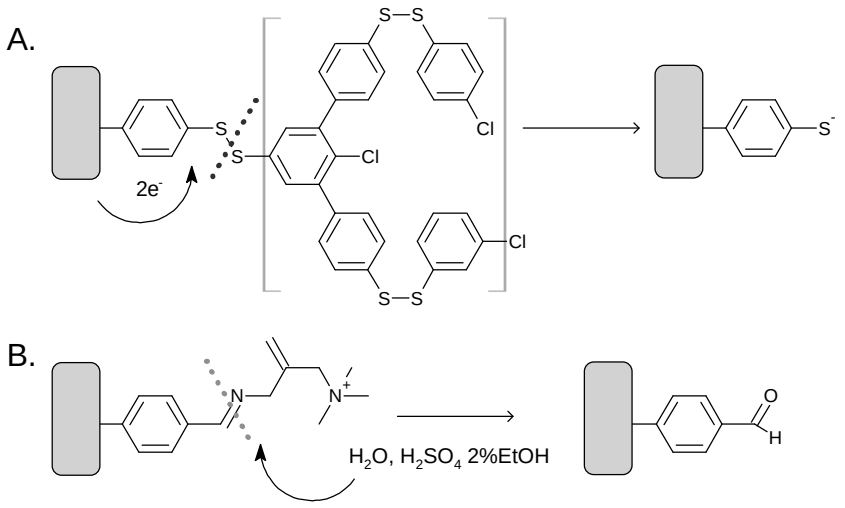


Figure. 15. Grafting a monolayer using the ‘’formation/degradation’’ approach : A) using the formation of a multilayer of diaryl disulfides and its reductive cleavage to a monolayer of nucleophilic thiophenolate [360] and B) using a grafted long chain alkyl hydrazone and its cleavage in acidic media to a monolayer of benzaldehyde[359].

Elegant control to form a monolayer is the use of steric effects during the grafting of diazoniums, by properly choosing the molecules structure: no grafting is observed with 2-ethyl or 2,6-dimethylbenzenediazonium tertrafluoroborate, a monolayer is obtained with 3,5-*t*-butyl benzenediazonium and multilayers are produced with 2-, 3-methyl, 2-methoxy, 3,5-dimethyl, 4-*t*-butylbenzenediazonium cations)[394].

Grafting of 4-nitrobenzenediazoniumtetrafluoroborate in an ionic liquid (1-ethyl-3-methylimidazolium bis(trifluoromethylsulfonyl)imid) on GC, points to the formation of monolayer although this conclusion is based only on the measurements of surface concentration, which is not really reliable in this case[395].

II.6.7. Patterning using the reduction of diazoniums

Nanoscale patterning of PPF (≈2µm wide patterns) is performed by grafting the entire surface, removing the grafted film with an AFM tip and second grafting of the scratched zone with another diazonium salt; this permits to incorporate different chemical functionalities in the pattern[396]. Patterning of different types of substrates (Au, Cu, Si, PPF) is also done by micro contact printing using poly(dimethylsiloxane) stamps inked with aqueous acidic solutions of aryldiazonium (aminophenyl or carboxyphenyl diazonium) salts; this permits to obtain ≈20µm wide patters[397][398]. Local doping of semiconductors can be used to form 1µm patterns on the dopped zone[399].

Grafted domains of ≈ 50 μm^2 on ITO are obtained by using polystyrene beads [326]. Auto organized arrays of polystyrene beads are used to mask the surface of gold; then, nanoscale patterns of an organic layer are grafted on the unmasked area. After grafting, the patterns are revealed by the removal of the polystyrene beads – forming an imprint of aryl layers with holes on which copper can be deposited or different organic layers can be grafted[400].

A localized (≈40 µm wide) grafted pattern is obtained through the electrochemical conversion of a nitrobenzene derivative (c=1 mM, in solution containing an equivalent amount of sodium nitrite) using an SECM tip (positioned 6 µm from the gold substrate, under potentiostatic conditions, -0.4 V for 5 s). The electrochemical conversion gives an aniline derivative, which is diazotized and then grafted to a gold substrate (polarized at -0.1 V). Nitrobenzene is reduced to an amine at the SECM tip; as aniline diffuses to the substrate, it is diazotized in the tip-to-substrate gap and attaches to the substrate[401]. Using SECM in a three-electrode configuration, by positioning a Pt microelectrode (serving as a microanode) above the gold substrate (polarized at -0.5 V) in a solution containing 5 mM 4-azidobenzenediazonium + 0.1 M NBu_4BF_4, it is possible to obtain localized grafted spots whose size can be tuned by choosing the tip diameter and the tip-gold plate distance. With a grafting time of 10 ms and by using a 50 µm diameter tip, the size of the grafted spot depends on the tip-substrate distance: 500 µm grafted spots are obtained when the electrode is positioned ≈3 µm above the substrate

and much smaller spot when the electrode is positioned at ≈1.5 µm. Reducing the tip diameter leads to smaller grafted spots[402].

II.6.8. Techniques for the characterization of the grafted layers

The characterization of the formed layers is achieved using a vast number of different techniques: cyclic voltammetry, EIS (Electrochemical Impedance Spectroscopy), infrared spectroscopy (IRRAS -InfraRed Reflexion Absorbtion Spectroscopy-, PMIRRAS -Polarization Modulation IRRAS-), SEM (Scanning Electron Microscopy), AFM (Atomic force Microscopy), XPS (X-ray Photoelectron Spectroscopy), EDS (Energy Dispersion Spectroscopy), Tof-SIMS (Time of Flight Secondary Ion Mass Spectroscopy), Rutherford Backscattering, EQCM (Electrochemical Quartz Crystal Microbalance) etc. Some of interesting informations about the grafted layer will be included for each technique:

Cyclic voltammetry is used to perform grafting, to analyze the surface and to calculate the concentration of the grafted group if the latter has redox propreties (as explained below, this method should be used whith great care)[298], and to analyze the blocking behavior of the layer. When the electrode is modified electrochemically with a diazonium salt containing a redox group (nitrophenyl, anthraquinonyl), the reduction potential of this group, in the layer, does not change very much from one substrate to another and is similar to that of the parent compound (nitrobenzene, anthraquinone) in the same solution[298]. For example, in the case of layers containing nitro groups, the presence of this group is observed by scanning the modified electrode at negative potential and considering a reduction peak related to the transformation of the nitro group into amino and/or hydroxylamino groups in aqueous acidic solution. The presence of grafted anthraquinone groups on the modified SWNTs is observed by depositing the modified SWCNTs on an electrode and performing voltammetric scans from 0.2 to −0.5 V vs. SCE (in a buffer solution of pH=1). After some scans, two peaks are observed in the 0/ -0.3 V vs. SCE range. They correspond to the transformation of the quinonyl into an hydroquinolyl group, thus demonstrating electrochemically the attachment of the anthraquinone molecule to the SWCNTs[403].

The reduction of diazoniums on gold sometimes give rise to multi peaks; this is related to the gold multicristalline structure of the gold electrode. The reduction on Au(111) facets gives a single narrow reduction peak, but when the reduction is performed on Au(100) facets, two reduction peaks are observed. On a polycrystalline electrode, during the cyclic voltammetry,

each observed sub peak corresponds to the reduction of the molecule on a distinct crystallographic site[313].

The indirect evaluation of the grafting and the evidence of an organic layer on the electrode surface are achieved simply by cyclic voltammetry using redox probes (a redox couple in solution, such as ferrocene/ferricinium or ferro/ferricyanide). This probe presents a fast reversible behavior on a clean unmodified electrode, but on a modified electrode, the voltammogram corresponds to a much slower electron transfer or even completely disappears. The observed blocking behavior of the electrode is strongly influenced by a number of factors among which the choosen redox probe (charged or not) and the compacity of the layers (for example, an aminophenyl layer is more compact than a nitrophenyl layer).

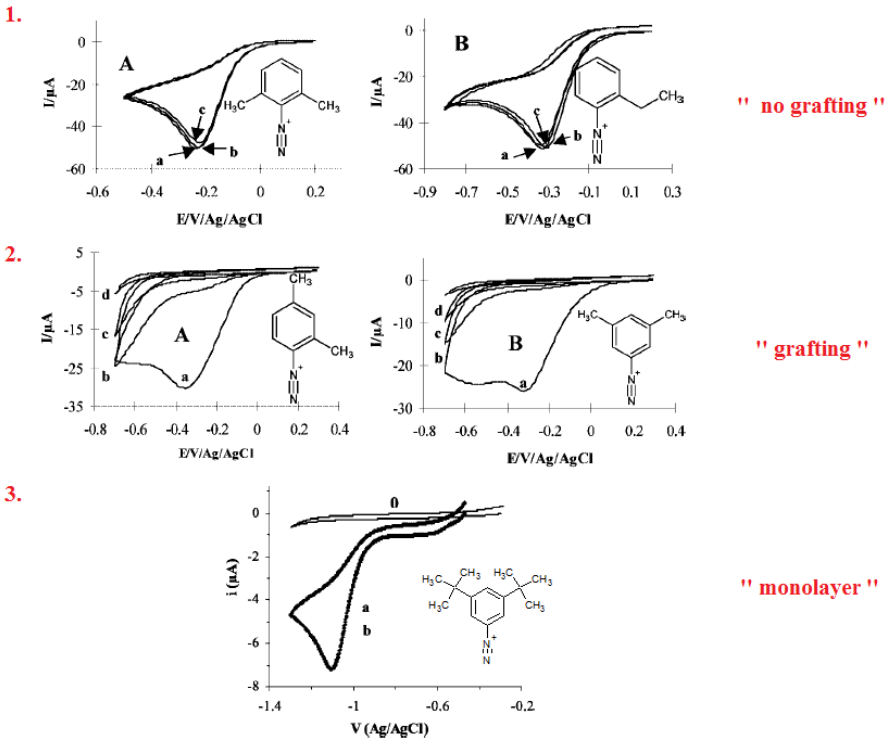


Figure. 16. Influence of the steric effects on the voltammetric behavior during the grafting of 4 mM substituted diazoniums salts in ACN + 0.1M NBu_4BF_4, Reference Ag/AgCl, 1,2) 2 mm glassy carbon electrode, scan rate 0.1 V s^{-1}. 3) 1 mm copper electrode, scan rate 50 mV s^{-1}. 1) (A) 2,6-dimethylbenzene diazonium, (a) first, (b) second, and (c) tenth scan, and (B) 2-ethylbenzenediazonium, (a) first, (b) second, and (c) fourth scan. 2) (A) 2,4- and (B) 3,5-dimethylbenzene diazonium, (a) first, (b) second, (c) third, and (d) fourth scan.[394] 3) 3,5-bis-*tert*-butylbenzenediazonium (a) first scan; (b) second scan; (0) blank[392].

The grafting efficiency on diamond depends strongly on its surface terminal groups, by cyclic voltammetry, during the attachment of 4-nitrobenzenediazonium tetrafluoroborate on the –H and –OH terminated diamond, the cathodic peak is located at the same potential in both cases, but the obtained current is 3 times higher on –H than –OH terminated diamond,

reflecting better grafting efficiency on the first one, on –O terminated diamond the reduction peak shifts toward more negative potential with a significantly smaller currents indicating a lesser grafting efficiency[404].

When grafting the 3,5-di-*t*-benzenediazonium tetrafluoroborate (Figure 16. 3), the current decreases slowly. In this case, the first grafted layer contains bulky steric groups that prevent further attack of 3,5-bis-*t*-butylphenyl radicals on this layer. As a consequence, a monolayer is obtained[392]. Conversely, during the grafting of 2,6-dimethyl or 2-ethyl benzenediazonium cations (Figure 16. 1), the successive scans are identical to the first one, indicating that, upon reduction, these diazoniums do not graft to the surface[394]. In the case of other diazonium salts with various substituents on different positions (2-, 3-methyl, 2-methoxy, 3,5- dimethyl, 4-*t*-butyl), the cyclic voltammograms are those usually observed during grafting (Figure 16. 2), the first reduction wave its observed and on second or third scan, the surface is blocked and the peak disappears[394].

The electrochemical stability of the films can also be evaluated by using redox probes. For a grafted electrode, the signal of the redox probe in solution may disappear. If the signal reappears by scanning at very negative or positive potentials, this indicates that the film has been removed. For example, this reappearance of the redox probe signal is observed when the potential reaches negative ca. -2 V vs. SCE or positive +1.8 V vs. SCE values - this means that the film is stable from +1.8 to -2 V vs. SCE [405].

Infrared and Raman spectroscopy permits to assess the presence of organic layers on reflective substrates. They can be used to ascertain the presence of a specific functional groups or its transformation in the grafted layer[379]. For example, the FTIR spectrum of CNTs modified with anthraquinone groups, measured using KBr pellet technique in the 1000- 2300 cm^{-1} region, shows the peaks related to 1695 cm^{-1} C=O stretching mode (of the quinonyl group) and 2926, 2858 cm^{-1} (C-H stretch)[403]. Some features for this technique are shown in Table 2.

A gold wafer modified with 4-nitrobenzenediazonium and analyzed by IRRAS contains a significant amount of physisorbed material (the products formed, in solution, upon reduction of the diazonium salt). The decreased intensity of $–NO_2$ stretch of the grafted plate upon sonication in ACN indicates the presence of only 35 % of the final grafted material, the remaining products being only deposited/adsorbed in/on the film[314] . Spontaneous grafting of

metals by simply dipping them in a diazonium salt solution can be observed through the increase of the peaks intensity with the immersion time (Figure 17)[302].

The bulk Raman spectra of grafted groups are very similar to those of the parent molecule. However, when a monolayer of azobenzene is grafted on GC, the vibration band at 1240-1280cm^{-1}, which is not observed in the parent molecule, corresponds to the covalent –C-C- bond between the GC and the layer. It is possible to observe by Raman spectroscopy the rotation of the grafted nitroazobenzene (NAB) group at the graphite edge plane about the C-C bond of the NAB/carbon interface by observing the depolarization ratios[407]. In the case of the spontaneous modification of the graphene layers with the 4-nitrobenzenediazonium cation, it is possible to demonstrate, using confocal Raman spectroscopy, that diazonium ions preferably bind to single layer graphene and only weakly to bi-layered areas. This shows different reactivities of the single and bi-layer graphene. In addition, grafting on graphene is a two-step mechanism, the first step being the adsorption of the diazonium cation onto graphene (see Chapter 4)[251].

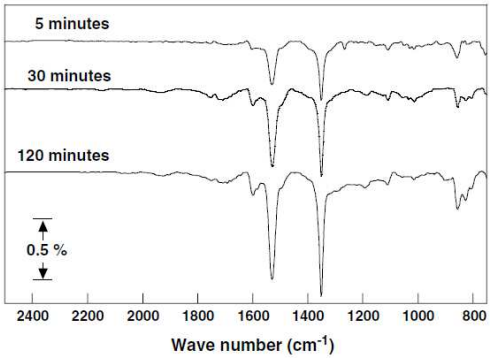
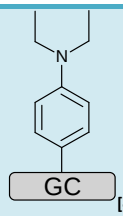
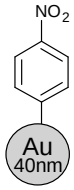
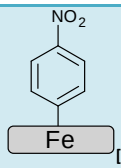
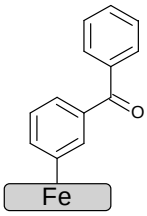
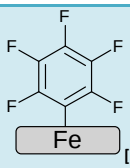
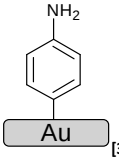


Figure. 17. Influence of immersion time on FT-IRRAS reflection spectra of nitrophenyl modified Zn surfaces. Modification of zinc surfaces consists in dipping the substrate in 10 mM 4-nitrobenzenediazonium tetrafluoroborate solution in ACN for 5, 30 and 120 min[302].

The orientation of molecules on PPF can be determined by Raman spectroscopy, using the selection rules for molecules on a surface. Only the components of the dipoles parralel to the vector of the polarized light are excited and give rise to adsorption. The average tilt angle with respect to the surface normal of 4-nitroazobenzene is 31.0 ± 4.5° and 44.2 ± 5.4° for fluorene, azobenzene, biphenyl, nitrobiphenyl (these layers are in upright orientation) [408].

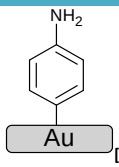
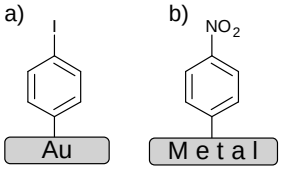
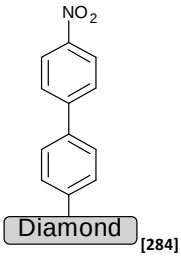
Table. 2. IRRAS (A), (B) PMIRRAS and (C) Raman spectroscopy characterization of grafted layers

Grafted molecule structure	Assigned to:
 [406] **(A)**	***3016 cm^{-1}*** aromatic C-H stretching ***2930-2850 cm^{-1}*** aliphatic C-H stretching ***1590 cm^{-1}*** aromatic C=C stretching ***1480-1500 cm^{-1}*** ring breathing ***1245 cm^{-1}*** phenyl-N stretching
 [318] **(C)**	***1589 cm^{-1}*** ring breathing ***1344 cm^{-1}*** symmetric NO_2 stretching ***1110 cm^{-1}*** C-N stretch + ring stretching ***1080(w) cm^{-1}*** CH in-plane bending ***852 cm^{-1}*** ONO scissor + ring stretching ***412 cm^{-1}*** Au-C stretch
 [296] **(B)**	***1600 cm^{-1}*** ring breathing ***1522 cm^{-1}*** NO_2 asymmetric stretching ***1350 cm^{-1}*** NO_2 symmetric stretching
 [296] **(B)**	***1658 cm^{-1}*** carbonyl group ***1311 cm^{-1}*** aromatic in-plane CH vibrations ***1278 cm^{-1}*** aromatic in-plane CH vibrations ***805 cm^{-1}*** CH out-of-plane
 [297] **(A)**	***1670 cm^{-1}*** C=C stretching ***1410 cm^{-1}*** C=C stretching ***1050 cm^{-1}*** CF stretching
 [374] **(A)** **‘’ in situ ‘’**	***3440 cm^{-1}*** (w) NH bond stretching ***1617 cm^{-1}*** deformation of N-H in NH_2 ***1515 cm^{-1}*** ring breathing ***1273 cm^{-1}*** aromatic C-N stretching ***908 cm^{-1}*** aromatic C-H out-of- plane

XPS (X-ray photoelectron spectroscopy) gives information about the surface concentration of the elements and about the thickness of the film. Some features of the use of this technique are shown on Table 3.

The grafted layers of azobenzene and 4-nitroazobenzene groups on GC give the expected N1s signal for a monolayer coverage. This surface coverage Γ is calculated by integration of the nitrogen peaks areas and by comparison with the C1s peak, $\Gamma = 1.4 \times 10^{-10}$ mol/cm^2.[407] The angle-resolved XPS C1s spectra of a grafted layer of 4-carboxyphenyl groups evidence a carbide type bond corresponding to the bonding between Fe and an organic layer, pointing to the covalent nature of this interface bonding [299]. In the case of grafted films on copper or Cu_2O, the observed XPS peaks indicate the presence of Cu-O-C and a Cu-C covalent bonding between the aryl ring and the substrate, and a high multilayer coverage containing different percentages of azo groups[308].

Table. 3. XPS energy peaks of different garted diazonium molecules

Grafted molecule structure	Assignments (eV)
 [374]	• 399.4 eV N1s organic nitrogen • 400.1 eV N1s azo bridges • 285.5 eV C1s carbon attached to amino groups • 284.4 eV and 284.9eV C1s carbon of aromatic rings
 [298]	• 622-633 eV I3d iodine doublet (a) • 406 eV N1s in NO_2 (b)
 [284]	• 399.9 eV N1s, nitrogen in N-H • 406.1 eV N1s, nitrogen in N-O • 531.7 eV O1s, oxygen in O-N • 286.9 eV C1s, carbon in C-O, C=O • 286.0 eV C1s, carbon in C-C

AFM (Atomic Force Microscopy) – permits to visualize surfaces and to measure the film thicknesses on a nanometric scale.

The thicknesses of the films can be measured by AFM on very flat surfaces such as PPF by scratching the layer with an AFM tip without carving the hard PPF surface and measuring, with another tip, the depth of the depression. A double AFM cantilever can also be used; then, the thickness between the scratched and pristine areas can be measured during the scratching.

A precise potential cycling can be used to control the formation of a monolayer, that can be controled by AFM scratching and by analyzing the height of these scratched areas with respect to the non-scratched ones (Figure 18)[258].

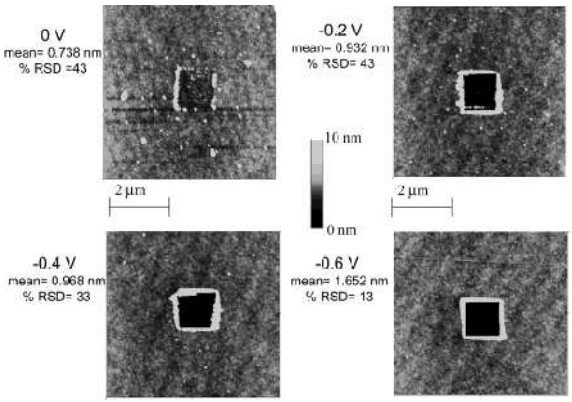


Figure. 18. Tapping mode images for a biphenyl-modified PPF surface following a contact mode scratch. Single derivatization scans from +0.4 to 0, -0.2, -0.4, and -0.6 V vs Ag/Ag+ were used to modify the PPF surface, as indicated[258].

Using this approach during the grafting of 4-nitrobenzene or 4'-nitroazobenzene-4-benzenediazonium, it was shown that the film increases with the modification time. It is also evidenced that the films formed on PPF during grafting in acetonitrile have a higher limiting thickness than those in aqueous media (collapsed films). This thickness increases with the deposition time to a limiting value but also depends on the structure of the diazonium salt: thicker films are obtained for 4-nitrobenzene than for 4'-nitroazobenzene-4-benzenediazonium[409].

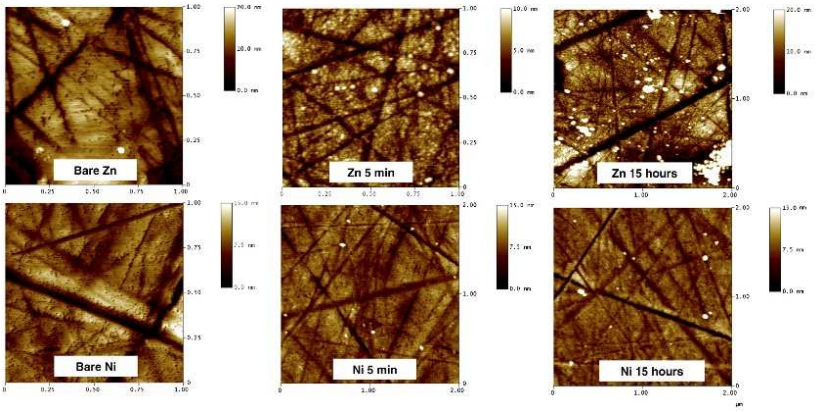


Figure. 19. AFM images of: bare zinc, bare nickel, and Zn and Ni surfaces modified with diethylaminobenzenediazonium by immersion of the sample for 5 min and 15 h in 10 mM 4-nitrobenzenediazonium tetrafluoroborate solution in ACN [302].

During the spontaneous grafting of metals by simply dipping them into a solution of diazonium salt + acetonitrile, AFM permits to show that grafting is more efficient when the metal is more reductive and also that the layer grows with the dipping time (Figure 19)[302].

SEM, TEM *(Scanning Electron Microscopy, Transmission Electron Microscopy)* are used to observe, measure or obtain chemical information on the grafted layer.

The surface morphology of graphite flakes can be observed after grafting 4-nitrobenzenediazoniuma and further transforming the grafted nitrophenyl groups to aminophenyl groups and then to aryldiazonium groups (using *tert*-butylnitrite). Finally, the covalent attachment of silicon powder onto the modified graphene flakes (Figure 20) can also be observed by SEM, and the silicon particle coverage is calculated by EDX ($2.6x10^{10}$ particles/cm^2)[245].

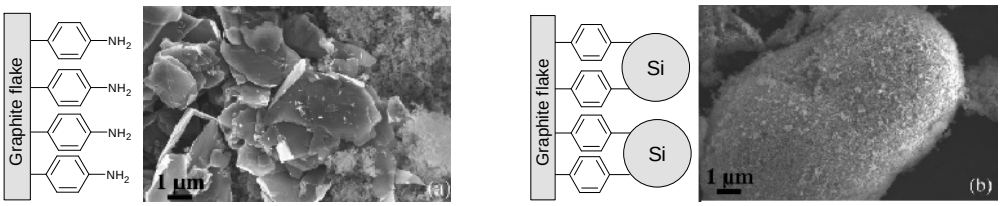


Figure. 20. SEM image of the modified graphite flake a) with 4-aminophenyl groups and b) subsequent transformation of $-NH_2$ group into diazo group followed by the covalent attachment of Si particles[245].

When the oxide powder, $Li_{1.1}V_3O_8$, is modified with the 4-nitrobenzenediazonium cation (by chronopotentiometry), the increase of the layer size is visible on TEM images. Its thickness changes with the modification time (Figure 21), th=1.5 nm (and formation of nodules) for t=10 min and th=2 nm (homogeneous layer covering all the powder nanograins) for t=60 min [410].

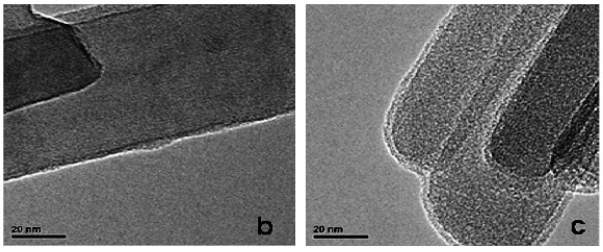


Figure. 21. TEM image of the modified oxide powder $Li_{1.1}V_3O_8$ with 4-nitrobenzene layer b) t=10min and c) t=60min [410].

During the grafting of HOPG, as observed by STM, the aryl layer formation is initiated at cleavage steps and later the film nucleation occurs on the basal plane at sites, which are likely

atomic scale defects (Figure 22). The film continues to grow both in 2- and 3-dimension through the radical binding on the entire surface[248].

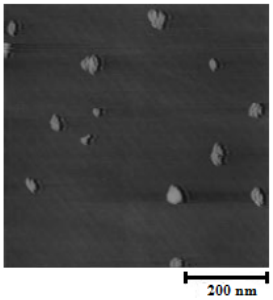


Figure. 22. Constant-current STM image (650 x 650 nm^2) of a HOPG substrate collected in air following 2 deposition cycles in 0.5 mM 4-diazo-*N*, *N*-diethylaniline fluoroborate. Bias voltage) 100 mV; tunneling current) 100 pA[248].

Observation of STM images of SiH grafted with bromophenyl under controlled charge conditions, shows the formation of an organized monolayer made of bromophenyl groups on the SiH surface. The modified layer derives from that of SiH by a (1√3)R30 transformation and the surface concentration is measured as Γ=6.7x10^{-10}mol cm^{-2} [333].

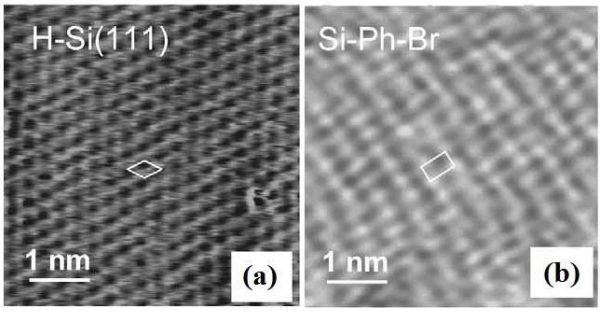


Figure. 23. STM 5nm x 5nm image of: a) SiH (111) surface and b) the same surface modified by bromphenyl groups[333].

ToF-SIMS (Time of flight Secondary Ion Mass Spectroscopy). The mass peaks corresponding to fragments of the layer or fragments obtained both from the layer and the substrate permit to characterize both the layer and its bonding to the surface. In the case of a layer obtained on GC by grafting 4-perfluorohexylphenyldiazonium tetrafluoroborate, the layer contains polymeric mass fragments [CH_2-CH_2-$C_6H_3C_6F_{13}$-$C_6H_4C_6F_{13}$]$^+$ corresponding to the polymeric chain and to the carbon substrate. In the same way, the films of 4-bromophenyl groups contain [C_6H_3-C_6H_4Br]$^+$ fragments, those of 4-carboxyphenyl groups contain fragments such as [$OCCH_2CH_2C_6H_4COOH$]$^-$, [$C_{20}H_{13}O_5$]$^-$. Such observations strongly evidence for the formation of multilayer films. The grafting efficiency is higher on

electrochemically modified plates than on spontaneously grafted ones; this can be assessed by analyzing and comparing the intensity of the mass fragments[411].

EQCM (Electrochemical Quartz Crystal Micro Balance). This mass sensitive technique can analyze simply the mass variation during the grafting reaction. When grafting very passivating diazonium salts, the effect of the surface passivisation is observed directly during the first potential scan in which nearly all the mass variation is observed; during the further scan cycles, no mass variation is observed. This is not the case with the 4-nitrobenzenediazonium salt: the largest mass effect is observed during the first scan but the mass increase is still observable during successive scans[313].

Thermogravimetric analysis (TGA). The thermal stability of functionalized carbon nanotubes (CNTs) is assessed by monitoring the mass loss during a temperature increase (from 100 – 1000 °C under inert atmosphere) by comparison with the unmodified ones. The native CNTs present a mass loss when the temperature reaches >100°C (caused by the desorption of water molecules); this loss is less significant for the modified CNTs. When rising the temperature to 175-700°C, the modified CNTs show a mass loss, which is very small compared to a non modified one; this mass loss is more pronounced at 165-225°C and continues up to 700°C [403]. From TGA data, the 24 % mass loss of microwave modified carbon nanohorns [using NH_2-C_6H_5-$O(CH_2)_6$-NH-Boc + isoamylnitrite)] corresponds to the presence of one grafted functional group for every 54 carbon atoms[277] .

II.6.9. Applications of diazonium salts grafting reactions.

Layers modified by reduction of diazonium salts are used for bonding polymers[412], biomacromolecules and nanoparticules[237][238]. In this way, diazonium salts can be considered as ***coupling agents.***

When iron is grafted with different diazonium salts, the grafting layer prevents the oxidation of iron -it ***inhibits corrosion-***. Iron grafted with different diazonium salts was tested in 0.01 M H_2SO_4 at open circuit potential. The film shows anticorrosive effects with an inhibition efficiency of 73% (in the case of grafted carboxyphenyl groups) with a slight increase to 85 % when the grafted layer is further derivatized with octyltriethoxysilane. When the grafted metal is left in the corrosion medium in the presence of the dissolved diazonium the inhibition efficiency increases up to 97 % [347]. No corrosion could be observed when the iron surface grafted with phenylcarboxylate functions is further modified with a thick polymeric film through attachment of poly(1,2-propanediyl fumarate)[412]. Modifying the surface of iron with

a layer of -C_6H_4-CH_3 permits to observe an inhibition efficiency against corrosion, which decreases from 78.1% to 53.6% after respectively 1.5 and 4.0 h of immersion in a solution of oxygenated 0.5 M NaCl [413].

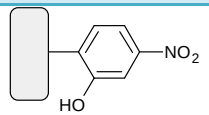
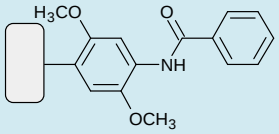
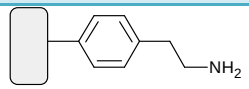
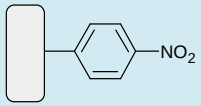
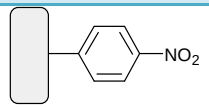
Grafing is also used to construct ***catalytic surfaces*** for oxidation (H_2O_2[414], methanol[415]) or for reduction (nitrate[414] , dihydrogen[416], oxygen [417]).

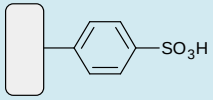
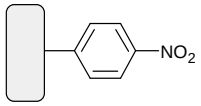
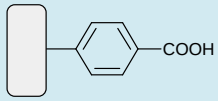
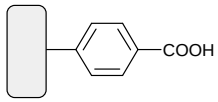
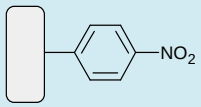
It is also applied in ***nanoelectronics***[418] – to build different devices such as molecular junctions[419], transistors[420], negative differential resistances[421], etc. In ***optoelectronic*** applications, grafting involves the attachment of conjugated molecules to the substrate to obtain increased photocurrents [422][423]. In ***batteries*** (Li-ion), grafting is used to stabilize and improve batteries performances[244][245][410]. In the ***fuel cell and hydrogen*** technology, grafting is performed on catalyst supports or catalysts to improve the final catalytic electrode performances[424-426].

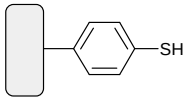
Modifying nanomaterials with diazonium salts increases their ***solubility*** and their dispersion in different solvents (the solubility can be tuned by attaching a chosen specific diazonium) [273]. It also allows to separate metallic nanotubes from semiconductive ones [427].

Different molecules or biomolecules can be covalently attached to surfaces opening vast possibilities for the construction of different ***sensors***[428] (Table 4). The sensing layer can be the grafted aryl layer itself[429-434] or a platform constructed from diazonium salts and reacted with linkers and then sensing groups[435-439] .

Table. 4. Some sensors constructed by diazonium grafting.

Grafted layer of diazonium and grafted material	Used for	Limits of detection, performance	Ref.
 Carbon screen printed electrode.	determination of ascorbic acid in fruit and vegetable juices	Detection of ascorbic acid from 2-20 µM, detection limit 0.86 µM, stable for 5 months with measurement taken every week (loss of only 16 % of its initial response during the whole period)	[429]
 Carbon-fiber microelectrode.	measuring real-time physiological pH changes in biological microenvironments	pH-dependent anodic peak potential response, sensitivity to acidic and basic changes detectable to 0.005 pH units. Used to measure dynamic *in vivo* pH changes occuring during neurotransmitter release in the central nervous system of the microanalytical model organism for Drosophila melanogaster.	[430]
 The grafted $-NH_2$ layer on GC serves as a binder for amino-modified probe DNA.	label-free electrochemical impedance spectroscopy method for sequence-specific detection of DNA	the sensor response increases linearly with the logarithm of concentration of target DNA in the range $2\times10^{-12} \div 2\times10^{-6}$ M. The limit is equivalent to the detection of circa 4×10^{7} copies of DNA in a 7 µL droplet or circa 5.7×10^{12} DNA copies in one litre of sample.	[431]
 Screenprinted carbon electrode is grafted with NBD, the $-NO_2$ is transformed electrochemically into $-NH_2$, followed by cross linking to the horseradish peroxidase (HRP) by using glutaraldehyde.	determination of H_2O_2	the HRP-modified electrode displays electrocatalytic activity towards the reduction of hydrogen peroxide (H_2O_2), without any mediator. H_2O_2 is determined in a linear range from 5.0 mM to 50.0 mM, with a detection limit of 1.0 mM.	[435]
 Screenprinted gold electrode is grafted with NBD, the $-NO_2$ is transformed electrochemically in $-NH_2$, followed by immobilizing the tyrosinase enzyme by using glutaraldehyde.	total phenolic content in tea	catechol displays the highest sensitivity (36.3 mA M^{-1}) and the lowest limit of detection (0.1 µmolL^{-1}). The biosensor is successfully applied to the detection of polyphenols in tea samples.	[436]

 Carbon fiber microelectrode.	determination of dopamine	increased sensitivity to dopamine and other positively charged analytes that is due to increased adsorption of analyte in the grafted layer. When this electrode is used in mouse brain slices, based on the signal to-noise ratios, a detection limit of 30 nM dopamine is calculated. This is a detection limit lower, by a factor of 5, than that of a bare non modified electrode.	[432]
 Screenprinted carbon electrode is grafted with NBD , the -NO_2 is transformed electrochemically into -NH_2, followed by covalent immobilization of enzymes, monoamine oxidase (MAO) /horseradish peroxidase (HRP) and diamine oxidase (DAO) /horseradish peroxidase (HRP)], by using hydroxysuccinimide and carbodiimide.	determination of biogenic amines	linear response range from 0.2 up to 1.6 µM and from 0.4 to 2.4 µM of histamine is obtained for DAO/HRP and MAO/HRP based biosensors, respectively. The biosensor construction is highly reproducible, yielding relative standard deviations for the sensivity of 10% and 11% for DAO/HRP and MAO/HRP based biosensors.	[437]
 Carbon-based screen-printed electrode.	determination of Cu(II)	detection of the Cu(II) as low as $5x10^{-9}$ to $1x10^{-8}$ M is achieved by immersing the grafted electrode in the solution of the analyte for 10 min followed by electrochemical measurement of the accumulated copper. In natural water measurements ther is no major interference of Pb(II) in the determination of Cu(II).	[433]
 Carbon-based screen-printed electrode.	determination of U(IV)	detection of the U(IV) with a detection limit $7x10^{-10}$ and $2x10^{-9}$ M (depending on accumulation time) is achieved by immersing the grafted electrode in the solution of the analyte followed by electrochemical measurement. No interference from Zn(II), Cd(II), Pb(II) and Cu(II) during the measurements.	[434]
 GC is grafted with NBD, the -NO_2 is transformed electrochemically into -NH_2 followed by covalent immobilization of *N*-(2-aminoethyl)-4,4'-bipyridine	determination of Ag(I)	detection is done electrochemically by preconcentrating the Ag(I) ions on the modified electrode due to their chemical interaction with bipyridine at -0.6 V, followed by oxidation of these ions at +0.34 V. The electrode reponse is linear in the range 0.05 µM to 1 µM Ag(I) with a detection limit of 0.025 µM and RSD = 3.6%.	[438]

by using glutaraldehyde.			
 GC electrode is grafted with a mercaptophenyl film on which firstly gold nanoparticules and secondly, a DNA layer is self-assembled.	detection of target DNA	a platform for the recognition of complementary single-stranded DNA with a detection limit of $7.2x10^{-11}$ M, showing a good selectivity, stability and regeneration ability for DNA detection.	[439]

II.7. Reduction of alkyl halides

The surfaces grafted by reduction of alkyl halides include hydrogenated Si[440], metals (Fe, Cu, Au)[441][442], TiN[441], GC[441-444], HOPG[443].

The reduction of alkyl bromides or iodides in dry deoxygenated ACN (typically 0.2 - 0.4 M alkyl halide + 0.2 M $LiBF_4$, ≈1.5min) on SiH, leads to the grafting of alkyl groups as revealed by IR spectroscopy. During this process, the peak intensity of the SiH bond (2120cm^{-1}) decreases with time, due to the grafting that replaces SiH bonds by Si-C bonds.

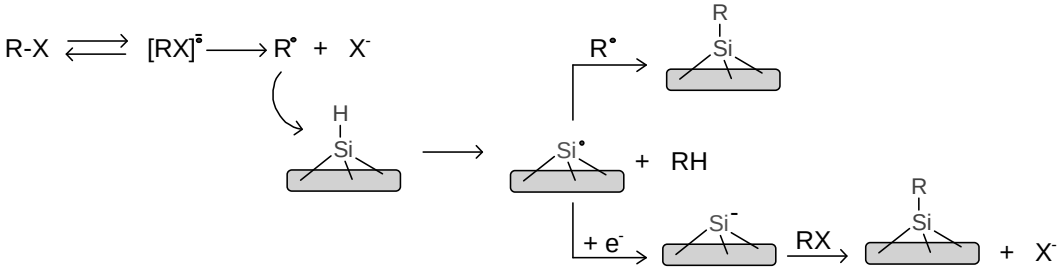


Figure. 24. Grafting mechanism of the reduction of alkyl halides on Si-H.

The grafting mechanism proceeds by abstraction of the hydrogen atom from the surface Si-H bond by the alkyl radical ($R^{\bullet}$) and formation of the $Si^{\bullet}$ radical that further couples with $R^{\bullet}$ or is reduced to Si^{-}, which reacts by nucleophilic attack with RX [440].

Multilayered films (≈ 6.54 nm thick) are obtained in the case of the electrochemical reduction of IC_6H_{13} and $ICH_2CH_2C_8F_{17}$ on Cu; their structure is assessed by Tof-SIMS and IRRAS spectroscopy - the grafted layer contains fragments of the alkyl chain and also Cu-organic fragments that confirm the grafting. During their grafting by cyclic voltammetry, a blocking behavior is observed: the current decreases steadily upon repetitive potential scans (Figure 25) [441].

Reduction of bromo- or iodo- acetonitriles leads to the cyanomethyl radical, that grafts to metal surfaces. The radical is reduced into the cyanomethyl anion at the potential where it is produced and it also attacks the first grafted cyanomethyl radical. This leads to a polymeric layer (Figure 25), which is thicker on copper than on gold; its thickness is on copper ≈ 6.8 nm, corresponding to ≈ 17 repeating units. A $-CH_2CH(NH_2)$ structure is proposed for the film[442].

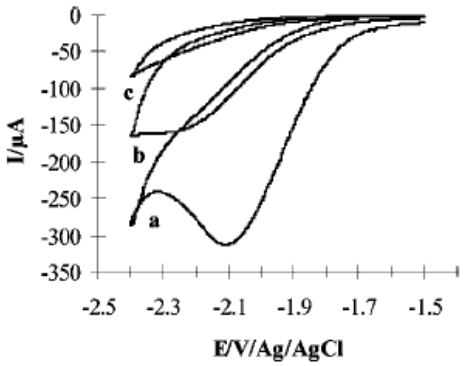


Figure. 25. Cyclic voltametry on a GC electrode (*d* =3 mm) in ACN+ 0.1 M NBu_4BF_4 of $I(CH_2)_2C_8F_{17}$ (*c* =10 mM), (a) first; (b) second and (c) third scans. Reference Ag/AgCl, v= 0.1 V s^{-1} [441].

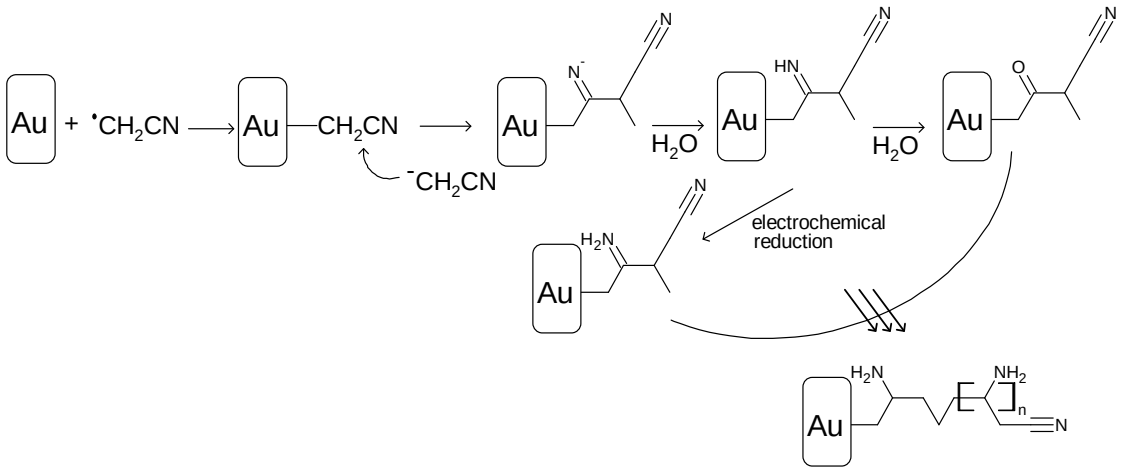


Figure. 26. Mechanism for the formation of an organic layer by electrografting of $^{\bullet}CH_2CN$[442].

On HOPG and GC, organic films are formed during the reduction of benzylbromide and 4-nitrobenzylbromide; the thickness of the layers increases with the deposition time and they can be observed by AFM and SEM [443].

II.8. Reduction of vinylics

Cathodic electrografting of vinylic polymers requires strictly anhydrous conditions and an organic aprotic solvent. The experiments are performed in a glove box (in solvents like ACN or DMF) using a large concentration of a vinylic monomer (ranging from 0.1 to 0.5 M) and high negative potentials (usually more negative than -2.5 V vs.SCE)[237][445][446]. By using specially designed monomers (vinylic monomers containing an ammonium group) grafting is possible in an aqueous solution[447]. The electrografted substrates include different materials

(Ni, Fe, Au, Cu, Pt, stainless steel, C, carbon nanotubes, Si, CdSe, Si_3N_4 and Teflon®)[237][445][446].

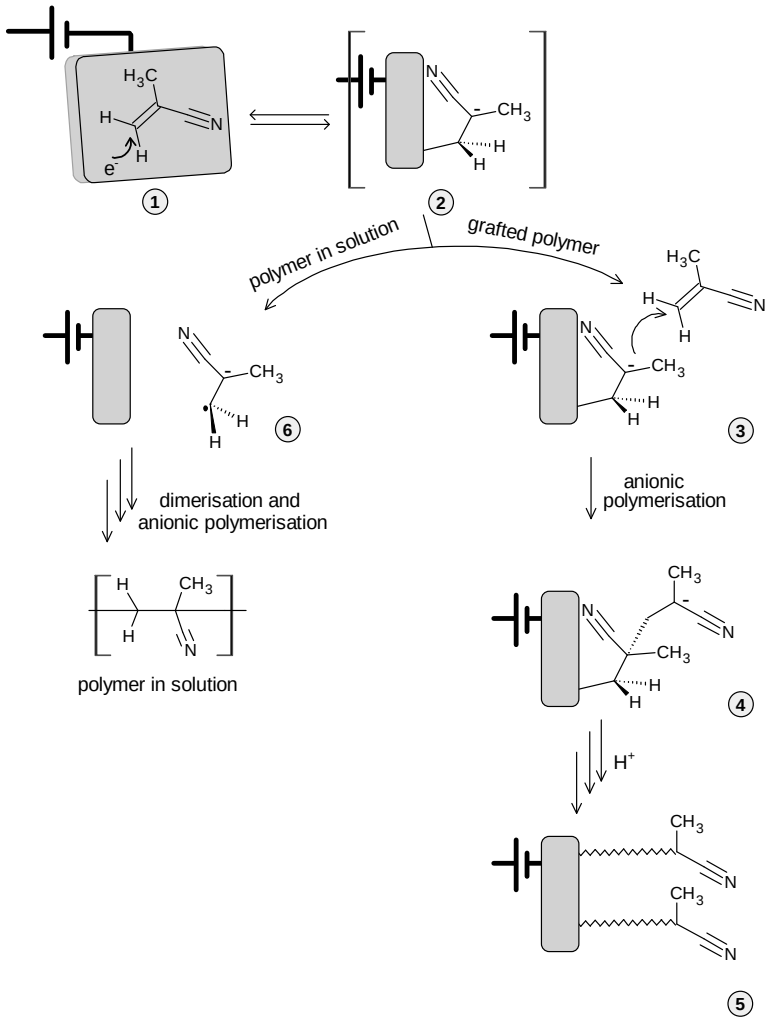


Figure. 27. Mechanism for the cathodic electrografting of the vinylics (i.e methacrylonitrile).

The mechanism for the electrochemical reduction of vinylics proceeds by adsorption of the vinylic monomer (1); then, by an electron transfer from the electrode to an adsorbed vinylic (2) leads to a radical anion that binds to the surface, forming a bonded anion. This bonded anion is not stable because the negative charge is repelled by the negatively charged cathode, but it can be stabilized by attacking a new monomer (3) to form a bonded dimer anion (4) whose negative charge is located far from the electrode. The layer continues to grow owning to an anionic mechanism. A second route is possible, in which the transient bonded anion (2) can be desorbed from the electrode and can polymerize in solution with the same

polymerization mechanism. The mechanism is electrochemical only in its initiation step, the further growth of the layer being a chemical reaction[237][446].

In the grafted layers of N-succinimidyl acrylate, the grafting density is 1 chain per 100 nm^2, the chains are separated by 10 nm with a 80 to 130 nm chain length (corresponding to a polymerization degree of 620 to 1016 monomer units, depending on the monomer concentration, 0.1 M or 1 M)[448] .

The anhydrous conditions and the use of the glove box to perform electrografting are overcome by the SEEP process (Surface Electroinitiated Emulsion Polymerization), which provides covalently grafted polymer films on conducting or semiconducting surfaces by radical polymerization in aqueous dispersed media. It relies on a cathodic electroinitiation, in which diazonium salts are used both to initiate the polymerization of the vinylic monomers in solution and to form a primer of grafted polyphenylene-like layer on the surface[449][450]. In the GraftFast© process, instead of electrochemistry, the radicals are formed by a reducing reagent in solution (iron, ascorbic acid, hypophosphorous acid). It is thus possible to graft insulating surfaces (oxides, polymers) as well as conductive or semiconductive ones[451] .

Direct localized (in the micrometric range) grafting of vinylics in aqueous solution (0.25 M H_2SO_4, NBD c = $2 \cdot 10^{-3}$ M and acrylic acid (AA) in concentration range from 0.5 to 7 M) is achieved by SECM in the direct mode, where the substrate is used as the cathode and an ultamicroelectrode as the anodic counter electrode. The control of the width and the thickness of the grafted spot can be adjusted by the time spent over the spot. For the same tip-sample distance, the radius of the formed spot depends on the tip diameter, increasing the tip diameter from 12.5 to 25 and 50 µm gives pattern with increased diameters increasing from 60 to 100 and 150 ± 10 µm. Coupling SECM with lithographic software enables drawing elegant grafted patterns on the substrate (Figure 28) [452].

A grafted layer of 4-vinylpyridine is able to complex rapidly copper ions from polluted wastewaters[453]. A nanocomposite material is formed by deposition of nanotubes modified with perfluoro chains on a gold surface electrografted by a layer of poly(acrylonitrile). It is used as an electrical contact lubricant under high vacuum conditions[454].

Local functionalization of surfaces (10 µm wide lines) with polymers using SEEP or GraftFast© processes is performed by lifting off a patterned mask (ink or SAM) previously drawn or stamped on the surface. The first simple method consist in handwriting a pattern

using water insoluble ink, grafting and then lifting-off by dissolving the ink (acetone or ethanol). The second method consists in stamping the substrate with a PDMS stamp immerged into alcoholic thiol solution, grafting the free surface, lifting-off the thiol layer using sonication in DMF or electrochemical reduction of the Au-S bond in an organic electrolyte[455].

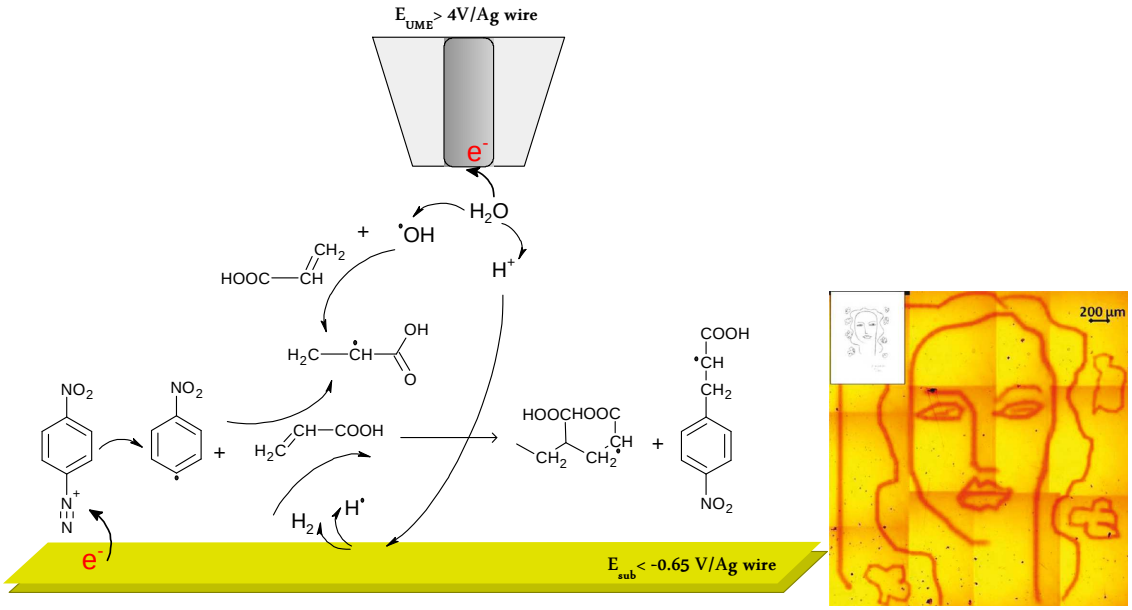


Figure. 28. ***Left:*** **Schematic view of the different electrochemical and chemical reactions occurring on the substrate, at the tip, and in the tip/substrate gap.** ***Right:*** **Reproduction of the "Madeleine" painted by Henri Matisse (inset) printed on the gold substrate by coupling SECM with Elecdraw software. (Conditions: [Acrylic Acid] = 2.0 mol L^{-1}, [DNB] = $2 \cdot 10^{-3}$ mol L^{-1}, [H_2SO_4] = 0.25 mol L^{-1})[452].**

Antibacterial films are obtained, for example, on stainless steel, by reduction of special monomers or inimers (polymer that further permits the initiation of an ATRP-Atom Transfer Radical Polymerization-). The antibacterial activity is obtained either by i) imbedding silver atoms in the film of poly(ethylacrylate) during its formation[456] or ii) by creating hyperbranched films with a large number of pyridinium groups (by attachment of a vinylic monomer with a chlorine atom followed by ATRP with a bromovinylic monomer and finally formation of pyridiniums by substitution of the bromines by pyridine)[457], or iii) by multilayer assembly of negatively (hyaluronic acid) and positively (chitosan) charged polyelectrolyte assembled on a negatively charged polyacrylate modified surface[458].

Grafted brushes on semi(conductive) surfaces are obtained by a two-step process, that consist in electrografting poly(*N*-succinimidyl acrylate) chains and further transforming these brushes by reaction with isopropylamine. In this way, a thermoreponsive layer of poly(N-

isopropylacrylamide) is obtained, as assessed by AFM; this coating in water at 20°C has a thickness of 80 ± 10 nm (swollen state) with a water drop contact angle of 33° (hydrophilic surface, T = 25°C). After raising the temperature to 42°C, the thickness decreases to 9±3 nm (collapsed state) and the water contact angle increases to 90° (hydrophobic surface, T=40°C)[459].

III. UV photochemical modification of surfaces

Using light for surface modifications offers many advantages. First, it produces directly the desired surface transformation without any contact to the surface, it applies to conductive as well as insulating surfaces, it requires a photon as a reagent (a clean reagent with little or no enviromental impact) and offers the possibility of surface patterning by illuminating through a mask[460]. Some photoreactions are:

- Elimination (the catalytic species, such as an acid or a base, can be produced on a photoactive molecule through an elimination reaction such as photodeprotection or photocleavage)
- Addition (*i.e.* photografting via, for example, the excited carbonyl group of benzophenone that abstracts an hydrogen atom from a neighboring compound, that forms a radical; then, benzophenone covalently binds to this radical through radical-radical combination)
- Rearrangment (i.e cis-trans isomerization in which the excitation of the double bond in an initially trans-azo compound leads to the formation of a less stable cis-azo conformer).

III.1. Modification using unsaturated compounds

This functionalization of surfaces by photochemical attachment of alkenes provides a pathway to stable interfaces; it has found great utility for attaching and sensing applications[461]. This photochemical grafting process of alkenes can be applied to different substrates, such as Si-H, diamond-H[462][463][464], carbon-H[465], GaN-H[466], thus broadening the possibilities for sensing and interface constructions.

The mechanism for the photochemical formation of monolayers is not clearly underestood. First, it was proposed (mechanism 1, Figure 29 A) that the reaction proceeds by UV

excitation and cleavage of the Si-H bond, producing a surface radical (a dangling bond) that reacts with a terminal olefin to form a Si-C bond. A neighboring surface hydrogen atom is then abstracted by the resulting secondary carbon radical to regenerate a new silicon radical and this process is repeated many times, yielding many adsorbates per initiation event[467][468].

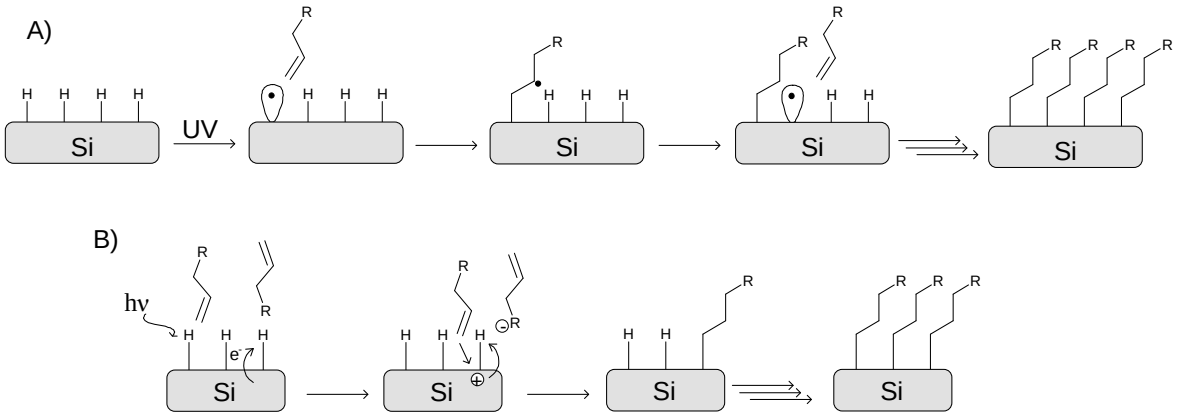


Figure. 29. Mechanism of photochemical grafting in Si-H: A) by excitaction and surface radical formation;B) by photoemission and nucleophilic attack of the alkene.

However, in a recently proposed mechanism, such as that proposed for the UV grafting of diamond, the UV light initiates photoemission from Si into the acceptor groups of a reactant (alkene) or another electron acceptor, leaving a valence-band hole that facilitates the nucleophilic attack by the alkene group (mechanism B, Fig.29. B). In the case of Si, at short wavelengths, where photons can excite the electron acceptor levels of the reactant molecule, photoemission is more efficient than excitation (mechanism A, Fig.29. A), but at longer wavelengths it is likely that only the excitation mechanism takes place (mechanism B)[469].

Grafting of Si-H with the same quality as thermal grafting, can be achieved under mild conditions by irradiation of the surface with visible light (447 to 658 nm) at room temperature in the presence of different 1-alkenes or 1-alkynes[470]. Using these mild photografting condition bio-active (i.e disaccharides) molecules can form directly monolayers[471].

Monolayer modification of the SiH surface with formation of the Si-O-C- interfacial bond is performed by UV irradiation of aliphatic alcohols and aldehydes with the last ones forming a chemically more resistant monolayer[472].

Hydrogen terminated Si nanowires grown on SiO_2 were selectively modified through UV irradiation with an alkene containing a protected amino group. After attachment of the linker,

the amino group is deprotected and used to covalently bind the DNA adducts. This method entails biomolecular recognition properties to the nanowires[473].

Photochemically grafted monolayer of 11-(2,4-dinitro-5-fluorobenzene)undecenamide is used to bind nucleophiles such as proteins or poly(ethyleneimine), using either micro-contact printing or a mask; micrometric patterns (≈ 5μm) can be photografted[474]. Hydrogen terminated diamond can be photopaterned throught a mask by UV photochemical grafting with alkenes (trifluoroacetamide-protected 1-aminodec-1-ene and 1-dodecene) down to 1 μm; the resolution is limited by diffraction effects associated with the use of a simple contact mask immersed directly in the reactant alkenes[464]. Hydrogenated gallium nitride is photo patterned (<12 μm width) with alkenes containing a protected amino group, which after deprotection is linked to single DNA-stranded nucleotides[466] .

Hydroxyl-terminated fused silica is modified by 1-alkenes under UV irradiation rendering it highly hydrophobic (water contact angle 109° for 8 h modification time, the non modified surface showing a ≈10° contact angle). It is possibile to create patterned hydrophobic sample (7.5 x 7.5 μm^2 squares with a 5 μm spacing); the modified surfaces are thermally stable up to at least 400°C[475].

Photochemical hydrosilylation is used to graft silicon quantum dots, thus modifying their physical properties and improving their oxidative and optical stability [476]. Magnetic monodisperse manganese ferrite nanoparticules modified with ω-alkenyl moieties are covalently anchored to the Si-H surface by UV irradiation [477] .

Formation of mixed monolayers with amine and triethylene glycol functionalities (through deprotection of the corresponding grafted alkenes) shows improvement of the ratio of specifically to non specifically bonded avidin. This confers to these layers an optimized ability to detect specifically bound avidin, while simultaneously reducing the nonspecific adsorption since the layer resists largely to nonspecific adsorption of proteins[463].

III.2. Modification using arylazides

The UV grafting of arylazides ($Ar\text{-}N_3$) is based on the formation of extremely reactive nitrene radicals (Ar-N) upon UV irradiation. Nitrenes can insert into C-H, N-H, O-H bonds forming an organic moiety covalently bonded to the polymer surface (Figure 30).

The photografted molecules include: heterocyclic azides[478], 4-substituted perfluorophenyl azides[479][480], 4-substituted arylazides[481], bis(aryl azides)[482], methyl azidocarboxylate[483],

azido derivatized polymers [poly(N,N-dimethylacrylamide-co-3-azidostyrene)[484], bis-4-azidobenzamide-polyethylene glycol[484], poly(styrene-co-3-azido-styrene)[484], poly(acrylic acid)[485], poly(ethylene glycol)[486], poly(cyclooctene) / poly(ethylene oxide) copolymer[487], poly(ethylene glycol)/poly(2,2,3,4,4,4-hexafluorobutyl acrylate)[488]], azide functionalized organic compounds (glucose[489], sucrose[489], dextrin[489], chitosan[490][491], photobiotin[492], lactamine[493]).

In general, this process is used to modify polymer surfaces such as polyethylene[478][483], polystyrene[479], polyimide[478], poly(3-octylthiophene)[479], polyacrylonitrile[481][494], polypropylene[495][489], glass[478][492], polyester[478], poly[1-(trimethyl-silyl)-1-propyne][482], nylon[490], tin oxide[478], aluminum[478], poly(vinyl alcohol)[484], poly(ether urethane)[496], poly(ether ether ketone)[480], poly(butylene terephthalate)[497], poly(ethylene terephthalate)[493][498], cotton fibres[488][499], expanded polytetrafluoroethylene[491], poly(vinylidene fluoride)[487], poly(methyl methacrylate)[500], quartz[501]. They can also bind to other molecules or materials[502].

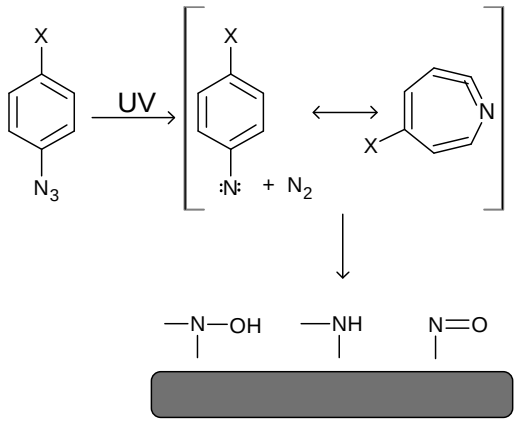


Figure. 30. Modification of polymers surface through photochemical process using azides.

The attachment of heterocyclic azides has been analyzed by XPS, IR, contact angle and ellipsometry. The modified quartz surface shows increased counting for C1s peak and a new N1s peak that is not present on an unmodified surface, presenting a clear evidence for the binding of the nitrene derived moiety to the surface. The IR spectra show a broad band at 1600 cm^{-1}, which is attributed to multilayered films containing also six or seven membered rings. The thickness of the film increases with the irradiation time; for 1, 15, 60 s and 30 min, the thickness is 0.8, 27 to 75 nm and 1 μm respectively.

Modification of hydrophobic surfaces such as polyethylene can be used to make them more hydrophilic (water contact angle of 60° upon irradiation in the presence of 4-azidopyridine - 95° for the non modified surface)[478].

The surface of GC is modified by the photolysis of different arylazides (deposited by spin coating on the surface). Diazonium salts are electrografted on carbon, and on top of such film, a second layer is attached by photopatterning arylazides[503].

The photografting process is used for different purposes. The modified film is used for the immobilization of horseradish peroxidase and for the creation of micrometer sized patterns (0.5 μm size) that are further reacted with fluorescein for visualization[479].

Using bolaammphiphiles[3] with two p-amidobenzoyl azide head groups, it is possible to deposit a monolayer of these molecules on polyacrylonitrile, to react the upper azide group with amines in the gas phase, converting the amine group to an amide, decomposing the other azide group (which is on the polyacrylonitrile surface), thus binding the molecule to the surface[494].

Surface modification of poly(etherurethanes) with arylazide containing phosphorylcholine end-groups, improves the polymers hemocompatibility[496].

It is possible to transform the hydrophobic polypropylene surface into an hydrophilic surface through the covalent bonding of sucrose residues via azide photolysis ("photochemical immobilization")[495].

Cross-linking of poly[1-(trimethyl-silyl)-1-propyne] membranes with bis(arylazide) renders them insoluble in solvents that typically dissolve the membranes and increases their separation factors for O_2 and N_2[482] It is possible to improve light stability and wettability of polyolefin polymers[489] as well as the nylon hemocompatibility[496]. The platelets adhesion are reduced onto these expanded polytetrafluoroethylene vascular grafts[491]. Acid treated glass can be modified with fluorescent-labeled arylazide and can be used to characterize site-selective photocatalyzed immobilization reactions on the surface[492].

Photo-crosslinking and photo-patterning of polyelectrolyte films is possible[501][504]. Many other reactions are reported: performing versatile photocrosslinking methodology based on sterically hindered bis(fluorophenyl azides), forming back-infiltrated and contiguous

[3] Bolaamphiphiles are amphiphilic molecules that have hydrophilic groups at both ends

interpenetrating donor–acceptor heterostructures for photovoltaic applications, providing the appropriate morphology for high-efficiency polymer-based photovoltaics, creating photopatternable polymer-based field-effect transistors and light-emitting diodes[501]. Crosslinking of poly(ethylene glycol) containing terminal azide groups to ionic liquid molecules by UV irradiation, greatly enhances the mechanical properties of the electrolyte and its conductivity for possible use in solar cells[486].Microfluidic surfaces can be modified to enable site-specific attachment of biological molecules[500].

Stable superhydrophobic cotton fabric can be produced, that displays high resistance to acids, bases and organic solvents[488]. Multi walled carbon nanotubes modified with fluoropolymers can be attached to cotton fabrics forming a self-cleaning superhydrophobic composite surface[499].

interpenetrating donor–acceptor heterostructures for photovoltaic applications, providing the appropriate morphology for high-efficiency polymer-based photovoltaics, creating photopatternable polymer-based field-effect transistors and light-emitting diodes[501]. Crosslinking of poly(ethylene glycol) containing terminal azide groups to ionic liquid molecules by UV irradiation, greatly enhances the mechanical properties of the electrolyte and its conductivity for possible use in solar cells[486].Microfluidic surfaces can be modified to enable site-specific attachment of biological molecules[500].

Stable superhydrophobic cotton fabric can be produced, that displays high resistance to acids, bases and organic solvents[488]. Multi walled carbon nanotubes modified with fluoropolymers can be attached to cotton fabrics forming a self-cleaning superhydrophobic composite surface[499].

References

[1] A. Ulman, *Chemical Reviews* **1996**, *96*, 1533-1554.
[2] D. Allara, R. Nuzzo, *Langmuir* **1985**, *1*, 45-52.
[3] D. Allara, R. Nuzzo, *Langmuir* **1985**, *1*, 52-66.
[4] H. Ogawa, T. Chihara, K. Taya, *Journal of the American Chemical Society* **1985**, *107*, 1365-1369.
[5] C. E. Taylor, D. K. Schwartz, *Langmuir* **2003**, *19*, 2665-2672.
[6] I. L. Liakos, R. C. Newman, E. McAlpine, M. R. Alexander, *Langmuir* **2007**, *23*, 995-999.
[7] H. Chen, X. Wu, Q. Yu, S. Yang, D. Wang, W. Seen, *Chin. J. Chem.* **2002**, *20*, 1467-1471.
[8] D. L. Allara, S. V. Atre, C. A. Elliger, R. G. Snyder, *Journal of the American Chemical Society* **1991**, *113*, 1852-1854.
[9] M. Moskovits, J. S. Suh, *Journal of the American Chemical Society* **1985**, *107*, 6826-6829.
[10] M. Samant, C. Brown, J. Gordon, *Langmuir* **1993**, *9*, 1082-1085.
[11] A. Raman, E. S. Gawalt, *Langmuir* **2007**, *23*, 2284-2288.
[12] T. Arita, J. Yoo, T. Adschiri, *J Nanopart Res* **2009**, *12*, 2567-2578.
[13] G. Kwak, M. Seol, Y. Tak, K. Yong, *The Journal of Physical Chemistry C* **2009**, *113*, 12085-12089.
[14] N. Karsi, P. Lang, M. Chehimi, M. Delamar, G. Horowitz, *Langmuir* **2006**, *22*, 3118-3124.
[15] D. Aswal, S. Lenfant, D. Guerin, J. Yakhmi, D. Vuillaume, *Analytica Chimica Acta* **2006**, *568*, 84-108.
[16] N. Chaki, K. Vijayamohanan, *Biosensors & Bioelectronics* **2002**, *17*, 1-12.
[17] S. Onclin, B. Ravoo, D. Reinhoudt, *Angewandte Chemie International Edition* **2005**, *44*, 6282-6304.
[18] C. Haensch, S. Hoeppener, U. S. Schubert, *Chem. Soc. Rev.* **2010**, *39*, 2323.
[19] J. Sagiv, *Journal of the American Chemical Society* **1980**, *102*, 92-98.
[20] C. Yam, A. Kakkar, *Journal of chemical society - Chemical communications* **1995**, 907-909.
[21] M. G. L. Petrucci, A. K. Kakkar, *Organometallics* **1998**, *17*, 1798-1811.
[22] J. Zhu, M. Yudasaka, M. Zhang, D. Kasuya, S. Iijima, *Nano Letters* **2003**, *3*, 1239-1243.
[23] Y. Wang, M. Lieberman, *Langmuir* **2003**, *19*, 1159-1167.
[24] P. Silberzan, L. Leger, D. Ausserre, J. Benattar, *Langmuir* **1991**, *7*, 1647-1651.
[25] S. Wasserman, Y. Tao, G. Whitesides, *Langmuir* **1989**, *5*, 1074-1087.
[26] C. M. Yam, S. S. Y. Tong, A. K. Kakkar, *Langmuir* **1998**, *14*, 6941-6947.
[27] K. Mathauer, C. W. Frank, *Langmuir* **1993**, *9*, 3446-3451.
[28] S. Brandriss, S. Margel, *Langmuir* **1993**, *9*, 1232-1240.
[29] M. E. McGovern, K. M. R. Kallury, M. Thompson, *Langmuir* **1994**, *10*, 3607-3614.
[30] C. Sun, D. E. Aston, J. C. Berg, *Journal of Colloid and Interface Science* **2002**, *248*, 96-102.
[31] M. E. McGovern, K. M. R. Kallury, M. Thompson, *Langmuir* **1994**, *10*, 3607-3614.
[32] K. Iimura, Y. Nakajima, T. Kato, *Thin Solid Films* **2000**, *379*, 230-239.
[33] K. Mathauer, C. W. Frank, *Langmuir* **1993**, *9*, 3002-3008.
[34] C. R. Kessel, S. Granick, *Langmuir* **1991**, *7*, 532-538.
[35] J. Gun, R. Iscovici, J. Sagiv, *Journal of Colloid and Interface Science* **1984**, *101*, 201-

213.
[36] N. Tillman, A. Ulman, J. Schildkraut, T. Penner, *Journal of the American Chemical Society* **1988**, *110*, 6136-6144.
[37] A. Franquet, C. Le Pen, H. Terryn, J. Vereecken, *Electrochimica Acta* **2003**, *48*, 1245-1255.
[38] E. Hoque, J. A. DeRose, P. Hoffmann, B. Bhushan, H. J. Mathieu, *The Journal of Physical Chemistry C* **2007**, *111*, 3956-3962.
[39] A. Batan, F. Brusciotti, I. De Graeve, J. Vereecken, M. Wenkin, M. Piens, J. Pireaux, F. Reniers, H. Terryn, *Progress in Organic Coatings* **2010**, *69*, 126-132.
[40] J. Bajat, I. Milosev, Z. Jovanovic, R. Jancic-Heinemann, M. Dimitrijevic, V. Miskovic-Stankovic, *Corrosion Science* **2010**, *52*, 1060-1069.
[41] J. Gun, J. Sagiv, *Journal of Colloid and Interface Science* **1986**, *112*, 457-472.
[42] C. N. Sukenik, N. Balachander, L. A. Culp, K. Lewandowska, K. Merritt, *J. Biomed. Mater. Res.* **1990**, *24*, 1307-1323.
[43] S. Xiao, M. Textor, N. D. Spencer, H. Sigrist, *Langmuir* **1998**, *14*, 5507-5516.
[44] A. Rezania, R. Johnson, A. R. Lefkow, K. E. Healy, *Langmuir* **1999**, *15*, 6931-6939.
[45] P. Dubruel, E. Vanderleyden, M. Bergada, I. De Paepe, H. Chen, S. Kuypers, J. Luyten, J. Schrooten, L. Van Hoorebeke, E. Schacht, *Surface Science* **2006**, *600*, 2562-2571.
[46] A. Nanci, J. Wuest, L. Peru, P. Brunet, V. Sharma, S. Zalzal, M. McKee, *Journal of Biomedical Materials Research* **1998**, *40*, 324-335.
[47] S. Marcinko, A. Y. Fadeev, *Langmuir* **2004**, *20*, 2270-2273.
[48] C. Allen, D. Baker, J. Albin, H. Oertli, D. Gillaspie, D. Olson, T. Furtak, R. Collins, *Langmuir* **2008**, *24*, 13393-13398.
[49] A. Arranz, C. Palacio, D. Garcia-Fresnadillo, G. Orellana, A. Navarro, E. Munoz, *Langmuir* **2008**, *24*, 8667-8671.
[50] S. Lenci, L. Tedeschi, C. Domenici, C. Lande, A. Nannini, G. Pennelli, F. Pieri, S. Severi, *Materials Science and Engineering: C* **2010**, *30*, 1221-1226.
[51] W. M. Liu, W. W. Zhao, H. Y. Zhang, P. F. Wang, Y. M. Chong, Q. Ye, Y. S. Zou, W. J. Zhang, J. A. Zapien, I. Bello, et al., *Appl. Phys. Lett.* **2009**, *94*, 183105.
[52] L. SelegArd, V. Khranovskyy, F. Soderlind, C. Vahlberg, M. Ahren, P. Kall, R. Yakimova, K. Uvdal, *ACS Applied Materials & Interfaces* **2010**, *2*, 2128-2135.
[53] Q. Ke, W. Fu, S. Wang, T. Tang, J. Zhang, *ACS Applied Materials & Interfaces* **2010**, *2*, 2393-2398.
[54] D. Li, W. Y. Teoh, D. Djunaedi, J. J. Gooding, C. Selomulya, R. Amal, *Adv. Eng. Mater.* **2010**, *12*, B210-B214.
[55] H. Wei, Z. Cleary, S. Park, K. Senevirathne, H. Eilers, *Journal of Alloys and Compounds* **2010**, *500*, 96-101.
[56] Y. Liang, M. Ozawa, A. Krueger, *ACS Nano* **2009**, *3*, 2288-2296.
[57] L. Min, L. Zhao-Yue, L. Qiang, Y. Hang, M. Lan, L. Jing-Hong, B. Yu-Bai, L. Tie-Jin, *Chin. J. Chem.* **2005**, *23*, 875-880.
[58] J. Han, S. Kim, J. Kim, H. Jeong, S. Jeong, G. Lee, *Industrial & Engineering Chemistry Research* **2010**, *49*, 6416-6421.
[59] L. Vast, L. Carpentier, F. Lallemand, J. Colomer, G. Van Tendeloo, A. Fonseca, J. Nagy, Z. Mekhalif, J. Delhalle, *Journal of the Materials Science* **2009**, *44*, 3476-3482.
[60] Q. Zhang, K. Naito, Y. Kagawa, *Journal of Nanoscience and Nanotechnology* **2009**, *9*, 267-274.
[61] Q. Chen, N. Yakovlev, *Applied Surface Science* **2010**, *257*, 1395-1400.
[62] K. Luo, S. Zhou, L. Wu, G. Gu, *Langmuir* **2008**, *24*, 11497-11505.
[63] D. L. Angst, G. W. Simmons, *Langmuir* **1991**, *7*, 2236-2242.
[64] A. Velamakanni, J. R. Torres, K. Ganesh, P. J. Ferreira, J. S. Major, *Langmuir* **2010**,

26, 15295-15301.
[65] W. van Ooij, D. Zhu, G. Prasad, S. Jayaseelan, Y. Fu, N. Teredesai, *Surface Engineering* **2000**, *16*, 386-396.
[66] W. van Ooij, D. Zhu, M. Stacy, A. Seth, T. Mugada, J. Gandhi, P. Puomi, *Tsinghua Science & Technology* **2005**, *10*, 639-664.
[67] T. Hofler, A. Track, P. Pacher, Q. Shen, H. Flesch, G. Hlawacek, G. Koller, M. Ramsey, R. Schennach, R. Resel, et al., *Materials Chemistry and Physics* **2010**, *119*, 287-293.
[68] K. Emoto, J. M. Van Alstine, J. M. Harris, *Langmuir* **1998**, *14*, 2722-2729.
[69] L. Velleman, G. Triani, P. J. Evans, J. G. Shapter, D. Losic, *Microporous and Mesoporous Materials* **2009**, *126*, 87-94.
[70] S. R. Cohen, R. Naaman, J. Sagiv, *The Journal of Physical Chemistry* **1986**, *90*, 3054-3056.
[71] N. L. Jeon, K. Finnie, K. Branshaw, R. G. Nuzzo, *Langmuir* **1997**, *13*, 3382-3391.
[72] M. Calistri-Yeh, E. J. Kramer, R. Sharma, W. Zhao, M. H. Rafailovich, J. Sokolov, J. D. Brock, *Langmuir* **1996**, *12*, 2747-2755.
[73] K. Iimura, T. Kato, S. Morita, Y. Ozaki, *Molecular Crystals and Liquid Crystals Science and Technology. Section A. Molecular Crystals and Liquid Crystals* **1999**, *337*, 113.
[74] A. Chandekar, S. Sengupta, J. Whitten, *Applied Surface Science* **2010**, *256*, 2742-2749.
[75] V. DePalma, N. Tillman, *Langmuir* **1989**, *5*, 868-872.
[76] B. Bhushan, A. V. Kulkarni, V. N. Koinkar, M. Boehm, L. Odoni, C. Martelet, M. Belin, *Langmuir* **1995**, *11*, 3189-3198.
[77] S. R. Wasserman, Y. T. Tao, G. M. Whitesides, *Langmuir* **1989**, *5*, 1074-1087.
[78] C. Bram, C. Jung, M. Stratmann, *Fresenius' Journal of Analytical Chemistry* **1997**, *358*, 108-111.
[79] C. Messerschmidt, D. K. Schwartz, *Langmuir* **2001**, *17*, 462-467.
[80] M. J. Pellerite, T. D. Dunbar, L. D. Boardman, E. J. Wood, *The Journal of Physical Chemistry B* **2003**, *107*, 11726-11736.
[81] R. Luschtinetz, A. F. Oliveira, J. Frenzel, J. Joswig, G. Seifert, H. A. Duarte, *Surface Science* **2008**, *602*, 1347-1359.
[82] E. S. Gawalt, M. J. Avaltroni, N. Koch, J. Schwartz, *Langmuir* **2001**, *17*, 5736-5738.
[83] E. S. Gawalt, M. J. Avaltroni, M. P. Danahy, B. M. Silverman, E. L. Hanson, K. S. Midwood, J. E. Schwarzbauer, J. Schwartz, *Langmuir* **2003**, *19*, 200-204.
[84] M. P. Danahy, M. J. Avaltroni, K. S. Midwood, J. E. Schwarzbauer, J. Schwartz, *Langmuir* **2004**, *20*, 5333-5337.
[85] J. Auernheimer, H. Kessler, *Bioorganic & Medicinal Chemistry Letters* **2006**, *16*, 271-273.
[86] A. Raman, M. Dubey, I. Gouzman, E. S. Gawalt, *Langmuir* **2006**, *22*, 6469-6472.
[87] M. Dubey, S. L. Bernasek, J. Schwartz, *Journal of the American Chemical Society* **2007**, *129*, 6980-6981.
[88] M. Dubey, T. Weidner, L. J. Gamble, D. G. Castner, *Langmuir* **2010**, *26*, 14747-14754.
[89] S. A. Paniagua, P. J. Hotchkiss, S. C. Jones, S. R. Marder, A. Mudalige, F. S. Marrikar, J. E. Pemberton, N. R. Armstrong, *The Journal of Physical Chemistry C* **2008**, *112*, 7809-7817.
[90] W. Luo, N. P. Westcott, A. Pulsipher, M. N. Yousaf, *Langmuir* **2008**, *24*, 13096-13101.
[91] T. Lewington, M. Alexander, G. Thompson, E. McAlpine, *Surface Engineering* **2002**, *18*, 228-232.
[92] J. G. Van Alsten, *Langmuir* **1999**, *15*, 7605-7614.
[93] H. Kim, P. E. Colavita, P. Paoprasert, P. Gopalan, T. Kuech, R. J. Hamers, *Surface*

Science **2008**, *602*, 2382-2388.
[94] O. Acton, I. Osaka, G. Ting, D. Hutchins, H. Ma, R. D. McCullough, A. K. Jen, *Appl. Phys. Lett.* **2009**, *95*, 113305.
[95] A. Pilbáth, I. Bertóti, I. Sajó, L. Nyikos, E. Kálmán, *Applied Surface Science* **2008**, *255*, 1841-1849.
[96] A. Pilbáth, I. Bertóti, É. Pfeifer, J. Mink, L. Nyikos, E. Kálmán, *Surface and Coatings Technology* **2009**, *203*, 1182-1192.
[97] G. Lecollinet, N. Delorme, M. Edely, A. Gibaud, J. Bardeau, F. Hindré, F. Boury, D. Portet, *Langmuir* **2009**, *25*, 7828-7835.
[98] J. McElwee, R. Helmy, A. Y. Fadeev, *Journal of Colloid and Interface Science* **2005**, *285*, 551-556.
[99] J. C. Love, L. A. Estroff, J. K. Kriebel, R. G. Nuzzo, G. M. Whitesides, *Chemical Reviews* **2005**, *105*, 1103-1170.
[100] C. D. Bain, E. B. Troughton, Y. T. Tao, J. Evall, G. M. Whitesides, R. G. Nuzzo, *Journal of the American Chemical Society* **1989**, *111*, 321-335.
[101] J. C. Love, D. B. Wolfe, R. Haasch, M. L. Chabinyc, K. E. Paul, G. M. Whitesides, R. G. Nuzzo, *Journal of the American Chemical Society* **2003**, *125*, 2597-2609.
[102] O. Dannenberger, J. J. Wolff, M. Buck, *Langmuir* **1998**, *14*, 4679-4682.
[103] M. Kawasaki, T. Sato, T. Tanaka, K. Takao, *Langmuir* **2000**, *16*, 1719-1728.
[104] P. E. Laibinis, G. M. Whitesides, D. L. Allara, Y. T. Tao, A. N. Parikh, R. G. Nuzzo, *Journal of the American Chemical Society* **1991**, *113*, 7152-7167.
[105] S. M. Han, W. R. Ashurst, C. Carraro, R. Maboudian, *Journal of the American Chemical Society* **2001**, *123*, 2422-2425.
[106] O. M. Magnussen, B. M. Ocko, M. Deutsch, M. J. Regan, P. S. Pershan, D. Abernathy, G. Grubel, J. Legrand, *Nature* **1996**, *384*, 250-252.
[107] N. Muskal, I. Turyan, D. Mandler, *Journal of Electroanalytical Chemistry* **1996**, *409*, 131-136.
[108] Z. Mekhalif, F. Laffineur, N. Couturier, J. Delhalle, *Langmuir* **2003**, *19*, 637-645.
[109] Z. Li, S. Chang, R. S. Williams, *Langmuir* **2003**, *19*, 6744-6749.
[110] T. Lin, T. Huang, Y. Liu, C. Yeh, Y. Lai, W. Hung, *The Journal of Physical Chemistry B* **2005**, *109*, 14079-14084.
[111] C. Nogues, P. Lang, *Langmuir* **2007**, *23*, 8385-8391.
[112] J. Hedberg, C. Leygraft, K. Cimatu, S. Baldelli, *Journal of Physical Chemistry C* **2007**, *111*, 17587-17596.
[113] T. Baum, S. Ye, K. Uosaki, *Langmuir* **1999**, *15*, 8577-8579.
[114] H. H. Park, A. Ivanisevic, *The Journal of Physical Chemistry C* **2007**, *111*, 3710-3718.
[115] D. Zerulla, T. Chasse, *Langmuir* **1999**, *15*, 5285-5294.
[116] A. R. Noble-Luginbuhl, R. G. Nuzzo, *Langmuir* **2001**, *17*, 3937-3944.
[117] M. Brust, M. Walker, D. Bethell, D. J. Schiffrin, R. Whyman, *Journal of the Chemical Society, Chemical Communications* **1994**, 801-802.
[118] A. C. Templeton, W. P. Wuelfing, R. W. Murray, *Accounts of Chemical Research* **2000**, *33*, 27-36.
[119] M. J. Hostetler, R. W. Murray, *Current Opinion in Colloid & Interface Science* **1997**, *2*, 42-50.
[120] S. Gomez, L. Erades, K. Philippot, B. Chaudret, V. Colliere, O. Balmes, J. Bovin, *Chemical Communications* **2001**, 1474-1475.
[121] C. K. Yee, R. Jordan, A. Ulman, H. White, A. King, M. Rafailovich, J. Sokolov, *Langmuir* **1999**, *15*, 3486-3491.
[122] Y. Shon, G. B. Dawson, M. Porter, R. W. Murray, *Langmuir* **2002**, *18*, 3880-3885.
[123] G. Viau, R. Brayner, L. Poul, N. Chakroune, E. Lacaze, F. Fiévet-Vincent, F. Fiévet,

Chemistry of Materials **2003**, *15*, 486-494.
[124] N. N. Mamedova, N. A. Kotov, A. L. Rogach, J. Studer, *Nano Letters* **2001**, *1*, 281-286.
[125] N. Gaponik, D. V. Talapin, A. L. Rogach, A. Eychmüller, H. Weller, *Nano Letters* **2002**, *2*, 803-806.
[126] M. A. Marcus, W. Flood, M. Stiegerwald, L. Brus, M. Bawendi, *The Journal of Physical Chemistry* **1991**, *95*, 1572-1576.
[127] T. Lover, W. Henderson, G. A. Bowmaker, J. M. Seakins, R. P. Cooney, *Chemistry of Materials* **1997**, *9*, 1878-1886.
[128] H. Dollefeld, K. Hoppe, J. Kolny, K. Schilling, H. Weller, A. Eychmuller, *Physical Chemistry Chemical Physics* **2002**, *4*, 4747-4753.
[129] H. Gu, P. Ho, K. W. T. Tsang, L. Wang, B. Xu, *Journal of the American Chemical Society* **2003**, *125*, 15702-15703.
[130] H. Gu, P. Ho, K. Tsang, C. Yu, B. Xu, *Chemical Communications* **2003**, 1966-1967.
[131] C. Xu, K. Xu, H. Gu, X. Zhong, Z. Guo, R. Zheng, X. Zhang, B. Xu, *Journal of the American Chemical Society* **2004**, *126*, 3392-3393.
[132] L. Wu, F. Camacho-Alanis, H. Castaneda, G. Zangari, N. Swami, *Electrochimica Acta* **2010**, *55*, 8758-8765.
[133] S. Chen, L. A. Truax, J. M. Sommers, *Chemistry of Materials* **2000**, *12*, 3864-3870.
[134] A. R. Kortan, R. Hull, R. L. Opila, M. G. Bawendi, M. L. Steigerwald, P. J. Carroll, L. E. Brus, *Journal of the American Chemical Society* **1990**, *112*, 1327-1332.
[135] V. Chechik, R. M. Crooks, C. J. M. Stirling, *Adv. Mater.* **2000**, *12*, 1161-1171.
[136] T. Sullivan, W. Huck, *European Journal of Organic Chemistry* **2003**, 17-29.
[137] P. L. Schilardi, P. Dip, P. C. dos Santos Claro, G. A. Benítez, M. H. Fonticelli, O. Azzaroni, R. C. Salvarezza, *Chem. Eur. J.* **2006**, *12*, 38-49.
[138] G. Wittstock, R. Hesse, W. Schuhmann, *Electroanalysis* **1997**, *9*, 746-750.
[139] C. Zhou, A. V. Walker, *Langmuir* **2007**, *23*, 8876-8881.
[140] J. Gooding, F. Mearns, W. Yang, J. Liu, *Electroanalysis* **2003**, *15*, 81-96.
[141] J. Stettner, A. Winkler, *Langmuir* **2010**, *26*, 9659-9665.
[142] J. Noh, E. Ito, M. Hara, *Journal of Colloid and Interface Science* **2010**, *342*, 513-517.
[143] D. Yang, C. P. Wilde, M. Morin, *Langmuir* **1996**, *12*, 6570-6577.
[144] M. Luo, J. Frechette, *Journal of Physical Chemistry C* **2010**, *114*, 20167-20172.
[145] C. A. Widrig, C. Chung, M. D. Porter, *Journal of Electroanalytical Chemistry and Interfacial Electrochemistry* **1991**, *310*, 335-359.
[146] J. Bucher, L. Santesson, K. Kern, *Langmuir* **1994**, *10*, 979-983.
[147] C. Vericat, G. Benitez, D. Grumelli, M. Vela, R. Salvarezza, *Journal of Physics: Condensed Matter* **2008**, *20*, 184004-184012.
[148] M. Linford, C. Chidsey, *Journal of the American Chemical Society* **1993**, *115*, 12631-12632.
[149] M. Linford, P. Fenter, P. Eisenberger, C. Chidsey, *Journal of the American Chemical Society* **1995**, *117*, 3145-3155.
[150] E. Faber, L. de Smet, W. Olthuis, H. Zuilhof, E. Sudholter, P. Bergveld, A. van den Berg, *ChemPhysChem* **2005**, *6*, 2153-2166.
[151] Q. Sun, L. de Smet, B. van Lagen, M. Giesbers, P. Thune, J. van Engelenburg, F. de Wolf, H. Zuilhof, E. Sudholter, *Journal of the American Chemical Society* **2005**, *127*, 2514-2523.
[152] H. Sano, T. Yaku, T. Ichii, K. Murase, H. Sugimura, *Journal of Vacuum Science & Technology B* **2009**, *27*, 858-862.
[153] L. J. Webb, N. S. Lewis, *The Journal of Physical Chemistry B* **2003**, *107*, 5404-5412.
[154] L. Scheres, M. Giesbers, E. Zuilhof, *Langmuir* **2010**, *26*, 10924-10929.

[155] J. T. C. Wojtyk, M. Tomietto, R. Boukherroub, D. D. M. Wayner, *Journal of the American Chemical Society* **2001**, *123*, 1535-1536.
[156] W. P. Voorthuijzen, M. D. Yilmaz, A. Gomez-Casado, P. Jonkheijm, W. G. van der Wiel, J. Huskens, *Langmuir* **2010**, *26*, 14210-14215.
[157] S. Ciampi, J. Harper, J. Gooding, *Chemical Society Reviews* **2010**, *39*, 2158-2183.
[158] A. Vilan, O. Yaffe, A. Biller, A. Salomon, A. Kahn, D. Cahen, *Advanced Materials* **2010**, *22*, 140-159.
[159] D. Aureau, J. Rappich, A. Moraillon, P. Allongue, F. Ozanam, J. Chazalviel, *Journal of Electroanalytical Chemistry* **2010**, *646*, 33-42.
[160] H. Sano, H. Maeda, T. Ichii, K. Murase, K. Noda, K. Matsushige, H. Sugimura, *Langmuir* **2009**, *25*, 5516-5525.
[161] M. Sung, G. Kluth, O. Yauw, R. Maboudian, *Langmuir* **1997**, *13*, 6164-6168.
[162] B. Barbier, J. Pinson, G. Desarmot, M. Sanchez, *J. Electrochem. Soc.* **1990**, *137*, 1757-1764.
[163] S. Antoniadou, A. D. Jannakoudakis, P. D. Jannakoudakis, E. Theodoridou, *Chemistry and Materials Science* **1992**, *22*, 1060-1064.
[164] R. S. Deinhammer, M. Ho, J. W. Anderegg, M. D. Porter, *Langmuir* **1994**, *10*, 1306-1313.
[165] A. Adenier, M. M. Chehimi, I. Gallardo, J. Pinson, N. Vilà, *Langmuir* **2004**, *20*, 8243-8253.
[166] F. Geneste, C. Moinet, *New Journal of Chemistry* **2005**, *2*, 269-271.
[167] R. Nasraoui, J. Bergamini, S. Ababou-Girard, F. Geneste, *Journal of Solid State Electrochemistry* **2010**, DOI 10.1007/s10008-010-1075-z.
[168] J. Ghilane, P. Martin, H. Randriamahazaka, J. Lacroix, *Electrochemistry Communications* **2010**, *12*, 246-249.
[169] M. Herlem, B. Fahys, G. Herlem, B. Lakard, K. Reybier, A. Trokourey, T. Diaco, S. Zairi, N. Jaffrezic-Renault, *Electrochimica Acta* **2002**, *47*, 2597-2602.
[170] J. Chretien, M. Ghanem, P. Bartlett, J. Kilburn, *Chemistry-A European Journal* **2008**, *14*, 2548-2556.
[171] M. Sosna, J. M. Chretien, J. D. Kilburn, P. N. Bartlett, *Physical Chemistry Chemical Physics* **2010**, *12*, 10018-10026.
[172] I. Gallardo, J. Pinson, N. Vilà, *The Journal of Physical Chemistry B* **2006**, *110*, 19521-19529.
[173] G. Yang, B. Liu, S. Dong, *Journal of Electroanalytical Chemistry* **2005**, *585*, 301-305.
[174] X. Li, Y. Wan, C. Sun, *Journal of Electroanalytical Chemistry* **2004**, *569*, 79-87.
[175] G. Yang, Y. Shen, M. Wang, H. Chen, B. Liu, S. Dong, *Talanta* **2006**, *68*, 741-747.
[176] X. Wei, F. Wang, Y. Yin, Q. Liu, L. Zou, B. Ye, *Analyst* **2010**, *135*, 2286-2290.
[177] G. Hu, Y. Ma, Y. Guo, S. Shao, *Electrochimica Acta* **2008**, *53*, 6610-6615.
[178] C. Yu, J. Guo, H. Gu, *Electroanalysis* **2010**, *22*, 1005-1011.
[179] M. Ghanem, J. Chretien, A. Pinczewska, J. Kilburn, P. Bartlett, *Journal of Materials Chemistry* **2008**, *18*, 4917-4927.
[180] G. Herlem, C. Goux, B. Fahys, F. Dominati, A. Goncalves, C. Mathieu, E. Sutter, A. Trokourey, J. Penneau, *Journal of Electroanalytical Chemistry* **1997**, *435*, 259-265.
[181] G. Herlem, B. Lakard, M. Herlem, B. Fahys, *J. Electrochem. Soc.* **2001**, *148*, 435-438.
[182] O. Buriez, E. Labbé, P. Pigeon, G. Jaouen, C. Amatore, *Journal of Electroanalytical Chemistry* **2008**, *619-620*, 169-175.
[183] P. Deveci, B. Taner, Z. Üstündag, E. Özcan, A. O. Solak, Z. KIlIç, *Journal of Molecular Structure* **2010**, *982*, 162-168.
[184] C. Cougnon, J. Mauzeroll, D. Belanger, *Angewandte Chemie International Edition* **2009**, *48*, 7395-7397.

[185] T. Kim, H. Choi, B. Go, J. Kim, *Electrochemistry Communications* **2010**, *12*, 788-791.
[186] M. Sandroni, G. Volpi, J. Fiedler, R. Buscaino, G. Viscardi, L. Milone, R. Gobetto, C. Nervi, *Catalysis Today* **2010**, *158*, 22-28.
[187] G. Hu, Y. Guo, S. Shao, *Electroanalysis* **2009**, *21*, 1200-1206.
[188] O. Segut, G. Herlem, B. Lakard, V. Blondeau-Patissier, M. Nardin, S. Gree, J. Rauch, *Synthetic Metals* **2010**, *160*, 1359-1364.
[189] A. J. Downard, A. B. Mohamed, *Electroanalysis* **1999**, *11*, 418-423.
[190] M. A. Ghanem, J. Chrétien, J. D. Kilburn, P. N. Bartlett, *Bioelectrochemistry* **2009**, *76*, 115-125.
[191] S. Tominaka, K. Goto, T. Momma, T. Osaka, *Journal of Power Sources* **2009**, *192*, 316-323.
[192] L. Wang, P. Huang, J. Bai, H. Wang, L. Zhang, Y. Zhao, *Microchimica Acta* **2007**, *158*, 151-157.
[193] I. E. MülazImoglu, A. D. MülazImoglu, E. YIlmaz, *Desalination* **2011**, *268*, 227-232.
[194] R. Nasraoui, D. Floner, C. Paul-Roth, F. Geneste, *Journal of Electroanalytical Chemistry* **2010**, *638*, 9-14.
[195] C. P. Andrieux, F. Gonzalez, J. Savéant, *Journal of the American Chemical Society* **1997**, *119*, 4292-4300.
[196] C. Andrieux, F. Gonzalez, J. Savéant, *Journal of Electroanalytical Chemistry* **2001**, *498*, 171-180.
[197] E. Coulon, J. Pinson, J. Bourzat, A. Commerçon, J. P. Pulicani, *Langmuir* **2001**, *17*, 7102-7106.
[198] F. Geneste, M. Cadoret, C. Moinet, G. Jezequel, *New J. Chem.* **2002**, *26*, 1261-1266.
[199] E. Coulon, J. Pinson, J. Bourzat, A. Commerçon, J. Pulicani, *The Journal of Organic Chemistry* **2002**, *67*, 8513-8518.
[200] P. A. Brooksby, A. J. Downard, S. S. C. Yu, *Langmuir* **2005**, *21*, 11304-11311.
[201] P. Astudillo, A. Galano, F. Gonzalez, *Journal of Electroanalytical Chemistry* **2007**, *610*, 137-146.
[202] L. S. Hernández-Muñoz, R. J. Fragoso-Soriano, C. Vázquez-López, E. Klimova, L. A. Ortiz-Frade, P. D. Astudillo, F. J. González, *Journal of Electroanalytical Chemistry* **2010**, *650*, 62-67.
[203] K. Vaik, U. Mäeorg, F. C. Maschion, G. Maia, D. J. Schiffrin, K. Tammeveski, *Electrochimica Acta* **2005**, *50*, 5126-5131.
[204] F. Geneste, C. Moinet, G. Jezequel, *New Journal of Chemistry* **2002**, *26*, 1539-1541.
[205] G. U. O. Bei, A. Jun-ichi, O. S. A. Tetsuo, *Chemical & pharmaceutical bulletin* **1996**, *44*, 860-862.
[206] H. Maeda, Y. Yamauchi, M. Yoshida, H. Ohmori, *Analytical Sciences* **1995**, *11*, 947-952.
[207] H. Maeda, T. Li, M. Hosoe, M. Itami, Y. Yamauchi, H. Ohmori, *Analytical Sciences* **1994**, *10*, 963-965.
[208] H. Maeda, T. Kitano, C. Huang, K. Katayama, Y. Yamauchi, H. Ohmori, *Analytical Sciences* **1999**, *15*, 531-536.
[209] M. Hatsuo, I. Munenori, Y. Yuji, O. Hidenobu, *Chemical & pharmaceutical bulletin* **1996**, *44*, 2294-2299.
[210] H. Maeda, M. Itami, K. Katayama, Y. Yamauchi, H. Ohmori, *Analytical Sciences* **1997**, *13*, 721-727.
[211] H. Maeda, K. Katayama, R. Matsui, Y. Yamauchi, H. Ohmori, *Analytical Sciences* **2000**, *16*, 293-298.
[212] F. Geneste, C. Moinet, *Journal of Electroanalytical Chemistry* **2006**, *594*, 105-110.
[213] J. Ledesma-Garcia, L. Arriaga, T. Chapman, R. Velazquez-Castillo, L. Godinez,

Journal of The Electrochemical Society **2010**, *157*, E1-E5.
[214] D. Quan, W. Shin, *Materials science & engineering. C, Biomimetic and supramolecular systems* **2004**, *24*, 113-115.
[215] J. M. Buriak, *Chemical Reviews* **2002**, *102*, 1271-1308.
[216] K. Perrine, A. Teplyakov, *Chemical Society Reviews* **2010**, *39*, 3256-3274.
[217] M. Warntjes, C. Vieillard, F. Ozanam, J. Chazalviel, *Journal of The Electrochemical Society* **1995**, *142*, 4138-4142.
[218] F. Ozanam, C. Vieillard, M. Warntjes, T. Dubois, M. Pauly, J. Chazalviel, *Canadian journal of chemical engineering* **1998**, *76*, 1020-1026.
[219] F. Yang, R. Hunger, K. Roodenko, K. Hinrichs, K. Rademann, J. Rappich, *Langmuir* **2009**, *25*, 9313-9318.
[220] T. Yamada, K. Shirasaka, M. Noto, H. Kato, M. Kawai, *Journal of Physical Chemistry B* **2006**, *110*, 7357-7366.
[221] A. Marrani, F. Cattaruzza, F. Decker, P. Galloni, R. Zanoni, *Electrochimica Acta* **2010**, *55*, 5733-5740.
[222] S. Fellah, R. Boukherroub, F. Ozanam, J. Chazalviel, *Langmuir* **2004**, *20*, 6359-6364.
[223] A. Bansal, X. Li, I. Lauermann, N. S. Lewis, S. I. Yi, W. H. Weinberg, *Journal of the American Chemical Society* **1996**, *118*, 7225-7226.
[224] T. Yamada, M. Kawai, A. Wawro, S. Suto, A. Kasuya, *Journal of Chemical Physics* **2004**, *121*, 10660-10667.
[225] J. Mukherjee, S. Peczonczyk, S. Maldonado, *Langmuir* **2010**, *26*, 10890-10896.
[226] N. Y. Kim, P. E. Laibinis, *Journal of the American Chemical Society* **1998**, *120*, 4516-4517.
[227] J. H. Song, M. J. Sailor, *Journal of the American Chemical Society* **1998**, *120*, 2376-2381.
[228] F. Yang, R. Hunger, K. Rademann, J. Rappich, *Physica Status Solidi (c) - Current Topics In Solid State Physics* **2010**, *7*, 161-164.
[229] A. Fidélis, F. Ozanam, J. -. Chazalviel, *Surface Science* **2000**, *444*, L7-L10.
[230] P. T. Hurley, E. J. Nemanick, B. S. Brunschwig, N. S. Lewis, *Journal of the American Chemical Society* **2006**, *128*, 9990-9991.
[231] S. Fellah, A. Teyssot, F. Ozanam, J. Chazalviel, J. Vigneron, A. Etcheberry, *Langmuir* **2002**, *18*, 5851-5860.
[232] A. Teyssot, A. Fidélis, S. Fellah, F. Ozanam, J. -. Chazalviel, *Electrochimica Acta* **2002**, *47*, 2565-2571.
[233] S. Fellah, A. Amiar, F. Ozanam, J. Chazalviel, J. Vigneron, A. Etcheberry, M. Stchakovsky, *J. Phys. Chem. B* **2007**, *111*, 1310-1317.
[234] S. S. S. Vegunta, J. N. Ngunjiri, J. C. Flake, *Langmuir* **2009**, *25*, 12750-12756.
[235] S. R. Puniredd, O. Assad, H. Haick, *Journal of the American Chemical Society* **2008**, *130*, 13727-13734.
[236] J. Pinson, F. Podvorica, *Chemical Society Reviews* **2005**, *34*, 429.
[237] D. Bélanger, J. Pinson, *Chemical Society Reviews* **2011**, DOI 10.1039/c0cs00149j.
[238] S. Mahouche-Chergui, S. Gam-Derouich, C. Mangeney, M. M. Chehimi, *Chemical Society Reviews* **2011**, DOI 10.1039/c0cs00179a.
[239] M. Delamar, R. Hitmi, J. Pinson, J. Saveant, *Journal of the American Chemical Society* **1992**, *114*, 5883-5884.
[240] P. Allongue, M. Delamar, B. Desbat, O. Fagebaume, R. Hitmi, J. Pinson, J. Saveant, *Journal of the American Chemical Society* **1997**, *119*, 201-207.
[241] R. D. Smith, P. G. Pickup, *Electrochimica Acta* **2009**, *54*, 2305-2311.
[242] M. Tanaka, T. Sawaguchi, Y. Sato, K. Yoshioka, O. Niwa, *Langmuir* **2011**, *27*, 170-178.

[243] B. P. Corgier, C. A. Marquette, L. J. Blum, *Journal of the American Chemical Society* **2005**, *127*, 18328-18332.
[244] Q. Pan, H. Wang, Y. Jiang, *Electrochemistry Communications* **2007**, *9*, 754-760.
[245] C. Martin, M. Alias, F. Christien, O. Crosnier, D. Belanger, T. Brousse, *Advanced Materials* **2009**, *21*, 4735-+.
[246] M. Bayati, J. Abad, C. Bridges, M. Rosseinsky, D. Schiffrin, *Journal of Electroanalytical Chemistry* **2008**, *623*, 19-28.
[247] P. Viel, X. Le, V. Huc, J. Bar, A. Benedetto, A. Le Goff, A. Filoramo, D. Alamarguy, S. Noel, L. Baraton, et al., *Journal of Materials Chemistry* **2008**, *18*, 5913-5920.
[248] J. Kariuki, M. McDermott, *Langmuir* **1999**, *15*, 6534-6540.
[249] A. Sarapuu, K. Helstein, D. Schiffrin, K. Tammeveski, *Electrochemical and Solid-State Letters* **2005**, *8*, E30-E33.
[250] C. Bradbury, L. Kuster, D. Fermin, *Journal of Electroanalytical Chemistry* **2010**, *646*, 114-123.
[251] F. Koehler, A. Jacobsen, K. Ensslin, C. Stampfer, W. Stark, *Small* **2010**, *6*, 1125-1130.
[252] E. Bekyarova, M. E. Itkis, P. Ramesh, C. Berger, M. Sprinkle, W. A. de Heer, R. C. Haddon, *Journal of the American Chemical Society* **2009**, *131*, 1336-1337.
[253] M. Hossain, M. Walsh, M. Hersam, *Journal of the American Chemical Society* **2010**, *132*, 15399-15403.
[254] A. Jacobsen, F. Koehler, W. Stark, K. Ensslin, *New Journal of Physics* **2010**, *12*, DOI 10.1088/1367-2630/12/12/125007.
[255] J. R. Lomeda, C. D. Doyle, D. V. Kosynkin, W. Hwang, J. M. Tour, *Journal of the American Chemical Society* **2008**, *130*, 16201-16206.
[256] A. Sinitskii, A. Dimiev, D. A. Corley, A. A. Fursina, D. V. Kosynkin, J. M. Tour, *ACS Nano* **2010**, *4*, 1949-1954.
[257] J. Englert, C. Dotzer, G. Yang, M. Schmid, C. Papp, J. Gottfried, H. Steinruck, E. Spiecker, F. Hauke, A. Hirsch, *Nature Chemistry* **2011**, *3*, 279-286.
[258] F. Anariba, S. DuVall, R. McCreery, *Analytical Chemistry* **2003**, *75*, 3837-3844.
[259] S. Ranganathan, R. McCreery, *Analytical Chemistry* **2001**, *73*, 893-900.
[260] P. A. Brooksby, A. J. Downard, *Langmuir* **2004**, *20*, 5038-5045.
[261] R. L. McCreery, J. Wu, R. Prasad Kalakodimi, *Phys. Chem. Chem. Phys.* **2006**, *8*, 2572.
[262] A. J. Gross, A. J. Downard, *Analytical Chemistry* **2011**, *83*, 2397-2402.
[263] E. Coulon, J. Pinson, J. Bourzat, A. Commerçon, J. P. Pulicani, *Langmuir* **2001**, *17*, 7102-7106.
[264] M. Toupin, D. Bélanger, *The Journal of Physical Chemistry C* **2007**, *111*, 5394-5401.
[265] M. Toupin, D. Belanger, *Langmuir* **2008**, *24*, 1910-1917.
[266] A. Pauric, B. MacLean, E. Easton, *Journal of The Electrochemical Society* **2011**, *158*, B331-B336.
[267] J. Lyskawa, A. Grondein, D. Bélanger, *Carbon* **2010**, *48*, 1271-1278.
[268] B. Bath, H. Martin, R. Wightman, M. Anderson, *Langmuir* **2001**, *17*, 7032-7039.
[269] T. Matrab, M. N. Nguyen, S. Mahouche, P. Lang, C. Badre, M. Turmine, G. Girard, J. Bai, M. M. Chehimi, *The Journal of Adhesion* **2008**, *84*, 684.
[270] J. L. Bahr, J. Yang, D. V. Kosynkin, M. J. Bronikowski, R. E. Smalley, J. M. Tour, *Journal of the American Chemical Society* **2001**, *123*, 6536-6542.
[271] C. Dyke, M. Stewart, F. Maya, J. Tour, *Synlett* **2004**, 155-160.
[272] P. Marcoux, P. Hapiot, P. Batail, J. Pinson, *New Journal of Chemistry* **2004**, *28*, 302-307.
[273] C. Dyke, J. Tour, *Chemistry - A European Journal* **2004**, *10*, 813-817.
[274] O. de Fuentes, T. Ferri, M. Frasconi, V. Paolini, R. Santucci, *Angewandte Chemie*

International Edition **2011**, *50*, 3457-3461.
[275] F. Tasca, W. Harreither, R. Ludwig, J. Gooding, L. Gorton, *Analytical Chemistry* **2011**, *83*, 3042-3049.
[276] G. Pagona, N. Karousis, N. Tagmatarchis, *Carbon* **2008**, *46*, 604-610.
[277] N. Rubio, M. A. Herrero, M. Meneghetti, Á. Díaz-Ortiz, M. Schiavon, M. Prato, E. Vázquez, *J. Mater. Chem.* **2009**, *19*, 4407.
[278] Z. Li, S. Dai, *Chemistry of Materials* **2005**, *17*, 1717-1721.
[279] Z. Li, W. Yan, S. Dai, *Langmuir* **2005**, *21*, 11999-12006.
[280] R. Liu, X. Wang, X. Zhao, P. Feng, *Carbon* **2008**, *46*, 1664-1669.
[281] X. Liu, M. Huang, H. Ma, Z. Zhang, J. Gao, Y. Zhu, X. Han, X. Guo, *Molecules* **2010**, *15*, 7188-7196.
[282] J. Wang, J. Carlisle, *Diamond and Related Materials* **2006**, *15*, 279-284.
[283] T. Matrab, M. Chehimi, J. Boudou, F. Benedic, J. Wang, N. Naguib, J. Carlisle, *Diamond and Related Materials* **2006**, *15*, 639-644.
[284] S. Lud, M. Steenackers, R. Jordan, P. Bruno, D. Gruen, P. Feulner, J. Garrido, M. Stutzmann, *Journal of the American Chemical Society* **2006**, *128*, 16884-16891.
[285] Y. Zhong, K. Loh, A. Midya, Z. Chen, *Chemistry of Materials* **2008**, *20*, 3137-3144.
[286] D. Shin, N. Tokuda, B. Rezek, C. Nebel, *Electrochemistry Communications* **2006**, *8*, 844-850.
[287] Y. Zhou, J. Zhi, *Electrochemistry Communications* **2006**, *8*, 1811-1816.
[288] G. Shula, P. Actis, B. Marcus, M. Opallo, R. Boukherroub, S. Szunerits, *Diamond and Related Materials* **2008**, *17*, 1394-1398.
[289] C. Agnès, J. Arnault, F. Omnès, B. Jousselme, M. Billon, G. Bidan, P. Mailley, *Phys. Chem. Chem. Phys.* **2009**, *11*, 11647.
[290] A. Bongrain, H. Uetsuka, L. Rousseau, L. Valbin, S. Saada, C. Gesset, E. Scorsone, G. Lissorgues, P. Bergonzo, *Physica Status Solidi (a) Applications and Materials Science* **2010**, *207*, 2078-2083.
[291] C. Mangeney, Z. Qin, S. Dahoumane, A. Adenier, F. Herbst, J. Boudou, J. Pinson, M. Chehimi, *Diamond and Related Materials* **2008**, *17*, 1881-1887.
[292] S. A. Dahoumane, M. N. Nguyen, A. Thorel, J. Boudou, M. M. Chehimi, C. Mangeney, *Langmuir* **2009**, *25*, 9633-9638.
[293] Y. Liang, M. Ozawa, A. Krueger, *ACS Nano* **2009**, *3*, 2288-2296.
[294] Y. Liang, T. Meinhardt, G. Jarre, M. Ozawa, P. Vrdoljak, A. Scholl, F. Reinert, A. Krueger, *Journal of Colloid and Interface Science* **2011**, *354*, 23-30.
[295] N. Yang, H. Uetsuka, E. Osawa, C. Nebel, *Angewandte Chemie International Edition* **2008**, *47*, 5183-5185.
[296] A. Adenier, M. Bernard, M. M. Chehimi, E. Cabet-Deliry, B. Desbat, O. Fagebaume, J. Pinson, F. Podvorica, *Journal of the American Chemical Society* **2001**, *123*, 4541-4549.
[297] A. Chaussé, M. M. Chehimi, N. Karsi, J. Pinson, F. Podvorica, C. Vautrin-Ul, *Chemistry of Materials* **2002**, *14*, 392-400.
[298] M. Bernard, A. Chaussé, E. Cabet-Deliry, M. M. Chehimi, J. Pinson, F. Podvorica, C. Vautrin-Ul, *Chemistry of Materials* **2003**, *15*, 3450-3462.
[299] K. Boukerma, M. M. Chehimi, J. Pinson, C. Blomfield, *Langmuir* **2003**, *19*, 6333-6335.
[300] T. Matrab, M. M. Chehimi, C. Perruchot, A. Adenier, A. Guillez, M. Save, B. Charleux, E. Cabet-Deliry, J. Pinson, *Langmuir* **2005**, *21*, 4686-4694.
[301] A. Adenier, C. Combellas, F. Kanoufi, J. Pinson, F. I. Podvorica, *Chemistry of Materials* **2006**, *18*, 2021-2029.
[302] A. Adenier, N. Barré, E. Cabet-Deliry, A. Chaussé, S. Griveau, F. Mercier, J. Pinson, C. Vautrin-Ul, *Surface Science* **2006**, *600*, 4801-4812.

[303] P. Doppelt, G. Hallais, J. Pinson, F. Podvorica, S. Verneyre, *Chemistry of Materials* **2007**, *19*, 4570-4575.
[304] T. Matrab, M. Save, B. Charleux, J. Pinson, E. Cabet-deliry, A. Adenier, M. M. Chehimi, M. Delamar, *Surface Science* **2007**, *601*, 2357-2366.
[305] M. Ceccato, A. Bousquet, M. Hinge, S. U. Pedersen, K. Daasbjerg, *Chemistry of Materials* **2011**, *23*, 1551-1557.
[306] M. Kullapere, L. Matisen, A. Saar, V. Sammelselg, K. Tammeveski, *Electrochemistry Communications* **2007**, *9*, 2412-2417.
[307] G. Chamoulaud, D. Bélanger, *The Journal of Physical Chemistry C* **2007**, *111*, 7501-7507.
[308] B. Hurley, R. McCreery, *Journal of The Electrochemical Society* **2004**, *151*, B252-B259.
[309] M. Hinge, M. Ceccato, P. Kingshott, F. Besenbacher, S. U. Pedersen, K. Daasbjerg, *New J. Chem.* **2009**, *33*, 2405.
[310] F. Berger, J. Delhalle, Z. Mekhalif, *Electrochimica Acta* **2008**, *53*, 2852-2861.
[311] G. Liu, J. Liu, T. Bocking, P. Eggers, J. Gooding, *Chemical Physics* **2005**, *319*, 136-146.
[312] A. Ricci, C. Rolli, S. Rothacher, L. Baraldo, C. Bonazzola, E. J. Calvo, N. Tognalli, A. Fainstein, *J Solid State Electrochem* **2007**, *11*, 1511-1520.
[313] A. Benedetto, M. Balog, P. Viel, F. Le Derf, M. Sallé, S. Palacin, *Electrochimica Acta* **2008**, *53*, 7117-7122.
[314] D. M. Shewchuk, M. T. McDermott, *Langmuir* **2009**, *25*, 4556-4563.
[315] J. Lehr, B. E. Williamson, B. S. Flavel, A. J. Downard, *Langmuir* **2009**, *25*, 13503-13509.
[316] M. Khoshroo, A. A. Rostami, *Journal of Electroanalytical Chemistry* **2010**, *647*, 117-122.
[317] F. Mirkhalaf, J. Paprotny, D. J. Schiffrin, *Journal of the American Chemical Society* **2006**, *128*, 7400-7401.
[318] L. Laurentius, S. Stoyanov, S. Gusarov, A. Kovalenko, R. Du, G. Lopinski, M. McDermott, *ACS Nano* **2011**, *5*, 4219-4227.
[319] M. Stewart, F. Maya, D. Kosynkin, S. Dirk, J. Stapleton, C. McGuiness, D. Allara, J. Tour, *Journal of the American Chemical Society* **2004**, *126*, 370-378.
[320] V. Stockhausen, J. Ghilane, P. Martin, G. Trippé-Allard, H. Randriamahazaka, J. Lacroix, *Journal of the American Chemical Society* **2009**, *131*, 14920-14927.
[321] J. Ghilane, M. Delamar, M. Guilloux-Viry, C. Lagrost, C. Mangeney, P. Hapiot, *Langmuir* **2005**, *21*, 6422-6429.
[322] M. Janin, J. Ghilane, H. Randriamahazaka, J. Lacroix, *Electrochemistry Communications* **2009**, *11*, 647-650.
[323] A. A. Isbir-Turan, Z. Üstündag, A. O. Solak, E. KIlIç, A. Avseven, *Thin Solid Films* **2009**, *517*, 2871-2877.
[324] O. I. Covaci, B. Bucur, M. P. Bucur, G. L. Radu, *Microchim Acta* **2010**, *169*, 335-343.
[325] O. Covaci, B. Bucur, L. Galateanu, F. Craciunoiu, G. Radu, *Digest Journal of Nanomaterials and Biostructures* **2011**, *6*, 731-738.
[326] S. Maldonado, T. Smith, R. Williams, S. Morin, E. Barton, K. Stevenson, *Langmuir* **2006**, *22*, 2884-2891.
[327] A. J. Haque, K. Kim, *Langmuir* **2011**, *27*, 882-886.
[328] F. Mirkhalaf, T. J. Mason, D. J. Morgan, V. Saez, *Langmuir* **2011**, *27*, 1853-1858.
[329] M. Joselevich, F. J. Williams, *Langmuir* **2008**, *24*, 11711-11717.
[330] N. Griffete, F. Herbst, J. Pinson, S. Ammar, C. Mangeney, *Journal of the American Chemical Society* **2011**, *133*, 1646-1649.

[331] P. Allongue, C. de Villeneuve, J. Pinson, F. Ozanam, J. Chazalviel, X. Wallart, *Electrochimica Acta* **1998**, *43*, 2791-2798.
[332] P. Allongue, C. Henry de Villeneuve, J. Pinson, *Electrochimica Acta* **2000**, *45*, 3241-3248.
[333] P. Allongue, C. Henry de Villeneuve, G. Cherouvrier, R. Cortès, M. -. Bernard, *Journal of Electroanalytical Chemistry* **2003**, *550-551*, 161-174.
[334] J. Rappich, A. Merson, K. Roodenko, T. Dittrich, M. Gensch, K. Hinrichs, Y. Shapira, *The Journal of Physical Chemistry B* **2006**, *110*, 1332-1337.
[335] A. Güell, K. Roodenko, F. Yang, K. Hinrichs, M. Gensch, F. Sanz, J. Rappich, *Materials Science and Engineering: B* **2006**, *134*, 273-276.
[336] K. Roodenko, M. Gensch, J. Rappich, K. Hinrichs, N. Esser, R. Hunger, *The Journal of Physical Chemistry B* **2007**, *111*, 7541-7549.
[337] J. Rappich, K. Hinrichs, *Electrochemistry Communications* **2009**, *11*, 2316-2319.
[338] B. S. Flavel, D. J. Garrett, J. Lehr, J. G. Shapter, A. J. Downard, *Electrochimica Acta* **2010**, *55*, 3995-4001.
[339] G. Valenti, L. Bardini, D. Bonazzi, S. Rapino, M. Marcaccio, F. Paolucci, *Journal of Physical Chemistry C* **2010**, *114*, 22165-22170.
[340] G. Collins, P. Fleming, C. O'Dwyer, M. Morris, J. Holmes, *Chemistry of Materials* **2011**, *23*, 1883-1891.
[341] C. Combellas, F. Kanoufi, D. Mazouzi, A. Thiébault, P. Bertrand, N. Médard, *Polymer* **2003**, *44*, 19-24.
[342] G. Liu, M. S. Freund, *Chemistry of Materials* **1996**, *8*, 1164-1166.
[343] D. Acevedo, C. Rivarola, M. Miras, C. Barbero, *Electrochimica Acta* **2011**, *56*, 3468-3473.
[344] C. Andrieux, J. Pinson, *Journal of the American Chemical Society* **2003**, *125*, 14801-14806.
[345] D. Jiang, B. Sumpter, S. Dai, *Journal of the American Chemical Society* **2006**, *128*, 6030-6031.
[346] J. Lehr, B. Williamson, B. Flavel, A. Downard, *Langmuir* **2009**, *25*, 13503-13509.
[347] C. Combellas, M. Delamar, F. Kanoufi, J. Pinson, F. I. Podvorica, *Chemistry of Materials* **2005**, *17*, 3968-3975.
[348] F. I. Podvorica, F. Kanoufi, J. Pinson, C. Combellas, *Electrochimica Acta* **2009**, *54*, 2164-2170.
[349] S. Baranton, D. Bélanger, *The Journal of Physical Chemistry B* **2005**, *109*, 24401-24410.
[350] S. Baranton, D. Bélanger, *Electrochimica Acta* **2008**, *53*, 6961-6967.
[351] S. E. Creager, B. Liu, H. Mei, D. DesMarteau, *Langmuir* **2006**, *22*, 10747-10753.
[352] G. Liu, J. Gooding, *Langmuir* **2006**, *22*, 7421-7430.
[353] B. Jousselme, G. Bidan, M. Billon, C. Goyer, Y. Kervella, S. Guillerez, E. Abou Hamad, C. Goze-Bac, J. Mevellec, S. Lefrant, *Journal of Electroanalytical Chemistry* **2008**, *621*, 277-285.
[354] Y. Tsukahara, T. Wada, K. Tanaka, *Chemistry Letters* **2010**, *39*, 1134-1135.
[355] D. R. Laws, J. Sheats, A. L. Rheingold, W. E. Geiger, *Langmuir* **2010**, *26*, 15010-15021.
[356] C. Fave, Y. Leroux, Trippé, H. Randriamahazaka, V. Noel, J. Lacroix, *Journal of the American Chemical Society* **2007**, *129*, 1890-1891.
[357] C. Fave, V. Noel, J. Ghilane, G. Trippe-Allard, H. Randriamahazaka, J. Lacroix, *The Journal of Physical Chemistry C* **2008**, *112*, 18638-18643.
[358] D. Alamarguy, A. Benedetto, M. Balog, S. Noel, P. Viel, F. Le Derfc, F. Houze, M. Salle, S. Palacin, *Surface and Interface Analysis* **2008**, *40*, 802-805.

[359] K. Malmos, M. Dong, S. Pillai, P. Kingshott, F. Besenbacher, S. U. Pedersen, K. Daasbjerg, *Journal of the American Chemical Society* **2009**, *131*, 4928-4936.
[360] L. Nielsen, K. Vase, M. Dong, F. Besenbacher, S. Pedersen, K. Daasbjerg, *Journal of the American Chemical Society* **2007**, *129*, 1888-+.
[361] G. Liu, M. Paddon-Row, J. Gooding, *Electrochemistry Communications* **2007**, *9*, 2218-2223.
[362] A. Adenier, E. Cabet-Deliry, A. Chaussé, S. Griveau, F. Mercier, J. Pinson, C. Vautrin-Ul, *Chemistry of Materials* **2005**, *17*, 491-501.
[363] P. Abiman, G. Wildgoose, R. Compton, *Journal of Physical Organic Chemistry* **2008**, *21*, 433-439.
[364] M. P. Stewart, F. Maya, D. V. Kosynkin, S. M. Dirk, J. J. Stapleton, C. L. McGuiness, D. L. Allara, J. M. Tour, *Journal of the American Chemical Society* **2004**, *126*, 370-378.
[365] O. Fontaine, J. Ghilane, P. Martin, J. Lacroix, H. Randriamahazaka, *Langmuir* **2010**, *26*, 18542-18549.
[366] J. Pinson, B. Christophe, *Use of a Diazonium Salt in a Method for Modifying Insulating or Semi-Conductive Surfaces, and Resulting Products*, U.S. Patent EP1948720 (B1).
[367] G. Wildgoose, N. Lawrence, H. Leventis, L. Jiang, T. Jones, R. Compton, *Journal of Materials Chemistry* **2005**, *15*, 953-959.
[368] J. Liu, M. Zubiri, B. Vigolo, M. Dossot, B. Humbert, Y. Fort, E. Mcrae, *Journal of Nanoscience and Nanotechnology* **2007**, *7*, 3519-3523.
[369] J. Bahr, J. Tour, *Chemistry of Materials* **2001**, *13*, 3823-+.
[370] C. Mangeney, Z. Qin, S. A. Dahoumane, A. Adenier, F. Herbst, J. Boudou, J. Pinson, M. M. Chehimi, *Diamond and Related Materials* **2008**, *17*, 1881-1887.
[371] L. Q. Shi, T. Sun, F. Yu, S. Dong, F. L. Yuan, *Advanced Materials Research* **2009**, *60-61*, 406-409.
[372] A. Gui, G. Liu, M. Chockalingam, G. Le Saux, E. Luais, J. Harper, J. Gooding, *Electroanalysis* **2010**, *22*, 1824-1830.
[373] M. A. Ghanem, J. Chrétien, A. Pinczewska, J. D. Kilburn, P. N. Bartlett, *J. Mater. Chem.* **2008**, *18*, 4917.
[374] J. Lyskawa, D. Bélanger, *Chemistry of Materials* **2006**, *18*, 4755-4763.
[375] T. Breton, D. Bélanger, *Langmuir* **2008**, *24*, 8711-8718.
[376] C. Louault, M. D'Amours, D. Belanger, *ChemPhysChem* **2008**, *9*, 1164-1170.
[377] P. Verma, P. Maire, P. Novák, *Electrochimica Acta* **2011**, *56*, 3555-3561.
[378] A. Holm, R. Moller, K. Vase, M. Dong, K. Norrman, F. Besenbacher, S. Pedersen, K. Daasbjerg, *New Journal of Chemistry* **2005**, *29*, 659-666.
[379] L. T. Nielsen, M. Ceccato, A. H. Holm, M. V. Kristensen, S. U. Pedersen, K. Daasbjerg, *Langmuir* **2009**, *25*, 12160-12168.
[380] J. Chrétien, M. Ghanem, P. Bartlett, J. Kilburn, *Chemistry - A European Journal* **2008**, *14*, 2548-2556.
[381] Z. Üstündag, A. O. Solak, *Electrochimica Acta* **2009**, *54*, 6426-6432.
[382] B. Chen, M. Lu, A. Flatt, F. Maya, J. Tour, *Chemistry of Materials* **2008**, *20*, 61-64.
[383] B. Chen, A. Flatt, H. Jian, J. Hudson, J. Tour, *Chemistry of Materials* **2005**, *17*, 4832-4836.
[384] X. Joyeux, P. Mangiagalli, J. Pinson, *Advanced Materials* **2009**, *21*, 4404-+.
[385] B. Flavel, D. Garrett, J. Lehr, J. Shapter, A. Downard, *Electrochimica Acta* **2010**, *55*, 3995-4001.
[386] K. Constantopoulos, C. Shearer, A. Ellis, N. Voelcker, J. Shapter, *Advanced Materials* **2010**, *22*, 557-571.
[387] O. de Fuentes, T. Ferri, M. Frasconi, V. Paolini, R. Santucci, *Angewandte Chemie*

International Edition **2011**, *50*, 3457-3461.
[388] J. Harnisch, A. Pris, M. Porter, *Journal of the American Chemical Society* **2001**, *123*, 5829-5830.
[389] J. Shi, X. Li, Y. Hu, Y. Hua, *Journal of Solid State Electrochemistry* **2008**, *12*, 1555-1559.
[390] P. Urchaga, M. Weissmann, S. Baranton, T. Girardeau, C. Coutanceau, *Langmuir* **2009**, *25*, 6543-6550.
[391] J. Noel, D. Zigah, J. Simonet, P. Hapiot, *Langmuir* **2010**, *26*, 7638-7643.
[392] C. Combellas, F. Kanoufi, J. Pinson, F. I. Podvorica, *Journal of the American Chemical Society* **2008**, *130*, 8576-8577.
[393] K. Malmos, J. Iruthayaraj, S. U. Pedersen, K. Daasbjerg, *Journal of the American Chemical Society* **2009**, *131*, 13926-13927.
[394] C. Combellas, D. Jiang, F. Kanoufi, J. Pinson, F. I. Podvorica, *Langmuir* **2009**, *25*, 286-293.
[395] J. Ghilane, P. Martin, O. Fontaine, J. Lacroix, H. Randriamahazaka, *Electrochemistry Communications* **2008**, *10*, 1060-1063.
[396] P. A. Brooksby, A. J. Downard, *Langmuir* **2005**, *21*, 1672-1675.
[397] A. Downard, D. Garrett, E. Tan, *Langmuir* **2006**, *22*, 10739-10746.
[398] J. Lehr, D. Garrett, M. Paulik, B. Flavel, P. Brooksby, B. Williamson, A. Downard, *Analytical Chemistry* **2010**, *82*, 7027-7034.
[399] J. Charlier, S. Palacin, J. Leroy, D. Del Frari, L. Zagonel, N. Barrett, O. Renault, A. Bailly, D. Mariolle, *J. Mater. Chem.* **2008**, *18*, 3136.
[400] B. P. Corgier, D. Bélanger, *Langmuir* **2010**, *26*, 5991-5997.
[401] C. Cougnon, F. Gohier, D. Bélanger, J. Mauzeroll, *Angewandte Chemie International Edition* **2009**, *48*, 4006-4008.
[402] M. Coates, E. Cabet, S. Griveau, T. Nyokong, F. Bedioui, *Electrochemistry Communications* **2011**, *13*, 150-153.
[403] M. Pandurangappa, T. Ramakrishnappa, *Materials Chemistry and Physics* **2010**, *122*, 567-573.
[404] N. Yang, J. Yu, H. Uetsuka, C. E. Nebel, *Electrochemistry Communications* **2009**, *11*, 2237-2240.
[405] M. D'Amour, D. Bélanger, *The Journal of Physical Chemistry B* **2003**, *107*, 4811-4817.
[406] J. K. Kariuki, M. T. McDermott, *Langmuir* **2001**, *17*, 5947-5951.
[407] Y. Liu, R. L. McCreery, *Analytical Chemistry* **1997**, *69*, 2091-2097.
[408] F. Anariba, U. Viswanathan, D. Bocian, R. McCreery, *Analytical Chemistry* **2006**, *78*, 3104-3112.
[409] P. A. Brooksby, A. J. Downard, *Langmuir* **2004**, *20*, 5038-5045.
[410] F. Tanguy, J. Gaubicher, A. Gaillot, D. Guyomard, J. Pinson, *Journal of Materials Chemistry* **2009**, *19*, 4771.
[411] C. Combellas, F. Kanoufi, J. Pinson, F. I. Podvorica, *Langmuir* **2005**, *21*, 280-286.
[412] A. Adenier, E. Cabet-Deliry, T. Lalot, J. Pinson, F. Podvorica, *Chemistry of Materials* **2002**, *14*, 4576-4585.
[413] T. Shimura, K. Aramaki, *Corrosion Science* **2006**, *48*, 3784-3801.
[414] J. Marwan, T. Addou, D. Belanger, *Chemistry of Materials* **2005**, *17*, 2395-2403.
[415] D. Guo, H. Li, *Carbon* **2005**, *43*, 1259-1264.
[416] M. Alonso-Lomillo, O. Rudiger, A. Maroto-Valiente, M. Velez, I. Rodriguez-Ramos, F. Munoz, V. Fernandez, A. De Lacey, *Nano Letters* **2007**, *7*, 1603-1608.
[417] M. Pita, C. Gutierrez-Sanchez, D. Olea, M. Velez, C. Garcia-Diego, S. Shleev, V. M. Fernandez, A. L. De Lacey, *The Journal of Physical Chemistry C* **2011**, DOI 10.1021/jp203643h.

[418] D. Aswal, S. Koiry, B. Jousselme, S. Gupta, S. Palacin, J. Yakhmi, *Physica E: Low-dimensional Systems and Nanostructures* **2009**, *41*, 325-344.
[419] R. McCreery, A. Bergren, *Advanced Materials* **2009**, *21*, 4303-4322.
[420] A. Scott, D. Janes, C. Risko, M. Ratner, *Applied Physics Letters* **2007**, *91*, DOI 10.1063/1.2750516.
[421] S. Koiry, D. Aswal, B. Jousselme, C. Majumdar, S. Gupta, S. Palacin, J. Yakhmi, *Chemical Physics Letters* **2010**, *493*, 135-140.
[422] W. Zhao, B. Tong, Y. Pan, J. Shen, J. Zhi, J. Shi, Y. Dong, *Langmuir* **2009**, *25*, 11796-11801.
[423] Y. Pan, B. Tong, J. Shi, W. Zhao, J. Shen, J. Zhi, Y. Dong, *The Journal of Physical Chemistry C* **2010**, *114*, 8040-8047.
[424] M. Weissmann, S. Baranton, J. Clacens, C. Coutanceau, *Carbon* **2010**, *48*, 2755-2764.
[425] A. Le Goff, V. Artero, B. Jousselme, P. Tran, N. Guillet, R. Metaye, A. Fihri, S. Palacin, M. Fontecave, *Science* **2009**, *326*, 1384-1387.
[426] P. Urchaga, M. Weissmann, S. Baranton, T. Girardeau, C. Coutanceau, *Langmuir* **2009**, *25*, 6543-6550.
[427] S. Ghosh, C. Rao, *Nano Research* **2009**, *2*, 183-191.
[428] J. Gooding, *Electroanalysis* **2008**, *20*, 573-582.
[429] L. Civit, H. Nassef, A. Fragoso, C. O'Sullivan, *Journal of Agricultural and Food Chemistry* **2008**, *56*, 10452-10455.
[430] M. Makos, D. Omiatek, A. Ewing, M. Heien, *Langmuir* **2010**, *26*, 10386-10391.
[431] A. Kowalczyk, A. Nowicka, R. Jurczakowski, M. Fau, A. Krolikowska, Z. Stojek, *Biosensors and Bioelectronics* **2011**, *26*, 2506-2512.
[432] A. Hermans, A. Seipel, C. Miller, R. Wightman, *Langmuir* **2006**, *22*, 1964-1969.
[433] S. Betelu, C. Vautrin-Ul, A. Chaussé, *Electrochemistry Communications* **2009**, *11*, 383-386.
[434] S. Betelu, C. Vautrin-Ul, J. Ly, A. Chausse, *Talanta* **2009**, *80*, 372-376.
[435] A. Radi, X. Munoz-Berbel, M. Cortina-Puig, J. Marty, *Electroanalysis* **2009**, *21*, 1624-1629.
[436] M. Cortina-Puig, X. Munoz-Berbel, C. Calas-Blanchard, J. Marty, *Microchimica Acta* **2010**, *171*, 187-193.
[437] M. Alonso-Lomillo, O. Dominguez-Renedo, P. Matos, M. Arcos-Martinez, *Analytica Chimica Acta* **2010**, *665*, 26-31.
[438] M. Radulescu, A. Chira, M. Radulescu, B. Bucur, M. Bucur, G. Radu, *Sensors* **2010**, *10*, 11340-11351.
[439] F. Li, Y. Feng, P. Dong, L. Yang, B. Tang, *Biosensors & Bioelectronics* **2011**, *26*, 1947-1952.
[440] C. Gurtner, A. Wun, M. Sailor, *Angewandte Chemie International Edition* **1999**, *38*, 1966-1968.
[441] M. M. Chehimi, G. Hallais, T. Matrab, J. Pinson, F. I. Podvorica, *The Journal of Physical Chemistry C* **2008**, *112*, 18559-18565.
[442] C. Combellas, F. Kanoufi, Z. Osman, J. Pinson, A. Adenier, G. Hallais, *Electrochimica Acta* **2010**, *In Press, Accepted Manuscript*, DOI 10.1016/j.electacta.2010.10.062.
[443] F. Hui, J. Noel, P. Poizot, P. Hapiot, J. Simonet, *Langmuir* **2011**, *27*, 5119-5125.
[444] J. Simonet, *Electrochemistry Communications* **2010**, *In Press, Accepted Manuscript*, DOI 10.1016/j.elecom.2010.10.021.
[445] S. Palacin, C. Bureau, J. Charlier, G. Deniau, B. Mouanda, P. Viel, *ChemPhysChem* **2004**, *5*, 1469-1481.
[446] S. Gabriel, R. Jérôme, C. Jérôme, *Progress in Polymer Science* **2009**, *35*, 113-140.
[447] M. Cecius, R. Jérôme, C. Jérôme, *Macromolecular Rapid Communications* **2007**, *28*,

948-954.
[448] S. Cuenot, S. Gabriel, R. Jerome, C. Jerome, C. Fustin, A. Jonas, A. Duwez, *Macromolecules* **2006**, *39*, 8428-8433.
[449] G. Deniau, L. Azoulay, L. Bougerolles, S. Palacin, *Chemistry of Materials* **2006**, *18*, 5421-5428.
[450] L. Tessier, G. Deniau, B. Charleux, S. Palacin, *Chemistry of Materials* **2009**, *21*, 4261-4274.
[451] V. Mévellec, S. Roussel, L. Tessier, J. Chancolon, M. Mayne-L'Hermite, G. Deniau, P. Viel, S. Palacin, *Chemistry of Materials* **2007**, *19*, 6323-6330.
[452] F. Grisotto, A. Ghorbal, C. Goyer, J. Charlier, S. Palacin, *Chemistry of Materials* **2011**, *23*, 1396-1405.
[453] P. Viel, S. Palacin, F. Descours, C. Bureau, F. Le Derf, J. Lyskawa, M. Salle, *Applied Surface Science* **2003**, *212*, 792-796.
[454] A. Benedetto, P. Viel, S. Noel, N. Izard, P. Chenevier, S. Palacin, *Surface Science* **2007**, *601*, 3687-3692.
[455] A. Mesnage, G. Deniau, L. Tessier, V. Mevellec, S. Palacin, *Applied Surface Science* **2011**, *257*, 7805-7812.
[456] S. Voccia, M. Ignatova, R. Jérôme, C. Jérôme, *Langmuir* **2006**, *22*, 8607-8613.
[457] M. Ignatova, S. Voccia, S. Gabriel, B. Gilbert, D. Cossement, R. Jérôme, C. Jérôme, *Langmuir* **2009**, *25*, 891-902.
[458] A. Charlot, S. Gabriel, C. Detrembleur, R. Jérôme, C. Jérôme, *Chemical Communications* **2007**, 4656-4658.
[459] S. Gabriel, A. Duwez, R. Jérôme, C. Jérôme, *Langmuir* **2007**, *23*, 159-161.
[460] E. Park, G. Carroll, N. Turro, J. Koberstein, *Soft Matter* **2009**, *5*, 36-50.
[461] X. Wang, E. C. Landis, R. Franking, R. J. Hamers, *Accounts of Chemical Research* **2010**, *43*, 1205-1215.
[462] T. Strother, T. Knickerbocker, Russell, J. E. Butler, L. M. Smith, R. J. Hamers, *Langmuir* **2002**, *18*, 968-971.
[463] T. Lasseter, B. Clare, N. Abbott, R. Hamers, *Journal of the American Chemical Society* **2004**, *126*, 10220-10221.
[464] X. Wang, P. Colavita, K. Metz, J. Butler, R. Hamers, *Langmuir* **2007**, *23*, 11623-11630.
[465] P. Colavita, B. Sun, K. Tse, R. Hamers, *Journal of Vacuum Science & Technology A* **2008**, *26*, 925-931.
[466] H. Kim, P. E. Colavita, K. M. Metz, B. M. Nichols, B. Sun, J. Uhlrich, X. Wang, T. F. Kuech, R. J. Hamers, *Langmuir* **2006**, *22*, 8121-8126.
[467] R. L. Cicero, M. R. Linford, C. E. D. Chidsey, *Langmuir* **2000**, *16*, 5688-5695.
[468] R. L. Cicero, C. E. D. Chidsey, G. P. Lopinski, D. D. M. Wayner, R. A. Wolkow, *Langmuir* **2002**, *18*, 305-307.
[469] X. Wang, R. E. Ruther, J. A. Streifer, R. J. Hamers, *Journal of the American Chemical Society* **2010**, *132*, 4048-4049.
[470] Q. Sun, L. de Smet, B. van Lagen, M. Giesbers, P. Thune, J. van Engelenburg, F. de Wolf, H. Zuilhof, E. Sudholter, *Journal of the American Chemical Society* **2005**, *127*, 2514-2523.
[471] L. de Smet, A. Pukin, Q. Sun, B. Eves, G. Lopinski, G. Visser, H. Zuilhof, E. Sudholter, *Applied Surface Science* **2005**, *252*, 24-30.
[472] C. Hacker, K. Anderson, L. Richter, C. Richter, *Langmuir* **2005**, *21*, 882-889.
[473] J. Streifer, H. Kim, B. Nichols, R. Hamers, *Nanotechnology* **2005**, *16*, 1868-1873.
[474] T. Ha, M. Park, H. Park, J. Choi, G. Kim, M. Hyun, B. Chung, *Chemical Communications* **2007**, 1611-1613.

[475] J. ter Maat, R. Regeling, M. Yang, M. N. Mullings, S. F. Bent, H. Zuilhof, *Langmuir* **2009**, *25*, 11592-11597.
[476] R. J. Clark, M. K. M. Dang, J. G. C. Veinot, *Langmuir* **2010**, *26*, 15657-15664.
[477] G. Leem, S. Zhang, A. Jamison, E. Galstyan, I. Rusakova, B. Lorenz, D. Litvinov, T. Lee, *ACS Applied Materials & Interfaces* **2010**, *2*, 2789-2796.
[478] M. A. Harmer, *Langmuir* **1991**, *7*, 2010-2012.
[479] M. Yan, S. Cai, M. Wybourne, J. Keana, *Journal of the American Chemical Society* **1993**, *115*, 814-816.
[480] C. Henneuse-Boxus, E. Duliere, J. Marchand-Brynaert, *European Polymer Journal* **2001**, *37*, 9-18.
[481] M. Ulbricht, H. Hicke, *Angewandte Makromolekulare Chemie* **1993**, *210*, 69-95.
[482] J. Jia, G. Baker, *Journal of Polymer Science Part B: Polymer Physics* **1998**, *36*, 959-968.
[483] J. Mosnacek, M. Bertoldo, C. Kosa, C. Cappelli, G. Ruggeri, I. Lakac, F. Ciardelli, *Polymer Degradation and Stability* **2007**, *92*, 849-858.
[484] T. Matsuda, T. Sugawara, *Journal of Biomedical Materials Research* **1995**, *29*, 749-756.
[485] G. Wu, F. Shi, Z. Wang, Z. Liu, X. Zhang, *Langmuir* **2009**, *25*, 2949-2955.
[486] J. Koh, J. Koh, N. Park, J. Kim, *Solar Energy Materials and Solar Cells* **2010**, *94*, 436-441.
[487] R. Revanur, B. McCloskey, K. Breitenkamp, B. Freeman, T. Emrick, *Macromolecules* **2007**, *40*, 3624-3630.
[488] G. Li, H. Zheng, Y. Wang, H. Wang, Q. Dong, R. Bai, *Polymer* **2010**, *51*, 1940-1946.
[489] S. Knaus, A. Nennadal, B. Froschauer, *Macromolecular Symposia* **2001**, *176*, 223-232.
[490] C. Mao, W. Zhao, C. Zhu, A. Zhu, J. Shen, S. Lin, *Carbohydrate Polymers* **2005**, *59*, 19-25.
[491] A. Zhu, Z. Ming, S. Jian, *Applied Surface Science* **2005**, *241*, 485-492.
[492] S. Chin, P. Pantano, *Microchemical Journal* **2006**, *84*, 1-9.
[493] L. Renaudie, C. Le Narvor, E. Lepleux, P. Roger, *Biomacromolecules* **2007**, *8*, 679-685.
[494] P. Bohme, H. Hicke, C. Boettcher, J. Fuhrhop, *Journal of the American Chemical Society* **1995**, *117*, 5824-5826.
[495] S. Knaus, A. Nennadal, *Macromolecular Symposia* **1998**, *127*, 257-263.
[496] A. P. van der Heiden, D. Goebbels, A. P. Pijpers, L. H. Koole, *J. Biomed. Mater. Res.* **1997**, *37*, 282-290.
[497] C. Salvagnini, A. Roback, M. Momtaz, V. Pourcelle, J. Marchand-Brynaert, *Journal of Biomaterials Science - Polymer Edition* **2007**, *18*, 1491-1516.
[498] P. Roger, L. Renaudie, C. Le Narvor, B. Lepoittevin, L. Bech, M. Brogly, *European Polymer Journal* **2010**, *46*, 1594-1603.
[499] G. Li, H. Wang, H. Zheng, R. Bai, *Langmuir* **2010**, *26*, 7529-7534.
[500] J. Mecomber, R. Murthy, S. Rajam, P. Singh, A. Gudmundsdottir, P. Limbach, *Langmuir* **2008**, *24*, 3645-3653.
[501] R. Png, P. Chia, J. Tang, B. Liu, S. Sivaramakrishnan, M. Zhou, S. Khong, H. Chan, J. Burroughes, L. Chua, et al., *Nature Materials* **2010**, *9*, 152-158.
[502] L. Liu, M. Yan, *Accounts of Chemical Research* **2010**, *43*, 1434-1443.
[503] A. J. Gross, S. S. C. Yu, A. J. Downard, *Langmuir* **2010**, *26*, 7285-7292.
[504] S. Khong, S. Sivaramakrishnan, R. Png, L. Wong, P. Chia, L. Chua, P. Ho, *Advanced Functional Materials* **2007**, *17*, 2490-2499.

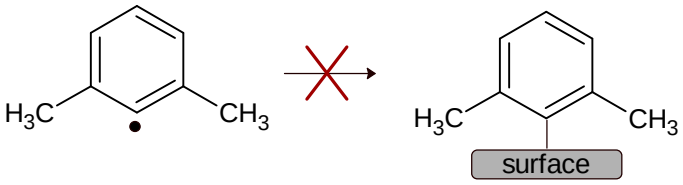
Chapter 2

Indirect Grafting of Acetonitrile-Derived Films on Metallic Substrates

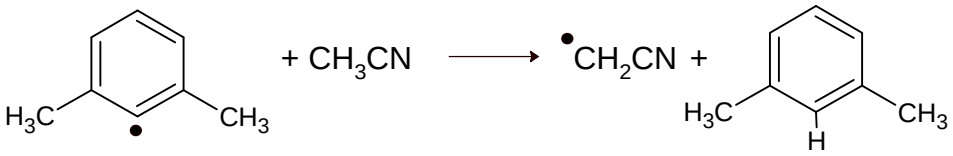
Chapter 2 : Indirect Grafting of Acetonitrile-Derived Films on Metallic Substrates

2.1. Introduction

Before this work was started, it had been shown that the 2,6-dimethylbenzenediazonium (2,6-DMBD) cannot be grafted on surfaces due to the steric hindrance of the two methyl groups ortho to the carbon radical[1].



Among the reactions of radicals, dimerization and H-atom abstraction are often observed. Under the conditions (diazonium salt concentration ≤ 100 mM) where the latter radical is formed, dimerization – a second order reaction- is certainly not favored. But hydrogen atom abstraction from the solvent:



is certainly an important reaction due to the high concentration of the solvent (~ 17 M). This hydrogen atom abstraction produces a new alkyl radical. The following paper tries to answer the question: is the cyanomethyl radical produced under H-atom abstraction able to react with surfaces?

The prospects for such a grafting reaction to occur are good as it had been shown previously that this same radical obtained upon cathodic reduction of ICH_2CN[2] could attach to surfaces.

Main results

- The reaction is indeed possible on various metals and on silicon.
- The formation of this layer is also possible without an electrochemical induction in the case of copper.
- The layers are fully characterized: functionality of the layer (IRRAS), surface hydrophobicity/hydrophilicity (contact angle), thickness (ellipsometry, profilometry or SEM), layer image (SEM), chemical composition (Tof-SIMS).
- A grafting mechanism is proposed accounting for the formation of the layer.

[1] C. Combellas, D. Jiang, F. Kanoufi, J. Pinson, F. I. Podvorica, Langmuir **2009**, *25*, 286.

[2] C.Combellas, F.Kanoufi,Z.Osman, J.Pinson, A. Adenier, G. Hallais, Electrochimica Acta **2011,** *56*, 1476.

2962 *Chem. Mater.* **2010,** *22,* 2962–2969
DOI:10.1021/cm100295n

CHEMISTRY OF MATERIALS
Article

Indirect Grafting of Acetonitrile-Derived Films on Metallic Substrates

Avni Berisha,[†,‡] Catherine Combellas,[†] Frédéric Kanoufi,[†] Jean Pinson,[†] Stéphane Ustaze,[§] and Fetah I. Podvorica*[,†,‡]

[†]*Physico-Chimie des Electrolytes, des Colloides et Sciences Analytiques, ESPCI ParisTech, CNRS UMR 7195, 10 rue Vauquelin, 75231 Paris Cedex 05, France,* [‡]*Chemistry Department of Natural Sciences Faculty, University of Prishtina, rr. "Nëna Tereze" nr. 5, 10 000 Prishtina, Kosovo, and* [§]*Alchimer, 15 rue du Buisson aux Fraises, 91300, Massy, France*

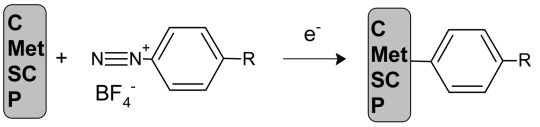
Received January 29, 2010. Revised Manuscript Received March 17, 2010

Strongly bonded organic films with amino groups are obtained on gold, copper, and silicon surfaces by reduction of 2,6-dimethyl benzenediazonium in acetonitrile (ACN). The sterically hindered 2,6-dimethylphenyl radical is unable to attach to the surface, but it abstracts an hydrogen atom from ACN to give the cyanomethyl radical ($\cdot CH_2CN$) that reacts with the surface. A spontaneous reaction is also possible on copper. The film is characterized by IR spectroscopy, scanning electron microscopy, ellipsometry, water contact angles, and cyclic voltammetry. A mechanism is elaborated that accounts for the formation, grafting of the cyanomethyl radical, and finally formation of amino multilayers.

Introduction

The reduction of aryl diazonium[1−7] and diaryliodonium[8] salts on various materials provides an easy method to ensure the covalent bonding of aryl layers to surfaces. The key point is the formation of aryl radicals, either by electrochemistry, or spontaneously[1b] (through a dissociative electron transfer and N_2 evolution[9]), or in the presence of an added reducing agent.[10] Once produced in aprotic or aqueous media, part of those aryl radicals reacts with carbon,[2b] metal,[2h] semiconductor,[2d] and polymer[10b] surfaces according to Scheme 1.

Scheme 1



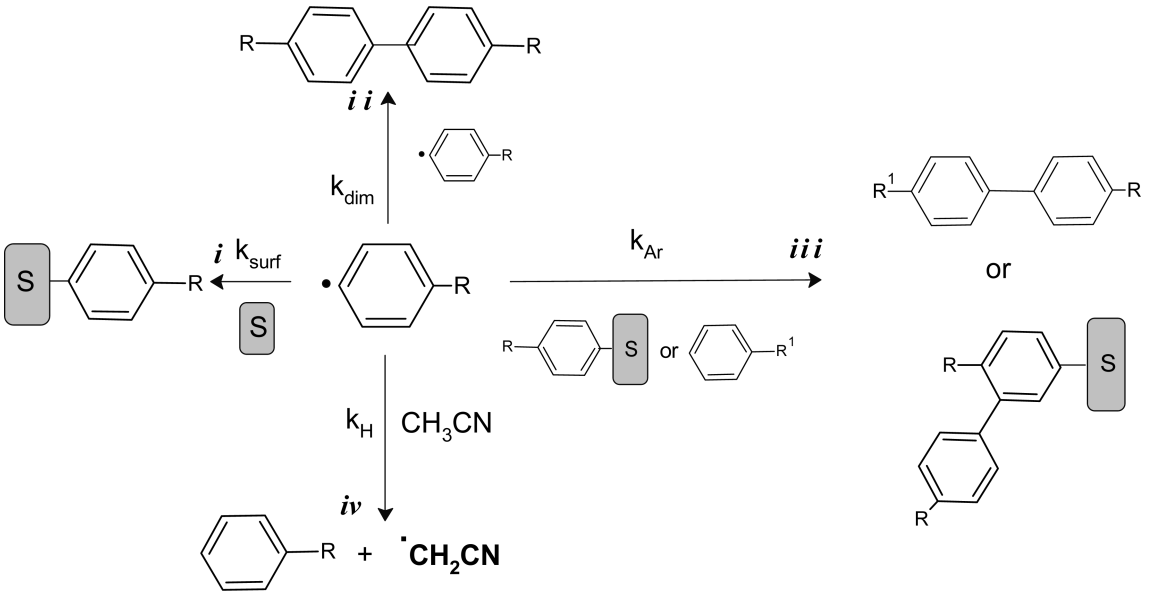
C =Carbon, Met =Metal, SC = Semiconductor, P=Polymer

*Corresponding author. E-mail: fetah.podvorica@fshmn.uni-pr.edu.

(1) (a) Pinson, J.; Podvorica, F. *Chem. Soc. Rev.* **2005**, *34*, 429. (b) Barrière, F.; Downard, A. *J. Solid State Electrochem.* **2008**, *12*, 1231. (c) McCreery, R., L. *Chem. Rev.* **2008**, *108*, 2646. (d) Gooding, J. J. *Electroanalysis* **2008**, *20*, 582.
(2) (a) Delamar, M.; Hitmi, R.; Pinson, J.; Savéant, J.-M. *J. Am. Chem. Soc.* **1992**, *114*, 5883. (b) Allongue, P.; Delamar, M.; Desbat, B.; Fagebaume, O.; Hitmi, R.; Pinson, J.; Savéant, J.-M. *J. Am. Chem. Soc.* **1997**, *119*, 201. (c) Henry de Villeneuve, C.; Pinson, J.; Bernard, M. C.; Allongue, P. *J. Phys. Chem. B* **1997**, *101*, 2415. (d) Allongue, P.; Henry de Villeneuve, C.; Pinson, J.; Ozanam, F.; Chazalviel, J. N.; Wallart, X. *Electrochim. Acta* **1998**, *43*, 2791. (e) Adenier, A.; Bernard, M. C.; Chehimi, M. M.; Cabet-Deliry, E.; Desbat, B.; Fagebaume, O.; Pinson, J.; Podvorica, F. *J. Am. Chem. Soc.* **2001**, *123*, 4541. (f) Chaussé, A.; Chehimi, M. M.; Karsi, N.; Pinson, J.; Podvorica, F.; Vautrin-Ul, C. *Chem. Mater.* **2002**, *14*, 392. (g) Adenier, A.; Cabet-Deliry, E.; Lalot, T.; Pinson, J.; Podvorica, F. *Chem. Mater.* **2002**, *14*, 4576. (h) Bernard, M. C.; Chaussé, A.; Cabet-Deliry, E.; Chehimi, M. M.; Pinson, J.; Podvorica, F.; Vautrin-Ul, C. *Chem. Mater.* **2003**, *15*, 3450. (i) Allongue, P.; Henry de Villeneuve, C.; Cherouvrier, G.; Cortes, R. *J. Electroanal. Chem.* **2003**, *550*, 161. (j) Combellas, C.; Kanoufi, F.; Pinson, J.; Podvorica, F. I. *Langmuir* **2005**, *21*, 280. (k) Adenier, A.; Cabet-Deliry, E.; Chaussé, A.; Griveau, S.; Mercier, F.; Pinson, J.; Vautrin-Ul, C. *Chem. Mater.* **2005**, *17*, 491. (l) Combellas, C.; Kanoufi, F.; Pinson, J.; Podvorica, F. I. *Chem. Mater.* **2005**, *17*, 3968. (m) Combellas, C.; Kanoufi, F.; Pinson, J.; Podvorica, F. I. *Chem. Mater.* **2006**, *18*, 2021. (n) Adenier, A.; Barré, N.; Cabet-Deliry, E.; Chaussé, A.; Griveau, S.; Mercier, F.; Pinson, J.; Vautrin-Ul, C. *Surf. Sci.* **2006**, *600*, 4801. (o) Podvorica, F. I.; Kanoufi, F.; Pinson, J.; Combellas, C. *Electrochim. Acta* **2009**, *54*, 2164.
(3) (a) Liu, Y. C.; McCreery, R. L. *J. Am. Chem. Soc.* **1995**, *117*, 11254. (b) Liu, Y. C.; McCreery, R. L. *Anal. Chem.* **1997**, *69*, 2091. (c) DuVall, S. H.; McCreery, R. L. *J. Am. Chem. Soc.* **2000**, *122*, 6759. (d) Ranganathan, S.; Steidel, I.; Anariba, F.; McCreery, R. L. *Nano Lett.* **2001**, *1*, 491. (e) Itoh, T.; McCreery, R. L. *J. Am. Chem. Soc.* **2002**, *124*, 1089. (f) Anariba, F.; DuVall, S. H.; McCreery, R. L. *Anal. Chem.* **2003**, *75*, 3837. (g) Hurley, B. L.; McCreery, R. L. *J. Electrochem. Soc.* **2004**, *151*, B252. (h) Anariba, F.; Viswanathan, U.; Bocian, D. F.; McCreery, R. L. *Anal. Chem.* **2006**, *78*, 3104. (i) Mahmoud, A. M.; Bergren, A. J.; McCreery, R. L. *Anal. Chem.* **2009**, *81*, 6972.
(4) (a) Saby, C.; Ortiz, B.; Champagne, G. Y.; Bélanger, D. *Langmuir* **1997**, *13*, 3837. (b) D'Amours, M.; Bélanger, D. *J. Phys. Chem B* **2003**, *107*, 4811. (c) Baranton, S.; Bélanger, D. *J. Phys. Chem B* **2005**, *109*, 24401. (d) Chamoulaud, G.; Bélanger, D. *Langmuir* **2004**, *20*, 4989. (e) Toupin, B.; Bélanger, D. *Langmuir* **2008**, *24*, 1910. (f) Cougnon, C.; Mauzeroll, J.; Bélanger, D. *Angew. Chem., Int. Ed.* **2009**, *48*, 7395.
(5) (a) Downard, A. J. *Langmuir* **2000**, *16*, 9680. (b) Downard, A. J.; Prince, M. J. *Langmuir* **2001**, *17*, 5581. (c) Brooksby, P. A.; Downard, A. J. *Langmuir* **2004**, *20*, 5038. (d) Paulik, M. G.; Brooksby, P. A.; Abell, A. D.; Downard, A. J. *J. Phys. Chem. C* **2007**, *111*, 7808. (e) Downard, A. J.; Garrett, D. J.; Tan, E. S. Q. *Langmuir* **2006**, *22*, 10739. (f) Lehr, J.; Williamson, B. E.; Flavel, B. S.; Downard, A. J. *Langmuir* **2009**, *25*, 13503.
(6) (a) Nielsen, L. T.; Vase, K. H.; Dong, M.; Besenbacher, F.; Pedersen, S. U.; Daasbjerg, K. *J. Am. Chem. Soc.* **2007**, *129*, 1888. (b) Peng, Z.; Holm, A. H.; Nielsen, L. T.; Pedersen, S. U.; Daasbjerg, K. *Chem. Mater.* **2008**, *20*, 6068. (c) Malmos, K.; Iruthayaraj, J.; Pedersen, S. U.; Daasbjerg, K. *J. Am. Chem. Soc.* **2009**, *131*, 13926.
(7) (a) Kariuki, J. K.; McDermott, M. T. *Langmuir* **1999**, *15*, 6534. (b) Kariuki, J. K.; McDermott, M. T. *Langmuir* **2001**, *17*, 5947. (c) Shewchuk, D. M.; McDermott, M. T. *Langmuir* **2009**, *25*, 4556.
(8) (a) Vase, K. H.; Holm, A. H.; Norman, K.; Pedersen, S. U.; Daasbjerg, K. *Langmuir* **2007**, *23*, 3786. (b) Matrab, T.; Combellas, C.; Kanoufi, F. *Electrochem. Commun.* **2008**, *10*, 1230.
(9) Andrieux, C.; Pinson, J. *J. Am. Chem. Soc.* **2003**, *125*, 14801.
(10) (a) Wildgoose, G. G.; Pandurangappa, M.; Lawrence, N. S.; Jiang, L.; Jones, T. G. J.; Compton, R. G. *Talanta* **2003**, *60*, 887. (b) Bureau, C.; Pinson, J. Fr Pat 0510914, PCT WO2007048894 (to Alchimer).

Published on Web 03/31/2010
© 2010 American Chemical Society

Scheme 2



In an ACN solution, the aryl radicals generated from diazonium salts can undergo various reactions that are presented in Scheme 2: (i) electrografting with the surface (k_{surf}), (ii) dimerization in solution (k_{dim}), (iii) reaction with another aromatic group (either from an aromatic compound in the solution or already grafted onto the surface) to give dimers or oligomers in solution or attached to the surface (k_{Ar}, Gomberg−Bachmann[11] reaction that involves a cyclohexadienyl intermediate), and (iv) abstraction of an hydrogen atom from the solvent, ACN, to give the cyanomethyl radical $\cdot CH_2CN$ (k_H).[12]

If we consider only the reactions with the surface (i and iii), the reduction of diazonium salts (by electrochemistry, a reducing agent, or a reducing surface) provides aryl radicals that for one part react with the surface, and for the other part attack the first attached aryl groups, leading to the growth of a polyphenylene film.[13] Previously, we showed that the steric hindrance is one of the parameters that controls the polyphenylene film growth: the two bulky *tert*-butyl groups of 3,5- di *tert*-butyl benzenediazonium prevent the growth of the film ($k_{Ar} \approx 0$) and a monolayer can be obtained;[14a] the two methyl groups of 2,6-dimethyl benzenediazonium (2,6-DMBD) prevent the attachment of the radical to the surface ($k_{Surf} \approx 0$).[14b] However, these two methyl groups should not prevent the abstraction of an hydrogen atom from the solvent and the formation of the cyanomethyl radical (iv or Scheme 3 [R2]). Besides, such a radical should be stabilized in the medium by the isotopic reaction with ACN itself (Scheme 3 [R3]). This paper deals with the reaction of this radical with the surface and the subsequent formation of an organic film of controllable thickness. In this case, an indirect grafting of an easily available solvent takes place through a diazonium salt.

Experimental Section

Chemicals. Anhydrous ACN (99.8%; <0.05% water) was from Aldrich as well as tetrabutylammonium tetrafluoroborate, which was kept in an oven at 95 °C. Milli-Q water (> 18 MΩ cm) was used for rinsing the samples. 2,6-DMBD was prepared by the standard procedure.[14b]

Samples. One (or 2) × 1 cm^2 gold-coated silicon wafer plates (Aldrich, 1000 Å coating) were cleaned in a "piranha" solution (1/3 v/v H_2O_2/H_2SO_4 for 10 min), and rinsed one time with Milli-Q water under sonication (10 min).

Massive 1 (or 2) × 1 cm^2 copper plates were polished with different grades of polishing paper and finally with a 0.04 μm alumina slurry on a polishing cloth, using a Presi Mecatech 234 polishing machine. After polishing, the plates were rinsed with Milli-Q water, left for 10 min in a 5% aqueous solution of citric acid, rinsed again with Milli Q water, and finally sonicated for 10 min in acetone.

P-doped silicon samples (Siltronic, resistivity 0.016 Ω cm) were hydrogenated by dipping for 5 min in 3% HF, and then rinsed in Milli-Q water for 5 min under sonication.

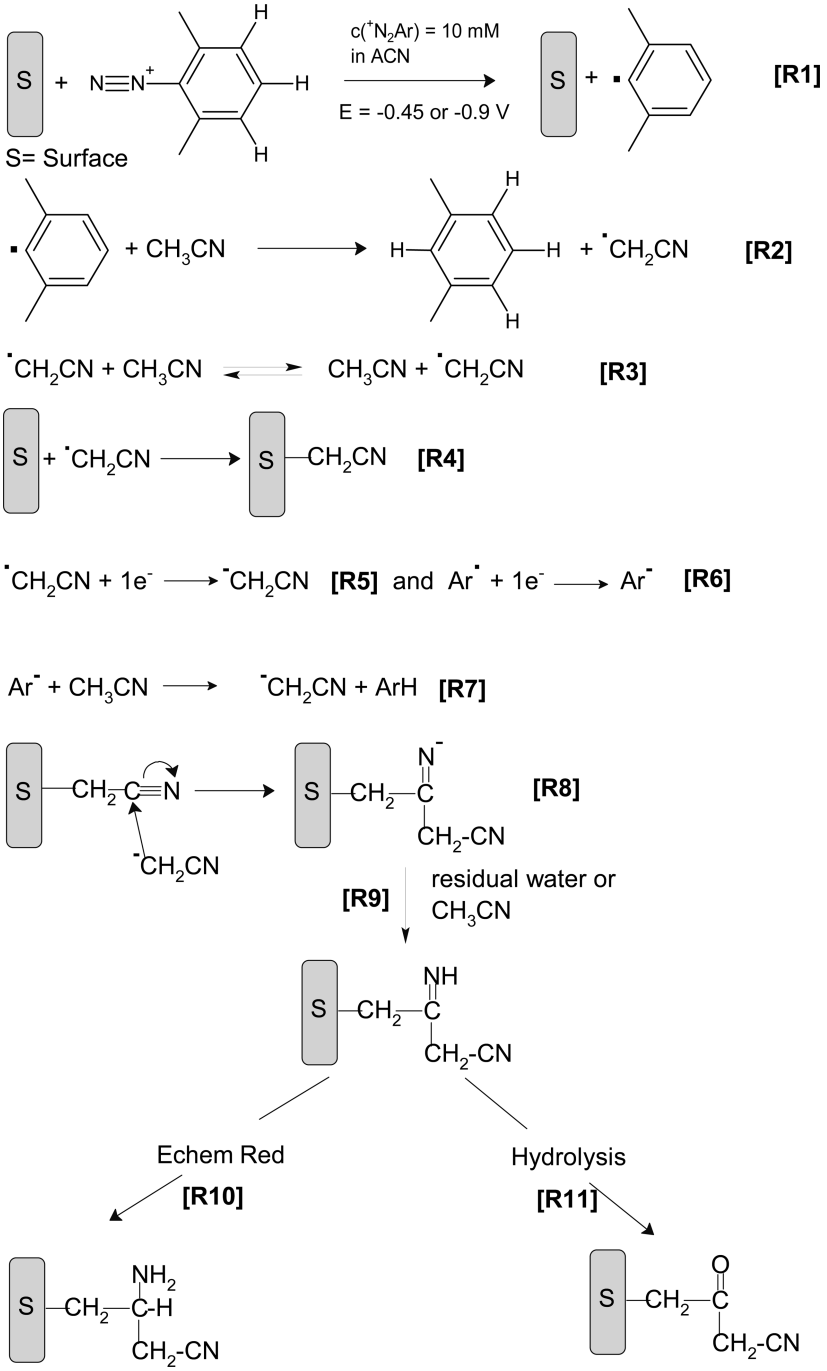
The electrodes for cyclic voltammetry were Cu or Au (diameter, 1 mm) wires imbedded in epoxy resin or a small silicon shard. Metallic electrodes were polished and rinsed as the copper plate above.

Electrochemical experiments were performed with an EG&G 263A potentiostat/galvanostat and an Echem 4.30 version software. Electrografting was performed by chronoamperometry in ACN + 0.1 M NBu_4BF_4 solutions with a 10 mM solution of 2,6-DMBD. The reference electrode was Ag/AgCl and the counter electrode a platinum foil. In the case of Si, the modification was achieved by chronopotentiometry at $E = -0.9$ V/Ag/AgCl for 900 s under light irradiation. The Si sample was scratched and connected in the back with silver conducting polymer and a piece of copper tape.

Spontaneous grafting of the copper plates was carried out by immersing the plates into ACN+ 0.1 M NBu_4BF_4 solutions in the presence of 10 or 100 mM of 2,6-DMBD for 30 min.

(11) Gomberg, M.; Bachmann, W. E. *J. Am. Chem. Soc.* **1924**, *45*, 2339.
(12) M'Halla, F.; Pinson, J.; Savéant, J.-M. *J. Am. Chem. Soc.* **1980**, *102*, 4120.
(13) Doppelt, P.; Hallais, G.; Pinson, J.; Podvorica, F.; Verneyre, S. *Chem. Mater.* **2007**, *19*, 4570.
(14) (a) Combellas, C.; Kanoufi, F.; Pinson, J.; Podvorica, F. I. *J. Am. Chem. Soc.* **2008**, *130*, 8576. (b) Combellas, C.; Jiang, D.; Kanoufi, F.; Pinson, J.; Podvorica, F. I. *Langmuir* **2009**, *25*, 286.

Scheme 3



IR spectra of the modified samples were recorded using a Jasco FT/IR-6100 Fourier Transform Infra Red Spectrometer equipped with a MCT detector. For each spectrum, 1000 scans were accumulated with a spectral resolution of 4 cm^{-1}.

TOF-SIMS spectra were obtained with an ION-TOF IV with Au^+ primary ions at 25 keV. The analyzed zone was 150 μm^2, and the acquisition time 75 s. Blank samples were analyzed in the same run as the modified samples. The peak intensity refers to the area of the peak normalized to the total intensity of the spectrum.

Thicknesses of films grafted onto Au and Cu were measured with a mono wavelength ellipsometer Sentech SE400. The following values were taken for gold, $n_s = 0.182$, $k_s = 3.489$; copper, $n_s = 0.265$, $k_s = 3.108$, and the polymeric layer $n_s = 1.210$, $k_s = 0$. These values were measured on clean surfaces before electrografting, and the thickness was determined from the same plate after electrografting. On Au, the thickness was also measured from the SEM image of the limit of the layer of a tilted sample. Thicknesses of films grafted onto Si were measured by carving a sharp furrow through the film with a sharp tip and measuring the depth of this furrow with an α Step IQ profilometer from KLA Tencor. The length of a chain with multiple $CH_2CH(NH_2)$ groups was calculated with ACD ChemSketch 12 after optimization (11.23 Å for ten groups).

SEM images were obtained using a Zeiss Ultra II electron microscope.

Contact angles were measured by a standard technique, in which the substrate was cooled by a Pelletier element and a drop of a few microliters of water was placed on it, using a microsyringe. A stereomicroscope allowed the droplet image enlargement and the contact angle measurement.

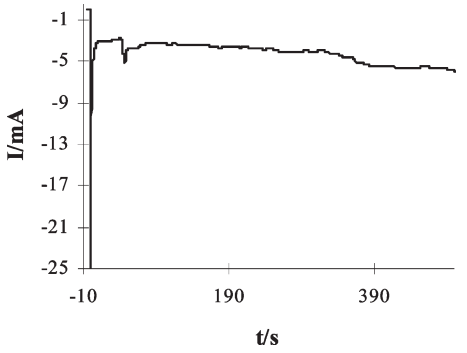


Figure 1. Chronoamperometry of a copper plate in a 10 mM 2,6-DMBD solution in ACN +0.1 M NBu_4BF_4. Electrode biased at $E = -0.9$ V/Ag/AgCl for 480 s.

Trifluoroacetylation. A modified gold plate was immersed into 5 mL of THF + 0.5 mL of $(CF_3CO)_2O$ and a few drops of triethylamine and left at room temperature overnight.[15] The plate was then rinsed with acetone and distilled water under sonication.

Results

Electrochemical Measurements. The chronoamperometry of a copper plate ($s = 1$ cm^2) in an ACN + 0.1 M NBu_4BF_4 + 10 mM 2,6-DMBD solution is shown in Figure 1. It is very different from the chronoamperogram usually observed with diazonium salts where for $t > 5$ s, the current is ~0. On the contrary, here, for $t > 5$ s, the absolute value of the current increases slightly with time, which indicates that the film formed on the electrode through a cathodic reaction is not blocking.[2m] At the end of the electrolysis, a gray film is observed on the surface. Similar results were observed with gold and hydrogenated silicon and the chronoamperograms are presented in Figures S1 and S2 (see the Supporting Information).

IRRAS Measurements. The IR spectrum of a 2 cm^2 copper plate submitted to a constant potential of -0.9 V/Ag/AgCl for 480 s is presented in Figure 2a. The main features of this spectrum are the absence of a $-C\equiv N$ stretching band[16] (2254 cm^{-1} for ACN itself) and the presence of bands corresponding to grafted amine groups at 1595 cm^{-1} (NH deformation) and at 3243 cm^{-1} ($-$NH stretching). A band at 1397 cm^{-1} (CH_2 scissoring) is also observed.[17]

The IR spectrum of a 2 cm^2 copper plate submitted to a lower potential (E = -0.45 V/Ag/AgCl) for 480 s is presented in Figure 2b. The latter amino bands at 3260 and 1595 cm^{-1} are still observed, although smaller, and a new strong C=O band is present at 1693 cm^{-1}. This indicates that changing the potential for electrografting results in a different structure for the grafted film.

Grafting on copper was also achieved under the same conditions as for Figure 2a except that ACN contained 1% H_2O. The main IR bands of the plate modified under these conditions are shown in the insert of Figure 2c together with the corresponding bands under dry conditions (Figure 2a). The IR bands have decreased by ~40%.

The electrochemical modification of a gold plate at $E = -0.9$ V/Ag/AgCl for 480 s is also possible as shown by IRRAS in Figure 3a. The IRRAS spectrum is similar to that obtained on copper (Figure 2a); however, the band at 1397 cm^{-1} is absent.

To ascertain the presence of amino groups on the surface, a gold plate modified with ACN was treated with trifluoroacetic anhydride (5% solution in THF) overnight to transform primary amine groups into trifluoroacetamide functions ($-NH_2+(CF_3C{=}O)_2O \leftrightarrow$-NHC(O)$CF_3$). The IR spectrum of Figure 3b shows that the NH deformation at 1617 cm^{-1} has disappeared and the band at 3243 cm^{-1} has decreased; it now corresponds to the NH stretching of amide functions. The presence of CF_3(CO) groups in the film is evidenced by the C=O band at 1785 cm^{-1} and the CF_3 stretching bands at 1210 and 1170 cm^{-1} (~3350, 3200, 1705, 1200, 1155 cm^{-1} for trifluoroacetamide, $CF_3C(=O)NH_2$).

An ACN-derived film can also be grafted on copper and iron electrodes by spontaneous reduction of 2,6-DMBD in an ACN solution (without supporting electrolyte). Figure 4 shows the presence of amino bands at 3300 and 1600 cm^{-1} and also of a strong C=O band at 1693 cm^{-1} as in the case of the electrochemical grafting at $E = -0.45$ V/Ag/AgCl. For such a spontaneous grafting, the intensity of the IR bands increases with the concentration of 2,6-DMBD (from 10 to 100 mM) (compare Figures 4 a and b).

ToF-SIMS. We have recorded the Tof-SIMS spectrum of a copper plate spontaneously grafted in ACN + 100 mM 2,6-DMBD for 30 min (without any supporting electrolyte). The main features of this spectrum are summarized in Table 1 and some significant peaks are presented in Figure 5.

Thickness of the Films. They were measured by ellipsometry, profilometry, or SEM and are gathered in Table 2.

The thickness of the layers corresponds to a quite large number of $-CH_2-CH(NH_2)-$ groups (see below). Because the size of this group is 1.1 Å along the chain axis, there should be ~500 of such groups on both gold and copper, indicating a very efficient process for the growth of the layer.

SEM Results. The acetonitrile derived films grafted electrochemically on gold or copper surfaces via 2,6-dimethyl phenyl radicals were observed by SEM (Figures 6a, b and c, d for gold and copper respectively). Figure 6b shows the interface between the film and the unmodified gold surface. Other images are given in the Supporting Information (see Figures S3−S5). The films are homogeneous and dense. On gold (Figure 6a,b), the surface is rather homogeneous with some bumps, and on copper a clear structure is visible, the origin of which is still unclear (Figures 6c,d and S5).

Contact Angle Measurements. The water contact angle measurements before and after treatment are gathered in

(15) Smith, M. B.; March, J. *March's Advanced Organic Chemistry*, 5th ed.; Wiley Interscience: New York, 2001; p 510.
(16) The nitrile band of acetonitrile is located at 2254 cm^{-1}. This position is very close to that of residual CO_2, but careful examination of the spectra before CO_2 correction indicates that, in any case, the CN band should not exceed the background noise.
(17) Socrates, G. *Infrared and Raman Characteristic Group Frequencies*, 3rd ed.; John Wiley & Sons: New York, 2008.

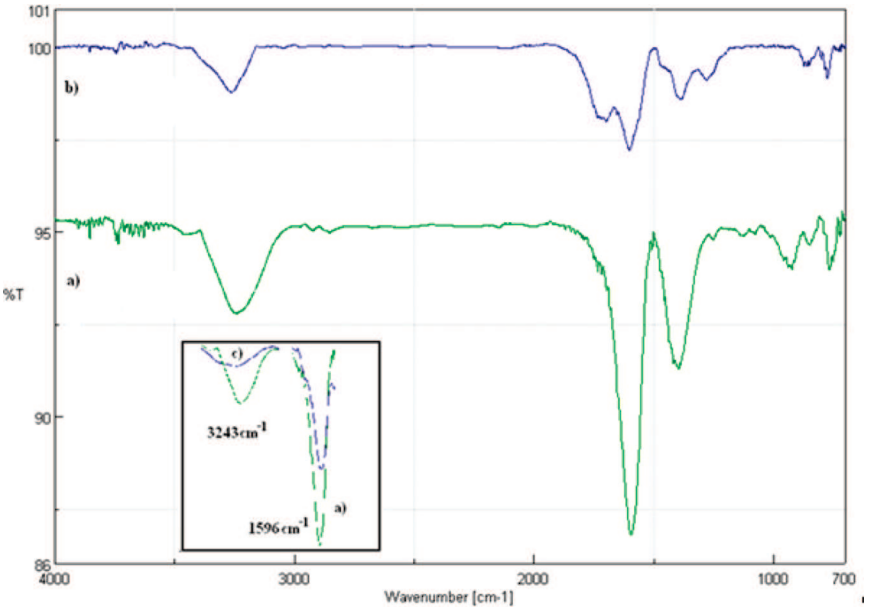


Figure 2. IRRAS spectra of a copper plate after electrolysis in an ACN solution of 10 mM 2,6-DMBD. Plate biased at E = (a) −0.90 and (b) −0.45 V/Ag/AgCl for 480 s under dry conditions; inset (c) in the presence of 1% H_2O. IR assignments in cm^{-1}: 3243, NH stretching; 1595, NH deformation; 1693, C═O stretching.

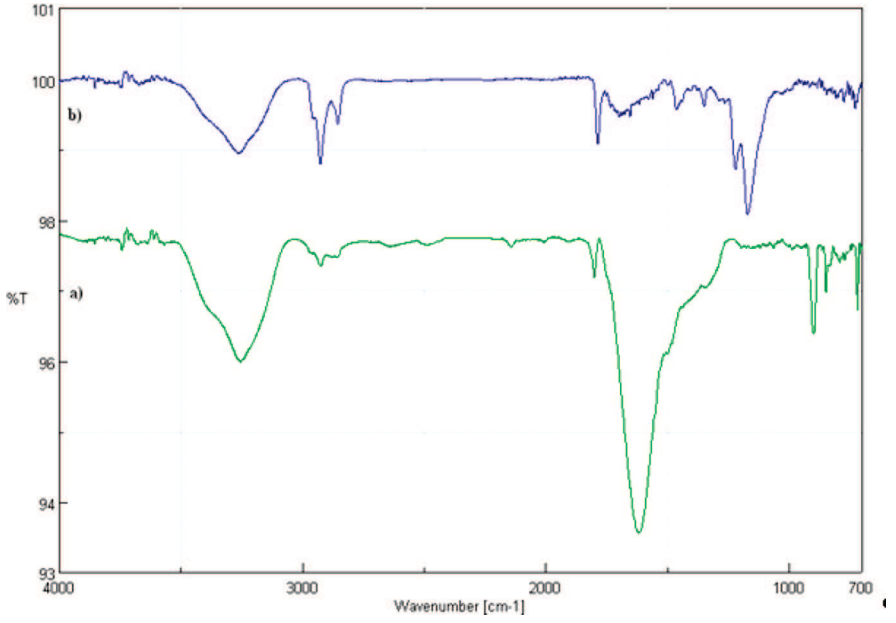


Figure 3. IRRAS spectra of a gold plate after electrolysis in a 10 mM 2,6-DMBD ACN solution. Plate biased at E = −0.9 V/Ag/AgCl for 480 s (a) before and (b) after reaction overnight with trifluoroacetic anhydride $(CF_3C{=}O)_2O$ in a THF solution. IR assignments in cm^{-1}: 3243, NH stretching; 1597, NH deformation; 1170 and 1210, CF_3 stretching.

Table 3 for gold and copper. They indicate that the surface has been modified by the treatment into a more hydrophobic one.

Discussion

The 2,6-DMBD salt is electrochemically reduced[14b] at E_p = −0.25 V/Ag/AgCl (gold electrode, 10 mM solution in ACN + 0.1 M NBu_4BF_4, scan rate v = 100 mV s^{-1}; see Figure S6 in the Supporting Information). In the above experiments, the electrolyses were performed at −0.9 or −0.45 V/Ag/AgCl to reduce the aryldiazonium salt into the aryl radical. We showed previously that, when using a 4 mM solution of 2,6-DMBD, the radical obtained does not attach to metal surfaces.[14b]

Besides, when diazonium salts are grafted to a metal, the structure of the film does not change with the grafting potential;[1] this is not the case with the ACN film presented above, as the IRRAS spectra are different when the grafting is performed at −0.45 or −0.90 V (Figure 2). In addition, in the case of spontaneous grafting, ACN is the only compound present in the solution besides the diazonium salt. Therefore, the observed grafted organic film should originate from ACN.

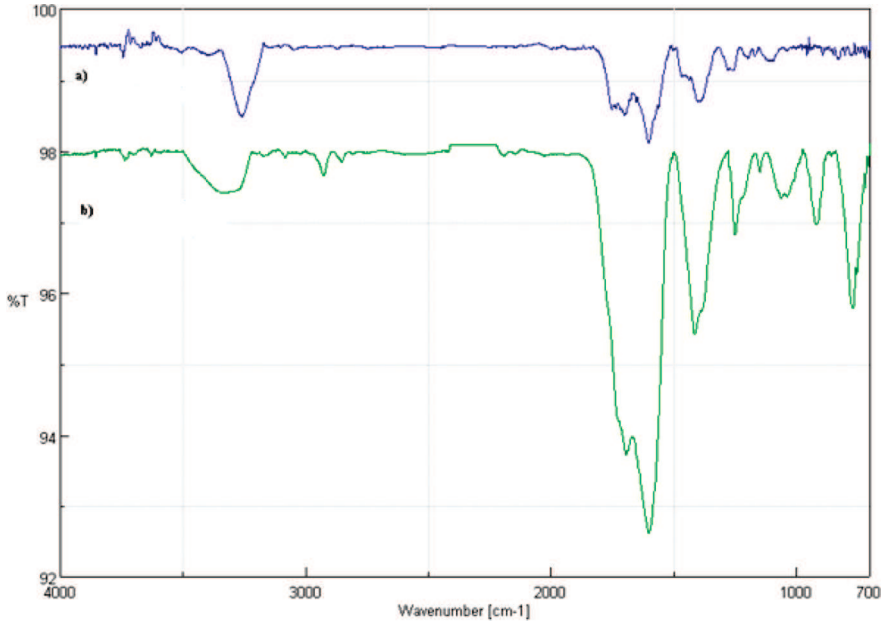


Figure 4. IRRAS spectra of a copper plate dipped for 30 min in (a) 10 and (b) 100 mM 2,6-DMBD in an ACN solution. IR assignments in cm^{-1}: 3250, NH stretching; 1595, NH deformation; 1693, C=O stretching.

Table 1. Tof-SIMS Spectrum of a Copper Plate Modified in ACN + 2,6-DMBD (positive fragments)

m/z	assignment	intensity on bare Cu	intensity on modified Cu
62.93	^{63}Cu	5034	766
64.93	^{65}Cu	2229	336
77.04	C_6H_5	289	1423
78.04	C_6H_6	63	390
91.05	$C_6H_4-CH_3$	223	751
105.07	$CH_3-C_6H_4-CH_3$	120	1514
115.05	$(CH_3)_2C_6H_4-CH$	70	620
146.10	$CH_2-C_6H_4-CH-CH-NH_2$	14	950
267.17	$[C_6H_4(CH_3)-CH-CH(NH_2)]_2$	12	254

In addition, the spectra do not indicate the presence of nitrile groups, alternatively they clearly present the signature of amine groups, and this is confirmed by the trifluoroacetylation reported above. Tof-SIMS spectra also present nitrogen containing fragments that can be assigned to amino groups. To account for these observations, we propose the mechanism reported in Scheme 3.

After its formation [R1], the 2,6-dimethylphenyl radical can dimerize in solution but the abstraction of an hydrogen atom from the solvent [R2] is favored by the large concentration of ACN (17 M) and by the fast rate of hydrogen atom abstraction (the pseudo first order rate constant of the reaction of the cyanophenyl radical measured in ACN[12] is $k_H = 4 \times 10^7\ s^{-1}$). Once formed, the cyanomethyl radical is stabilized by the isotopic reaction [R3][18] and reacts with the surface in reaction [R4]. However, the IR spectra do not show any significant $-C\equiv N$ bands but present strong amino bands. To rationalize this fact, we propose that the surface $-CH_2CN$ be attacked by the cyanomethyl anion as in reaction [R8]. When the reaction is performed electrochemically, this anion can be obtained in two ways: by reduction of the radical or by deprotonation of ACN. The redox potential $E°(\cdot CH_2CN/^-CH_2CN) = -0.69$ V/SCE that is -0.66 V/Ag/AgCl has been measured by Gennaro;[19] therefore, at the electrolysis potential of -0.9 V, the cyanomethyl radical should be reduced to its anion by the electrode [R5]. At this potential, the 2,6-dimethyl phenyl radical should also be reduced to its anion [R6][20] and this aryl anion should also be able to deprotonate ACN [R7].[21]

In the case of spontaneous reactions, the problem is more complicated, the only reducing agent in the experiment is copper. The open circuit potential measured for a copper plate in a 100 mM ACN solution of 2,6-DMBD is -0.44 V/Ag/AgCl; therefore, reduction of the cyanomethyl radical should be possible, at least in part. The cyanomethyl anion should attack the first grafted cyanomethyl group in the same [R8] reaction as in electrochemistry. The attack of the grafted cyanomethyl group by the cyanomethyl anion is known as the Thorpe reaction,[22] a reaction analogous to the aldol reaction. In both cases—electrochemical or spontaneous—one obtains an iminium ion that should be protonated by the very small amount of residual water or by abstraction of a proton from ACN,

(18) The increase in the current observed during the chronopotentiometry is most likely related to the increasing concentration of the cyanomethyl radical in the solution .

(19) Isse, A. A.; Gennaro, A. *J. Phys. Chem. A* **2004**, *108*, 4180.

(20) (a) The reduction potential of the phenyl radical to its anion was measured by Andrieux,[20b] $E_p = -0.64$ V/SCE, and Vase,[20c] $E_p = -0.95$ V/SCE. The reduction potential of the 2,6-dimethyl phenyl radical should be slightly more negative because of the effect of the methyl groups. (b) Andrieux, C. P.; Pinson, J. *J. Am. Chem. Soc*. **2003**, *125*, 14801. (c) Vase, K. Ph.D. Thesis, University of Aarhus, Aarhus, Denmark, **2007**.

(21) (a) The pKa of acetonitrile is 31.3[21b] and that of phenyllitium is about 43;[21c] therefore, the 2,6-dimethylbezene anion should be able to deprotonate acetonitrile to give the cyanomethyl anion. (b) Rossi, L.; Feroci, M.; Inesi, A. *Mini-Rev. Org. Chem*. **2005**, *2*, 79. (c) Smith, M. B.; March, J. *March's Advanced Organic Chemistry*, 5th ed.; Wiley Interscience: New York, 2001; p 331.

(22) Smith, M. B.; March, J. *March's Advanced Organic Chemistry*, 5th ed.; Wiley Interscience: New York, 2001; p 1238.

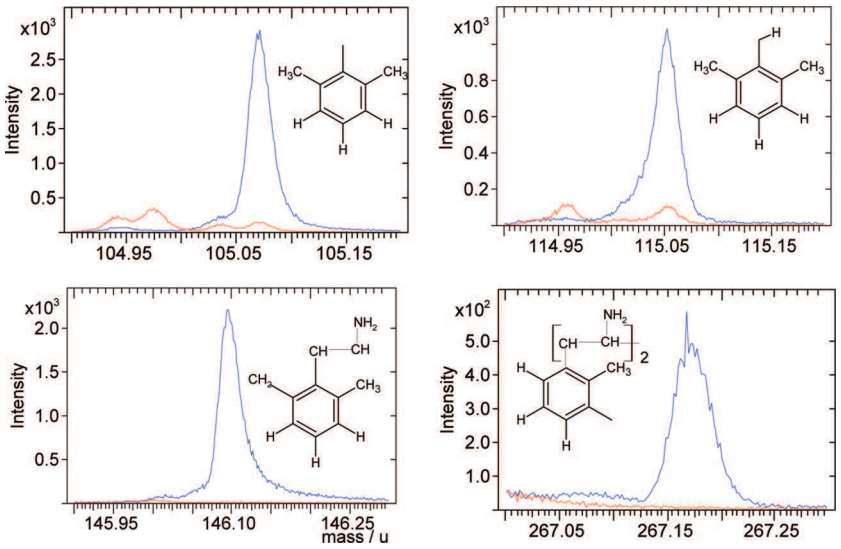


Figure 5. Some characteristic ToF-SIMS peaks.

Table 2. Thickness of the Layers Prepared by Reduction of 2,6-DMBD in ACN at $E = -0.90$ V/Ag/AgCl for 480 s

Au[a]	Cu[b]	Si[c]
56 ± 1 nm	49 ± 3 nm	9 ± 4 nm

[a] Measured by SEM. [b] Measured by ellipsometry. [c] Measured by profilometry. [2,6-DMBD] = (a,b) 100 mM, (c) 10 mM.

regenerating the cyanomethyl anion [R9]. Imines are known to be reducible,[23] leading to amines via [R10] that are characterized through their IR spectra and their transformation into trifluoroacetamide. However, during the spontaneous reaction, the potential is less negative than during the electrochemical reaction and only part of the imines is reduced. As imines are known to be very easily hydrolyzed,[24] the unreduced part is transformed to ketones [R11], most probably during the rinsing of the samples as the experiments were performed under dry conditions. This is in agreement with the IR spectra that show the formation of both amines and ketones. The absence of IR bands corresponding to the terminal nitrile group is a consequence of the low proportion of nitrile groups compared to $-CH_2CH(NH_2)-$ groups (1 for 500).

In addition, the ToF−SIMS spectra indicate that the aryl radical is able to react with the polymeric chain obtained from acetonitrile, in agreement with some fragments presented in Table 1. Such reaction, if sufficiently effective, should also be observed by a less sensitive method such as IR. Then bands similar to those of 2,6-dimethylaniline could be expected, such as CH_3 stretching at 2967 and 2921 cm^{-1} and ring vibrations at 1622 and 1480 cm^{-1}; on the spectrum of Figure 2, the 2967, 2921, and 1480 cm^{-1} bands are clearly absent. The bands at 848 and 770 cm^{-1} can be attributed to aromatic groups, but the 848 cm^{-1} signal could also correspond to an aliphatic amine (strong 856 cm^{-1} band for isopropylamine). This indicates that the number of aryl groups attached to the chain is limited or small. Indeed, once formed the 2,6-dimethylphenyl radical can react either with acetonitrile (17 M) or with the thin organic layer present on the surface; in view of the relative concentrations, the reaction with ACN is favored.

The results described here can be compared with the reaction observed when hydrogenated diamond is treated with peroxides in ACN.[25] The mechanism, which is shown in Scheme 4, involves the formation of the peroxy radical that abstracts an hydrogen atom from the diamond surface; the diamond radical also abstracts an hydrogen from ACN and recombination of a diamond radical with the cyanomethyl radical provides a surface that is functionalized with $-CH_2CN$ groups. The presence of the $-C\equiv N$ group is observed through its vibration at 2271 cm^{-1} that increases with time. But the IR spectrum[25] does not show any signal corresponding to an amine. Even if the grafted radical is the same, the layer is quite different from that observed here; this is due to the absence of an anion that could attack the first grafted cyano group.

This reaction can also be compared with that described by Deniau et al. who were able to form composite polynitrophenylene-polyvinyl films by simultaneous reduction of the 4-nitrobenzenediazonium salt and a vinylic compound.[26] In this case, the nitrophenyl radicals initiate the radical polymerization of vinylic monomers under protic conditions. This reaction has been called SEEP (surface electroinitiated emulsion polymerization). The main difference with our procedure is that the 2,6-DMBD

(23) (a) Lund, H. *Reduction of Azomethines in Organic Electrochemistry*, 4th ed.; Lund, H., Hammerich, O., Eds.; Marcel Dekker: New York, 2001, p435. (b) Reed, R. C.; Wightman, R. M. In *Encyclopedia of Electrochemistry of the Elements*; Bard, A. J., Lund, H., Eds.; Marcel Dekker: New York, Vol. *XV.1*, pp 54. (c) Largeron, M.; Fleury, M.-B. *Org. Lett.* **2009**, *11*, 883. (d) Largeron, M.; Chiaroni, A.; Fleury, M.-B. *Chem. Eur. J.* **2008**, *14*, 996.
(24) Smith, M. B.; March, J. *March's Advanced Organic Chemistry*, 5th ed.; Wiley Interscience: New York, 2001; p 1177.
(25) Tsubota, T.; Shintaro, I.; Osamu, H.; Nagaoka, S.; Masanori, M.; Yasumichi, M. *Phys. Chem. Chem. Phys.* **2002**, *4*, 3881.
(26) (a) Deniau, G.; Azoulay, L.; Bougerolles, L.; Palacin, S. *Chem. Mater.* **2006**, *18*, 5421. (b) Tessier, L.; Deniau, G.; Charleux, B.; Palacin, S. *Chem. Mater.* **2009**, *21*, 4261.

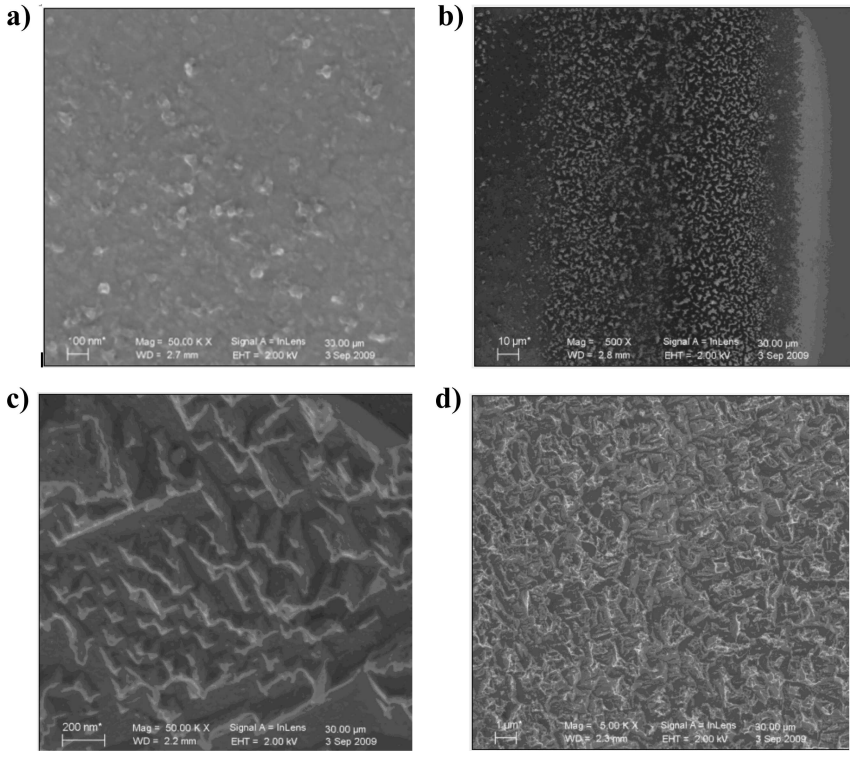
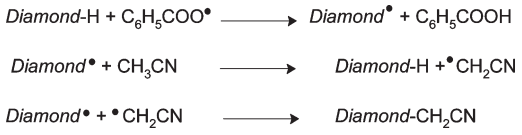


Figure 6. SEM of (a, b) gold and (c, d) copper plates immersed into a 100 mM 2,6-DMBD + 0.1 M NBu_4BF_4 ACN solution for (a, b) 900 s at $E = -0.9$ V/Ag/AgCl, (c, d) 1800 s without electrochemical assistance. Scale bars: (a) 100 nm, (b) 10 μm (c) 200 nm, (d) 1 μm. Secondary electron analysis.

Table 3. Water Contact Angles

	Au (deg)	Cu (deg)
bare surface	44 ± 2	35 ± 2
modified surface	53 ± 4	52 ± 4

Scheme 4. Grafting of the Cyanomethyl Radical on Hydrogenated Diamond Surfaces[25]



radical itself is not grafted on the electrode surface, but is able to provide radicals from the solvent by hydrogen atom abstraction. A film derived from acetonitrile is formed, but in our case, aryl radicals are not incorporated into the film, at least, to a large extent.

Conclusion

Under electrochemical or spontaneous grafting conditions, the 2,6-dimethyl benzenediazonium salt does not lead to the modification of the surface by 2,6-dimethylphenyl groups. This is related to the steric hindrance in the positions ortho to the nitrogen atom. The 2,6-dimethyl phenyl radical is formed but instead of reacting with the surface, it abstracts an hydrogen atom from ACN to give the cyanomethyl radical, that reacts with the surface. The reaction is triggered by electrochemistry or started spontaneously with reducing metals such as copper. It should also be triggered by other reducing metals, such as iron, nickel, zinc, etc. The growth of the layer results from the further attack of the cyanomethyl anion on the first grafted cyanomethyl group. This provides a surface containing amino groups and, in some cases, keto groups. A mechanism is proposed to account for the formation of such grafted surfaces.

As both amino and keto groups are very reactive, this method provides surfaces that can be easily further derivatized, for example, for controlled protein immobilization.[27] The method can be extended to other molecules (RH) that can transfer an hydrogen atom to the 2,6-dimethylphenyl radical to give a new radical (R·) able to react with a surface. Work is in progress to explore new grafting reactions along these lines.

Acknowledgment. We are grateful to the Alchimer society for the use of the SEM microscope and to Dr. Xavier Joyeux for recording the images. The "Agence Nationale de la Recherche" is gratefully acknowledged for its financial support via the ANR-06-BLAN-0368 project.

Supporting Information Available: Additional figures (PDF). This material is available free of charge via the Internet at http://pubs.acs.org.

(27) Kim, J.; Cho, J.; Seidler, P.; Kurland, N.; Yadavalli, V. *Langmuir* **2010**, *26*, 2599.

Supporting information

Indirect Grafting of Acetonitrile Derived Films on Metallic Substrates

Avni Berisha[$,§], Catherine Combellas[$], Frédéric Kanoufi[$], Jean Pinson[$] Stéphane Ustaze[‡] and Fetah I. Podvorica[$,§*]

Chronoamperometry

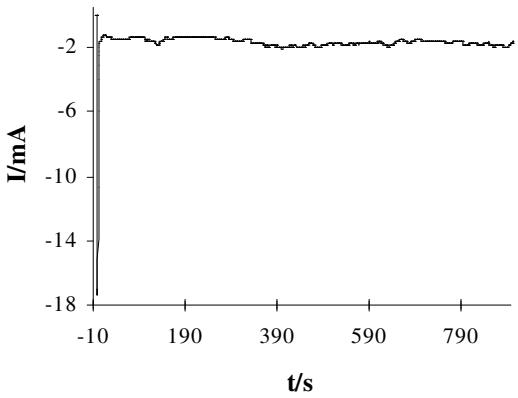


Figure S1 Chronoamperometry of a gold plate in a 100 mM solution of 2,6-DMBD in ACN. Electrode biased at E = - 0.9 V/Ag/AgCl for 900 s.

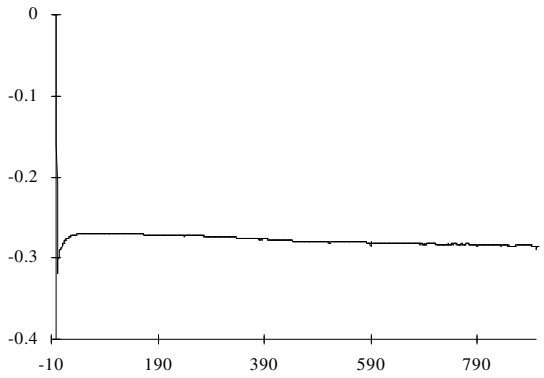


Fig. S2. Chronoamperometry of an hydrogenated silicon plate in a 10 mM 2,6-DMBD ACN solution. Electrode biased at E = - 0.9 V/Ag/AgCl for 900 s.

* Corresponding author : fetah.podvorica@fshmn.uni-pr.edu

SEM images
Gold surfaces

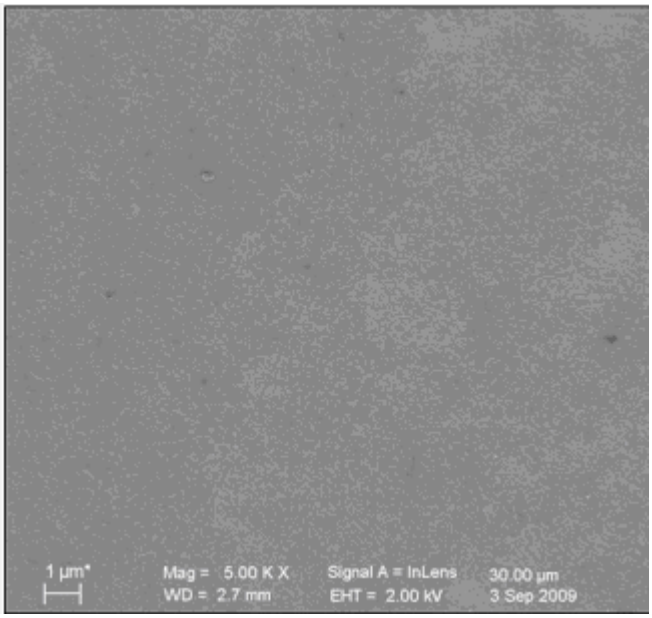


Figure S3. SEM image of a gold plate grafted for 900 s in an ACN + 100 mM 2,6-DMBD + 0.1 M NB_4BF_4 solution at E = - 0.9 V/Ag/AgCl. Scale bar 1µM. Secondary electrons analysis.

At the 1µm scale, the surface is homogeneous.

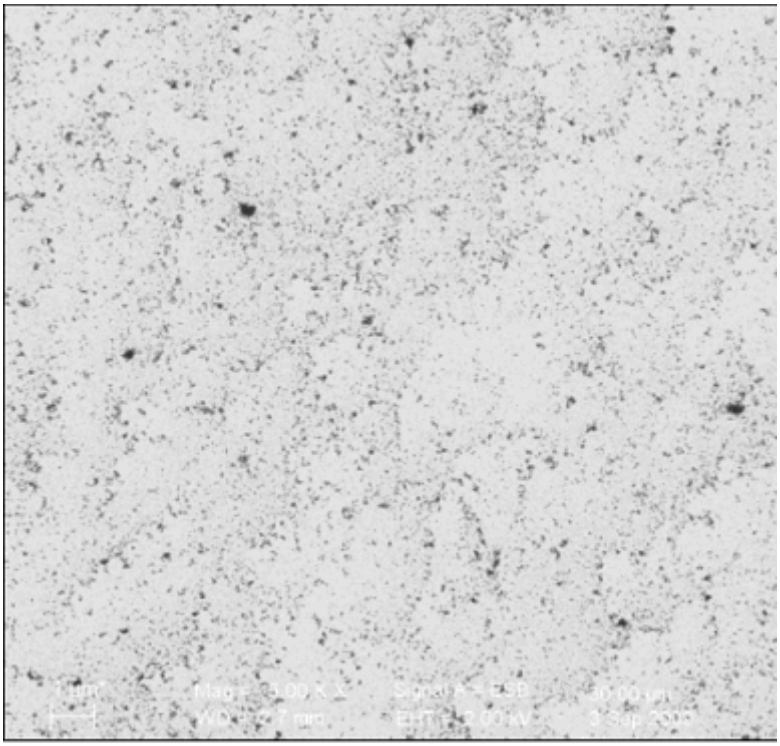


Figure S4. SEM of a gold plate grafted for 900 s at ACN + 100 mM 2,6-DMBD + 0.1 M NB_4BF_4 solution at E = - 0.9 V/Ag/AgCl. Scale bar 1µm. Backscattered electrons analysis.

By tilting the sample, it is possible to measure the thickness of the layer: 56 nm.

Copper surfaces

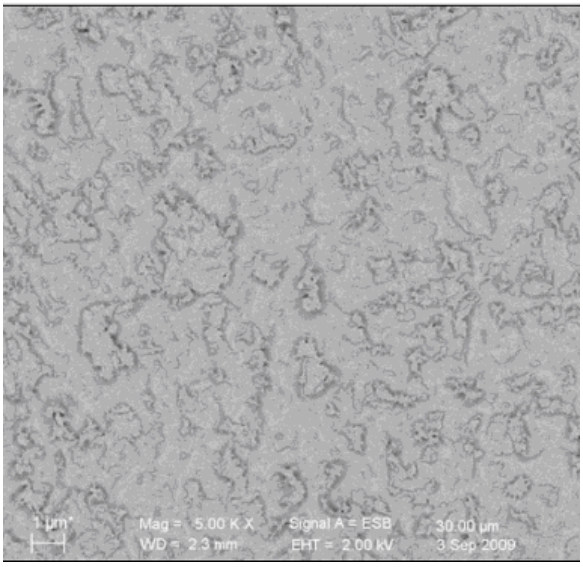


Figure S5. SEM image of a copper plate immersed in a 100 mM 2,6-DMBD + 0.1 M NBu_4BF_4 ACN solution during 1800 s. Scale bar 1 µm. Backscattered electrons analysis.

As in Figure 5c,d the structured surface of the organic film on top of copper is observed. The film is chemically homogeneous.

Cyclic voltammetry

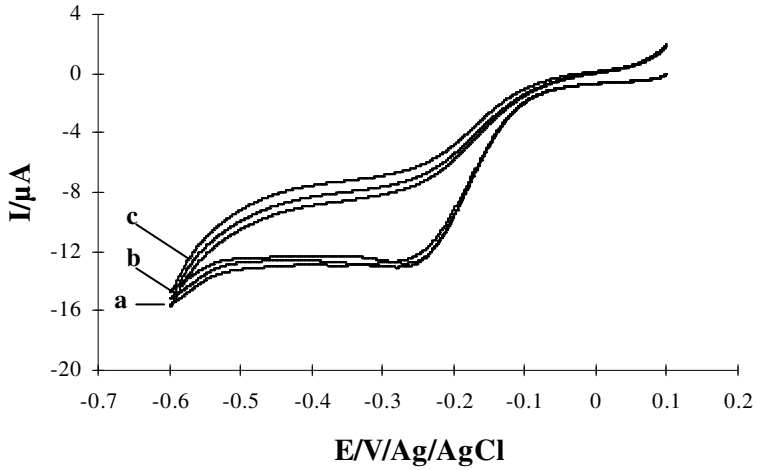


Figure S6. Cyclic voltammetry of gold a electrode (1 mm diameter) in a 10 mM 2,6-DMBD + 0.1 M NBu_4BF_4 ACN solution. a) 1st; b) 2nd and c) 3rd scan. v = 0.1 V/s. Ref. Ag/Ag/AgCl.

Figure S6 shows that the height of the wave (Ep = -0.25 V/(Ag/AgCl) does not decrease with the number of scans as usually observed with diazonium salts. This indicates that the electrode is not blocked and therefore that grafting does not occur.

2.4. Analysis

We have shown that the formation of radicals by H-atom abstraction leads to a radical derived from the solvent and that this radical is able to attach to surfaces. Is it possible to generalize this reaction by changing the solvent? The answer is certainly yes, provided some conditions are fulfilled.

- the solvent should be able to dissolve concentrations of c ~ 10 mM of the diazonium salt and a supporting electrolyte.

- the bond pertaining to the solvent that should be cleaved has to be weaker than the C-H bond of 2,6-DMBD (~ 480 $kJ.mol^{-1}$). As the latter is very strong, this should be possible with the lots of aliphatic solvents such as usual electrochemical solvents (DMF, DMSO, etc).

Aromatic solvents should not work very well (but this is a small drawback as aryl diazonium themselves are able to modify surfaces with aryl groups. Hydrogen abstraction from more complex molecules should also be possible. It should also be possible to abstract halogen atoms such as iodine to produce a variety of radicals that should react with surfaces.

Another interesting point of the method described above is that it permits to produce radicals at moderate potentials (the reduction potential of the 2,6-DMBD, Ep = -0.25V/(Ag/AgCl). This constitutes a catalytic reduction of the solvent. For example, IC_6H_{13} is reduced at -2.8V/(Ag/AgCl) in acetonitrile but the formation of the radical should be possible at -0.25V/(Ag/AgCl); this means that a catalytic effect of more than 2V is expected. These reactions are presently under investigation.

Chapter 3

Photochemical grafting and Patterning of Metallic Surfaces by Organic Layers Derived from Acetonitrile

Chapter 3 : Photochemical grafting and Patterning of Metallic Surfaces by Organic Layers Derived from Acetonitrile

3.1. Introduction

As explained in the introduction of this thesis, modification of the surfaces properties constitutes a large field of investigation. However, it is interesting to search for new methods as these methods of grafting cannot be interchanged, and many of them have a field of applications that is limited in one way or another. For example, oxidative electrografting is not possible on oxidizable materials such as industrial metals. In addition, the tendency is to achieve fast, simple and efficient grafting. Photochemistry may be simpler than electrochemistry as there is no need to contact the substrate, to insert a reference and a counter electrode in the solution. Photochemistry only necessitates a UV or visible lamp. However, in order to obtain a reactive intermediate in the solution (a radical for example), the solution must absorb light. Therefore, the number of reactive species produced will depend on the thickness and absorbance of the solution layer. It must be somewhat controlled to allow for the light to reach the surface and to obtain reproducible results.

Besides, micro or nanopatterning is a mandatory step for the development of sensors and biosensors, photochemistry is well suited for this purpose through the use of a mask, (this is the technique widely used by the microelectronic industry). In the following paper, we present the relatively large patterning of a copper surface, but the resolution of the pattern can certainly be further improved.

We have seen in the introduction that many grafting reactions rely on the formation of radicals or carbenes and also that nearly all electrografting reactions are due to radicals. Radicals can be produced by photochemistry as reported in the introduction. Other examples of radicals formed by photochemistry are, for example[1]: alkyl, benzyl, phenyl, ketyl radicals.

In this chapter, we present a relatively unexpected radical, the cyanomethyl radical: $^{\bullet}CH_2CN$ deriving from acetonitrile. Acetonitrile is widely used as a solvent for recording UV spectra down to low wavelength. However, it absorbs below 200 nm but its photochemical reactions have not been much investigated. We have performed these irradiations with a simple equipment: a small mercury lamp.

Main results

- A new methodology for the grafting of surfaces which is based on the formation of the cyanomethyl radical through the UV irradiation of acetonitrile.
- The photografting to different metals: Cu, Au, Ni, Fe.
- The possibility of patterning surfaces.
- The characterisation of the layer: functionality of the layer (IRRAS), surface hydrophobicity/hydrophilicity (contact angle), thickness (ellipsometry, profilometry or SEM), layer compactness (SEM) and elemental composition (EDX), chemical composition (Tof-SIMS), topography (AFM), solution composition (electrospray ionization mass spectroscopy).
- The proposition of a grafting mechanism and the formation of the layer by combining all the data obtained through the use of these techniques.

(Article in Press, Chemistry of Materials; *dx.doi.org/10.1021/cm200579b*)

---

[1] Nichola J. Turro, V. Ramamurthy, J.C. Sciano, Modern Molecular Photochemistry of Organic Molecules, University Science Books, Sausalito, USA, 2010

3.2. Paper

Photochemical Grafting and Patterning of Metallic Surfaces by Organic Layers Derived from Acetonitrile

Avni Berisha,[$,§] Catherine Combellas[$], Géraldine Hallais[‡], Frédéric Kanoufi[$], Jean Pinson*[$] and Fetah I. Podvorica[$]

[$] *Physico-Chimie des Electrolytes, des Colloïdes et Sciences Analytiques, ESPCI, CNRS UMR 7195, 10 rue Vauquelin, 75231 Paris Cedex 05, France.* [§] *Chemistry Department of Natural Sciences Faculty, University of Prishtina, rr. "Nëna Tereze" nr. 5, 10000 Prishtina, Kosovo.*[‡] *Ecole Normale Supérieure, CNRS-ENS-UPMC 8640, 24 rue Lhomond, 75005 Paris, France*

Abstract

Metallic substrates are modified by a polymeric layer obtained under photochemical irradiation of acetonitrile. The reaction involves a photogenerated radical and leads to the covalent bonding of the organic layer to the metal. Different characterization techniques allow to unravel the structure of the layer: *Substrate*-CH_2-CH-(NH_2)[-CH_2-CH-(NH_2)-]$_n$-[CH_2-C(=O)]$_m$. A mechanism is discussed that accounts for the formation of the layer. The method is quite easy to implement, it only necessitates a UV lamp and a very common solvent. Photografting is well suited to pattern surfaces with polymeric layers by irradiation through a mask and finally, the patterning of copper at the micrometer scale is described as a proof of concept.

Introduction

Electrografting is a well recognized technique for the covalent modification of surfaces, for example by reduction of vinylics or diazonium salts.[1,2] These methods permit to obtain strongly bonded organic layers on carbon, metals, semiconductors and dielectric substrates.

Such coatings range from monolayers to micrometric thick polymer layers and can include a very large number of organic functions.

Some examples of localized electrografting of surfaces have been published. A first series of experiments use AFM for patterning surfaces. For example, the localized electrografting of diazonium salts has been achieved by electrografting a uniform film, removing lines of the film with an AFM tip and electrografting a second diazonium in the lines.[3] In this way,

patterns down to 0.33 µm width of methyl and nitro groups were obtained on a flat carbon surface. AFM also permitted the targeted delivery of a single molecule.[4] For that, gold coated AFM tips were modified by electrografting a vinylic polymeric chain that reacts with the surface when the tip is brought into contact. When the tip is retracted the weakest bond between the tip and the surface is broken (Au(tip)–C(vinylic polymer) bond) and finally the polymer chain remains bonded to the surface.

A second method used poly(dimethylsiloxane) (PDMS) molds with 22 µm channels that were applied on flat carbon surfaces. The channels were filled with a diazonium salt that was electrografted. Spontaneous grafting of metallic surfaces can also be achieved with this technique,[5] as well as the modification of already grafted layers[6] . Instead of using a stamp, an Au or GC surface has been covered with an array of polystyrene beads (down to 0.1 µm) that mask part of the surface. Then, the aryldiazonium electrografting process is followed by subsequent removal of the polystyrene beads, the ungrafted surface areas become available for either another aryldiazonium electrografting or a metal electrodeposition.[7]

SECM (Scanning ElectroChemical Micoscopy) permits to pattern conductive and insulating surfaces. A nitro aryl derivative is reduced at the tip of a SECM to an amine and as this amine diffuses to the substrate, it is diazotized (by $NaNO_2$ added in the solution) and the diazonium salt is reduced and electrografted on the substrate maintained at -0.1 V/SCE; 40 µm wide spots were obtained. [8] Organic bands (110 µm wide) were electrografted onto a gold surface by direct reduction of a diaryliodonium ion at the surface, the SECM tip acting as a counter-electrode.[9] Since an organic layer of bromobenzyl groups attached to a gold substrate acts as an initiator for ATRP (Atom Transfer Radical Polymerization), by locally reducing the C-Br bond, no polymerization is possible where the bromine atoms have been cleaved and a ~ 100 µm pattern was obtained in the polymeric layer. [10,11] By electrogenerating highly reducing radical anions at a SECM tip, it was possible to reduce 200 µm spots of polytetrafluoroethylene into carbon and to attach a polymer to this carbon. [12] By reducing a solution containing a diazonium and a vinylic, intricate deposited polymer patterns made of ~ 0.2 µm lines were obtained by atomic force - scanning electrochemical microscopy (AFM-SECM). [13]

On semiconductors, localized doping may promote localized electrografting; this was demonstrated for example, on p-doped Si(100) covered with its native oxide. [14-16] It is also possible to produce localized electrografting by using surfaces made of two different

materials. With a silicon sample partly plated with gold,[17] only the gold part of the sample is electrografted whatever silicon or gold is used for contact. In this way, thin patterns such as interdigitated gold electrodes with 0.5 µm between the two electrodes can be selectively covered with polymeric films.

Looking at these different methods for patterning polymers on surfaces, it appears that SECM and AFM are very slow methods that will be difficult to use on a larger size than a few µm; the use of PDMS stamps seems also difficult on a production scale. On the contrary, photopatterning is widely used by the microelectronic industry to produce integrated circuits with patterns down to 32 nm and the fabrication of very complicated masks is now routinely achieved by this industry. In the biological field, bio-micropatterning onto polyethyleneglycol covered glass using deep UV light is an elegant method to control cell adhesion geometry on surfaces. [18] It would therefore be interesting to find out photochemical methods for patterning various substrates including metals and carbon, starting from simple chemicals.

Among the already existing photografting methods, the modification of the surface of polymers has been the most widely investigated. Some examples involve the grafting of i) polyethylene by acrylic acid in the presence of benzophenone or formaldehyde, [19-21] ii) benzoylated polystyrene by polyethyleneglycol chains to give a polystyrene-graft-polyethyleneglycol, [22] iii) polydimethylsiloxane by polyvinylic acid.[23] In a different reaction, alkenes and alkynes have been grafted, under irradiation, on a variety of substrates (diamond, [24-38] glassy carbon,[39-43] pyrolyzed photoresist,[44] amorphous carbon,[45] carbon nanotubes,[46] silicon, [47-56]). These alkenes or alkynes can be end functionalized to permit further modification. [37,57] Alkyl halides have also been photografted on diamond (hydrogenated or not) and metal surfaces, using X-ray beams or UV irradiation. [58-60]

Heterocyclic azides[61] and other substituted phenyl azides[62] can be photopatterned by UV through masks onto polymer surfaces (polyethylene, polyimide, polyester,...), giving micrometer sized patterns on polystyrene.[62] Patterning through a photoresist is also possible.[63]

A photoresist deposited on Si(100) was irradiated through a mask, after lift-off, a diazonium salt was electrografted on Si to give patterns of 4-aminophenyl groups (down to 1 µm).[64]

In this paper, we present a method for photografting a very simple compound, acetonitrile (ACN) or haloacetonitriles, to give nanometer thick amino layers. When irradiation takes place through a mask, 100-200 micrometer wide lines are obtained.

In a recent paper, the electrochemical reduction of I- and Br-CH_2CN was reported to give an amino layer through an intermediate cyanomethyl radical ($^{\bullet}CH_2CN$).[65] The indirect electrografting of ACN has also been described by reducing 2,6-dimethylphenyl diazonium.[66] Due to the steric hindrance of the two methyl groups, the 2,6-dimethylphenyl radical obtained cannot bind to the substrate,[67] but it can abstract an hydrogen atom from the solvent (ACN). This leads to the cyanomethyl radical that reacts with the metallic (Au, Cu) or Si-H surfaces to give a bonded organic layer that can be described as *Substrate*-$[CH_2CH(NH_2)]_n$ with carbonyl groups included in the chains. A mechanism has been proposed to account for the formation of this layer.

Photografting of ACN was also observed on Carbon NanoTubes (CNT) and the following structure was assigned to the modified nanotube: *CNT*-CH_2-CH_2-NH_2 on the basis of XPS and IR spectra, without any evidence concerning the thickness of the film and the mechanism for its formation.[68] As we will see below our results do not agree with this structure.

Experimental section

Chemicals. Anhydrous acetonitrile (99.8%), 4- nitrobenzoyl chloride, 4-*tert*-butyl and 4-nitrophenyl isocyanate were from Sigma-Aldrich and iodoacetonitrile (ICH_2CN) from Acros Organics. They were used as received. One irradiation experiment was performed with a freshly opened bottle of 99.9% Chromasolv ACN; similar IR spectra were observed on copper (Figure. S1, Supporting Information, SI). Acetone, sulphuric acid (96%) were from Acros Organics and hydrogen peroxide (30%) from Merck Schuchardt. Milli-Q water (>18 MΩ) was used for plate rinsing and solutions preparation. *Caution: ICH_2CN should be handled with gloves*.

Plates. 1x1 cm Gold coated wafers (Aldrich, gold coated silicon wafer, 1000 angstrom coating) were cleaned with 'piranha' solution (1:3 v/v H_2O_2:H_2SO_4) for 10 min at room temperature, and rinsed under sonication for 10 min in Milli-Q water. Before modification, the plates were dried under a stream of nitrogen. *Caution : Piranha solutions are highly aggressive and should be handled with full protection, gloves, mask,...*

Massive (1 cm^2) iron or nickel plates were polished using 2 µm alumina slurry on DP-NAP polishing cloth with a Mecatech 234 polishing machine (Presi). For the measurements on copper, Si wafers covered with 150 nm of polished copper were used without further polishing, they were rinsed with Milli-Q water, left for 10 min into 5% aqueous solution of

citric acid, rinsed again with Milli-Q water and sonicated for 10 min in acetone, and dried under a stream of nitrogen.

Photografting. Photochemical modification was achieved via wide spectrum UV irradiation mercury Pen Ray lamp UVPC-86079 (20 mA AC, 4400 µW cm^{-2} at 254 nm for a distance of ~ 2 cm) with emission at 184.9 (3%, ~ 150 µW cm^{-2}) , 253.6 (100%,) , 312.5-313.1,356.0-356.3, 407.7, 435.8 nm. Prior to irradiation, a thin film of neat ACN or ICH_2CN was deposited onto the metallic plates that were placed 4 cm under the UV light source. The experiments were performed in the laboratory atmosphere with some exceptions in a glove box containing less than 1 ppm O_2. After UV irradiation for 10, 20 or 30 min, the plates and wafers were rinsed with ACN, acetone, ultrasonicated for 10 min in acetone two times and finally ultrasonicated for 10 min in toluene. For localized photografting, the Teflon® mask was held on top of the Cu wafer and the chromed quartz mask was separated from the copper wafer by a Teflon® ribbon (0.225 mm), so that a thin layer of ACN was present between the mask and the metal surface. The irradiation time was longer than without the mask (40 min) because the light intensity at the surface was lowered by the presence of the mask.

For the identification of amine groups, a copper wafer irradiated for 10 min and rinsed under sonication in acetone for another 10 min was reacted overnight in an ACN saturated solution of 4-nitrobenzoyl chloride; some corrosion of the layer was observed. In other experiments, copper wafers irradiated for 2 min in ACN and rinsed as above were derivatized in 5 mL toluene + 300 µL 4- tert-butylphenylisocyanate or 5 mL DMF + 300 µL 4-nitrophenylisocyanate , left overnight and rinsed in acetone for 480 s under sonication.

Instrumentation. IR spectra of modified plates were recorded using a purged (low CO_2, dry air) Jasco FT/IR-6100 Fourier Transform Infra Red Spectrometer equipped with MCT (mercury-cadmium-telluride) detector. For each spectrum, 1000 scans were accumulated with a spectral resolution of 4 cm^{-1}. The background recorded before each spectrum was that of a clean substrate. The profiles were recorded with an IRRAS Jasco IRT 700S microscope, using a 40x40 μm^2 beam size and 800 accumulations with a spectral resolution of 4 cm^{-1}.

Thicknesses of the films on Au and Cu were measured with a mono wavelength ellipsometer Sentech SE400. The following values were taken for gold: ns = 0.153, ks = 3.567; for copper: ns= 0.101, ks = 3.513. These values were measured on clean surfaces before photografting and the film thicknesses were determined from the same plates after modification, taking n_s = 1.46 , ks = 0 for the polymeric layer.

The thickness profile was recorded with an interferometric profilometer Microsurf 3D from Fogale. The real thickness reported in Figure 11D2, z, is obtained from the interferometric profile (not shown). This profile presents a height decrease in the pattern region where a layer was expected to have grown. This is explained from the loss of light reflectivity induced by the beam light transport into the dielectric grafted layer: the ungrafted copper surface is more reflecting than the copper surface covered by a thin dielectric layer. The interferometric topographic profile, Z_{topo}, is converted into local grafted film thickness, z, from $z = -Z_{topo}/2n$ where n= 1.46 is chosen for the grafted layer refractive index.

Contact angles were measured using the Krüss DSA30 instrument. The samples were horizontally placed on the instrument stage and 3 µL of Milli-Q water was automatically delivered on the top of the sample. At least five measurements were made for each sample. The values of the contact angles were calculated by the tangent method using Drop Shape Analysis software.

AFM images. AFM measurements were performed using a 5100 Atomic Force Microscope (Agilent technologies- Molecular Imaging) operated in a dynamic tip deflection mode (Acoustic Alternating Current mode, AAC). All AFM experiments were done using Silicon Probes (Applied NanoStructures-FORT) in the tapping mode with 3 N m^{-1} spring constant at 69 kHz. The images were scanned in topography, amplitude and phase mode with a resolution of 512×512 pixels and are representative of 1×1 μm^2 regions over different locations on the studied surfaces.

ToF-SIMS spectra were obtained with an ION-TOF IV with Au^+ primary ions at 25 keV, the analyzed zone was 150 μm^2 and the acquisition time 75 s. Blank samples were analyzed in the same run as the modified samples. The peak intensity refers to the area of the peak normalized to the total intensity of the spectrum. The images were obtained with Au_3^+ ions for 100 scans (~ 40 min).

Scanning electron microscopy (SEM) **images and energy-dispersive X-ray** (EDS) **spectra** were obtained using a Hitachi S-4300 microscope.

Solution Analysis. Acetonitrile was irradiated for 1 hour, evaporated to about one tenth of its initial volume and diluted (50/50) with 0.1% phosphoric acid and injected by electrospray in positive mode in a Q-Tof-2 mass spectrometer from Micromass (m/z in the 90-1600 range, scan time= 1 min, inter scan time= 0.1 s, capillary voltage= 3.0 V, cone voltage= 40 V,

MCP= 2100 V, source temperature = 150°C, desolvation temperature = 300°C).The chemical formula was obtained from the best match of the isotopic mass using the ChemCalc software.

Results

Since acetonitrile absorbs below 200 nm, photochemical modification of metallic surfaces was achieved by irradiating at 184.9 nm a thin film of neat ACN deposited onto the metallic plate (4 cm under the UV light source). The irradiation time varied from 10 to 30 min. After irradiation, the samples were rinsed under different conditions, as described in the Experimental Section. After the initial rinsing, IRRAS spectra did not change upon further 15 min rinsing in acetone under sonication. This indicated that the layers are bonded to the surface.

IRRAS and ellipsomeric measurements. Without irradiation, no significant spectrum is observed. The IR spectra of copper surfaces UV irradiated for different times are presented in Figure 1. The main features of these spectra are the presence of a weak -C≡ N stretching band at 2211 cm^{-1} (2254 cm^{-1} for ACN itself) and the presence of bands corresponding to grafted amino groups at 1600 cm^{-1} (NH_2 deformation) and at 3300 cm^{-1} (-NH_2 stretching). A band at 1399 cm^{-1} (CH_2 scissoring) is also observed. [66,69] Upon increased irradiation time, the transmittance decreases, which indicates the formation of thicker films (same for Au, see Figure S1, SI). The spectra obtained with Au, Ni and Fe are presented in Figures S2-4 (SI) along with the blank experiments without irradiation and the main peaks are assigned in Table 1. IR bands in similar wavenumbers ranges are observed for all metals, but the NH_2 deformation band cannot be distinguished on Au.

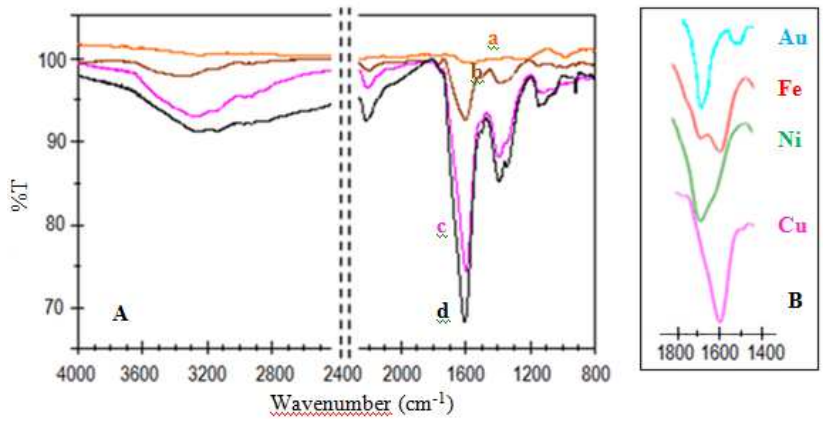


Figure 1. IRRAS spectra of A) a copper wafer a) left in ACN without irradiation for 30 min; b-d) submitted to UV irradiation in ACN for b) 10, c) 20 and d) 30 min and B) the 1500-1800 cm^{-1} range for Au, Fe, Ni and Cu, photografted for 20 min (C=O stretching and NH_2 deformation bands). Ultrasonication for 10 min in acetone after photografting.

Table 1. IRRAS Spectra of the Different Metallic Surfaces Modified with ACN under UV Irradiation. Wavenumbers in cm^{-1}.

Metal	Peak position cm^{-1}	Peak assignment
Cu	3300	$-NH_2$ stretching
	~1670 sh	C=O stretching
	1600	$-NH_2$ deformation
Au	3260	$-NH_2$ stretching
	1690	C=O stretching
Ni	3320	$-NH_2$ stretching
	1675	C=O stretching
	~1600 sh	$-NH_2$ deformation
Fe	3400	$-NH_2$ stretching
	1685	C=O stretching
	1600	$-NH_2$ deformation

For comparison, the spectra of a copper wafer irradiated in a solution of neat ICH_2CN was recorded (Figure 2; bands at 3280, 1600, 1420 cm^{-1}); it is similar to that of a copper wafer irradiated in ACN and the transmittance also decreases with time.

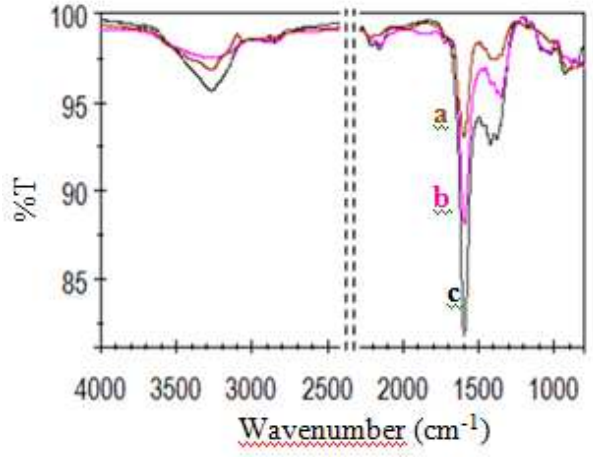


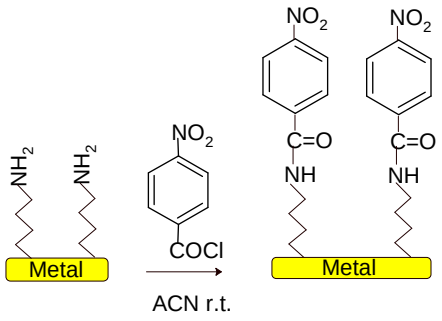
Figure 2. IRRAS spectrum of a copper wafer irradiated in neat ICH_2CN for a) 10, b) 20 and c) 30 min. Ultrasonication for 10 min in acetone after photografting.

The IRRAS data reported in Table 1 favor of the presence of $–NH_2$ groups on copper, gold, nickel and iron surfaces after UV irradiation (by comparison with neat isopropyl amine: 3358, 3282, 1608 cm^{-1}, with isopropylamine chemisorbed on Ni:[70] 3300 cm^{-1}, and with a Self-Assembled Monolayer of 11-amino-1-undecanethiol that presents a broad band in the 3100-

3400 cm^{-1} region[71]). Carbonyl groups are also observed (1670-1690 cm^{-1}), by comparison with acetone (1715 cm^{-1}) and with 4-hydroxy-4-methylpentan-2-one,[72] where a hydroxyl group located in the β-position (1707 cm^{-1}) is hydrogen bonded (we could not find data with a β-substituted NH_2 group). Figure 1B presents an enlargement of the 1400-1800 cm^{-1} region that shows the relative variation of the C=O stretching and -NH_2 deformation bands with the different metals.

In order to understand the origin of the carbonyl band, we have recorded the IRRAS spectra of gold wafers irradiated in a glove box containing less than 1 ppm of dioxygen (Figure S5, SI) and of copper wafers prepared in order to minimize or increase the amount of surface oxides. On gold, in the presence of dioxygen, a C=O band can be observed at 1690 cm^{-1} (Figure 1B) and there is no significant band at ~ 1600 cm^{-1}; in absence of dioxygen, the C=O band shifts to 1677 cm^{-1} due to overlapping with another band at 1616 cm^{-1}, that can be assigned to the NH_2 deformation (Figure S5, SI). Therefore, even in the absence of dioxygen, a C=O band is still present, this indicates that the oxygen of the carbonyl groups comes, at least in part in part, from surface oxides. This experiment also shows that in the absence of dioxygen, an NH_2 deformation band appears, that was not observed in the presence of dioxygen and therefore the formation of the C=O and NH_2 groups should be in competition. However, in these experiments, the surfaces have been sonicated before and after irradiation and it has been shown that bare Au surfaces are subject to uncontrollable, solvent dependent changes during sonication; such sonication prior to grafting may increase the reactivity of surface oxides.[73]

To ascertain the presence of amino groups, the modified copper wafers have been reacted with 4-nitrobenzoyl chloride (Scheme 1):



Scheme 1. Reaction of surface amino groups from an irradiated copper wafer with 4-nitrobenzoyl chloride.

After reaction, the IRRAS spectrum (Figure 3) shows the disappearance of the 1600 cm^{-1} band due to NH_2 deformation and the appearance of several bands at 1692 cm^{-1} (overlapping C=O and NH amide bands), 1604 cm^{-1} (aromatic ring) and the two strong antisymetric (1532 cm^{-1}) and symmetric (1350 cm^{-1}) bands of the nitro group. The spectra of irradiated copper surfaces post modified with 4-butyl or 4-nitrophenylisocyanate are presented in Figure S6 (SI); the reaction is sluggish and the characteristic bands are small.

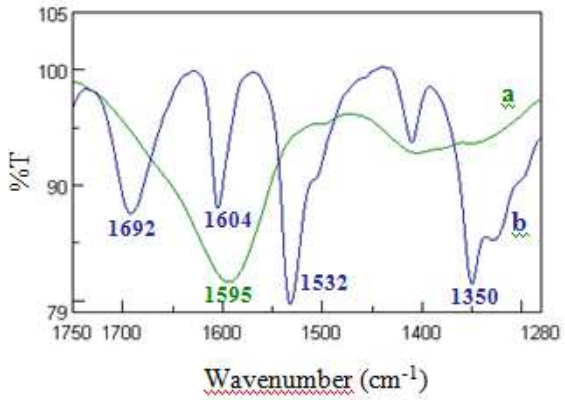


Figure 3. Copper wafer a) photografted by UV irradiation in ACN for 10 min , and b) immersed overnight in a saturated solution of 4-nitrobenzoyl chloride. Ultrasonication for 10 min in acetone after reaction.

In order to determine a grafting mechanism, water (1%) or acetic acid (1 %) was added to ACN during irradiation of a copper wafer and no change of the IRRAS spectrum was observed, (Figures S7 and 8, SI). Conversely, when a radical trap, TEMPO (2,2,6,6-tetramethylpiperidine 1-oxyl), was added to ACN (1%, 60 mM), photografting was completely suppressed as shown in Figure 4.

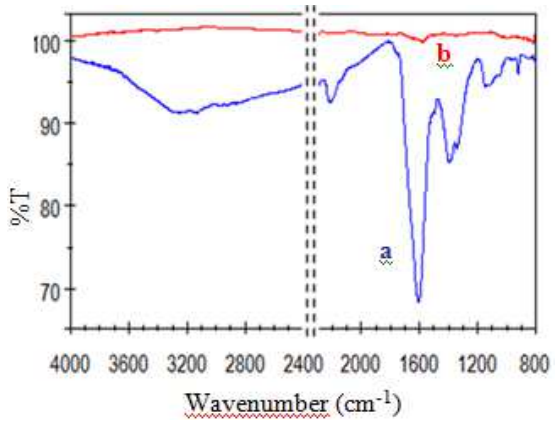


Figure 4. Copper wafer irradiated in ACN for 20 min a) and b) in the presence of 1% TEMPO. Ultrasonication for 10 min in acetone after irradiation.

The homogeneity of the layer was examined by recording IRRAS profiles at 1600 cm^{-1} along a ~ 1x0.2 mm^2 line on a copper wafer (Figure 5). The profiles show that after 10-30 min irradiation, the absorbance does not present any zero value, which indicates that there is no ungrafted region at the 30 µm scale. The mean absorbance, A, increases with the irradiation time - a) 10 min, A ≈ 0.01; b) 20 min, A ≈ 0.02; c) 30 min, A ≈ 0.025- indicating thicker layers as the photografting time increases, in agreement with the IR spectra (Figure 1). Some bumps are observed on these profiles.

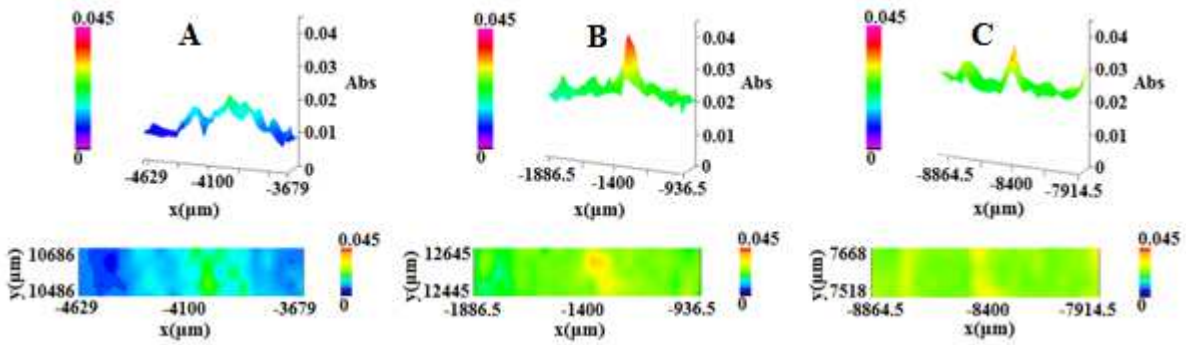


Figure 5. IRRAS surface absorbance profiles at 1600 cm^{-1} of a copper wafer photografted in ACN with irradiation time: A) 10, B) 20 and C) 30 min. 40x40 µm beam size.

Thickness of the layers. The values (d) obtained by ellipsometry on copper and the relative intensity of IR absorption at 1600 cm^{-1} are represented in Figure 6 for different irradiation times in ACN. A good correlation between ellipsometric and IR measurements is observed altogether. Both vary quasi linearly with time.

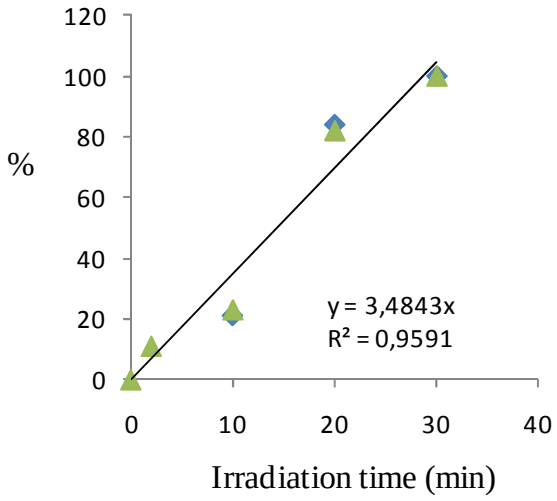


Figure 6. Relative IR intensities of the 1600 cm^{-1} band (▲) and thickness (z) (♦) vs irradiation time on copper wafers. A relative 100 % thickness corresponds to 85 nm.

Scanning Electron Microscopy (SEM) and Energy Dispersive Spectroscopy (EDS). Figure 7A presents the SEM images of a bare copper wafer and Figure 7B the same wafer after 30 min irradiation in ACN. The two images are clearly different and a coating can be observed on the photografted sample (Figure 7B). In order to confirm that the difference in the two images of Figure 7 corresponds to the grafted organic coating, we have recorded the EDS spectra of the modified copper wafer at two different positions: the first one corresponds to the organic layer, the second one to the interface between the organic layer and a scratched line (Figures 8A and B).

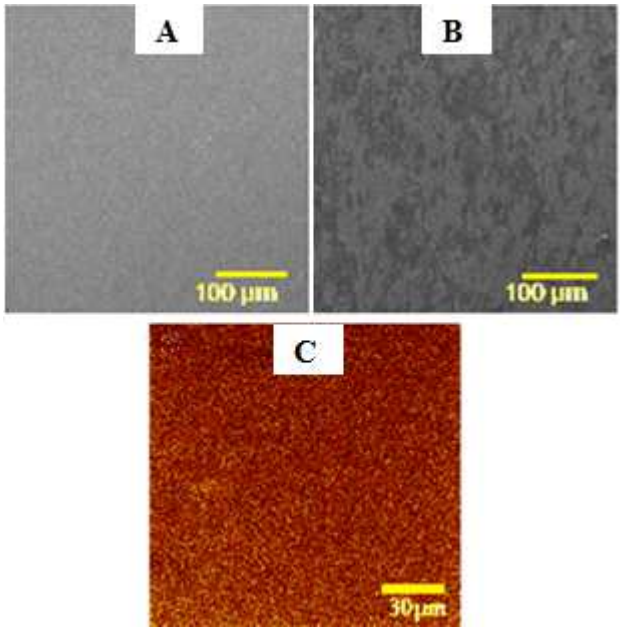


Figure 7. A, B) **SEM** image of A) a bare copper wafer; B) the same wafer photografted by UV irradiation under ACN for 30 min; C) ToF-SIMS image obtained from the sum of the positive ions (fragments containing both Cu and C), UV irradiation in ACN for 30 min.

Inside the grafted layer (Figures 8A, C), besides Cu and Si, a small amount of Ti (that probably corresponds to an intermediate layer of the wafer) is observed (~ 22% C, 8% N and 9% O, mass %). Inside the scratch, most of the Cu has been removed (Figure 8B, D), Si appears (60-85%), C decreases to ~ 6 %, N and O become negligible. This is in good agreement with the IRRAS spectra and confirms the presence of an organic layer containing C, N and also O.

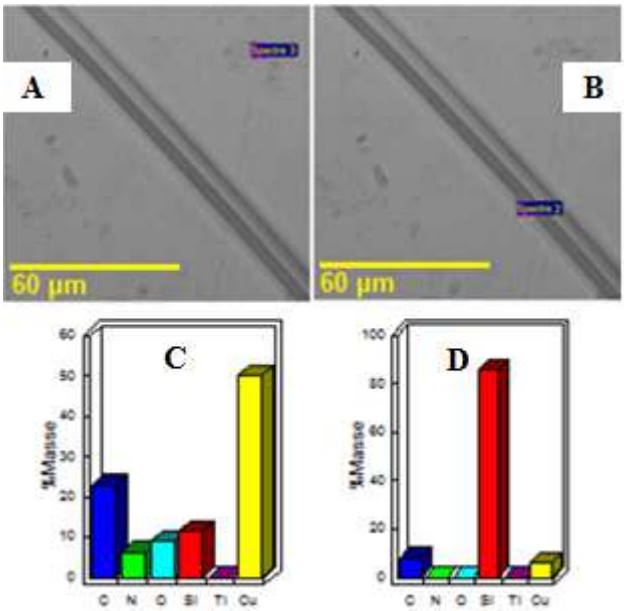


Figure 8. A, B) EDS images of a copper wafer after 30 min irradiation in ACN. C, D) Relative mass distribution of C, N, O, Si, Ti and Cu atoms at the grafted surface and scratched line of the copper wafer. C) on the modified surface along the rectangle indicated in A. D) in the center of the scratched line along the rectangle indicated in B.

AFM images have been captured on copper and gold (Figure 9). With both metals, the layer appears compact. The film thickness on copper is ~ 20 nm, in good agreement with the ellipsometric measurements; on gold, the layer is very thin and close to a monolayer. Figures S9 and 10 (SI) present the topographic, phase and amplitude AFM images. The topographic profiles present some dips that should correspond to small (10-100 nm diameter) holes in the layer.

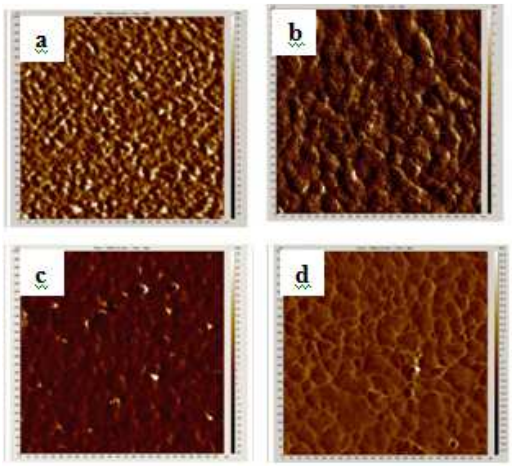
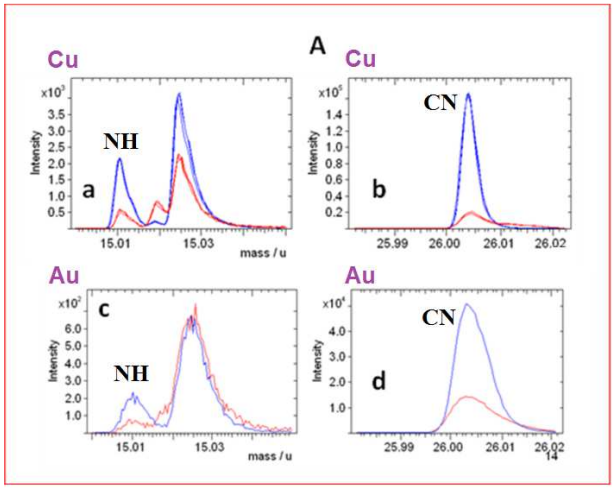


Figure 9. AFM phase images (1 x 1 μm^2) of clean copper and gold wafers (respectively a, b,) and after irradiation for 10 min in ACN (respectively c, d).

ToF-SIMS spectra have been recorded for photografted Cu and Au surfaces. The main characteristic peaks are presented in Figure 10. Figure 10A presents negative ions assigned to NH (m/z = 15.01) and CN (m/z = 26.00), indicating the presence of nitrogen on the surface. Figure 10B presents some positive ions characteristic of the structure of the layer: C_4H_8NO [m/z = 86.06, CH_2-$CH(NH_2)$-CH_2-C(=O)-H], $C_4H_{10}N_2$ [m/z = 86.09, CH_2-$CH(NH_2)$-CH_2-$CH(NH_2)$-] and $C_4H_9N_2$ [m/z = 85.08, CH_2-$CH(NH_2)$-CH_2-CNH_2-] on copper; $C_6H_{15}N_2$ [(m/z = 115.12, CH_2-$CH(NH_2)$-CH_2-$CH(NH_3)$-CH_2-CH_2] on gold. Figure 10C presents positive ions that contain both an atom from the substrate (Cu, Au) and carbon from the organic layer: CuCHN [m/z = 89.94],[63] CuC_2H_3N [m/z = 103.96, ^{63}Cu-CH_2-NH], AuC_2N [m/z = 234.96]. Figure 7C is a 150x150 μm^2 ToF-SIMS image of the sum of all the positive ions containing a copper atom and a carbon fragment. As the MEB images, it indicates a homogeneous grafting. Note that, on gold, although the IRRAS NH_2 deformation band is too small to be distinguished from the neighboring C=O band, ToF-SIMS, that is more sensitive, allows observing the presence of NH_2 groups in the layer.



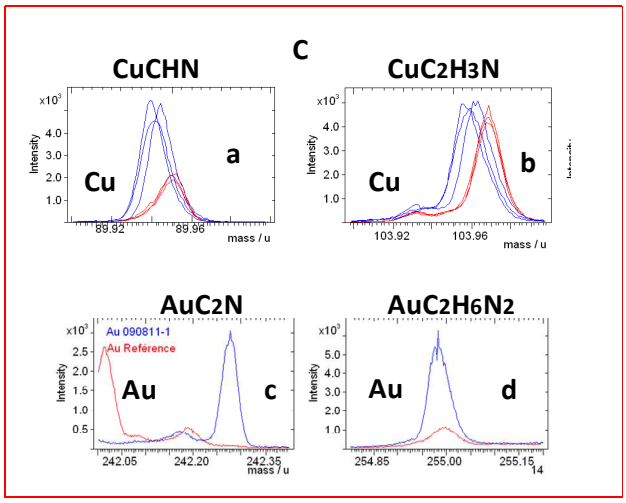


Figure 10. ToF-SIMS spectra. A) negative ions, B, C) positive ions; a, b) copper wafer, c,d) gold wafer. Blue lines: samples irradiated in ACN for 30 min; red lines: untreated samples. Some spectra are recorded three times on three different locations on the sample.

Analysis of the irradiated solution. After irradiation, a sample of acetonitrile was analyzed by electrospray ionization mass spectroscopy. The spectrum presents the base peak at m/z = 242.605 (relative intensity 100%) and smaller peaks at m/z =243.625 (32%); 409.35 (5%); 429.26 (12%); 430.28 (5%). The base peak can be assigned to the protonated oligomer ($C_{11}H_{26}N_6$, exact monoisotopic mass: 242.222), in good agreement with the proposed structure of the organic layer:

$$NC\text{-}[CH_2\text{-}CH(NH_3^+)]_4\text{-}\ CH_2CN$$

Open circuit potential (ocp) under irradiation. In order to assess the possible involvement of electron transfer between the metallic substrate and the organic layer, we have measured the ocp without and under irradiation and compared these data with the ratio of amino to keto groups measured by IRRAS (Table 2, Figures S11-14, SI).

Table 2. Open Circuit Potentials Without and Under Irradiation (V(Ag/AgCl))

Open circuit potential	Cu	Au	Ni	Fe
without irradiation	-0.34	-0.27	-0.19	-0.12
under irradiation	-0.37	-0.29	-0.19	-0.11
NH_2 vs C=O[a]	~90:10	~0	~30:70	~50:50

a) Ratio of IR intensities of the NH_2 deformation and the C=O stretching bands in Figure1B.

The ocp increases (becomes less cathodic) in the order Cu, Au, Ni, Fe. This order of ocp is different from that of the ratio of the IRRAS intensities of the amino deformation over the carbonyl stretching bands (Cu, Fe, Ni, Au).

Localized Grafting. To obtain patterned surfaces, we have irradiated a copper wafer through a mask that was either i) a Teflon® plate with 2 mm holes or ii) a chromed quartz mask with 133 µm wide lines (Figure 11C1).

The Teflon® mask was used to get an IR image of the spot obtained on the copper wafer with a 40x40 µm beam size (Figure 11A). The image was recorded at 1600 cm^{-1} (NH_2 deformation vibration) and represents approximately a quarter of the spot. The highest intensity is observed on the upper left corner (center of the spot) in a zone whose dimensions are in agreement with those of the Teflon® mask.

With the chromed quartz mask, the resulting lines were imaged by ToF-SIMS. Figures 11B2 and 3 represent the images for, respectively, the sum of the intensities of all positive ions, and the intensity of the peak at m/z = 132.99 [$CuCH_2CH(NH_2)CH_2CH^+$]. The latter, which is recorded in the line, is represented in Figure 11B1. Optical images of the quartz mask and the irradiated copper wafer are presented, respectively, in Figures 11C1 and 2. The two images are in good agreement; 166 µm wide lines are visible on the patterned wafer. The same lines were also imaged by optical microscopy (11D1). Profilometry across the line (11D2) permits to measure the thickness and the width of the line: ~40 nm and ~ 200 µm respectively (in fair agreement with the optical image).

These different images indicate that localized photografting is possible on metals and that the lines observed optically correspond to the organic layer obtained from the photochemical reaction of ACN.

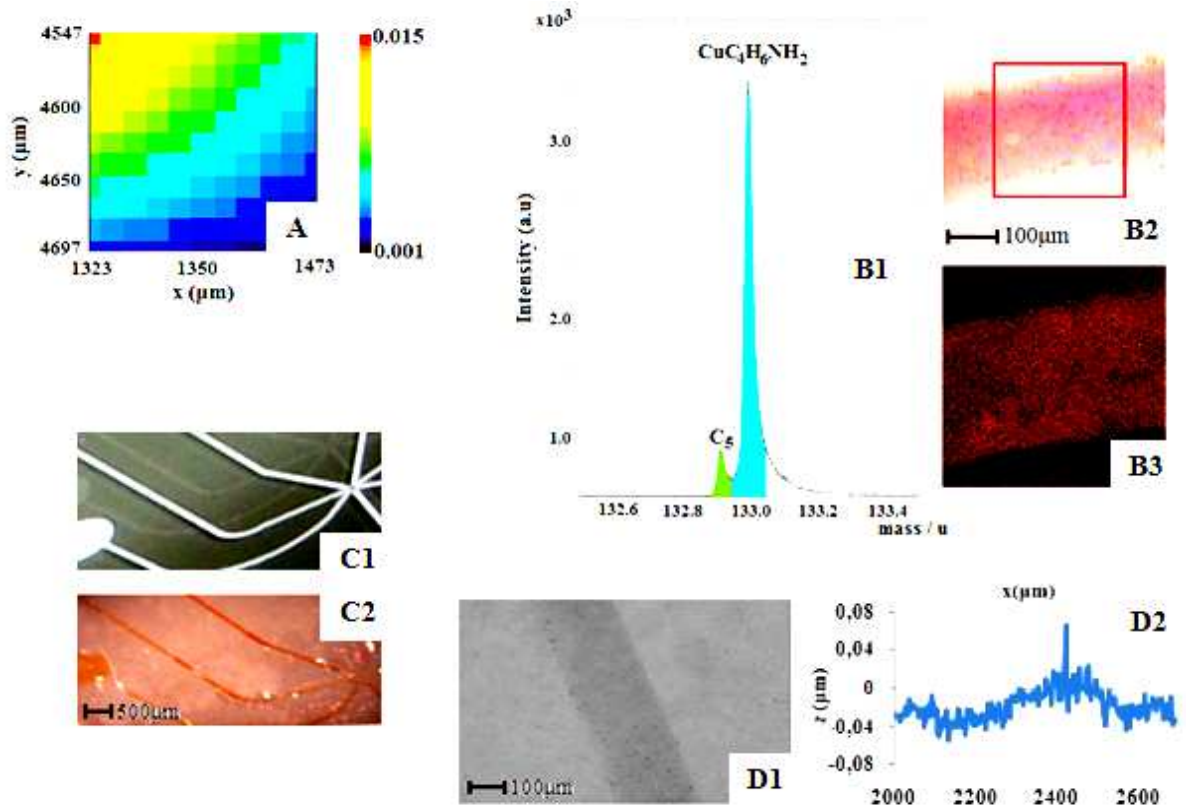


Figure 11. Localized photografting of a copper wafer: A) IR map of a spot grafted through a Teflon® mask with 2 mm holes (40x40 µm^2 beam size, recorded at 1600 cm^{-1}). B-D) Line grafted through a chromed quartz mask with 133 µm wide lines: B1) Tof-SIMS positive fragments at m/z = 132.99. B2, 3) images obtained from B2) the sum of the intensities of all positive ions and B3) the intensity of the m/z = 132.99 ion (in the red rectangle in B2). C) optical images of C1) the mask and C2) the obtained pattern (note that the scale is nearly the same). D1) optical image of the grafted line; D2) the corresponding interferometric profile across the grafted band.

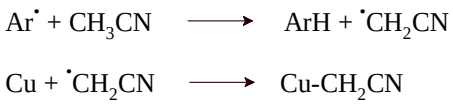
Discussion

The existence of an organic layer on metallic surfaces due to the photochemical grafting of ACN is evidenced by the surface IR spectra, the SEM images and the Tof-SIMS spectra that are different from those of the background. This layer contains nitrogen as shown by EDS and ToF-SIMS measurements, and this nitrogen is present as amines that are identified through their stretching and deformation bands in IRRAS. IRRAS also shows carbonyl bands and weak nitrile bands, while the latter are very strong in pure acetonitrile. Ellipsometry shows that these layers are in the 10-100 nanometer range, they are homogeneous as observed by SEM and ToF-SIMS. These layers are strongly bonded to the surface as they resist ultrasonication for 15 min; this strong attachment is due to a chemical bond as evidenced by

ToF-SIMS through the peaks containing both a metallic atom and part of the organic layer such as CuC_2H_3N (Figure 10C).

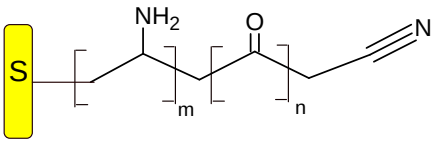
A remarkable difference between photo and electrografting can be mentioned. Under photografting, the thickness of the layer increases linearly with time since the radicals are continuously generated in the solution and bind to the growing layer. Conversely, under electrografting, the layer is self-limiting and reaches a limit after a certain time[74] since the electron must transfer from the electrode to the solution through the layer; as the layer grows, the electron transfer becomes slower and slower and finally stops.

These coatings can be compared with the layers obtained by indirect electrografting of ACN through hydrogen atom abstraction from ACN by the 2,6-dimethylphenyl radical ($Ar^{\bullet}$)[66] to give the cyanomethyl radical (Scheme 2):



Scheme 2

In this case, a structure containing amino and carbonyl groups was assigned to the layer. Here, a similar structure can be assigned to the photografted layer. It is presented in Scheme 3 along with the characteristic ToF-SIMS fragments. The layer obtained on a copper wafer after 10 min irradiation in ACN is 20 nm thick (Figure 6); for comparison, a $-CH_2-CH(NH_2)-$ group is 0.11 nm long.



S= substrate

ToF-SIMS fragments:

$-CH_2-CH(NH_2)-CH_2-C(=O)-H^+$,

$-CH_2-CH(NH_2)-CH_2-CH(NH_2)-^+$,

$-CH_2-CH(NH_2)-CH_2-CH(NH_3)-CH_2-CH_2-^+$

Scheme 3

A mechanism for the formation of the above layers is summarized in Scheme 4. We propose that the same cyanomethyl radical be responsible for the photografting of ACN and ICH_2CN.

The photografting of alkyl halides on metals (Cu, Au) under UV irradiation[60] and on diamond surfaces (hydrogenated or not) using X-ray beams[58] or UV irradiation with an Hg arc[59] has been reported and the alkyl radical was deemed responsible for the reaction with the metal. The electrochemical reduction of I, $BrCH_2CN$ has been described and the resulting cyanomethyl radical was shown to react with metallic surfaces to give amino layers.[65] The cyanomethyl radical has been previously identified in acetonitrile under irradiation [R1].[68,75] For example, this radical has been characterized by esr upon irradiation with a mercury lamp.[75a] Therefore, we propose that the cyanomethyl radical is formed by irradiation of either CH_3CN [R1] or ICH_2CN [R2]. It reacts with the surface along reaction [R3].

In the course of indirect electrografting, the growth of the layer was assigned to the reduction of the cyanomethyl radical into the cyanomethyl anion, which further reacts with the nitrile group already grafted to the surface (Thorpe reaction). In this case, the potential of the electrode (- 0.90 V(Ag/AgCl) on Au and Cu) or the open circuit potential (-0.44 V(Ag/AgCl) on Cu permitted the reduction of the radical to the anion.[66] Addition of 1% water completely suppressed the grafting reaction by protonation of the anion.

Here, upon addition of 1% water or acetic acid during photograting, there was no change in the IRRAS spectrum of the surface. Moreover, by adding TEMPO, the photografting was completely suppressed, indicating a radical reaction. This clearly shows that i) no anion and, ii) no electron transfer from the metal to the cyanomethyl radical are involved in the process. The ocp under irradiation (-0.37 V/(Ag/AgCl)) is not very different from the ocp measured during the indirect electrografting in the presence of 0.1 M 2,6-dimethylbenzene diazonium (-0.44 V/(Ag/AgCl)). [66] Therefore, the difference of mechanism between photochemical and electrochemical reactions (radical vs anionic reaction) cannot be explained by different potentials of the metal. It should originate from kinetics differences: the radical reaction would be faster than the anionic reaction under photochemical irradiation due to the increased concentration of the radical. Note that the cyanomethyl radical should be quite stable in ACN as the only reaction it may undergo in solution is a hydrogen atom abstraction from ACN, that regenerates the same radical.

Therefore, we propose that the growth of the layer be due to the attack of the cyanomethyl radical on the nitrile group of the first grafted $-CH_2CN$ group [R4]. The attack of the radical takes place on the carbon atom of the nitrile group. This reaction has already been reported in the litterature: [76] i) the cyanobutyl radical cyclizes to give cyclopentanone through an

intermediate iminyl radical, [77] (reaction rate: $4.5x10^2$ s^{-1} at 259 K);[78] ii) iminyl radicals are generated by 5-*exo* cyclisation of alkyl, vinyl and aryl *C*-centred radicals with nitriles;[79] iii) the fluoroformyl radical reacts with acetonitrile to give an iminyl radical [80] and the esr spectrum of iminyl radicals has been observed.[81] In Scheme 4, the iminyl radical can be hydrogenated to an imine by hydrogen atom transfer from ACN, regenerating a cyanomethyl radical [R5]; therefore, the reaction is a chain reaction. For comparison, the fast rate constants for the reaction of the 2-methyl-6,6-diphenyl-5-hexeniminyl radical with good hydrogen donors such as thiophenol and chlorothiophenol are: k = $0.6x10^7$ and $1.4x10^7$ M^{-1} s^{-1}, respectively. [82]

The formation of keto groups during the indirect electrografting [66] was assigned to the hydrolysis of the imine during the rinsing of the samples. But in the present photografting reaction, addition of 1% water or acetic acid does not change the $–NH_2$/C=O ratio measured by IRRAS. Therefore, the –C=O group does not originate from the hydrolysis of the imine. On gold, in the absence of dioxygen, the IR intensity of the carbonyl group is smaller but does not completely disappear; on copper this band increases when the copper surface is left in contact with air. This indicates that the sources of oxygen are atmospheric dioxygen *and* the surface oxides [R6]. The differences between the samples prepared with or without sonication indicate that sonication influences the results.[73] For samples prepared under the standard conditions described in the experimental section, it is difficult to explain why the –C=O band intensity increases in the order Cu<Fe<Ni<Au, it probably depends on many factors among which the structure of the oxide, its thickness, its bond dissociation energy. The high amount of carbonyl groups on gold can be related to the high activity of gold as a catalyst. This catalytic activity has been assigned to the extremely reactive nature of atomic oxygen bound in 3-fold coordination sites on metallic gold. This is the predominant form of O at low concentrations on the surface.[83] The formation of the carbonyl group can originate either from the iminyl radical or from the imine, but imines are stable in the presence of oxygen, therefore the reaction of the iminyl radical both with dioxygen and surface oxides is the most likely route to the carbonyl group [R6].

The photoreduction of imines in the presence of an hydrogen atom donor has been documented,[84,85] it occurs along reaction [R7] that also regenerates the cyanomethyl radical. This leads to amines that have been observed by IRRAS, and chemical derivatization. In the case of indirect electrografting,[66] we had assigned the reduction of the imine into an amine to an electron transfer. We have examined this possibility in the present case by recording the

open circuit potential (ocp) for the different metals under irradiation and the ratio of keto to amino groups (Table 2). The order of ocp is Cu, Au, Ni, Fe while that of -NH_2/C=O is Cu, Fe, Ni, Au. This difference of order does not support an electron transfer as the main route to the reduction of the imine.[86]

The chain grows by repeating these reactions of the cyanomethyl radical on the terminal nitrile, giving both amines and keto groups in the chain [R8]. The process is a chain reaction as cyanomethyl radicals are generated through [R5 and R7]. The small nitrile bands observed in IRRAS correspond to the terminal nitrile groups.

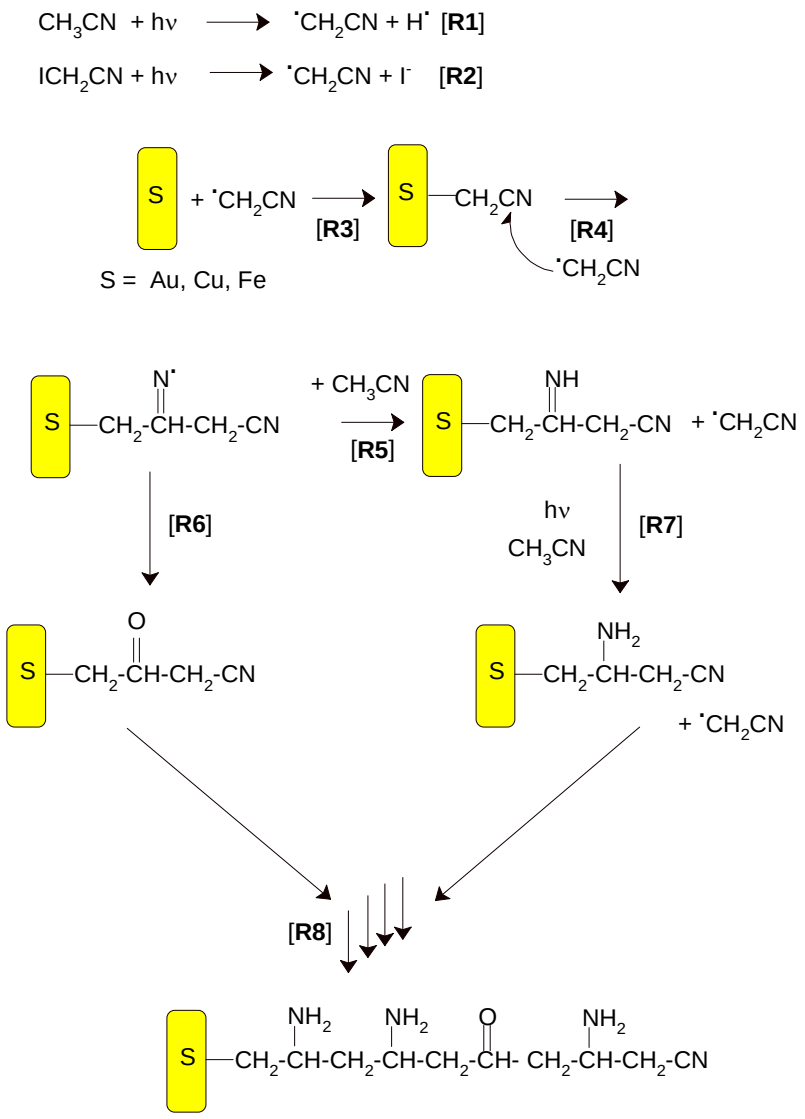
Localized grafting through a mask gives a pattern whose size is similar to that of the mask (~150-200 µm lines). Such pattern size compares well with patterns obtained with SECM. It is a little larger than those obtained with PDMS stamps and 3 orders of magnitude larger than those obtained with polystyrene beads. Clearly, the interest of the method we propose is not in the size that it is possible to reach. But with grafting by irradiation through masks or by SECM, the pattern can be tailored at the micrometer scale, which is the size suited for biological applications. With nanobeads or particles, the pattern is fixed since the patterned zone corresponds to the free electrode surface left between the beads arranged in a hexagonal structure. Smaller patterns would necessitate smaller masks or grids and likely a more powerful UV source.[87]

Conclusion

The photochemical grafting of ACN is possible on metals, it gives thin organic layers functionalized with amino and keto groups. This method is quite easy to implement, it only necessitates a UV lamp and a very common solvent. Interestingly, the structure of the layers is similar to that obtained through indirect electrografting or through electrografting of I and $BrCH_2CN$, but the mechanism is different, as indicated by the addition of water that stops the electrografting reaction, but does not change the photografting reaction. Therefore, a mechanism involving only radicals is proposed.

Localized grafting is easily performed by carrying out the photografting reaction through a mask. The size of the pattern, which is similar to that of the mask, compares well with patterns obtained with SECM. The interest of the method is not in the size that it is possible to reach, but in the easiness to implement it in the micrometer range, that is well suited for

biological applications. Since amino groups are easily post functionalized, it should be possible to use this localized grafting for the construction of biosensors.



Scheme 4

Acknowledgments. We are grateful to Alchimer society for the Tof-SIMS spectra, to Ms. Sandra Nunige for the SEM spectra, and to Dr Didier Thiébaut and Ms. Ramia Bakain for the ESI-MS spectrum of the solution. The Langlois foundation is acknowledged for financial support to one of us (F. I. P.).

Supporting Information Available: experimental section, IRRAS spectra for Ni, Fe, Au surfaces photografted with ACN and blank experiments without irradiation, determination of ocp, contact angles. This material is available free of charge via the Internet at http://pubs.acs.org.

---

[1] Palacin, S.; Bureau, C.; Charlier, J.; Deniau, G.; Mouanda, B.; Viel, P. *ChemPhysChem.* **2004**, *5*, 1468.

[2] a) Pinson, J.; Podvorica, F. *Chem. Soc. Rev*. **2005**, *34*, 249. b) Bélanger, D.; Pinson, J. *Chem. Soc. Rev*. **2011**, *40*, 3995.

[3] Brooksby P. A.; Downard, A. J. *Langmuir* **2005,** *21*, 1672.

[4] Duwez, A.-S.; Cuenot, S.; Jérôme, C.; Gabriel, S.; Jérôme, R.; Rapino S.; Zerbetto, F. *Nature Nanotech.* **2006**, *1*, 122.

[5] Garrett, D. J.; Lehr, J.; Miskelly G. M.; Downard, A. J. *J. Am. Chem. Soc.* **2007**, *129*, 15456.

[6] Downard, A. J.; Garrett D. J.; Tan, E. S. Q. *Langmuir* **2006,** *22*, 10739.

[7] Corgier, B. P.; Bélanger, D. *Langmuir* **2010**, *26*, 5991.

[8] Cougnon, C.; Gohier, F.; Bélanger, D.; Mauzeroll, J. *Angew. Chem., Int. Ed*. **2009**, *48*, 4006.

[9] Matrab, T.; Combellas, C.; Kanoufi, F. *Electrochem. Commun.*, **2008**, *10*, 1230.

[10] Matrab, T.; Combellas, C.; Kanoufi, F. *Electrochem. Commun.*, **2008**, *10*, 1230.

[11] Hauquier, F.; Matrab, T.; Kanoufi, F.; Combellas, C. *Electrochim. Acta* **2009**, *54*, 5127.

[11] Matrab, T.; Hauquier, F.; Combellas, C.; Kanoufi, F. *ChemPhysChem*. **2010**, *11*, 670.

[12] Combellas, C.; Kanoufi, F.; Nunige, S. *Chem. Mater.* **2007**, *19*, 3830.

[13] Ghorbal A., A.; Grisotto, F.; Charlier, J.; Palacin, S; Goyer, C.; Demaille, C. *ChemPhysChem* **2009**, *10*, 1053.

[14] Charlier, J.; Palacin, S.; Leroy, J.; DelFrari, D.; Zagonel, L.; Barrett, N.; Renault, O.; Bailly, A.; Mariolle, D. *J. Mater. Chem.* **2008**, *18*, 3136.

[15] Charlier, J.; Clolus, E.; Bureau, C.; Palacin, S. *J. Electroanal. Chem.* **2009**, *625*, 97.

[16] Charlier, J.; Baraton, L.; Bureau, C.; Palacin, S. *ChemPhysChem.* **2005**, *6*, 70.

[17] Charlier, J.; Ameur, S.; Bourgoin, J.-P.; Bureau C.; Palacin, S. *Adv. Funct. Mater.* **2004**, *14*, 125.

[18] Azioune, A.; Storch, M.; Bornens, M.; Thery, M.; Piel, M. *Lab. On Chip* **2009**, *9*, 1640.

[19] Allméar, K.; Hult, A.; Rånby, B. *J. Appl. Polym. Sci.* **1988,** *26***,** 2099.

[20] Yang, W.; Rånby B. J. Appl. Polym. Sci. 1996, 62 , 545.

[21] Han, J.; Wang, H. *J. Appl. Polym. Sci* **2009**, *113*, 2062

[22] Yong, G.; Zhihua; N.; Huaming, L. *J. Polym. Res.* **2009**, *16*,709.

[23] Subramanyam, U.; Kennedy, J. P. *J. Polym. Sci., Part A* **2009**, *47*, 5272.

[24] Szunerits, S.; Boukherroub, R. *J. Solid State Electrochemistry* **2008**, *12*, 1205.

[25] Kim, C. S.; Mowrey, R. C.; Butler, J. E.; Russell, Jr. J. N. *J. Phys. Chem. B* **1998**, *102*, 9290.

[26] Strother, T.; Knickerbocker, T.; Russell, Jr., J. N.; Butler, J. E.; Smith, L. M.; Hamers R. J. *Langmuir* **2002**, *18*, 968.

[27] Yang, W.; Baker, S. E.; Butler, J. E.; Lee, C.-s.; Russell Jr., J. N.; Shang, L.; Sun, B; Hamers R. J. *Chem. Mater.* **2005**, *17*, 938.

[28] Lasseter, T. L.; Clare, B. H.; Abbott, N. L.; Hamers, R. J. *J. Am. Chem. Soc.* **2004**, *126*, 10220.

[29] Nichols, B.M.; Butler, J. E.; Russell Jr., J. N.; Hamers R. J. *J. Phys. Chem. B* **2005**, *109*, 20938.

[30] Nichols, B.M.; Metz, K. M.; Tse, K.-Y.; Butler, J. E.; Russell Jr, J. N.; Hamers R. J. *J. Phys. Chem. B* **2006**, *110*, 16535.

[31] Nebel, C. E.; Shin, D.; Takeuchi, D.; Yamamoto, T.; Watanabe, H.; Nakamura T. *Langmuir* **2006**, *22*, 5645.

[32] Steenackers, M.; Lud, S. Q.; Niedermeier, M.; Bruno, P.; Gruen, D. M.; Feulner, P.; Stutzmann, M.; Garrido, J. A.; Jordan, R. *J. Am. Chem. Soc.* **2007**, *129*, 15655.

[33] Wang, X.; Colavita, P. E.; Metz, K. M.; Butler, J. E.; Hamers, R. J. *Langmuir* **2007**, *23*, 11623.

[34] Nebel, C. E.; Uetsuka, H.; Rezek, B.; Shin, D.; Tokuda, N.; Nakamura, T. *Mater. Res. Soc. Symp. Proc*. **2007**, *956*, 113.

[35] Chong, K. F.; Loh, K. P.; Vedula, S. R. K.; Lim, C. T.; Sternschulte, H.; Steinmüller, D.; Sheu, F.-s.; Zhong Y. L. *Langmuir* **2007**, *23*, 5615.

[36] Zhong, Y. L.; Chong, K. C.; May, P. W.; Chen, Z.-K.; Loh K. P. *Langmuir* **2007**, *23*, 5824.

[37] Rezek, B.; Shin, D.; Nebel C. E. *Langmuir* **2007**, *23*, 7626.

[38] Yang, N.; Uetsuka, H.; Watanabe, H.; Nakamura, T.; Nebel C. E. *Diamond Rel. Mater.* **2008**, *17*, 1376.

[39] Colavita, P. E.; Sun, B.; Wang, X.; Hamers, R. J. *J. Phys. Chem. C* **2009**, *113*, 1526.

[40] Landis, E. C.; Hamers, R. J. *J. Phys. Chem. C* **2008**, *112*, 16910.

[41] Colavita, P. E.; Sun, B.; Tse, K.-Y.; Hamers, R. J. *J. Vacuum Sci. Tech.* A **2008**, 26, 925.

[42] Colavita, P. E.; Streifer, J. A.; Sun, B.; Wang, X.; Warf, P.; Hamers, R. J. *J. Phys. Chem. C* **2008**, *112*, 5102.

[43] Colavita, P. E.; Sun, B.; Tse, K.-Y.; Hamers, R. J. *J. Am. Chem. Soc*. **2007**, *129*, 13554.

[44] Yu, S. S. C.; Tan, E.S.Q.; Jane, R.T.; Downard A. J. *Langmuir* **2007**, *23*, 4662.

[45] Lockett, M. R.; Shortreed, M. R.; Smith, L. M. *Langmuir* **2008**, *24*, 9198.

[46] Ellison, M. D.; Buckley, L. K.; Lewis, G. G.; Smith, C. E.; Siedlecka, E. M.; Palchak, C. V.; Malarchik, J. M. *J. Phys. Chem. C* **2009**, *113*, 18536.

[47] Dyer, D.J. *Adv. Polym. Sci.* **2006,** *197*, 47.

[48] Pellegrino, G.; Motta, A.; Cornia, A.; Spitaleri, I.; Fragala, I. L.; Condorelli, G. G. *Polyhedron* **2009**, *28*, 1758.

[49] Moraillon, A.; Gouget-Laemmel, A. C.; Ozanam, F.; Chazalviel, J.-N. *J. Phys. Chem. C* 2008, *112*, 7158.

[50] Bellec, N.; Faucheux, A.; Hauquier, F.; Lorcy, D.; Fabre, B. *Int. J. Nanotech.* **2008**, *5*, 741.

[51] Faucheux, A.; Gouget-Laemmel, A. C.; Allongue, P.; Henry de Villeneuve, C.; Ozanam, F.; Chazalviel, J.-N. *Langmuir* **2007**, *23*, 1326.

[52] Coffinier, Y.; Boukherroub, R.; Wallart, X.; Nys, J.-P.; Durand, J.-O.; Stievenard, D.; Grandidier, B. *Surf. Sci.* **2007**, *601*, 5492.

[53] Ha, T. H.; Park, M.-R.; Park, H. J.; Choi, J.-S.; Kim, G.; Hyun, M. S.; Chung, B. H. *Chem. Commun*. **2007**, *16*, 1611.

[54] Mischki, T. K.; Donkers, R. L.; Eves, B. J.; Lopinski, G. P.; Wayner, D. D. M. *Langmuir* **2006**, *22*, **8359**.

[55] Gauthier, N.; Argouarch, G.; Paul, F.; Humphrey, M. G.; Toupet, L.; Ababou-Girard, S.; Sabbah, H.; Hapiot, P.; Fabre, B. *Adv. Mater*. **2008**, *20*, 1952.

[56] Yang, M.; Teeuwen, R. L. M.; Giesbers, M.; Baggerman, J.; Arafat, A.; de Wolf, F. A.; van Hest, J. C. M.; Zuilhof, H. *Langmuir* **2008**, *24*, 7931.

[57] Fabre, B. *Acc. Chem. Res*. **2010**, *43*, 1509.

[58] Smentkowski, V. S.; Yates, J. T., Jr. *Science* **1996**, *271*, 193.

[59] Kim, C. S.; Mowrey, R. C.; Butler, J. E.; Russell, J.N. *J. Phys.Chem. B* **1998**, *102*, 9290.

[60] Chehimi, M. M.; Hallais, G.; Matrab, T.; Pinson, J., Podvorica, F. I. *J. Phys. Chem. C* **2008,** *112*, 18559.

[61] Harmer, M. A. *Langmuir* **1991**, *7*, 2010-2012.

[62] Yan, M. D.; Cai S. X.; Wybourne M. N.; Keana J. W. F. *J. Am. Chem. Soc*. **1993**, *115*, 814-816.

[63] Charlier, J.; Clolus, E.; Bureau, C.; Palacin, S. *J. Electroanal. Chem*. **2008**, *622*, 238.

[64] Flavel, B. S.; Gross, A. J.; Garrett, D. J.; Nock, V.; Downard, A. J. *ACS Appl. Mater. Interfaces* **2010**, *2*, 1184.

[65] Combellas, C.; Kanoufi, F.; Osman, Z.; Pinson, J.; Adenier, A.; Hallais, G. *Electrochim. Acta*, **2011**, *56*, 1476.

[66] Berisha, A.; Combellas, C., Kanoufi, F.; Pinson, J.; Ustaze, S.; Podvorica, F. I. *Chem. Mater.* **2010**, *22*, 2962.

[67] Combellas, C.; Jiang, D.; Kanoufi, F.; Pinson, J.; Podvorica F. I. *Langmuir* **2009**, *25*, 286.

[68] Nakamura, T.; Ohana, T.; Ishihara, M.; Hasegawa, M.; Koga, Y. *Diamond Rel Mater.* **2008**, *17*, 559.

[69] Socrates, G. *Infrared and Raman Characteristic Group Frequencies*, 3rd ed. ; John Wiley & Sons: New York, **2008**.

[70] Sheets, R.W.; Blyholder, G. *J. Catalysis* **1981**, *67*, 308.

[71] Rozkiewicz, D. I.; Ravoo, B. J.; Reinhoudt, D. N. *Langmuir* **2005**, *21*, 6337.

[72] Acros Organics catalog ; http://www.acros.com, RN 123-42-2

[73] Paulik, M. G.; Brooksby, P. A.; Abell, A. D.; Downard A. J. *J. Phys. Chem.* C **2007**, *111*, 7808.

[74] Brooksby P. A.; Downard, A. J. *J. Phys. Chem. B* **2005,** *109*, 8791.

[75] a) Svejda, P.; Volman, D. H. *J. Phys. Chem.* **1970**, *74,* 1872. b) Lesiecki, M. L.; Guillory, W. A. *J. Chem. Phys.* **1978**, *69*, 4572. c) Halpern, J. B.; Tang, X. *Chem. Phys. Lett.* **1985**,*122*, 294. d) Chuang, C. C.; Wu, W. C.; Lee, M. X.; Lin, J. L. *PhysChemChemPhys*. **2000**, *2*, 3877.

[76] de Lijser, H. J. P.; Arnold, D. R. *J. Phys. Chem. A* **1998**, *102*, 5592 and references therein.

[77] (a) Ogibin, Yu. N.; Troyanski, E. I.; Nikishin, G. I. *Izv. Akad. Nauk. SSSR, Ser. Khim.* **1975**, 1461. (b) Ogibin, Yu. N.; Troyanski, E. I.; Nikishin,G. I. *Izv. Akad. Nauk. SSSR, Ser. Khim*. **1977**, 843.

[78] (a) Griller, D.; Schmid, P.; Ingold, K. U. *Can. J. Chem*. **1979**, *57*, 831. (b) Roberts, B. P.;Winter, J. N. *J. Chem. Soc., Perkin Trans. 2* **1979**, 1353.

[79] Russell Bowman, W.; Bridge, C. F.; Brookes P. *Tet. Lett.* **2000**, *41*, 8989.

[80] Bucher, G.; Kolano, C.; Schade, O.; Sander, W. *J. Org. Chem*. **2006**, *71*, 2135.

[81] Portela-Cubillo, F.; Alonso-Ruiz, R.; Sampedro, D.; Walton**,** J. C. *J. Phys. Chem. A* **2009,** *113*, 10005.

[82] Le Tadic-Biadatti, M.-H.; Callier-Dublanchet, A.-C. ; Horner, J. H.; Quiclet-Sire, B. ; Zard, S. Z.; Newcomb, M. *J. Org. Chem.* **1997,** *62*, 559.

[83] Baker, T. A.; Liua, X.; Friend, C. M. *Phys. Chem. Chem. Phys*. **2011**, *13*, 34.

[84] Coyle, D.J., *Introduction to Organic Photochemistry*, 5°ed, Wiley Interscience, New York, **1998**, p144.

[85] Ortega, M.; Rodriguez, M. A.; Campos, P. J. *Tetrahedron* **2005**, *61*, 11686.

[86] As indicated in the Discussion Section, the open circuit potentials in the indirect electrografting and under irradiation are not very different. Therefore, in the case of Cu there may be some involvement of the electron transfer during the reduction of the imine.

[87] Yee, C. K. ; Amweg, M. L. ; Parikh, A.N. *J. Am. Chem. Soc*. **2004**, *126*, 13962.

3.3. Supporting informations

Photochemical grafting and Patterning of Metallic Surfaces by Organic Layers Derived from Acetonitrile

Avni Berisha, Catherine Combellas, Géraldine Hallais, Frédéric Kanoufi, Jean Pinson and Fetah I. Podvorica

Supporting Information

Comparison of two different qualities of ACN and influence of atmospheric oxygen before treatment

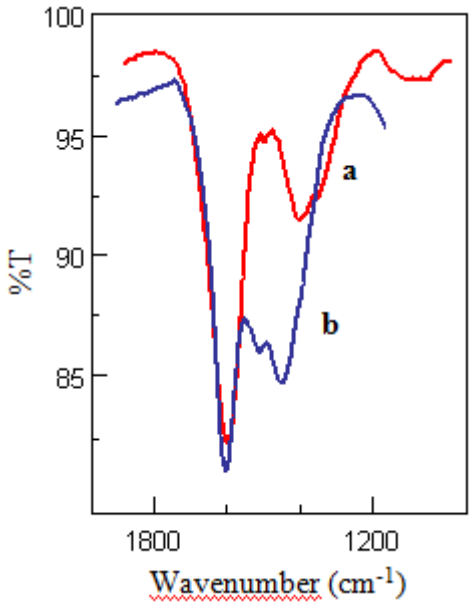


Figure S1. Copper wafer irradiated for 30 min in a) 99.8% anhydrous ACN and b) 99.9% Chromasolv ACN (Aldrich).

Two pieces of copper wafers were cleaned as indicated in the experimental section, The two different qualities of acetonitrile (99.8% anhydrous acetonitrile and 99.9% Chromasolv, Aldrich) provide identical results.

IRRAS spectra of Au, Ni and Fe surfaces photografted with ACN along with the blank experiments without irradiation are given in Figures S2-4.

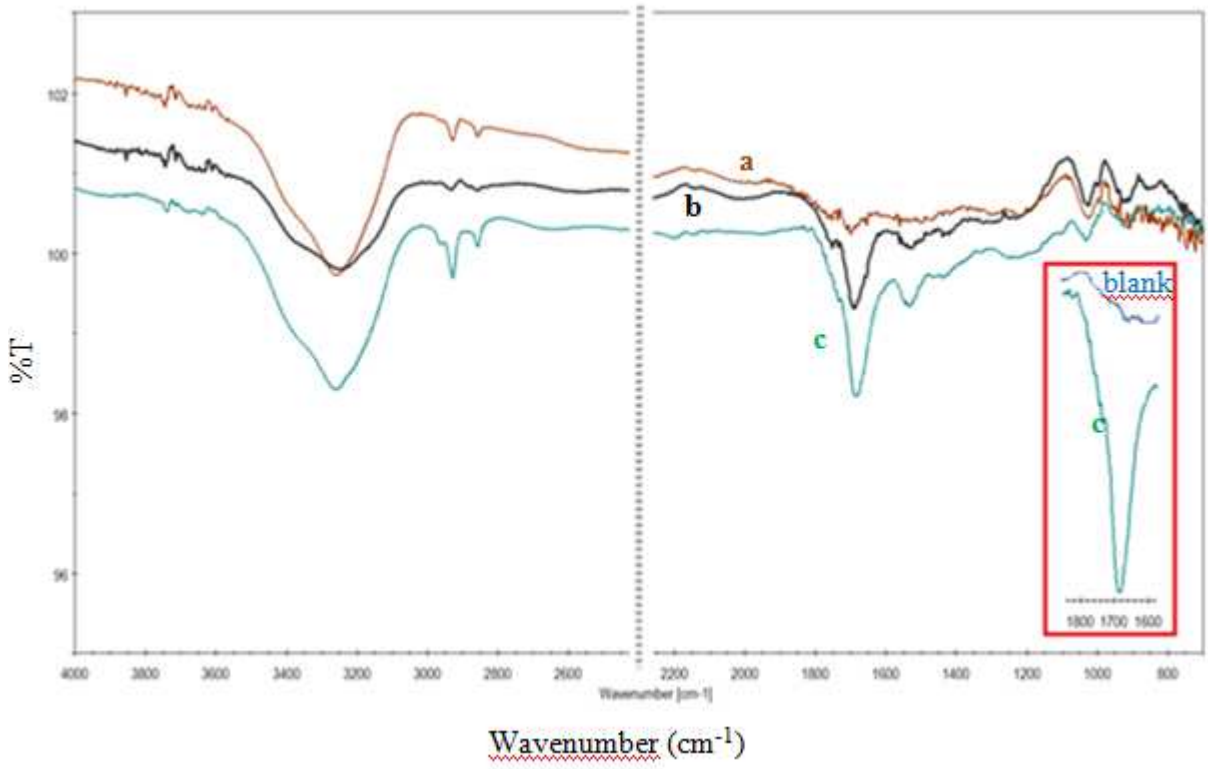


Figure S2. Au wafer after UV irradiation in ACN for a) 10, b) 20 and c) 30 min. Inset: blank) Gold wafer left in the ACN solution without irradiation for 30 min compared with c), the same wafer irradiated for 30 min. Ultrasonication for 10 min in acetone after photografting.

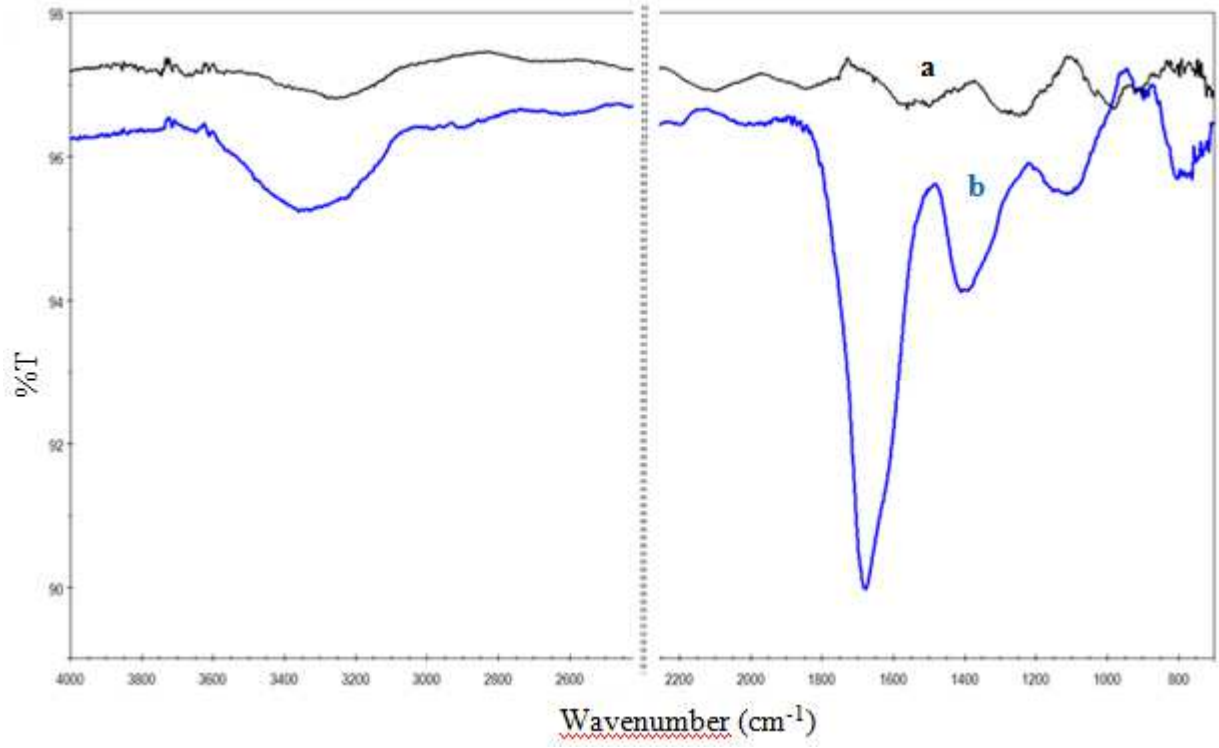


Figure S3. Ni plate a) left in the ACN solution for 30 min without irradiation), b) after UV irradiation in ACN for 20 min.

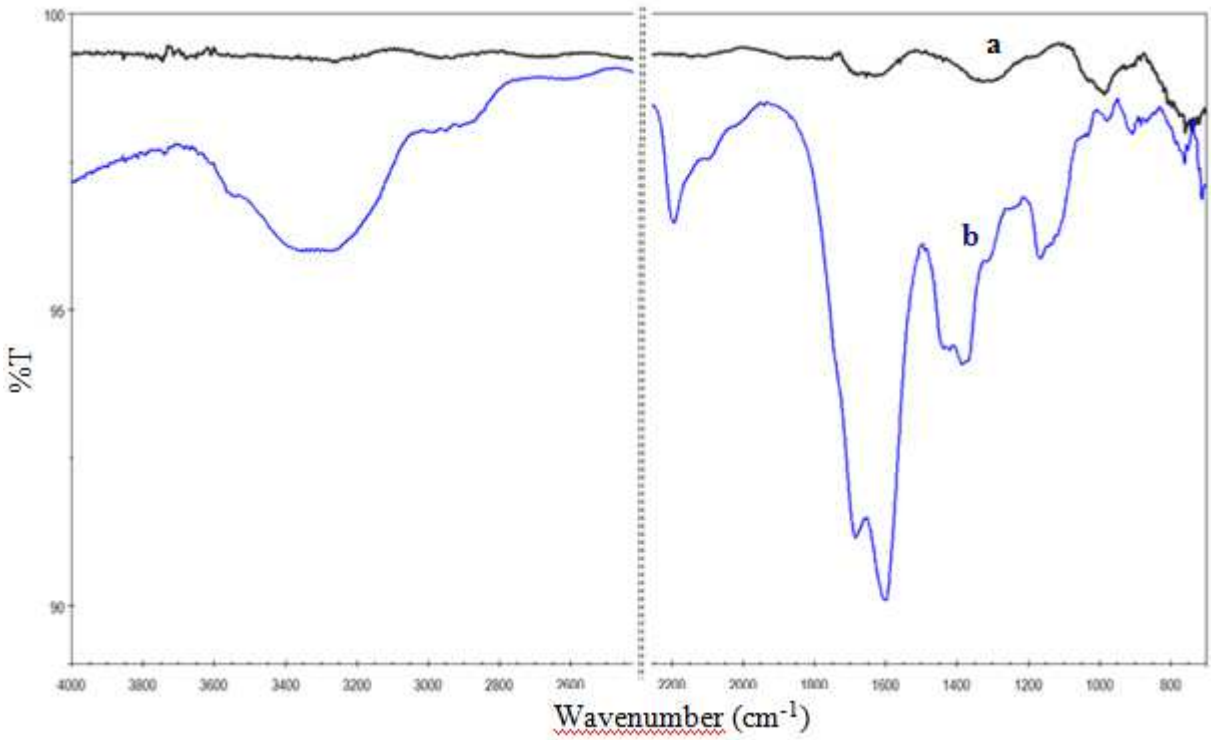


Figure S4. Fe plate a) left in the ACN solution for 30 min without irradiation), b) after UV irradiation in ACN for 20 min.

IRRAS spectra of gold and copper plates modified in the absence of dioxygen.

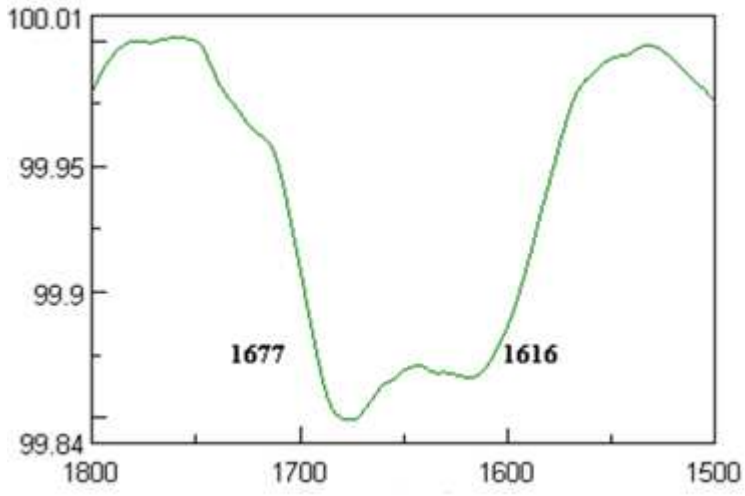
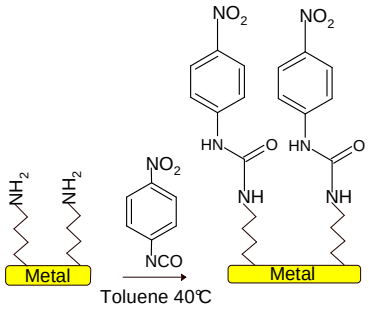


Figure S5. Gold wafer after UV irradiation in ACN for a) 10 min in a glove box containing less than 1ppm of dioxygen. Ultrasonication for 10 min in acetone after photografting.

Characterization of the amino groups by reaction with isocyanate

To ascertain the presence of amino groups, the modified copper wafers have been reacted with 4-nitro- or 4- *tert*-butylphenylisocyanates (Scheme 1):



Scheme S1. Reaction of surface amino group on a copper wafer with 4-nitrophenylisocyanate.

After reaction of a modified copper wafer with 4-nitrophenylisocyanate, the IRRAS spectrum (Figure S7 Ab) shows the presence of two new peaks at 1505 and 1330 cm^{-1} (designated by ∗) that are attributed to the asymmetric and symmetric stretching of the -NO_2 group (by comparison with nitrobenzene: 1521 and 1347 cm^{-1}). After reaction of a modified copper wafer with *t*-butylphenylisocyanate (Figure S7 Bc), a peak corresponding to -CH_3 stretching appears at 2965 cm^{-1} (designated by ∗), by comparison with *t*-butylbiphenyl: 2954 and 2926 cm^{-1}). These results confirm the reaction of grafted –NH_2 groups with 4-nitro or 4-*t*-

butylphenylisocyante. The reactions are less efficient than the reaction with 4-nitrobenzoyl chloride.

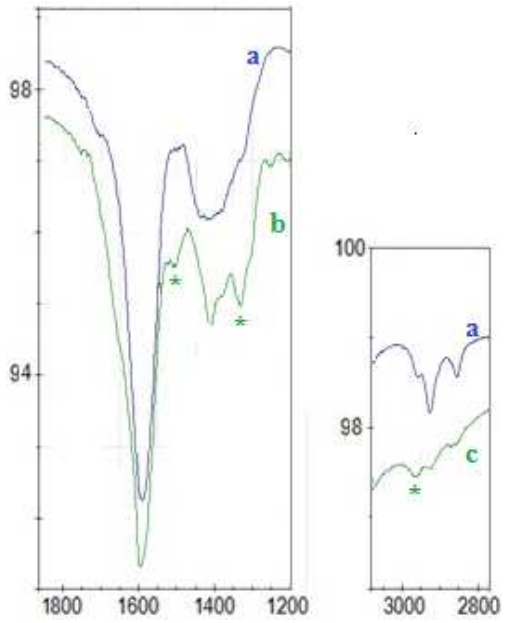


Figure S6. Copper wafer a) photografted by UV irradiation in ACN for 2 min , and immersed overnight in a 60 mM solution of b) 4-nitrophenylisocyanate and c) 4-*t*-butylphenylisocyanate in toluene at 40°C. Ultrasonication for 10 min in acetone after reaction**.**

Copper wafers modified for 20 min under UV irradiation in ACN + either 1% H_2O or acetic acid.

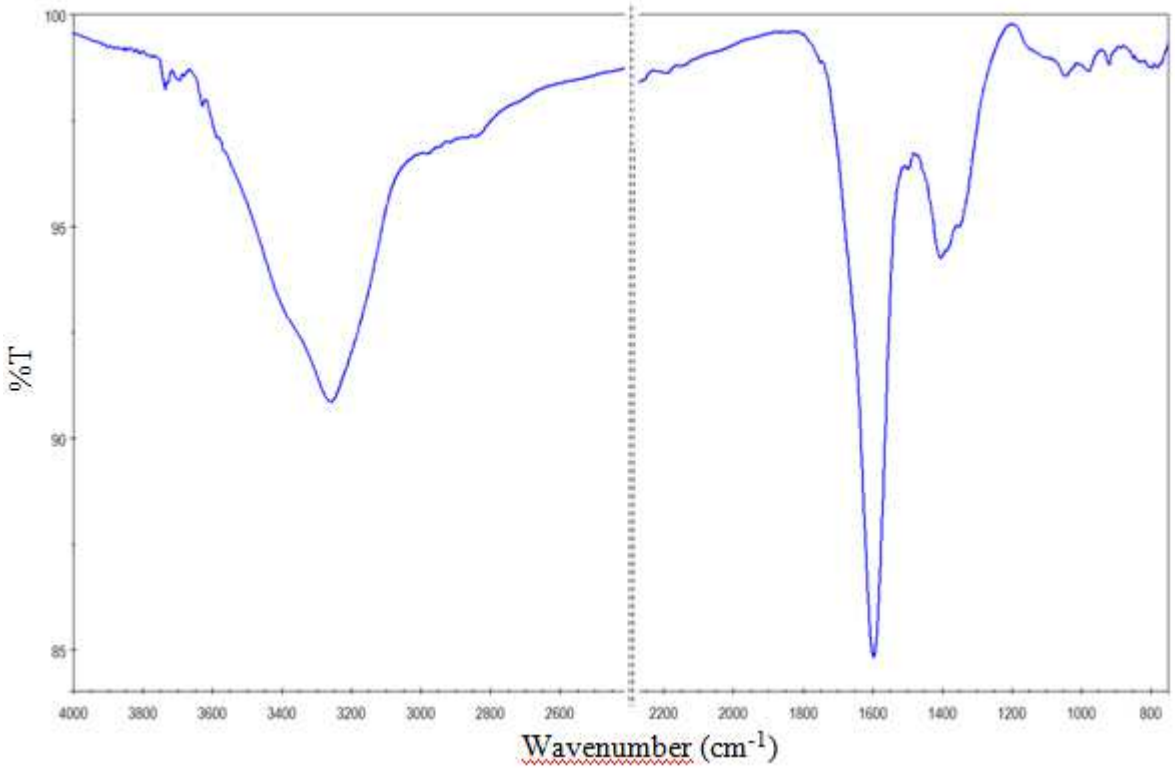


Figure S7. Cu wafer after UV irradiation in ACN +1% H_2O for 20 min.

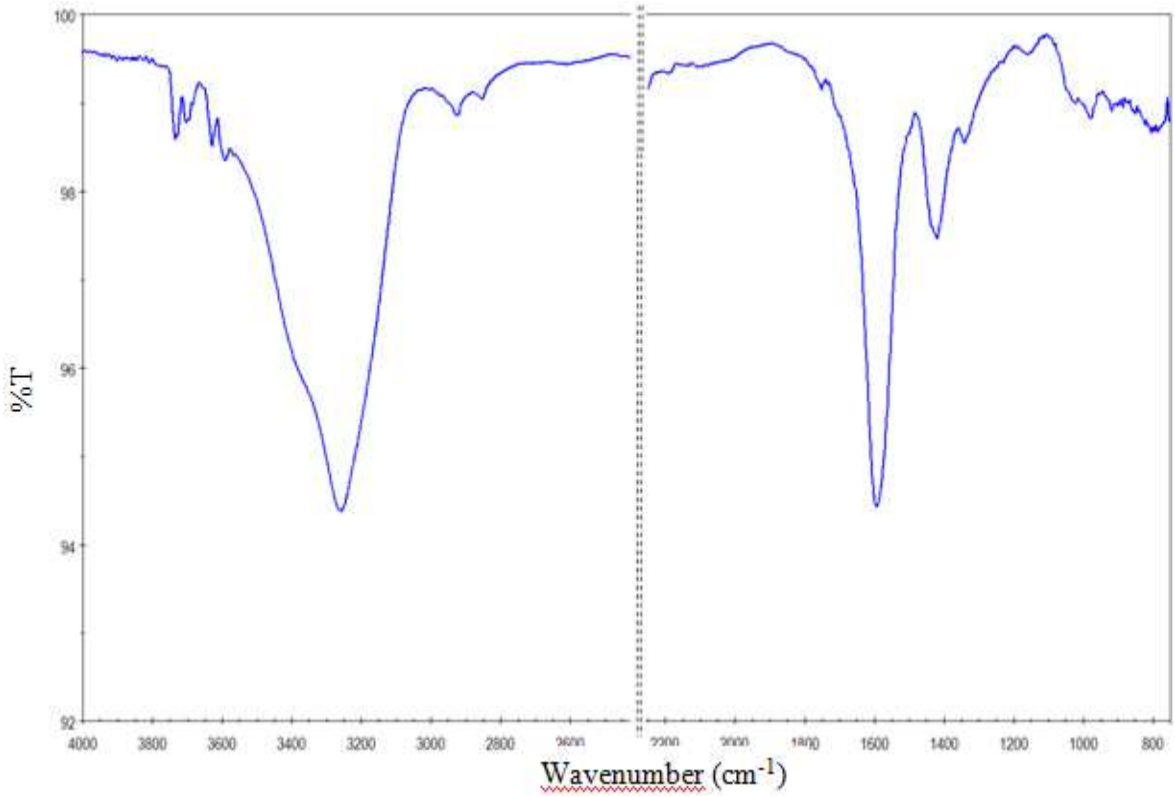


Figure S8. Cu wafer after UV irradiation in ACN +1% acetic acid for 20 min.

AFM images

Copper

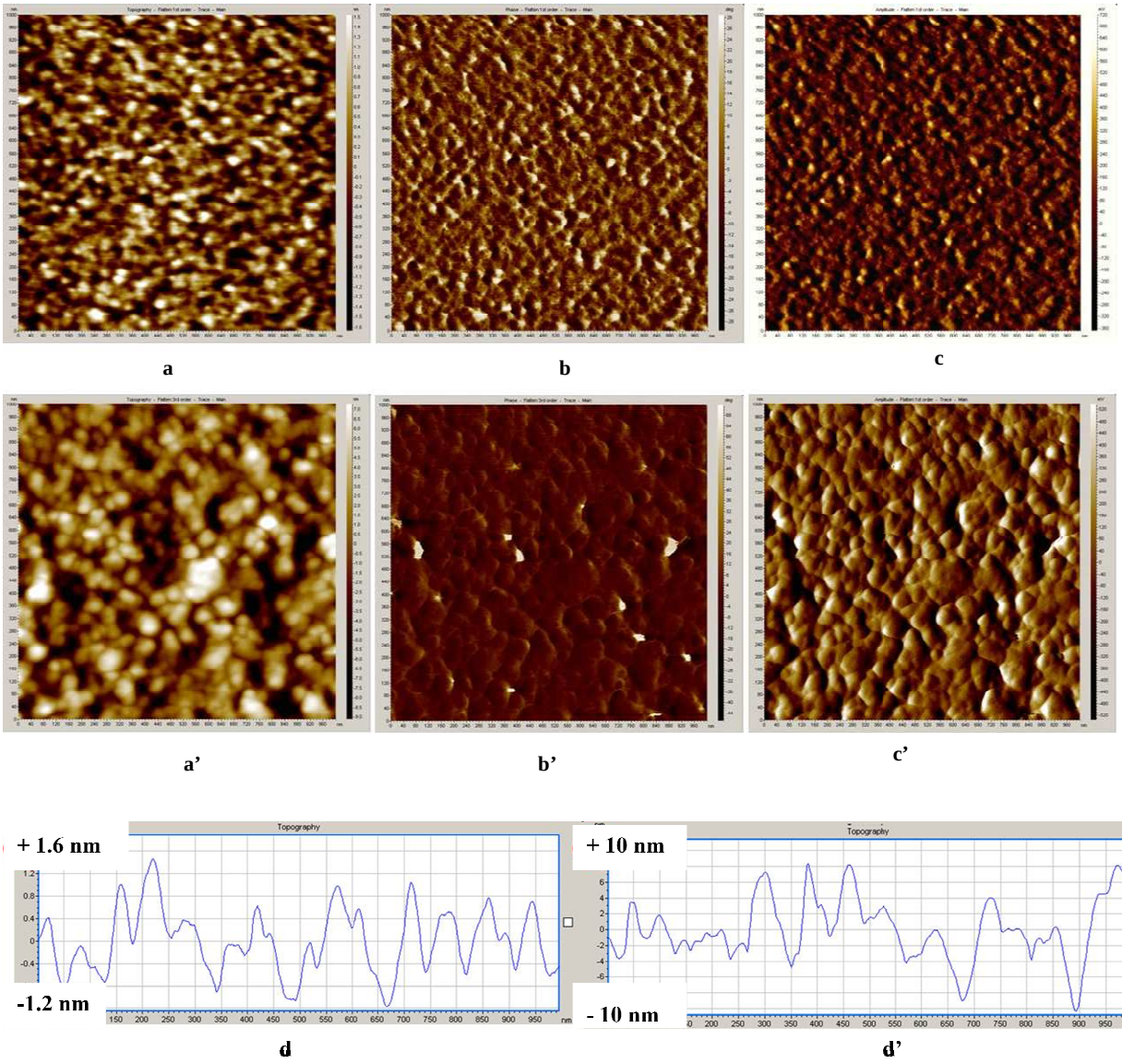


Figure S9. AFM images (1 x 1 µm^2). a, a') topographic; b, b') phase; c, c') amplitude images; d, d') topographic profiles. a, b, c, d) clean copper wafer; a', b', c', d') copper wafer irradiated for 10 min in ACN.

Gold

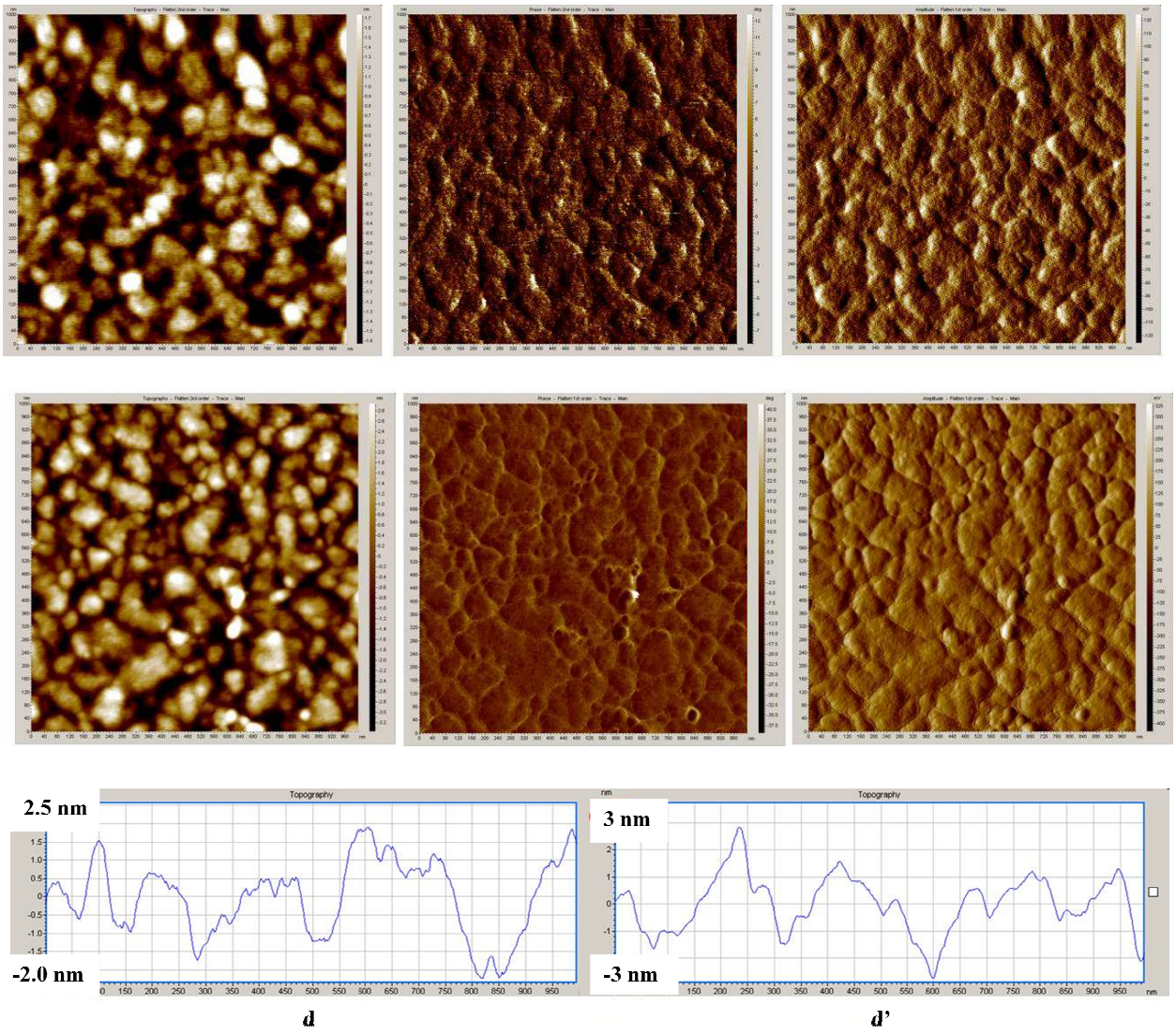


Figure S10. AFM images (1 x 1 μm^2). a, a') topographic; b, b') phase; c, c') amplitude images; d, d') topographic profiles. a, b, c, d) clean gold wafer; a', b', c', d') gold wafer irradiated for 10 min in ACN.

Chronopotentiometry and determination of open circuit potentials (ocps)

The metallic plates (or wafers) were connected with an insulated copper wire. The system consisted of an Ag/AgCl reference electrode, a carbon paper with a large area as the counter electrode and the metal plate as the working electrode. The UV lamp was held 4 cm from the plate surface during the measurements. The solution contained 20 mM NBu_4BF_4 in ACN. Chronopotentiometry curves of Cu, Au, Ni and Fe plates (or wafers) without and under UV irradiation are given in Figures S11-14.

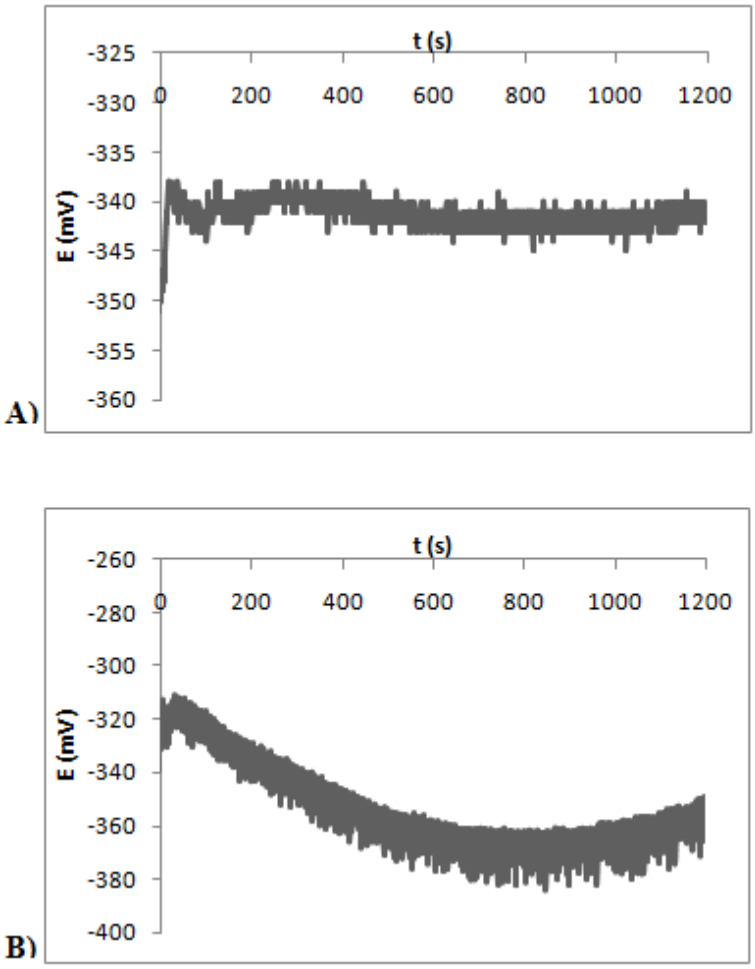


Figure S11. Chronopotentiometry for a copper wafer A) without and B) under UV irradiation.

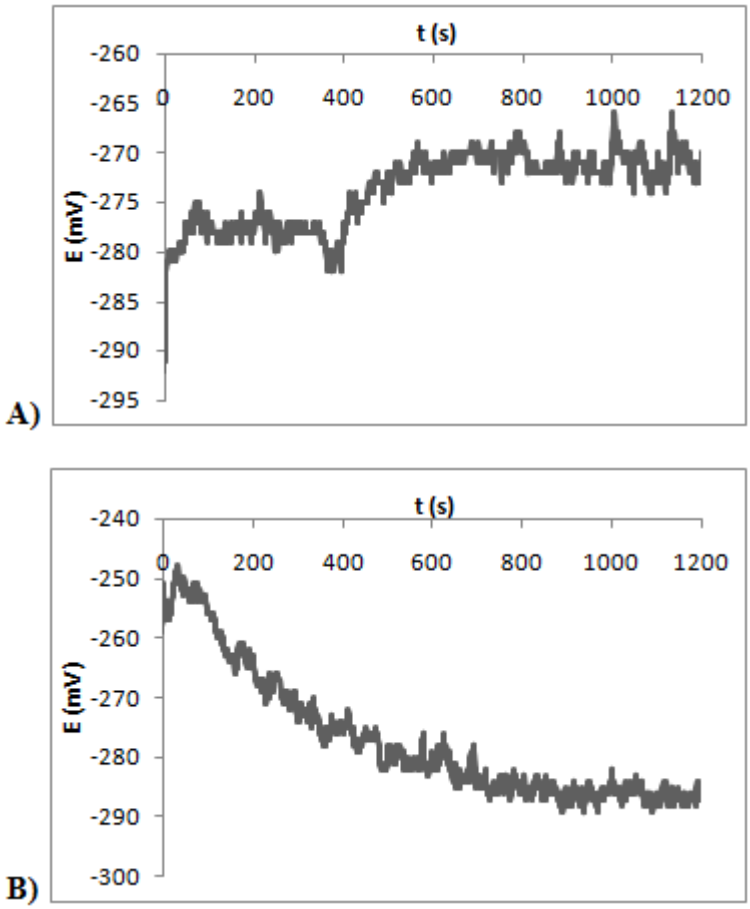


Figure S12. Chronopotentiometry for a gold wafer A) without and B) under UV irradiation.

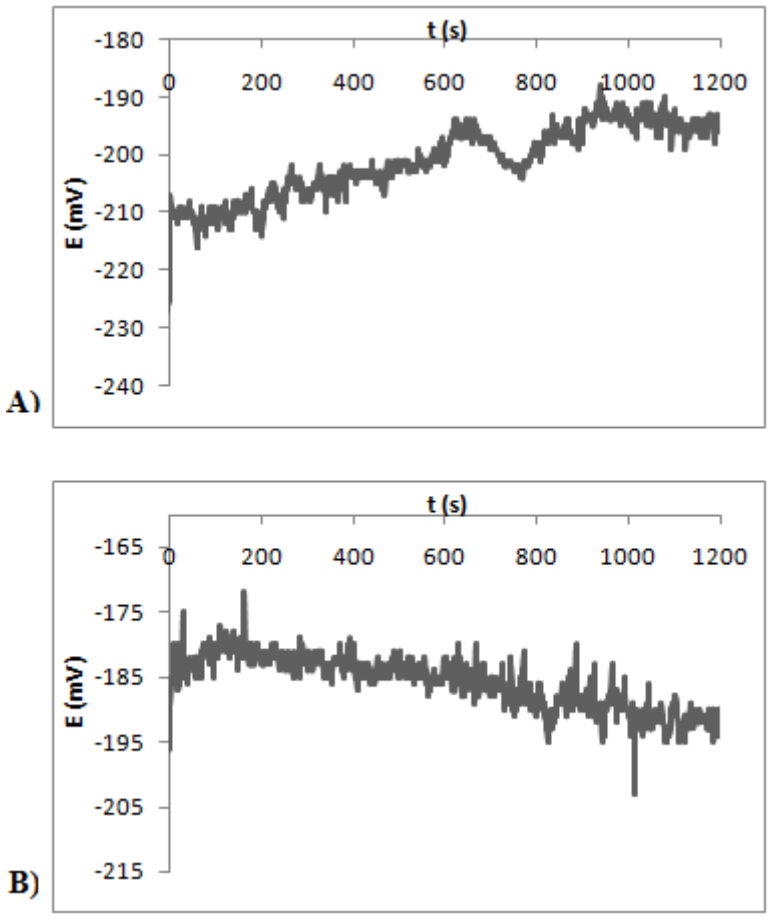


Figure S13. Chronopotentiometry for a nickel plate A) without and B) under UV irradiation.

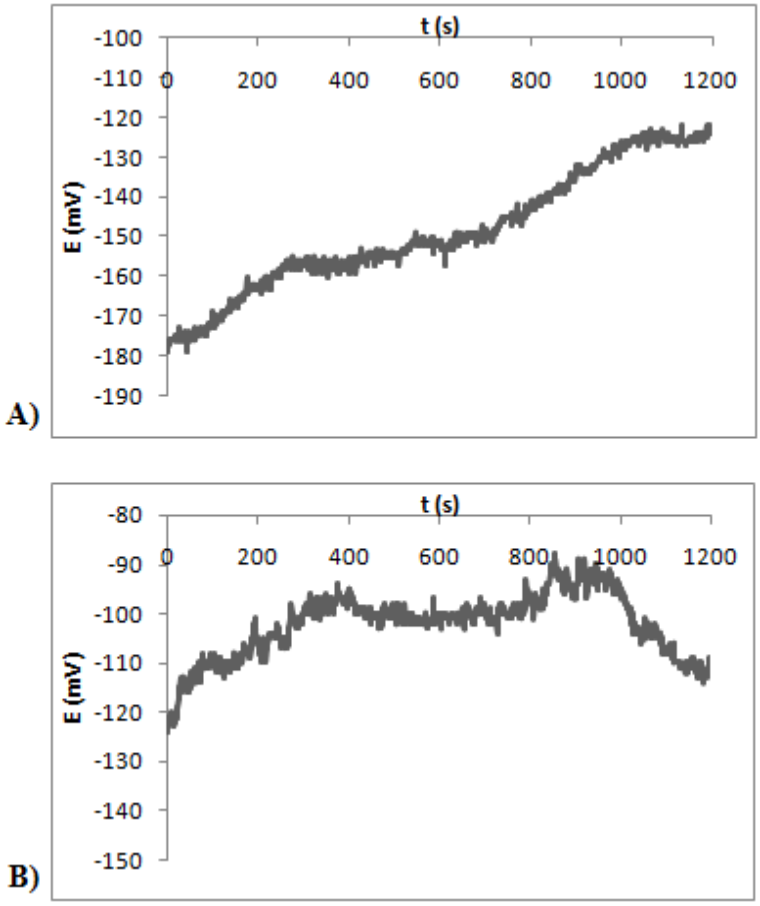


Figure S14. Chronopotentiometry for an iron plate A) without and B) under UV irradiation.

Water Contact angles

They were measured on bare and irradiated Cu and Au plated Si wafers (they are referred as Cu and Au wafers) in ACN for different time durations (Table 1). Once irradiated in CH_3CN, the contact angles for both surfaces are about the same (~60°), and they do not change with the treatment time (10, 20 or 30 min). This indicates that the surface energy of the organic film deposited onto the substrate is constant, whatever the substrate or the treatment time. For comparison, the advancing angles of a Si crystal covered by $-(CH_2)_{17}NH_2$ and $-(CH_2)_{16}CN$ are 58 and 69°, respectively[i]

Table SI1. Water Contact Angles on Bare and Modified Gold and Copper Plates upon Irradiation of ACN.[a,b]

	bare	10 min	20 min	30 min
Cu	45	59	60	61
Au	57	60	58	61

a) ° ± 4° , b) neat liquids.

[i] Margel, S.; Sivan, O.; Dolitzky, Y *Langmuir* **1991**, *7*, 2317.

3.4. Analysis

It had already been shown that alkyl radicals deriving from alkyl halides[1] or from haloacetonitrile[2] could be and could react with metallic surfaces. The previous paper describes the photochemical formation and grafting of the cyanomethyl radical starting from acetonitrile.

The obtained films are similar to those produced by the same radical under electrochemical conditions. But very surprisingly, the mechanisms responsible for the growth of the chain are different; an anion is involved in the electrochemical reaction and a radical in the photochemical reaction although the potentials of the metals are not very different. As stated in the paper, the difference likely stems from kinetics and it would be interesting to obtain some kinetic data on both processes.

This is a new example of the photogeneration of a radical followed by its coupling to a metallic surface. It can be assumed that this type of reaction can be generalized since many radicals can be produced by photochemistry. Looking at the reaction of these radicals with metals, carbon, or semiconducting surfaces, it should be an interesting field of research. Primary radicals should be favored as it has been shown - during the electrochemical grafting of amines - that the secondary radicals are much less reactive and that tertiary radicals do not react at all[3].

---

[1] M. M. Chehimi, Géraldine Hallais, Tarik Matrab, Jean Pinson, and Fetah I. Podvorica, The Journal of Physical Chemistry C **2008**, *112*, 18559–18565.

[2] C.Combellas, F.Kanoufi,Z.Osman, J.Pinson, A. Adenier, G. Hallais, Electrochimica Acta **2011,** *56*, 1476.

[3] R. S. Deinhammer, M. Ho, J. W. Anderegg and M.D. Porter, Langmuir, **1994**, *10*, 1306

Chapter 4

Physisorption vs grafting of aryldiazonium salts onto iron: A corrosion study

Chapter 4 : Physisorption vs grafting of aryldiazonium salts onto iron: A corrosion study

4.1. Introduction

Electro and spontaneous grafting of diazonium salts has gained recognition among the methods for surface modification. As explained in the introduction, the mechanism that permits the attachment of the aryl ring to various surfaces involves, most often, a radical. Based on the attack of this aryl radical on the surface, a mechanism has been proposed that also describes the growth of the layer. In addition, the electrochemical reaction leading to the aryl radical has been described as concerted, that is the transfer of one electron to the diazonium salt and the cleavage of dinitrogen constitutes a single step. As the electron transfer takes place on a diazonium cation “close” to the electrode, the radical is also formed “close” to the electrode and is ready to react with the surface. “Close” can have two meanings: i) if the molecules diffuse to the electrode, the electron transfer will take place in the double layer at the outer Helmotz plane ; ii) the diazonium salt can also be adsorbed on the surface. In the latter case, the electron transfer takes place on a cation already on the surface and the radical will also be formed on the surface. Therefore, the problem of a possible adsorption of the diazonium salt on the surface is a key step in the grafting mechanism.

Two papers have described the previous adsorption of diazonium cations on carbon surface. The first paper by Strano and al., uses Raman spectroscopy and photoluminescence to analyze the kinetics of the spontaneous grafting reaction of 4-chlorobenzene diazonium on SWCNTs. However, right from the start, this paper suffers from a error; the experimental section states that:” Prior to the reaction, the pH of the SWNT solution (1wt% SDS/D_2O) was increased from 5.5 to 11 using NaOH solution”; it is well known that only diazoates and not diazonium salts are present at such pH. Therefore, this paper should demonstrate that diazoates are adsorbed, although the adsorption of negatively charged diazoates on electron rich SWCNT is less likely that of a diazonium cation. The Raman and photoluminescenece spectra show two successive first order reactions. A long-lived intermediate selectively and non covalently binds and partially dopes the nanotube surface (τ = 2.4 min). A slower, covalent reaction is tracked using the time-dependent increase in the disorder mode in Raman (τ =73 min).

The second paper from Stark and al. examines the spontaneous grafting of graphene sheets with 4-nitrobenzenediazonium by Raman spectroscopy. In this case, the reaction was performed in unbuffered water where diazoates are also the main species in solution. Adsorption is observed through a shift of the G band of graphene (a collective vibration of the surface), while the covalent bonding is observed through the appearance of a D band corresponding to the formation of sp^3 carbons.

We have examined the possibility of an adsorption step during the grafting of 3,5- and 2,6-dimethylbenzene diazoniums. The experiments have been performed under conditions where the diazonium salts are stable at low pH.

Main results

- Elucidation of the possible involvement of an adsorption step during the grafting of iron.
- Confirmation of the grafting by IRRAS.
- Corrosion measurements to evaluate the inhibiton efficiency of the grafted layer.
- Characterization of the grafted surface layer hydrophobicity/hydrophilicity by measurements of water contact angles.

Monica L.Usrey, Ethan S. Lippmann and Michael S.Strano, Journal of American chemical Society, **2005**, *127*,16129 16135

Fabian M. Koehler, Arnhild Jacobsen, Klaus Ensslin, Christoph Stampfer and Wendelin J. Stark Small **2010**, *6*, No.10, 1125–1130

Electrochimica Acta xxx (2011) xxx–xxx

Contents lists available at ScienceDirect

Electrochimica Acta

journal homepage: www.elsevier.com/locate/electacta

Physisorption vs grafting of aryldiazonium salts onto iron: A corrosion study

Avni Berisha[a,b], Catherine Combellas[a], Frédéric Kanoufi[a], Jean Pinson[a], Fetah I. Podvorica[a,b,*]

[a] Physico-Chimie des Electrolytes, des Colloïdes et Sciences Analytiques, ESPCI ParisTech, CNRS UMR 7195, 10 rue Vauquelin, 75231 Paris Cedex 05, France
[b] Chemistry Department of Natural Sciences Faculty, University of Prishtina, rr. "Nëna Tereze" nr. 5, 10 000 Prishtina, Kosovo

ARTICLE INFO

Article history:
Received 15 November 2010
Received in revised form 10 January 2011
Accepted 11 January 2011
Available online xxx

Keywords:
Aryldiazonium salts
Physisorption
Electrografting
Iron
Corrosion inhibition

ABSTRACT

The possible involvement of an adsorption step in the course of the electrografting of aryldiazonium salts is tested by investigating the effect of 3,5-dimethylbenzenediazonium and of 2,6-dimethyl benzene diazonium salts (respectively 3,5- and 2,6-DMBD) on the corrosion of iron. In the case of 3,5-DMBD, the grafting is confirmed by infra red reflection absorption spectroscopy (IRRAS). Polarization curves of iron modified electrodes show increased protection against corrosion, particularly in the presence of 3,5-DMBD in the corrosion medium. Conversely, in the presence of 2,6-DMBD, whose radical does not attach onto the iron surface, no inhibition is observed. This indicates that, besides the absence of grafting, there is no physical adsorption of diazoniums onto iron prior to the grafting reaction, in contrast with graphene and carbon nanotubes.

© 2011 Elsevier Ltd. All rights reserved.

1. Introduction

Electrochemical and chemical reduction of aryl diazonium salts [1], (isolated or prepared in situ [2]) in organic media [3,4], acidic [5] or basic [6] aqueous solutions) lead to the covalent attachment of aryl radicals onto the surface of glassy carbon [7–10], carbon nanotubes [11–14], graphene [15–17], metals [18], semiconductors [19,20] and polymers [21–24] (Fig. 1). The reduction potential of aryl diazonium salts, which is ~0 V/SCE allows the easy formation of aryl radicals, electrochemically and/or chemically either by electron transfer with the surface (through a dissociative electron transfer and N_2 evolution) or with an added reagent [1]. Such radicals are responsible for the grafting of the organic moiety onto the surface.

It was shown recently that grafting of diazonium salts onto carbon nanotubes [13] and graphene [17] occurs along a two-step mechanism involving adsorption (physisorption) prior to the grafting step (chemisorption). On carbon nanotubes [13] in the presence of 4-chlorobenzenediazonium, a long-lived intermediate selectively and non-covalently binds to and partially dopes the nanotube surface (τ = 2.4 min). A slower, covalent reaction is tracked by the time-dependent increase in the disorder mode in Raman (τ = 73 min). These two steps are well described using a series of two first-order reactions. The adsorption (physisorption) of the 4-nitrobenzenediazonium on a graphene flake, prior to its reaction (Fig. 2), is observed by Raman spectroscopy [17] through (i) an initial slight shift of the G band of the graphene structure, (ii) the peaks at 1400 and 1440 cm^{-1} that can be attributed to adsorbed diazonium ions forming a charge-transfer complex with the graphene surface. This first step is followed by the appearance of a strong D band related to the formation of sp^3 carbons and therefore to the grafting reaction. Similar experiments indicate that nitrobenzene adsorbs but does not react onto graphene. The two-step reaction can be sketched as in Fig. 2.

Such adsorption that is clearly related to π-stacking of the aryl group is also a consequence of the electrostatic interaction between the positively charged diazonium group and the electron rich graphene. This is why we examine here if such prior adsorption is possible between an electron rich metal and a diazonium salt.

To test this assumption, we have considered the effect of two diazonium salts on the corrosion of iron. The 3, 5-dimethylbezenediazonium (3,5-DMBD) can be easily grafted, while the sterically hindered 2,6-dimethylbezenediazonium (2,6-DMBD) is unable to attach to the surface [25]; however, such hindrance is limited since the 2,6-dimethyl benzene radical is able to abstract an hydrogen atom from acetonitrile and also to react with alkyl chains [26]. On the other hand, many common corrosion inhibitors adsorb on the surface of iron (mercaptobenzothiazole, polyamines [27], benzotriazole [28], and propargylic alcohols [29]). Therefore, the corrosion of iron should be inhibited by the 3,5-DMBD as previously shown before with other diazonium salts [18,30–33] but some corrosion inhibition should also be observed with the 2,6-DMBD if it adsorbs flat on the surface of iron. There-

* Corresponding author at: Physico-Chimie des Electrolytes, des Colloïdes et Sciences Analytiques, ESPCI ParisTech, CNRS UMR 7195, 10 rue Vauquelin, 75231 Paris Cedex 05, France. Tel.: +33 1 40 79 47 54.
E-mail addresses: fetah.podvorica@espci.fr, fetah.podvorica@fshmn.uni-pr.edu (F.I. Podvorica).

0013-4686/$ – see front matter © 2011 Elsevier Ltd. All rights reserved.
doi:10.1016/j.electacta.2011.01.049

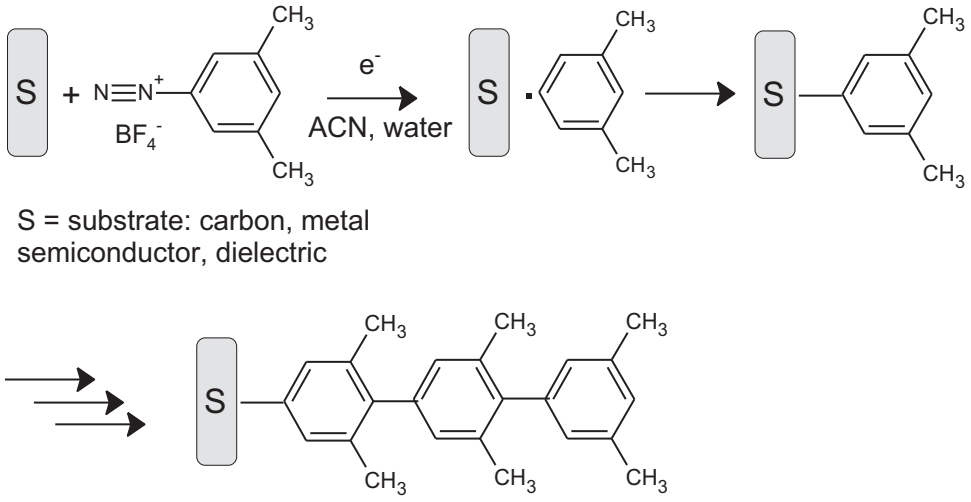


Fig. 1. Electrografting of the 3,5-dimethylbezenediazonium salt.

fore, the observation of an inhibition with the 2,6-DMBD would indicate that a two-step mechanism is possible as with carbon nanotubes and graphene, but the absence of inhibition would make this mechanism unlikely on iron.

This paper presents the results of the reduction of both diazonium salts, the IRRAS spectra of the surfaces after electrolysis and the corrosion curves in the absence and in the presence of diazonium salts. The surfaces will be referred as *Fe*-3,5-DMBD, and *Fe* + 2,6-DMBD.

2. Experimental

2.1. Chemicals

Milli-Q water (>18 MΩ cm) was used for rinsing the samples. 3,5- and 2,6-DMBD were prepared by the standard procedure [25].

2.2. Samples

Massive 1 (or 2) cm × 1 cm iron plates were polished with different grades of polishing paper and finally with a 0.04 μm alumina slurry on a polishing cloth, using a Presi Mecatech 234 polishing machine. After polishing, the plates were rinsed with Milli-Q water and finally sonicated for 10 min in acetone.

The electrodes for cyclic voltammetry were Fe wires (1 mm diameter) imbedded in epoxy resin. Metallic electrodes were polished and rinsed as the iron plate above.

With both diazonium salts, after grafting, the iron electrode was either (i) rinsed with acetone in an ultrasonic bath and then immersed into the pure aqueous acidic solution for physical characterizations by chronoamperometry, contact angles and IRRAS or, (ii) left in the acidic medium used for grafting (without rinsing) to perform corrosion measurements.

2.3. Electrochemical experiments

Electrochemical experiments were performed with an EG&G 263A potentiostat/galvanostat and an Echem 4.30 version software. Electrografting was performed by chronoamperometry in water + 10^{-2} mol dm^{-3} H_2SO_4 solutions with a 10^{-2} mol dm^{-3} solution of 3,5-DMBD or 2,6-DMBD. The reference electrode was the saturated calomel electrode (SCE) and the counter electrode a platinum foil. The potentiostatic polarization curves were carried out by applying a 1 mV/s scan rate. All experiments were performed at room temperature in aerated solutions under unstirred conditions. Before any measurement, the iron electrodes were left in the acidic corrosion medium until the corrosion potential, E_{corr}, stabilized to a constant value. The corrosion values, I_{corr}, were deduced from the semilogarithmic polarization curves by extrapoling the linear cathodic and anodic branches at the corrosion potential.

2.4. IRRAS spectra

IRRAS spectra of the modified samples were recorded using a Jasco FT/IR-6100 Fourier Transform Infra Red Spectrometer equipped with a MCT detector. For each spectrum, 1000 scans were accumulated with a spectral resolution of 4 cm^{-1}. Polished iron plates (as above) were used as references for the spectra.

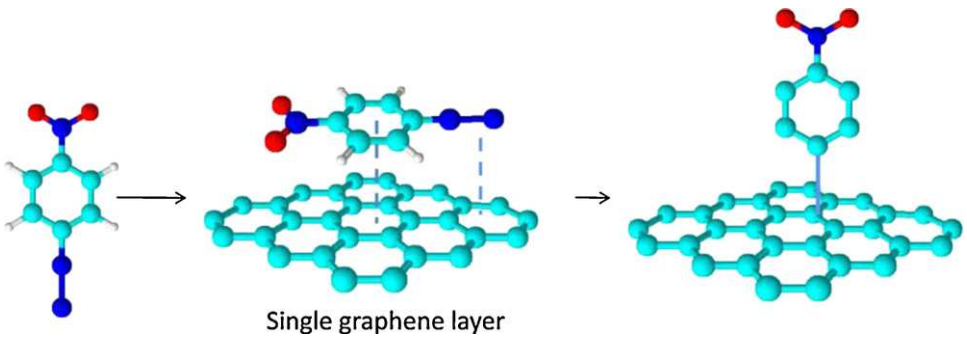


Fig. 2. Two-step mechanism for the grafting of diazonium salts onto graphene.

Please cite this article in press as: A. Berisha, et al., Physisorption vs grafting of aryldiazonium salts onto iron: A corrosion study, Electrochim. Acta (2011), doi:10.1016/j.electacta.2011.01.049

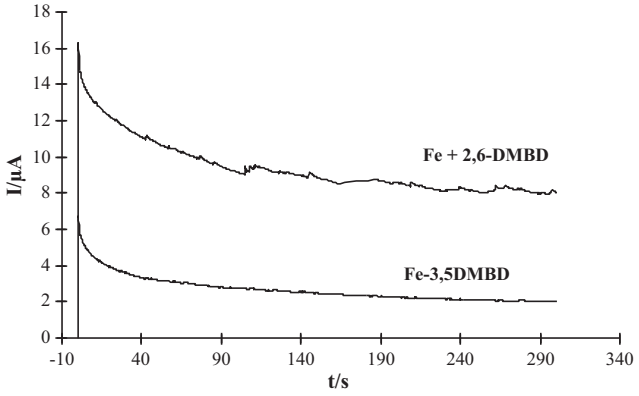


Fig. 3. Chronoamperometry curves for an iron electrode (d = 1 mm) immersed into a 10^{-2} mol dm^{-3} H_2SO_4 solution containing 10^{-2} mol dm^{-3} 3,5-DMBD or 2,6-DMBD: Fe-3,5-DMBD or Fe + 2,6-DMBD, respectively. Electrode potential: −0.7 V/SCE.

2.5. Contact angle measurements

Contact angle measurements were made by delivering a 2 μL drop of Milli-Q water from a micro syringe onto the surface of the modified plate that was mounted horizontally on an illuminated stage and the sample was cooled by a Pelletier element. The image of the static water drop was captured with a Canon PowerShot A640 photo camera attached to a Stemi 2000C microscope. The contact angle was measured using the ImageJ 1.42 software. The value of the contact angle is the average for 10 water drops taken in different parts of the plate.

3. Results and discussion

3.1. Chronoamperometry

Fig. 3 shows the chronomperometric curves obtained when immersing the polished iron electrode into 10^{-2} mol dm^{-3} of 3,5- or 2,6-DMBD aqueous solutions containing 10^{-2} mol dm^{-3} sulfuric acid. After grafting, the iron electrode was rinsed with acetone in an ultrasonic bath and then immersed into the pure aqueous acidic solution (except in the case where the corrosion measurements are performed in the same solution as the grafting). In the case of 3,5-DMBD electrolyzed at −0.7 V/SCE (about 130 mV negative to the corrosion potential), after a sharp increase, the current decreases to ∼2 μA while in the case of 2,6-DMBD, it does not decrease below 8 μA.

3.2. Contact angles

The contact angle of a bare iron electrode immersed into a 10^{-2} mol dm^{-3} H_2SO_4 solution and electrolysed for 5 min at E = −0.7 V/SCE is 58 ± 2°. It increases to 76.5 ± 2° when the electrolysis solution contains 10^{-2} mol dm^{-3} of 3,5-DMBD. This indicates the presence of an hydrophobic organic film, although under such conditions, the electrochemical reduction of 3,5-DMBD competes with protons reduction; on the contrary, for Fe + 2,6-DMBD the contact angle value is identical to that of a bare iron surface.

3.3. IRRAS

Fig. 4 shows the IR spectra of iron plates electrolyzed in aqueous acidic solutions without or in the presence of diazonium salts. After electrolysis for 5 min at −0.7 V/SCE in the absence of any diazonium salt (Fig. 4a) or in the presence of 2,6-DMBD (Fig. 4b), there are no differences between the spectra. Both spectra present a strong and broad band in the region between 1300 and 1000 cm^{-1} with two

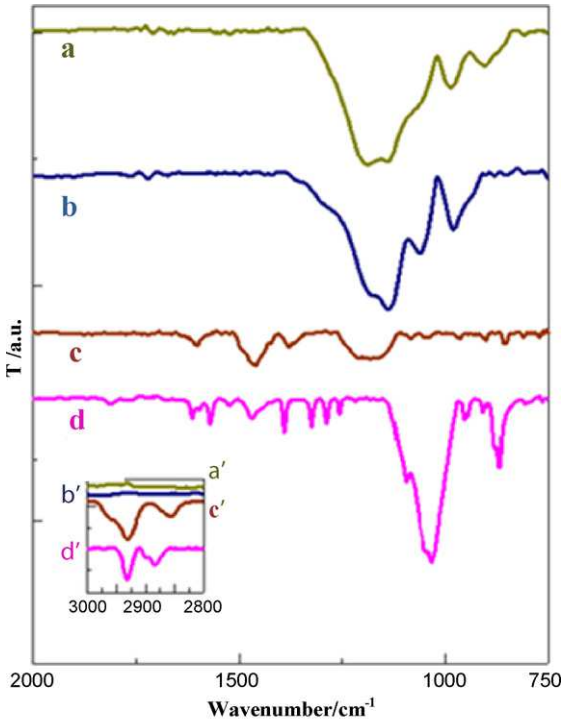


Fig. 4. IRRAS spectra for an iron plate electrolyzed for 5 min at E = −0.7 V/SCE in a 10^{-2} mol dm^{-3} H_2SO_4 solution (a) blank experiment; (b and c) in the presence of (b) 2,6-DMBD (Fe + 2,6-DMBD) and (c) 3,5-DMBD (Fe-3,5-DMBD). (d) ATR spectrum of the 3,5-DMBD diazonium salt. (a'–d'): inset, CH stretching region.

peaks at 1191 and 1137 cm^{-1} due to surface oxides (by comparison 1160, 1020 and 750 cm^{-1} for lepidocrocite).

When the electrolysis has been performed in the presence of 3,5-DMBD, a different spectrum is obtained (Fig. 4c). Iron oxides are still present, but with a lower intensity and this spectrum does not present any IR absorption at 2280 cm^{-1}, which confirms the loss of the diazonium group during the electrochemical reduction. Aromatic C–C stretching vibrations are observed at 1601, 1459 and 1377 cm^{-1} (by comparison 1614, 1568, 1465 and 1390 cm^{-1} for 3,5-DMBD – Fig. 4d – that also shows the strong absorption of the BF_4^- ion at 1100 cm^{-1}). An aromatic C–H out of plane vibration is present at 853 cm^{-1} for Fe-3,5-DMBD that can be attributed to 1,3,4,5-tetrasubsituted benzenes (by comparison, very strong band at 848 cm^{-1} for 1,2,3,5-tetramethylbenzene). The CH stretching of the methyl groups is also observed in the 2800–3000 cm^{-1} region, as shown in the inset of Fig. 4c'.

Therefore, contact angles and IRRAS spectra indicate that 3,5-DMBD can be grafted on the surface, in contrast to 2,6-DMBD. This means that chemisorption occurs with 3,5-DMBD but not with 2,6-DMBD.

3.4. Polarization curves

Polarization curves. Fig. 5 shows the semilogarithmic polarization curves of iron electrodes treated with 3,5- or 2,6-DMBD by the above mentioned procedure. While 2,6-DMBD has no significant effect to protect the iron electrode from oxidation, with 3,5-DMBD the corrosion current decreases (mostly on the cathodic side) and the corrosion potential shifts by 30 mV. Therefore, 3,5-DMBD shows the properties of a corrosion inhibitor.

Fig. 6 shows that the corrosion current of the Fe-3,5-DMBD electrode decreases about ten times in the cathodic region when the electrode is not withdrawn from the 3,5-DMBD aqueous acidic solution after the 5 min electrolysis at −0.7 V/SCE. The reduction

Please cite this article in press as: A. Berisha, et al., Physisorption vs grafting of aryldiazonium salts onto iron: A corrosion study, Electrochim. Acta (2011), doi:10.1016/j.electacta.2011.01.049

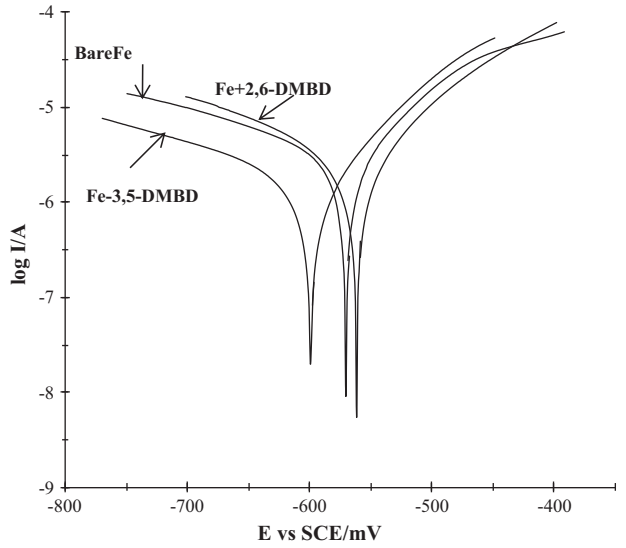


Fig. 5. Polarization curves for iron electrodes ($d = 1$ mm) in a 10^{-2} mol dm^{-3} H_2SO_4 solution: bare Fe, Fe-3,5-DMBD and Fe + 2,6-DMBD. The latter two were grafted for 5 min at −0.7 V/SCE in 10 mM of, respectively, 3,5- or 2,6-DMBD in 10^{-2} mol dm^{-3} H_2SO_4. $v = 1$ mV/s.

of protons is considerably hampered by the formation of a dense and hydrophobic (see the water contact angles above) film of 3,5-dimethylphenyl groups. A strong decrease of the current in the anodic region is also observed until −0.475 V/SCE. For higher potentials, the organic layer seems to be removed. This was previously observed with a grafted iodophenyl layer whose stability was tested as a function of the electrode potential [18]. The organic iodophenyl layer was still present after a 75 mV anodic potential shift from the corrosion potential but after a 150 mV shift, the film had been removed. In the case of an iron electrode modified with 3,5-DMBD, the grafted layer is stable after an anodic potential shift of 115 mV. When the iron electrode is maintained at −0.7 V/SCE for 5 min in an acidic water solution containing the 2,6-DMBD salt and is not withdrawn from the solution, the corrosion potential shifts 35 mV toward cathodic potentials by reference to an iron electrode in the absence of diazonium salt. This results from the presence of two oxidizing agents in the solution, protons and the diazonium ions (that are unable to graft to the surface). The polarization curves

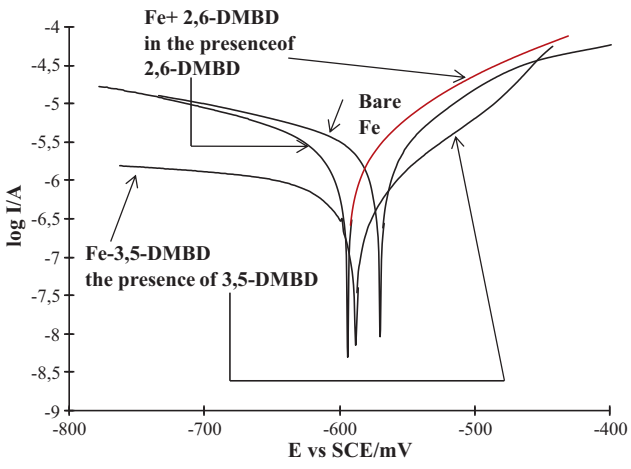


Fig. 6. Polarization curves for iron electrodes ($d = 1$ mm) in a 10^{-2} mol dm^{-3} H_2SO_4 solution: bare Fe, Fe-3,5-DMBD and Fe + 2,6-DMBD. The latter two were grafted for 5 min at −0.7 V/SCE in 10 mM of, respectively, 3,5- or 2,6-DMBD in 10^{-2} mol dm^{-3} H_2SO_4 and then left in the diazonium solution. $v = 1$ mV/s.

Table 1
Corrosion currents and inhibition efficiencies of bare and treated iron electrodes by electrochemical reduction of 3,5- or 2,6-DMBD.

Diazonium salt	E_{corr} vs SCE/mV	$(I_{corr}/10^{-6})$/A	IE (%)
None[a]	−570	3.2	–
3,5-DMBD[a]	−597	1.5	53
2,6-DMBD[a]	−560	3.1	2
3,5-DMBD[b]	−590	0.5	84
2,6-DMBD[b]	−595	3.2	–

[a] Measurements in a 10^{-2} mol dm^{-3} H_2SO_4 aqueous solution. Electrode diameter = 1 mm.
[b] In the presence of 10^{-2} mol dm^{-3} of the corresponding diazonium salt.

in Fig. 6 show that at $E = -0.7$ V/SCE – the potential used to perform the electrografting – no change in the current intensity is observed between an iron electrode electrolyzed in 2,6-DMBD and a bare iron electrode. On the anodic side, the current is somewhat larger than that on a bare electrode.

This result can be interpreted by the absence of any physical adsorption. Note that in Fig. 3 the chronoamperometric curve obtained with 2,6-DMBD shows some oscillations of the cathodic current, which are due to the formation of gaseous hydrogen. This also indicates the absence of adsorption of the diazonium salt.

For comparison, 1-octyne-3-ol, a classical inhibitor, is adsorbed onto iron and the corrosion current decreases by 80% in the presence of a 10^{-2} mol dm^{-3} concentration [29]. The same result can be expressed by calculating the inhibition efficiencies, IE (Table 1), from:

$$\mathrm{IE} = 100\left(1 - \frac{I_{corr}^{film}}{I_{corr}}\right) \quad (1)$$

where I_{corr}^{film} and I_{corr} represent the current intensities at respectively, the coated and bare iron electrodes.

Table 1 shows that 3,5-DMBD, once grafted onto the iron surface, acts as a cathodic inhibitor, the lowest corrosion current and the highest inhibition efficiency (84%) are obtained in the presence of the 3,5-DMBD salt. The electrografted organic film acts as a physical barrier at the interface between the metal and the corrosion medium. The 2,6-DMBD isomer that differs only by the position of the methyl groups does not show any inhibitor efficiency against iron corrosion and therefore does not adsorb (physisorb) onto the iron surface.

4. Conclusion

The 3,5-DMBD is effective as a corrosion inhibitor due to the formation of an organic film covalently bonded [34] to the surface of iron. Conversely, 2,6-DMBD does not present any effect on the corrosion. This can be interpreted both by the absence of electrografting reaction onto the surface due the steric hindrance of the two methyl groups α of the radical and also by the absence of adsorption of this diazonium onto the iron surface. This makes the adsorption of a diazonium salt prior to its grafting onto a metal unlikely.

References

[1] J. Pinson, F. Podvorica, Chem. Soc. Rev. 34 (2005) 429.
[2] S. Baranton, D. Bélanger, J. Phys. Chem. B 109 (2005) 24401.
[3] M. Delamar, R. Hitmi, J. Pinson, J.M. Savéant, J. Am. Chem. Soc. 114 (1992) 5883.
[4] P. Allongue, M. Delamar, B. Desbat, O. Fagebaume, R. Hitmi, J. Pinson, J.M. Savéant, J. Am. Chem. Soc. 119 (1997) 201.
[5] M. Delamar, G. Désarmot, O. Fagebaume, R. Hitmi, J. Pinson, J.M. Savéant, Carbon 35 (1997) 801.
[6] F.I. Podvorica, F. Kanoufi, J. Pinson, C. Combellas, Electrochim. Acta 54 (2009) 2164.
[7] C. Saby, B. Ortiz, G.Y. Champagne, D. Bélanger, Langmuir 13 (1997) 837.
[8] J.K. Kariuki, M.T. McDermott, Langmuir 15 (1999) 6534.
[9] A.J. Downard, M.J. Prince, Langmuir 17 (2001) 5581.

Please cite this article in press as: A. Berisha, et al., Physisorption vs grafting of aryldiazonium salts onto iron: A corrosion study, Electrochim. Acta (2011), doi:10.1016/j.electacta.2011.01.049

[10] T. Itoh, R.L. McCreery, J. Am. Chem. Soc. 124 (2002) 1089.
[11] J.L. Bahr, J. Yang, D.V. Kosynkin, M.J. Bronikowski, R.E. Smalley, J.M. Tour, J. Am. Chem. Soc. 123 (2001) 6536.
[12] P.R. Marcoux, P. Hapiot, P. Batail, J. Pinson, New J. Chem. 28 (2004) 302.
[13] M.L. Usrey, E.S. Lippmann, M.S. Strano, J. Am. Chem. Soc. 127 (2005) 16129.
[14] H. Wang, J. Xu, Chem. Phys. Lett. 477 (2009) 176.
[15] J.R. Lomeda, C.D. Doyle, D.V. Kosynkin, W.F. Hwang, J.M. Tour, J. Am. Chem. Soc. 130 (2008) 16201.
[16] R. Sharma, J.H. Baik, C.J. Perera, M.S. Strano, Nano Lett. 10 (2010) 398.
[17] F.M. Koehler, A. Jacobsen, K. Ensslin, C. Stampfer, W.J. Stark, Small 6 (2010) 1125.
[18] A. Adenier, M.C. Bernard, M.M. Chehimi, E. Cabet-Deliry, B. Desbat, O. Fagebaume, J. Pinson, F. Podvorica, J. Am. Chem. Soc. 123 (2001) 4541.
[19] P. Allongue, C. Henry de Villeneuve, J. Pinson, F. Ozanam, J.N. Chazalviel, X. Wallart, Electrochim. Acta 43 (1998) 2791.
[20] P. Allongue, C. Henry de Villeneuve, G. Cherouvrier, R. Cortès, J. Electroanal. Chem. 550 (2003) 161.
[21] C. Bureau, J. Pinson, European Patent EP1948720 (2007) (to Alchimer).
[22] V. Mévellec, S. Roussel, L. Tessier, J. Chancolon, M. Mayne-L'Hermite, G. Deniau, P. Viel, S. Palacin, Chem. Mater. 19 (2007) 6323.
[23] C. Combellas, F. Kanoufi, D. Mazouzi, A. Thiébault, P. Bertrand, N. Médard, Polymer 44 (2003) 19.
[24] A. Adenier, C. Combellas, F. Kanoufi, J. Pinson, F.I. Podvorica, Chem. Mater. 18 (2006) 2021.
[25] C. Combellas, D.e. Jiang, F. Kanoufi, J. Pinson, F.I. Podvorica, Langmuir 25 (2009) 286.
[26] A. Berisha, C. Combellas, F. Kanoufi, J. Pinson, F.I. Podvorica, Chem. Mater. 22 (2010) 2962.
[27] D. Landolt, Corrosion et Chimie de Surfaces des Métaux, Presses Polytechniques et universitaires Romandes, Lausanne, 1997.
[28] J.V. Custódio, S.M.L. Agostinho, A.M.P. Simões, Electrochim. Acta 55 (2010) 5531.
[29] J. O'M. Bockris, B. Yang, J. Electrochem. Soc. 138 (1991) 2237.
[30] A. Chaussé, M.M. Chehimi, N. Karsi, J. Pinson, F. Podvorica, C. Vautrin-Ul, Chem. Mater. 14 (2002) 392.
[31] C. Combellas, M. Delamar, F. Kanoufi, J. Pinson, F.I. Podvorica, Chem. Mater. 17 (2005) 3968.
[32] T. Shimura, K. Aramaki, Corros. Sci. 48 (2006) 3784.
[33] T. Shimura, K. Aramaki, Corros. Sci. 49 (2007) 1378.
[34] K. Boukerma, M.M. Chehimi, J. Pinson, C. Blomfield, Langmuir 19 (2003) 6333.

Please cite this article in press as: A. Berisha, et al., Physisorption vs grafting of aryldiazonium salts onto iron: A corrosion study, Electrochim. Acta (2011), doi:10.1016/j.electacta.2011.01.049

4.3. Analysis

The adsorption step prior to the covalent grafting step of diazonium salts has been investigated on carbon (SWCNT and graphene) under conditions where diazonium salts are not stable on and on metals by examining the effect of a particular diazonium on the corrosion of iron. Clearly more studies should be dedicated to this problem to confirm the adsorption by other methods on other materials. For example,

i) the Raman measurements on a graphene sheet should be repeated in an acidic medium,

ii) one could examine by Multiple Infrared Reflexion a thin layer of metal (gold,…) deposited on silicon, the solution being above the metal and the IR beam reflecting inside the gold plated silicon

iii) another method could involve a quartz microbalance; a preliminary adsorption step should translate into a two-step increase of weight.

General conclusions

General conclusions

The main part of this thesis describes the grafting of the cyanomethyl radical ($^{\cdot}CH_2CN$) on various surfaces. This radical is electron deficient, due to the presence of the cyano group on the same carbon as the unpaired electron. It is able to react with surfaces, like other radicals such as:

i) alkyl radicals such as $^{\cdot}CH_2$-C_5H_{11} with the alkyl electron donating substituent (obtained from halides).

ii) benzyl radicals such as $^{\cdot}CH_2$-C_6H_4-R , R = NO_2 or H, (obtained from carboxylates or halides).

iii) aromatic radicals $^{\cdot}$Ar with a variety of electron attracting or donating substituents (obtained either by reduction of diazonium salts or by oxidation of Grignard reagents)

iv) heteroaromatic radicals (derived from thiophene)

v) aminyl radicals, $^{\cdot}$NH-R.

DFT calculations have shown that radicals are indeed able to react with carbon or metallic surfaces to give stable constructions. Therefore, the reaction of radicals on metals -and also on carbon- is general, and should be considered as a classical reaction in the rich chemistry of radicals.

Oxygen centered radicals constitute a particular case; we have shown in the introduction that oxidation of alcohols on carbon leads to the formation of *Surface-O-R* assemblies, but it remains to be demonstrated that oxygen radicals are really involved. On the other hand, oxygen centered radicals are easily produced by oxidation of phenoxides, they have been widely investigated, but apparently no grafting reaction has ever been reported.

The above list of radicals is certainly not limitative and many other radicals should be able to react with surfaces. The main restricting factor seems to be the steric hindrance of the radical: primary aminyl radicals attach very efficiently to carbon, secondary radicals are much less reactive and tertiary radicals do not react; in the aryl radicals series, the steric hindrance of the 2,6-dimethylphenyl radical prevents its binding to surfaces.

The drawback of the steric hindrance can be turned into an advantage to graft other radicals. As the 2,6-dimethylphenyl radical (and most likely, other hindered radicals) is unable to react with surfaces, it abstracts an hydrogen atom from the solvent giving rise to another radical (in our case the cyanomethyl radical). This reaction can be generalized to other solvents and most likely to other organic compounds. If the hydrogen donor is the solvent, the condition is that the diazonium salt be soluble in this solvent; if it is a compound added in the solution, it must be a much better hydrogen atom donor than the solvent to compensate the concentration effect by a kinetic effect. Relative hydrogen donor abilities are known that should facilitate the design of proper candidates to graft onto surfaces.

Electrochemistry (or related reductions by the substrate or a reagent added in the solution) has been mostly used for modifying surfaces with strong covalent-like bonds. We have shown that acetonitrile can also be grafted to surfaces by photochemistry. Alkyl halides are also able to give radicals and their attachment on surfaces has been described. More substituents should be investigated to open the way to further applications. These reactions can certainly be generalized since many radicals can be produced by photochemistry. For example, irradiation of ketones is described in the literature as a means to produce radicals, but in this case the radical is a secondary radical and experiments must be performed to demonstrate that grafting is possible.

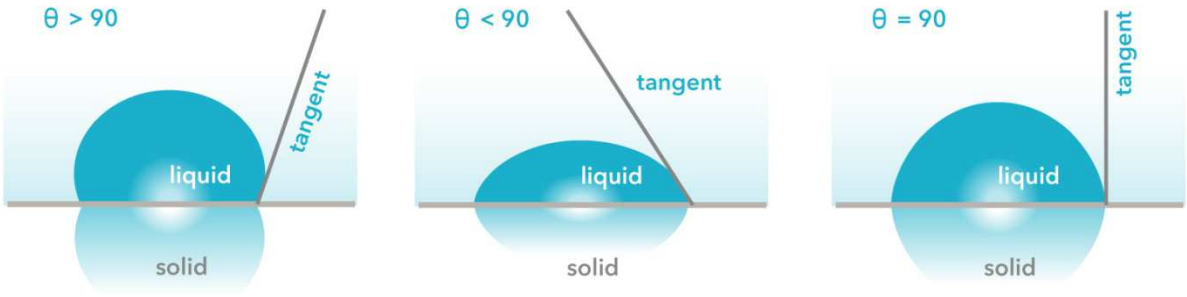
This brief discussion shows that a lot of problems and a number of new possible reactions are possible in this field of research. As this type of reaction is not far from real-life applications, we expect it to give rise to new industrial applications.

Annexes

Annexes

Annex 1: Water contact angles

Contact angle, θ, is a quantitative measure of the wetting of a solid by a liquid. It is defined geometrically as the angle formed by a liquid at the three-phase boundary where a liquid, gas and solid intersect, as shown below:



It can be seen from this figure that a low value of the contact angle (θ) indicates that the liquid spreads (the surface is hydrophilic), or wets well, while a high contact angle indicates poor wetting (the surface is hydrophobic). If the angle θ is less than 90°, the liquid is said to wet the solid. If it is greater than 90° it is said to be non-wetting. A zero contact angle represents complete wetting.

M E A S U R E M E N T S

A) The substrate was cooled by a Pelletier element and a drop of a few microliters of water was placed on it, using a microsyringe. A stereomicroscope allowed the droplet image enlargement and the contact angle measurement using ImageJ software.

B) **Krüss DSA30 instrument**

Samples were horizontally placed on the instrument stage and 3 µL of Milli-Q water was automatically delivered on the top of the sample. At least five measurements were made for each sample. The values of the contact angles were calculated by the tangent method using Drop Shape Analysis software.

Annex 2: Ellipsometry

Ellipsometry measures the change in the polarization state of light reflected from the surface of a sample. The measured values are expressed as Ψ and Δ. These values are related to the ratio of Fresnel reflection coefficients, respectively for p and s-polarized light.

$$\tan(\Psi)\, e^{i\Delta} = \frac{R_p}{R_s} \quad (1)$$

Because ellipsometry measures the ratio of two values, it can be highly accurate and very reproducible. From Eq. (1) the ratio is seen to be a complex number; thus, it contains phase information, which makes the measurement very sensitive. In Fig.1, a linearly polarized input beam is converted to an elliptically polarized reflected beam. For any angle of incidence greater than 0° and less than 90°, p-polarized light and s-polarized will be reflected differently.

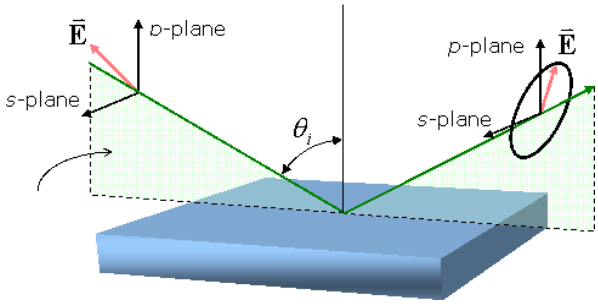


Fig. 1. Schematic of the geometry of an ellipsometry experiment.

MEASUREMENTS

SENTECH SE 400 ellipsometer , He-Ne laser with λ=6328 Å, angle =70.02°

Model: the values for ns and ks were measured on a clean wafer and then these values were further used in the determination of the thickness of a grafted layer: n(ambient)=1, n(upper)=1.00, n(lower)=1.46. The thickness is evaluated directly by the ellipsometer software.

Annex 3: Profilometry

Profilometry is a technique used to measure the surface roughness, film thickness, etc. There are two types of profilometers (contact and non-contact (optical)).

Contact profilometry uses a probe, or stylus, to physically measure the surface texture of a sample. As the probe is moved across the surface of the sample, the vertical movement of the stylus is captured and a two dimensional map of the sample surface is made. In this manner, step heights and surface roughness can be measured. The contact profilometer has a resolution of several nanometers and can measure film thicknesses up to 500 microns.

Optical profilometry. The optical profiler utilizes white-light interferometry to perform non-contact surface measurements. Step heights, surface roughness and surface curvature can all be measured quickly with no sample preparation required. While a contact profilometer is limited to line scans, the optical profiler produces three-dimensional maps of the sample surface with sub-nanometer resolution.

M E A S U R E M E N T S

R Step IQ profilometer from KLA Tencor (contact profilometer)

Thicknesses of films grafted onto Si were measured by carving a sharp furrow through the film with a sharp tip and measuring the depth obtained with the profilometer.

Microsurf 3D interferometric profilometer from Fogale (non-contact)

The interferometric topographic profile is recorded; the real layer thickness z is obtained from the interferometric profile by converting Z_{topo} into $z= -Z_{topo}/2n$, where n= 1.46 is chosen for the grafted layer refractive index.

Annex 4: IRRAS spectroscopy

There are a number of ways in which the IR technique may be implemented for the study of adsorbates on surfaces. For solid samples possessing a high surface area:

Transmission IR Spectroscopy: employing the same basic experimental geometry as that used for liquid samples and mulls. This is often used for studies on supported metal catalysts where the large metallic surface area permits a high concentration of adsorbed species to be sampled. The solid sample must, of course, be IR transparent over an appreciable wavelength range.

Diffuse Reflectance IR Spectroscopy (DRIFTS): in which the diffusely scattered IR radiation from a sample is collected, refocused and analysed. This modification of the IR technique can be employed with high surface area catalytic samples that are not sufficiently transparent to be studied in transmission.

For studies on low surface area samples (e.g. single crystals):

Reflection-Absorption IR Spectroscopy (RAIRS or IRRAS) : where the IR beam is specularly reflected from the front face of a highly-reflective sample, such as a metal single crystal surface.

Multiple Internal Reflection Spectroscopy (MIR) : in which the IR beam is passed through a thin, IR transmitting sample in a manner such that it alternately undergoes total internal reflection from the front and rear faces of the sample. At each reflection, some of the IR radiation may be absorbed by species adsorbed on the solid surface - hence the alternative name of Attenuated Total Reflection (ATR).

M E A S U R E M E N T S

Jasco FT/IR-6100 Fourier Transform Infra Red Spectrometer equipped with MCT detector.

For each spectrum, 1000 scans were accumulated with a spectral resolution of 4 cm^{-1}. The background recorded before each spectrum was that of a clean substrate.

A **Jasco IRT 700S microscope**, 40x40 μm^2 beam size and 800 accumulations with a spectral resolution of 4 cm^{-1} was used for surface maping.

Annex 5: Tof-SIMS

Time-of-Flight Secondary Ion Mass Spectrometry (ToF-SIMS) is a surface-sensitive analytical method that uses a pulsed ion beam (Cs, Au or microfocused Ga) to remove molecules from the very outermost surface of the sample. The particles are removed from atomic monolayers on the surface (secondary ions). These particles are then accelerated into a "flight tube" and their mass is determined by measuring the exact time at which they reach the detector (i.e. time-of-flight). Three operational modes are available using ToF-SIMS: surface spectroscopy, surface imaging and depth profiling. Analytical capabilities of ToF-SIMS include:

- Mass resolution of 0.00x amu. Particles with the same nominal mass (e.g. Si and C_2H_4, both with amu = 28) are easily distinguished from one another.
- Mass range of 0-10,000 amu; ions (positive or negative), isotopes, and molecular compounds (including polymers, organic compounds, and up to ~amino acids) can be detected.
- Trace element detection limits in the ppm range.
- Sub-micron imaging to map any mass number of interest.
- Depth profiling capabilities; sequential sputtering of surfaces allow analysis of the chemical stratigraphy on material surfaces (typical sputtering rates are ~ 100 A/minute).
- Retrospective analysis. Every pixel of a ToF-SIMS map represents a full mass spectrum. This allows an analyst to retrospectively produce maps for any mass of interest, and to interrogate regions of interest for their chemical composition via computer processing after the data set has been instrumentally acquired.

MEASUREMENTS

ION-TOF IV, with Au^+ primary ions at 25 keV.

The analyzed zone was 150 μm^2, and the acquisition time 75 s. Blank samples were analyzed in the same run as the modified samples. The peak intensity refers to the area of the peak normalized to the total intensity of the spectrum. The images were obtained with Au_3^+ ions for 100 scans (~ 40 min).

Annex 6: SEM, EDX

The scanning electron microscope (SEM) uses a focused beam of high-energy electrons to generate a variety of signals at the surface of solid specimens. The signals that derive from electron-sample interactions reveal information about the sample including external morphology (texture), chemical composition, and crystalline structure and orientation of materials making up the sample. The SEM is also capable of performing analyses of selected point locations on the sample; this approach is especially useful in qualitatively or semi-quantitatively determining chemical compositions by using EDX.

Accelerated electrons in an SEM carry significant amounts of kinetic energy, and this energy is dissipated as a variety of signals produced by electron-sample interactions when the incident electrons are decelerated in the solid sample. These signals include secondary electrons (that produce SEM images), backscattered electrons (BSE), diffracted backscattered electrons (EBSD that are used to determine crystal structures and orientations of minerals), photons (characteristic X-rays that are used for elemental analysis and continuum X-rays), visible light and heat. Secondary electrons and backscattered electrons are commonly used for imaging samples: secondary electrons are most valuable for showing morphology and topography on samples and backscattered electrons are most valuable for illustrating contrasts in composition in multiphase samples (i.e. for rapid phase discrimination). X-ray generation is produced by inelastic collisions of the incident electrons with electrons in discrete orbitals (shells) of atoms in the sample. As the excited electrons return to lower energy states, they yield X-rays that are at a fixed wavelength (that is related to the difference in energy levels of electrons in different shells for a given element). Thus, characteristic X-rays are produced for each element in a mineral that is "excited" by the electron beam.

M E A S U R E M E N T S

SEM images were obtained using a **Zeiss Ultra II** or **Hitachi S-4300** electron microscope**.**

The energy-dispersive X-ray (EDX) spectra were obtained using a Hitachi S-4300 microscope equipped with an energy dispersive X-ray spectrometer (Oxford Instruments INCA system).

Annex 7: AFM

AFM provides a 3D profile of the surface on a nanoscale, by measuring *forces* between a sharp probe (<10 nm) and a surface at very short distance (0.2-10 nm probe-sample separation). The probe is supported on a flexible cantilever. The deflection of the probe is typically measure by a *"beam bounce" method*. A semiconductor diode laser is bounced off the back of the cantilever onto a position sensitive photodiode detector. This detector measures the bending of cantilever when the tip is scanned over the sample. The measured cantilever deflections are used to generate a map of the surface topography.

MEASUREMENTS

5100 Atomic Force Microscope (Agilent technologies-Molecular Imaging), operated in a dynamic tip deflection mode (Acoustic Alternating Current mode, AAC).

AFM experiments were performed using Silicon Probes (Applied NanoStructures-FORT) in the tapping mode with 3 $N \cdot m^{-1}$ spring constant at 69 kHz. The images were scanned in topography, amplitude and phase modes with a resolution of 512×512 pixels and are representative of 1×1 μm^2 regions over different locations on the studied surfaces.

Annexes references

(Water contact angle)

http://www.attension.com/contact-angle.aspx

(Ellipsometry)

http://www.uta.edu/optics/research/ellipsometry/ellipsometry.htm

(Profilometry)

http://diarkis.com/index.php/analytics/profilometry/

(IRRAS)

http://www.chem.qmul.ac.uk/surfaces/scc/scat5_4.htm

(Tof-SIMS)

http://serc.carleton.edu/research_education/geochemsheets/techniques/ToFSIMS.html

(SEM, EDX)

http://serc.carleton.edu/research_education/geochemsheets/techniques/SEM.html

(AFM)

http://asdlib.org/onlineArticles/ecourseware/Bullen/SPMModule_BasicTheoryAFM.pdf

Abstract

Two different processes for the attachment of the cyanomethyl radical ($^{\bullet}CH_2CN$), deriving from acetonitrile, to metallic and semiconducting surfaces are described.

- The first method is based on an H-abstraction reaction. A specially designed aryl radical can abstract an hydrogen atom from acetonitrile.
- In the second method, the same cyanomethyl radical is produced by deep UV irradiation of acetonitrile.

This radical attaches covalently to the surface and is also responsible for the growth of an amino functionalized layer. The functionalized film is characterized by various methods (IRRAS, ellipsometry, profilometry, contact angle measurements, SEM, EDX, AFM and chemical derivatization).

Adsorption as a preliminary step in the grafting of diazonium salts is examined in the last chapter. From corrosion measurements on iron, it is concluded that there is no adsorption step prior to the grafting step.

Key words: surface modification, surface patterning, photochemistry, cyanomethyl radical, diazonium salts, 2,6-dimethylbenzenediazonium, adsorption.

Résumé

Cette thèse décrit deux procédés différents pour le greffage du radical cyanométhyle ($^{\bullet}CH_2CN$), dérivé de l'acétonitrile sur des métaux et des semi-conducteurs.

- La première méthode est basée sur une réaction d'abstraction d'un atome d'hydrogène de l'acétonitrile par un radical aryle stériquement encombré.
- Dans la deuxième méthode, le même radical cyanométhyle est produit par irradiation dans l'UV lointain.

Ce radical réagit avec la surface métallique pour former une liaison covalente, il est aussi responsable de la croissance d'une couche organique comportant des fonctions amines. Ce film fonctionalisé a été caractérisé par de nombreuses techniques (IRRAS, ellipsometrie, profilometrie, angle de contact, SEM, EDX, AFM et dérivatisation chimique).

Dans le dernier chapitre l'adsorption d'un sel de diazonium sur la surface du fer préalablement à son greffage a été examinée. Les résultats indiquent l'absence d'une telle adsorption.

Mots clés: Modification de surface, modification localisée, photochimie, radical cyanométhyle, sels de diazonium, 2,6-diméthylbenzenediazonium, adsorption.